



PONTIFICIA UNIVERSIDAD CATOLICA DE CHILE
ESCUELA DE INGENIERIA

PART I: RESPONSE OF REINFORCED CONCRETE BUILDINGS IN CONCEPCION DURING THE MAULE EARTHQUAKE

BENJAMÍN WESTENENK ORREGO

Thesis submitted to the Office of Research and Graduate Studies in partial fulfillment of the requirements for the Degree of Master of Science in Engineering

Advisor:

JUAN CARLOS DE LA LLERA MARTIN

Santiago de Chile, (December, 2011)

© 2011, Benjamín Westenenk Orrego



PONTIFICIA UNIVERSIDAD CATOLICA DE CHILE
ESCUELA DE INGENIERIA

PART I: RESPONSE OF REINFORCED CONCRETE BUILDINGS IN CONCEPCIÓN DURING THE MAULE EARTHQUAKE

BENJAMÍN WESTENENK ORREGO

Members of the Committee:

JUAN CARLOS DE LA LLERA M.

MATÍAS HUBE G.

EDUARDO IZQUIERDO V.

LUCIANO CHIANG S.

Thesis submitted to the Office of Research and Graduate Studies in partial fulfillment of the requirements for the Degree of Master of Science in Engineering

Santiago de Chile, (December, 2011)

To my father Cornelio and mother Loreto. Thanks for the support through all these years. I love you both.

ACKNOWLEDGMENTS

I am grateful of many people and institutions that made possible this research. I would like to thank the following professors: José Antonio Inaudi, Carl Lüders, Rafael Riddell, Rodrigo Jordán, Hernán Santa María, Christian Ledezma, Raúl Alvarez; engineers: Carlos Medel, Alfredo Payer, Guillermo Gerbaudo, Narciso Novillo, Mario Alvarez, Roberto Mollinedo, Jorge Quintanilla, Gabriel Sanhueza, Rocío Rivera, Jaime Arriagada, Emiliano Pinto, Walter Quintana, Fabiola Santibañez, Jeff Dragovich, Carlos Sempere, Lorena Larrea, Felipe Cuevas, Cesar Ahumada, Sebastián De la Fuente, Francisco Vega, Germán Pavez, Paula Valderrama; students: Santiago Brunet, Alan Sternberg; and companies: SIRVE S.A., DICTUC S.A. Special thanks goes to professor Jack Moehle, Rosita Jünemann and Juan José Besa. This research has been funded by the Chilean *Fondo Nacional de Ciencia y Tecnología*, Fondecyt, through Grant #1110377. Last but not least, I would like to thank professor Juan Carlos de la Llera for his constant support and guidance through all these years. Without his motivation and drive I would surely not be the same professional and person I am today.

TABLE OF CONTENTS

	Page
DEDICATION	ii
ACKNOWLEDGMENTS	iii
LIST OF TABLES	vii
LIST OF FIGURES	ix
RESUMEN.....	xvi
ABSTRACT.....	xvii
1. INTRODUCTION	1
2. BUILDING INVENTORY	4
3. BUILDING PROPERTIES	13
4. OTHER INDICES	23
5. DYNAMIC BUILDING PROPERTIES	28
6. CHARACTERICTIC DAMAGE	36
6.1 Building AA-1.....	36
6.2 Building AH-2.....	37
6.3 Building CM-3	37
6.4 Building TL-4.....	38
6.5 Building MD-5	39
6.6 Building PR-6.....	40
6.7 Buildings PP-7 and RT-8	40
6.8 Building TO-9	41

7.	STATISTICS OF BUILDING DAMAGE	43
7.1	Wall Damage.....	44
7.2	Beam Damage	49
7.3	Column Damage.....	56
7.4	Slab Damage	61
7.5	Total Damage	67
8.	TYPES OF DAMAGE	72
8.1	Wall Damage.....	72
8.2	Beam Damage	75
8.3	Slab Damage	77
9.	REPRESENTATION OF DAMAGE.....	79
10.	TRENDS IN SEISMIC BUILDING BEHAVIOR.....	82
10.1	Orientation of the Building	82
10.2	Vertical and Plan Irregularities	87
10.3	Structural Detailing of Walls and Construction	94
10.4	Inter-Story Damage Patterns	98
10.5	Energy Dissipation Sources	101
11.	INTERPRETATION OF TO-9 BUILDING	104
12.	BUILDING CODE TYPE ANALYSIS	110
12.1	Walls Analysis	110
12.2	Beam Analysis	118
12.3	General Comments.....	132
12.4	Comparison with Observed Damage	133
12.5	Drifts and Displacements	136
13.	CONCLUSIONS	141

REFERENCES.....	145
A P P E N D I C E S	148
APPENDIX A : Damage Drawings	149
APPENDIX B : D/C Drawings	159

LIST OF TABLES

	Page
Table 2-1: RC buildings considered.....	4
Table 3-1: Summary of average building parameters	21
Table 4-1: Plan irregularities indices	23
Table 4-2: Vertical irregularities indices.....	25
Table 5-1: Dynamic properties of analyzed buildings	34
Table 5-2: H/T ratios of analyzed buildings	35
Table 7-1: Damage in walls	47
Table 7-2: Damage in beams.....	53
Table 7-3: Damage in columns	59
Table 7-4: Damage in slabs.....	64
Table 7-5: Total damage	70
Table 8-1: Type of wall damage and stories where behavior is observed	73
Table 8-2: Type of beam damage and stories where behavior is observed	77
Table 8-3: Type of slab damage and stories where behavior is observed.....	78
Table 12-1: Grouping of D/C ratios	110
Table 12-2: Total results for shear in walls.....	112
Table 12-3: Total results for flexure in walls.....	116

Table 12-4: Total results for shear in beams	120
Table 12-5: Total results for positive bending in beams	124
Table 12-6: Total results for negative bending in beams	129
Table 12-7: Drifts and displacements for all considered buildings.....	140

LIST OF FIGURES

	Page
Figure 2-1: Geographical location of building studied in Concepción	5
Figure 2-2: Specific location of building studied in Concepción	6
Figure 2-3: Geographical orientation of buildings considered	7
Figure 2-4: Typical building plan drawings, building photos, and building axes.....	12
Figure 3-1: Width in the X-direction versus normalized height, b_x	13
Figure 3-2: Width in the Y-direction versus normalized height, b_y	14
Figure 3-3: Aspect ratio versus normalized height, b_1/b_2	15
Figure 3-4: Slenderness ratio versus normalized height, h/d	16
Figure 3-5: Story area versus normalized height, A	17
Figure 3-6: Average wall thickness versus normalized height, \bar{e}	18
Figure 3-7: X-direction shear wall density versus normalized height, ρ_x	19
Figure 3-8: Y-direction shear wall density versus normalized height, ρ_y	20
Figure 3-9: Density of vertical elements versus normalized height, ρ_z	20
Figure 4-1: Mass irregularity index versus normalized height, $ M_i / M_{i+1} $	26
Figure 5-1: Linear 3-D models for analyzed buildings	33
Figure 6-1: Examples of wall damage in building AA-1	36
Figure 6-2: Examples of wall damage in building AH-2	37

Figure 6-3: Examples of wall damage in building CM-3	38
Figure 6-4: Examples of wall damage in building TL-4.....	39
Figure 6-5: Examples of column damage in building MD-5	39
Figure 6-6: Examples of wall damage in building PR-6.....	40
Figure 6-7: Examples of wall damage in buildings (a), (b) PP-7; (c), (d) RT-8.....	41
Figure 6-8: Building TO-9; (a) Shear damage in axis 1A; (b) main collapse in story 12... ..	42
Figure 7-1: Examples of light, moderate and severe damage	43
Figure 7-2: Light damage in walls	44
Figure 7-3: Moderate damage in walls.....	45
Figure 7-4: Severe damage in walls	45
Figure 7-5: Total damage in walls	46
Figure 7-6: Examples of severe wall damage	49
Figure 7-7: Light damage in beams	50
Figure 7-8: Moderate damage in beams.....	50
Figure 7-9: Severe damage in beams	51
Figure 7-10: Total damage in beams.....	52
Figure 7-11: Examples of severe beam damage	55
Figure 7-12: Light damage in columns	56

Figure 7-13: Moderate damage in columns	57
Figure 7-14: Severe damage in columns	57
Figure 7-15: Total damage in columns	58
Figure 7-16: Examples of severe column damage	61
Figure 7-17: Light damage in slabs	62
Figure 7-18: Moderate damage in slabs	62
Figure 7-19: Severe damage in slabs	63
Figure 7-20: Total damage in slabs	63
Figure 7-21: Examples of severe slab damage.....	66
Figure 7-22: Total light damage.....	67
Figure 7-23: Total moderate damage	68
Figure 7-24: Total severe damage.....	68
Figure 7-25: Total damage	69
Figure 9-1: Example of damage observed in structural drawings.....	80
Figure 9-2: Comparison between recorded and actual damage for axis 1A of TO-9.....	81
Figure 10-1: Severely damaged walls at buildings (a) TL-4, (b) AH-2.....	84
Figure 10-2: Building PR-6; (a) Schematic elevation V-W, (b) Story plan and damaged area, (c) Torsion in axis N, (d) Ground settlement near axis V, (e) Settlement in PR-6.....	85

Figure 10-3: Building MD-5: (a) schematic plan; (b) collapsed columns; (c) elevation I; bending moment diagram in collapsed columns for (d) E-W, and (e) N-S	87
Figure 10-4: Severe irregularities in buildings (a) AA-1, (b) TO-9, (c) inverted wall and damage at the 11 th story of TO-9, axis 10.....	89
Figure 10-5: (a) Typical flag-shaped wall; (b) damage observed in flag shaped walls; Examples at buildings (c) AA-1 and (d) AH-2	90
Figure 10-6: (a) Opening formation at vertical irregularities; damage in upper stories of (b) AA-1, (c) AH-2, (d) CM-3; damage in lower stories of (e) CM-3, (f) building in Chillan	92
Figure 10-7: Building AH-2. (a) Story 1 of AH-2, (b) story 2 of AH-2, (c) shear damage in first story wall, (d) slab movement and (e) punching of walls through slabs.....	93
Figure 10-8: (a) Beams supported at orthogonal walls and (b) beams coupled with transverse shear walls. Beam punching at (c) RT-8, (d) TO-9, (e) PP-7. (f) Damage in coupling beams of PP-7	94
Figure 10-9: Typical thin wall failure. Buildings (a), (b): AH-2, (c) CM-3 and (d) PR-6.....	96
Figure 10-10: (a) Inadequate anchorage of beam-wall connection, (b) reinforcement outside of the confined area, (c) unconfined longitudinal reinforcement and lack of stirrups, (d) typical observed hooks.....	97
Figure 10-11: Multistory damage at CM-3. (a) Structural plan of story 2, (b) N-E corner, (c) N-W corner and (d) S-W corner	98

Figure 10-12: (a) Location of walls in plan CM-3, (b) observed damage, (c) shear failure at central wall and (d) induced damage in elevation F.....	99
Figure 10-13: Building PR-6. (a) Structural plan of 1 st story, (b) shear damage propagation through the slab, (c) zoom of damaged slab and superimposed flexural and shear stress cracking. (d) Multistory damage	100
Figure 10-14: Slabs working as coupling beams in buildings (a) AA-1, (b), (c) AH-2 and (d) PP-7	102
Figure 10-15: (a) Titanium building, (b) 280-ton energy dissipation device used and (c) C-shaped dissipators.....	103
Figure 11-1: Building TO-9. (a) West view, (b) East view, (c) South view and deformed axis J, (d) top view, (e) main collapse at story 12, (f) short column damage along axis 1A and (g) condition of 21 st story	105
Figure 11-2: Building TO-9. (a) Structural plan of 12 th story, (b) partial collapse of the 16 th story, (c) partial collapse of the 20 th story, (d) beams at 12 th story, (e) column in axes G-5 of 12 th story and (f) column in axes G-4	107
Figure 11-3: Building TO-9. (a) Axis 1A at story 14, (b) slab deformation at story 16, (c) damage at 18 th story, (d) severely damaged column at 21 st story	108
Figure 11-4: Important damage at core. (a) Explanation of observed behavior, (b) location of wall in story 12, (c) flexure-axial damage in story 11, (d) shear induced damage in story 12	109
Figure 12-1: Percentage of analyzed walls with shear D/C ratios within each group.....	111
Figure 12-2: Shear D/C ratios in walls as histograms.....	114

Figure 12-3: Shear D/C ratios in walls as cumulative probability	115
Figure 12-4: Flexural D/C ratios in walls as histogram for building TO-9	117
Figure 12-5: Flexural D/C ratios in walls of TO-9 as cumulative probability	117
Figure 12-6: Percentage of analyzed beams with shear D/C ratios within each group	119
Figure 12-7: Shear D/C ratios in beams as histograms	121
Figure 12-8: Shear D/C ratios in beams as cumulative probability	122
Figure 12-9: Percentage of analyzed beams with positive bending D/C ratios within each group	124
Figure 12-10: Positive bending D/C ratios in beams as histograms	126
Figure 12-11: Positive bending D/C ratios in beams as cumulative probability	127
Figure 12-12: Percentage of analyzed beams with negative bending D/C ratios within each group	129
Figure 12-13: Negative bending D/C ratios in beams as histograms	131
Figure 12-14: Negative bending D/C ratios in beams as cumulative probability	132
Figure 12-15: Example of deficient D/C ratios in structural drawings	135
Figure 12-16: Drifts and displacements for building AA-1	137
Figure 12-17: Drifts and displacements for building CM-3	137
Figure 12-18: Drifts and displacements for building PR-6	138
Figure 12-19: Drifts and displacements for building TO-9	139

Figure A-1: Damaged elements in story 2 of building AA-1.....	150
Figure A-2: Damaged elements in story 1 of building AH-2.....	151
Figure A-3: Damaged elements in story 2 of building CM-3	152
Figure A-4: Damaged elements in story 2 of building TL-4	153
Figure A-5: Damaged elements in story 3 of building MD-5	154
Figure A-6: Damaged elements in story 1 of building PR-6	155
Figure A-7: Damaged elements in story 1 of building PP-7	156
Figure A-8: Damaged elements in story 2 of building RT-8	157
Figure A-9: Damaged elements in story 12 of building TO-9	158
Figure B-1: D/C ratios in story 2 of building AA-1	160
Figure B-2: D/C ratios in story 2 of building CM-3	161
Figure B-3: D/C ratios in story 1 of building PR-6.....	162
Figure B-4: D/C ratios in story 12 of building TO-9	163

RESUMEN

El terremoto del 27 de febrero, de magnitud $M_w=8.8$, ocurrido en Chile, afectó aproximadamente a 13 millones de personas y a la parte más industrializada del país, dejando al descubierto todo tipo de problemas y fortalezas de las estructuras. Se presentan observaciones detalladas para nueve edificios severamente dañados de la región de Concepción. Estos edificios utilizan, en general, una configuración en base a muros de corte. Aunque menos del 1% de los edificios de media altura en Chile que fueron expuestos mostraban daños de gravedad, se mostraron patrones repetitivos ocurridos en estructuras y lugares diferentes, lo que implica que hay espacio para mejoras en la norma sísmica y sus recomendaciones. El carácter repetitivo de algunos años indica que estas observaciones pueden ser aplicables a edificios similares en otros lugares, mientras que otros daños pueden ser únicos. Bastantes muros de corte experimentaron fallas que aparentemente empezaron en los extremos debido a la alta compresión en estos bordes no confinados, haciendo que la falla se propagara al resto del muro. Otros muros experimentaron fallas debido al corte. El daño también se observó en columnas, vigas y losas de acoplamiento. En la mayoría de los casos, el porcentaje de elementos dañados fue inferior al diez por ciento de los elementos fuerza resistente del edificio, lo que sugiere que estas estructuras no fueron capaces de distribuir los daños. Se calculan varios índices, incluyendo los períodos de vibración y los índices de regularidad. Los daños en los muros de corte fueron frágiles, ocurrieron en estructuras relativamente nuevas de hormigón armado apoyadas en suelos blandos con algún grado de irregularidad vertical y/o de planta. Se deduce comportamiento no dúctil ya que no hay evidencia de daño extendido en la estructura y también del hecho que existen configuraciones estructurales muy similares que no mostraron ningún daño.

Palabras Claves: Evaluación de daños, Daños por terremotos, Análisis de fallas, Muros de hormigón armado, Estructuras de hormigón armado.

ABSTRACT

The February 27, magnitude $M_w=8.8$, Chile earthquake, affected approximately 13 million people and the most industrialized part of the country, exposing all sorts of problems and also strengths of structures. Detailed observations are reported for nine shear wall buildings from the Concepción region that experienced severe damage. Although less than 1% of the medium rise buildings in Chile that were exposed showed severe damage, such damage showed some repetitive patterns and occurred in different structures and locations, implying that there is space for seismic code improvements and recommendations. The repetitive nature of some of the damage suggests that these field observations may be applicable to similar buildings elsewhere, whereas other damage may be unique. Several shear walls experienced failures that apparently started at the boundaries due to the high compression in these unconfined edges, and propagated into the wall web. Other walls, including horizontal and vertical wall segments in perforated walls, experienced shear failure. Damage also was observed in columns, beams, and coupling slabs. In most cases, the percentage of damaged elements was less than ten percent of the lateral force-resisting elements of the building, suggesting that these structures were not capable of distributing damage. Several building indices are calculated, including vibration periods and regularity indices, for comparison with observed behavior. Damage in shear walls was brittle, occurred mainly in recent RC structures supported on soft soils with some degree of vertical and/or plan irregularity. Non ductile behavior has been inferred since there is no evidence of damage being spread in the structure and also from the fact that very similar structural configurations existed at nearby locations and showed no damage.

Keywords: Damage assessment, Earthquake Damage, Failure analysis, Reinforced concrete shear walls, Reinforced concrete structures.

1 INTRODUCTION

The February 27 Maule earthquake in central and southern Chile ($M_w=8.8$) caused severe damage in some medium rise buildings, industries, other civil infrastructure and lifelines, leading to an estimated earthquake cost of USD 30 billion (*Instituto de la Construcción*, 2010). This earthquake is the first in known Chilean seismic history which rupture propagated bilaterally north and south. Ground motion records suggest a fault zone with at least two main slip spots with displacements of about 14.5m (Hayes and USGS, 2010), one at the latitude of Cobquecura, and the other at the latitude of Curicó. The rupture zone propagated more toward the north than to the south because of the 1960 great Valdivia earthquake.

The seismic performance of some shear wall buildings was in some respects unexpected. The shear-wall building structural configuration, so positively evaluated after the 3-M 1985 Chile earthquake, showed this time to be vulnerable and most likely incapable of dissipating the energy consistent with the demand reduction factor used in their design. This thesis focuses on the observed shear-wall building damage of a specific group of 9 buildings located in Concepción, Talcahuano, and San Pedro; damage which is unprecedented in seismic literature. The inventory of buildings larger than five stories exposed to this earthquake was close to 10,000, from which one collapsed to ground level and about eighty sustained severe damage. In the Bio-Bio Region, the estimated number of severely damaged midrise concrete buildings is around 20. The high concentration of damaged buildings in and around Concepción provides an opportunity to conduct a comparative study of several buildings, likely subjected to similar though not identical ground motions, for which geometric characteristics and failure types can be identified. Seven of the nine damaged structures examined were 8 or fewer years old, and are counted among a total of 102 buildings nine stories or taller constructed in the

Bio-Bio region between 1985 and 2009 (*Instituto Nacional de Estadísticas de Chile*, 2010). Several lessons of universal applicability will be obtained from the interpretation and study of such damage, as well as from the building evaluation carried out prior to their demolition or retrofit.

This investigation is intended with two main purposes, one of archival nature and the other of a reconnaissance report. The information reported here comes from different sources, most notably, an initial reconnaissance by members of the EERI Learning from Earthquakes team that included the author in March 2010 and subsequent building surveys by US and Chilean teams during subsequent months. Local teams also developed stabilization solutions of some of the buildings and planned their demolition—seven of the nine buildings are scheduled to be demolished. The work performed produced extensive information about materials, a thorough survey of the internal damage state of the buildings, structural drawings and specifications, and linear structural models.

There is little doubt that structural damage is often a multi-factorial problem. As presented herein building performance was condition by factors such as: (i) the long duration of ground motion (2 minutes and 45 seconds), (ii) ground motion directivity effects, (iii) simultaneity of ground motion components, (iv) local soil conditions, (v) considerable vertical component of ground motions, (vi) structural orientation, (vii) wrong characterization of design spectra for long periods, (viii) excessive axial loads, (ix) lack of detailing, (x) construction aspects, etc. Many interest aspects not conventionally considered in design may result from the observation of damage in these structures and provoke questions such as: Why did shear failures occurred in some components of the buildings in Concepción and not in Santiago (Moehle, 2010)?, Why is there exceptions in the general correlation of structural damage with soil type and topographical accidents?, or Why did similar building concepts, close to each other, perform very differently?

This thesis provides a quick overview of the geometry of the structures, their most relevant structural characteristics, and their damage status. By using field data, the

survey performed on the structures, and the information contained in structural drawings, a number of building indices were computed in order to classify the structures. Particular trends observed in the seismic performance will be presented, which intends to expose some interpretation of the building response as it results from reconnaissance and surveying work. A more detailed analysis, but still preliminary, for one of the high rise buildings will also be presented. For buildings that showed a more critical structural condition, results of a linear response and code-type analysis are presented. The interpretation of data will leave several questions open for future research work. The information presented herein resulted in two articles sent to international journals (Westenenk et al, 2011)

2 BUILDING INVENTORY

The city of Concepción is 105km SSW from the epicenter and its building inventory was particularly affected by the earthquake. As a result of the strong ground shaking, several shear-wall type buildings underwent severe damage and one of them collapsed. The nine buildings listed in Table 2-1 belong to this group and their location is identified in Figure 2-1. The information presented in the Table includes for each building the number of stories, year of construction, geographical coordinates, longitudinal axis orientation, and soil type.

Table 2-1: RC buildings considered

ID	# of Stories	Construction Year	Geographic Coordinates		Longitudinal axis orientation	Soil type
AA-1	20+1	2002	36°49'06.98''S	73°02'28.44''W	64°N	II
AH-2	15+2	2009	36°50'12.45''S	73°06'06.97''W	85°W	III
CM-3	18+1	2005	36°49'06.98''S	73°02'41.49''W	62°W	II
TL-4	17+1	1973	36°49'42.70''S	73°03'10.62''W	62°W	III
MD-5	5+1	1957	36°43'11.25''S	73°06'31.27''W	0°W	III
PR-6	12	2006	36°49'14.42''S	73°03'42.90''W	62°W	III
PP-7	10	2004	36°47'46.81''S	73°05'05.77''W	4°N	III
RT-8	10	2006	36°47'44.29''S	73°05'05.67''W	4°N	III
TO-9	21+2	2008	36°49'45.97''S	73°03'18.45''W	62°W	III

Buildings are all reinforced concrete (RC) structures with a number of stories above grade ranging from 5 to 21; the number of basements is indicated by the number after the + sign in Table 2-1. Please note that the orientation of their longitudinal axis is denoted in clockwise direction from the indicated cardinal point. Soil type II represents a dense gravel or clay with shear wave velocity larger than 400m/s in the upper 10m, and type III to unsaturated gravel or clay with shear wave velocity less than 400m/s (NCh 433Of.96, 1996).

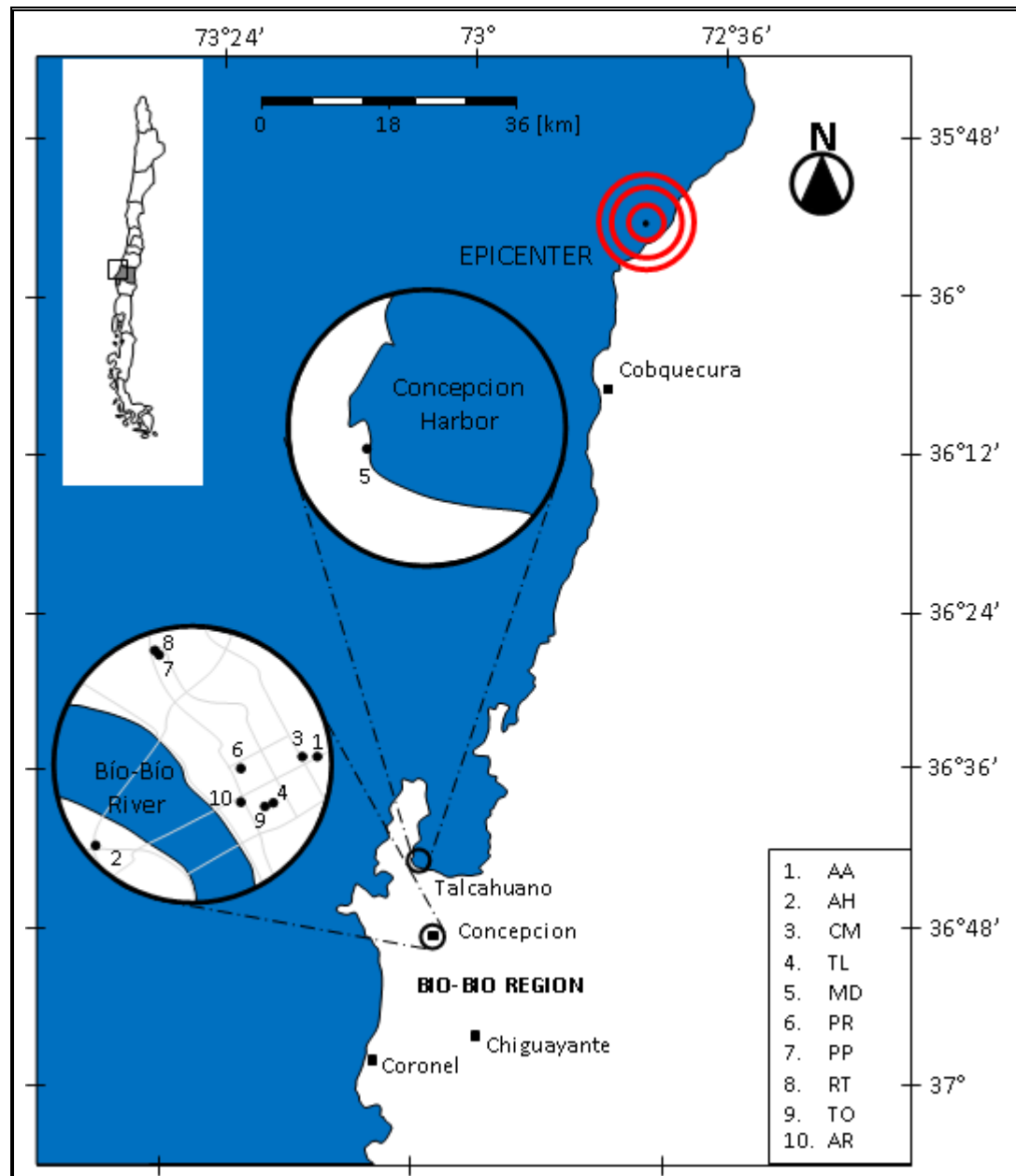


Figure 2-1: Geographical location of building studied in Concepción

Building 10 showed in Figure 2-1 is the only collapsed high rise building in Concepción. For a more specific location of the structures analyzed, see Figure 2-2.



Figure 2-2: Specific location of building studied in Concepción

Shown in Figure 2-3 are satellite images of the footprints of the buildings considered enclosed by rectangles for better identification. It also shows the orientation of the only building that collapsed in Concepción before and after the earthquake. It is seen that most buildings have principal axes oriented predominantly in the N-S and E-W and their orientation seems to be positively correlated with their most damaged direction. Indeed, without any detailed structural analysis, it is interesting to note that the most serious damage in these structures occurred in resisting planes along the E-W direction. Please also note that because of the kinematics of the subduction interplate mechanism, the co-seismic displacement of the ground occurred predominantly westward and up (smaller). This can also be confirmed by looking at the differential GPS vectors of co-seismic displacements of the crust presented elsewhere (Alimoradi and Naeim, 2010).

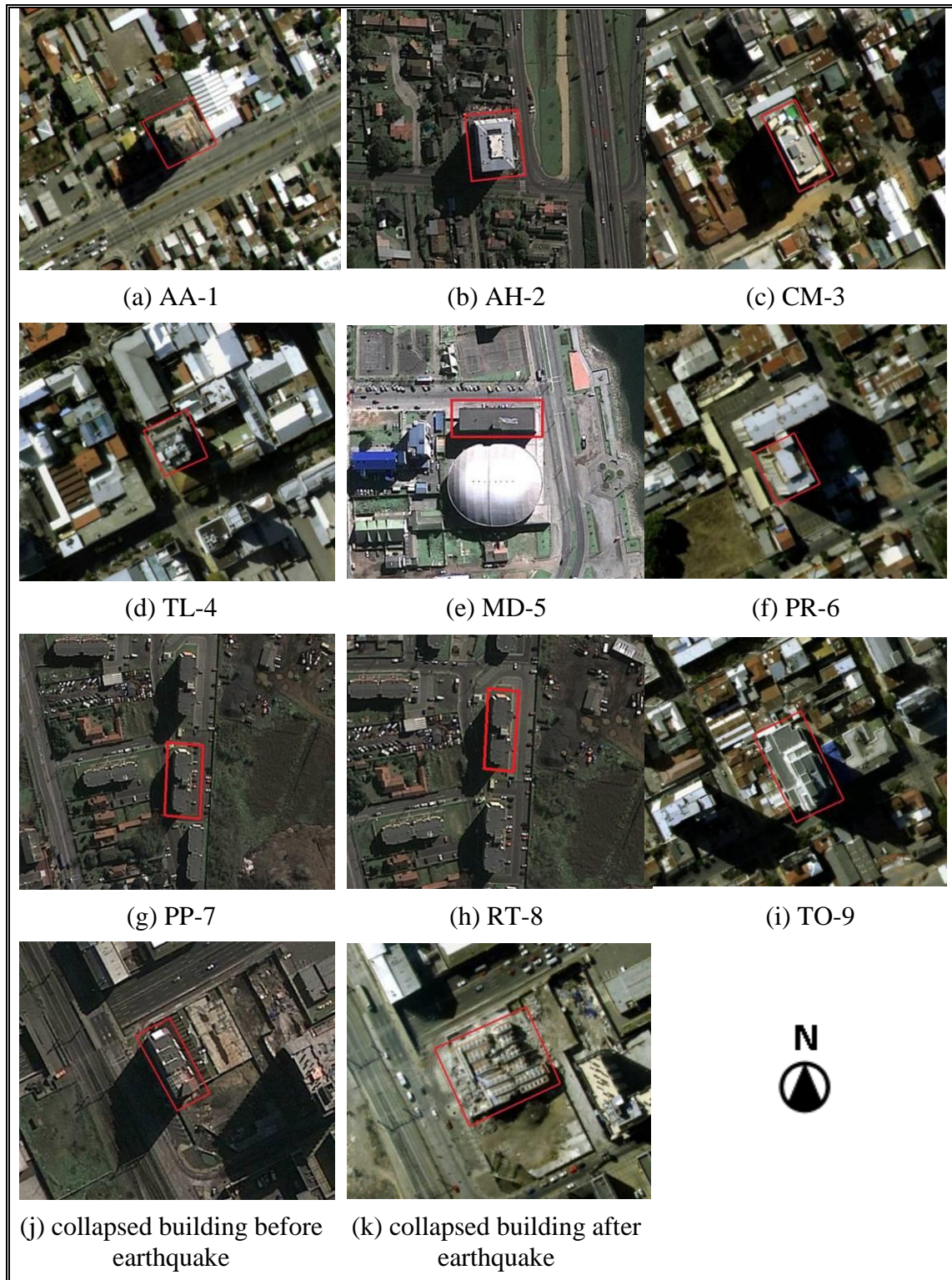
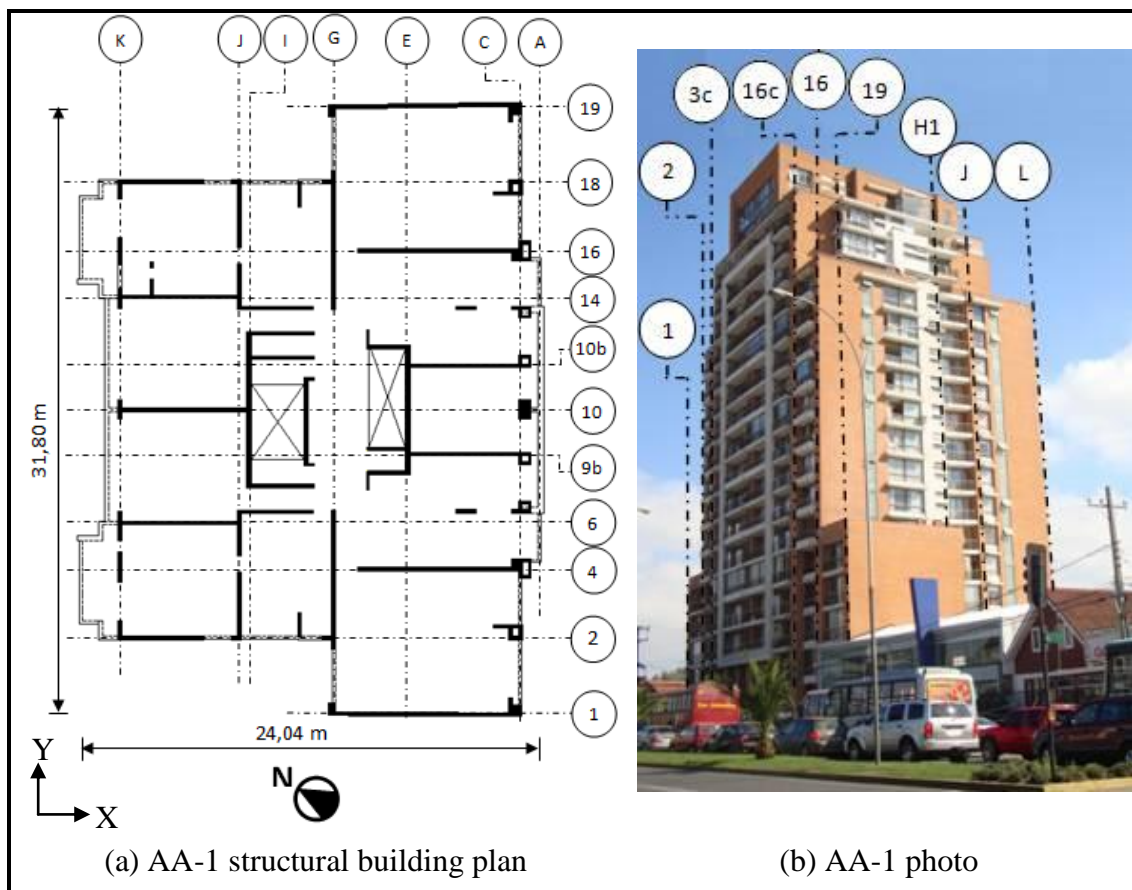
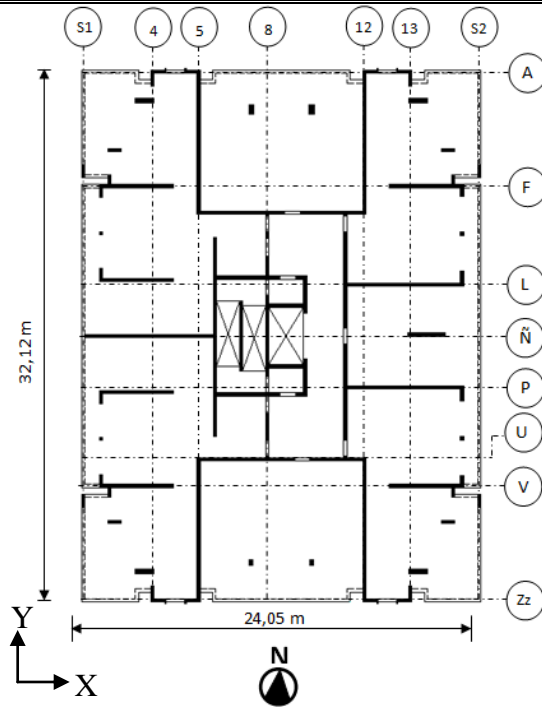


Figure 2-3: Geographical orientation of buildings considered

Representative building plans and panoramic photographs of the group of buildings are presented in Figure 2-4. Some of these structures have very peculiar geometries and vertical as well as plan irregularities. Therefore, they would require a complete set of drawings to describe and qualitatively analyze their behavior properly. However, the single plan included in this Figure provides some insight on the building configuration and helps understanding certain damage patterns presented later.

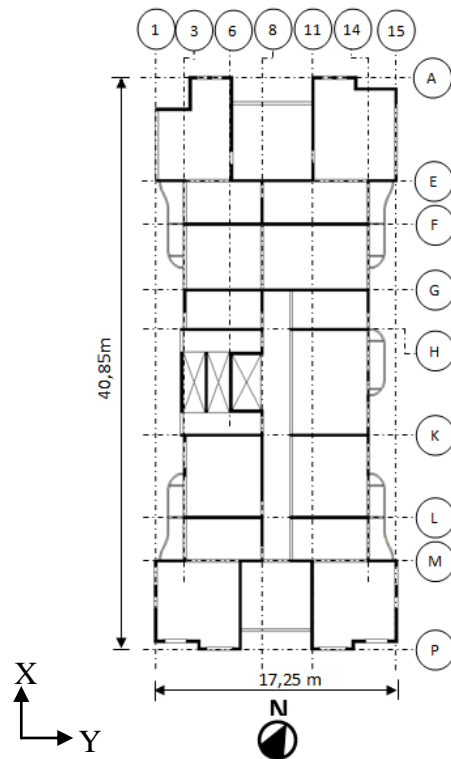




(c) AH-2 structural building plan



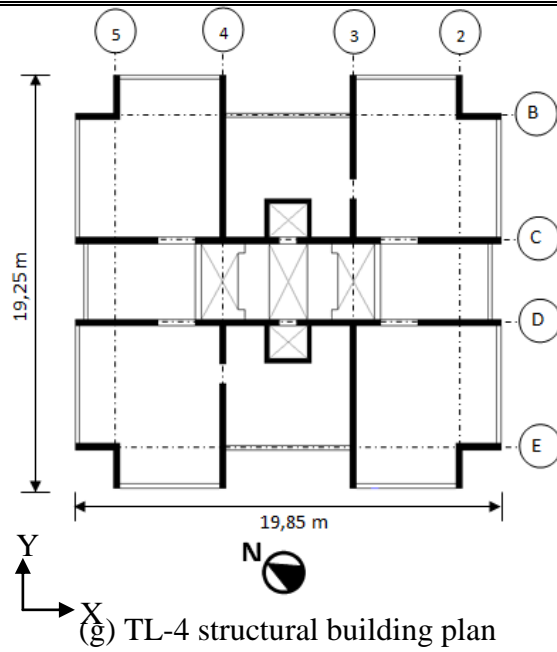
(d) AH-2 photo



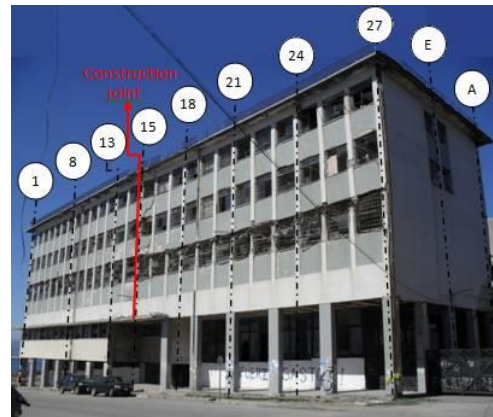
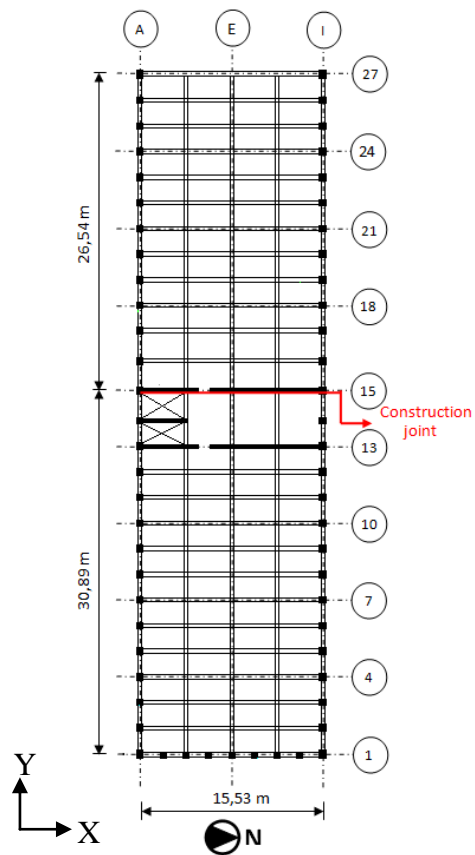
(e) CM-3 structural building plan



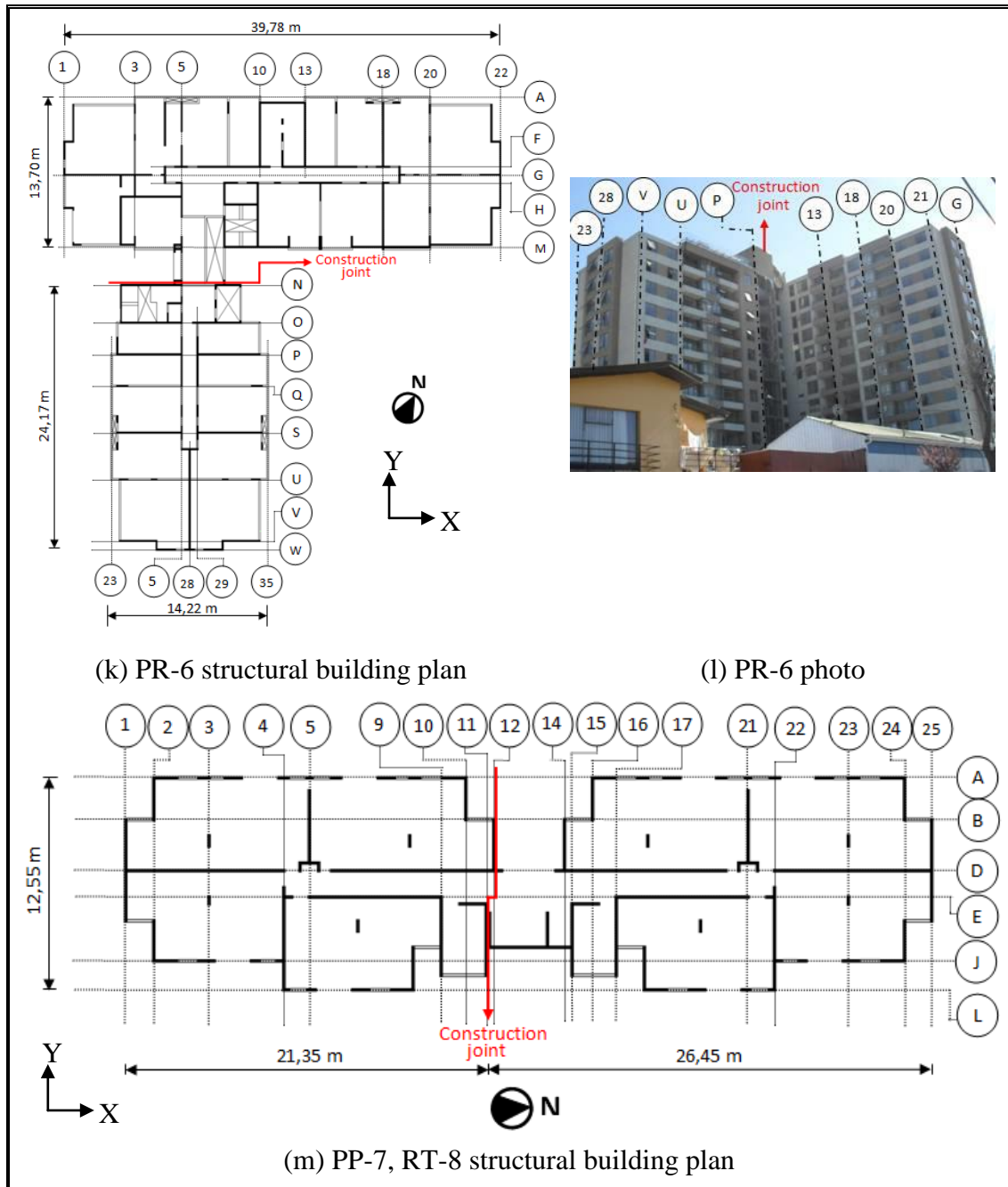
(f) CM-3 photo



(h) TL-4 photo



(j) MD-5 photo



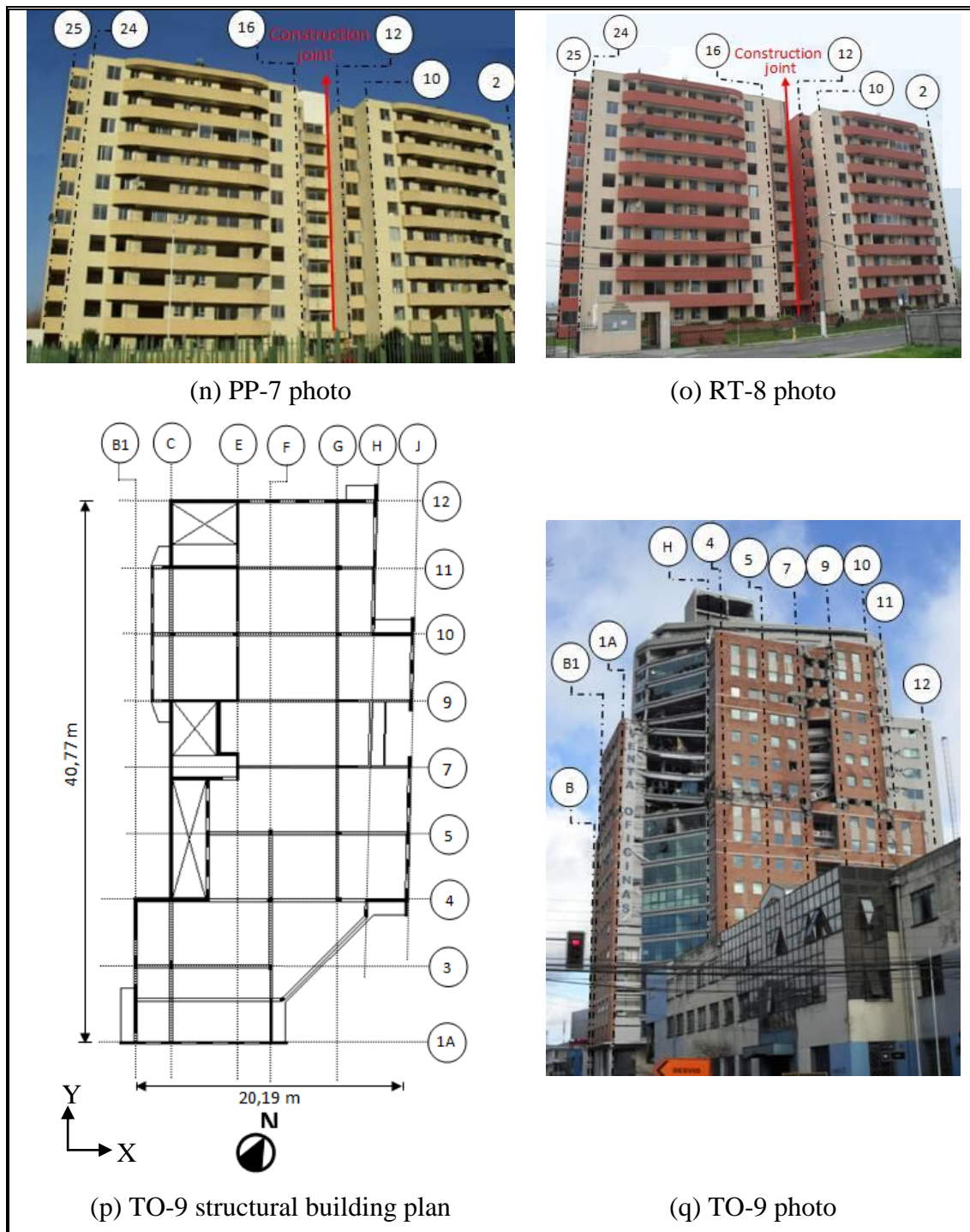


Figure 2-4: Typical building plan drawings, building photos, and building axes

3 BUILDING PROPERTIES

Some basic geometric building properties are summarized in this section. It is important to note that buildings MD-5, PP-7, and RT-8 are composed by two different blocks each separated by a construction joint, so figures and tables will differentiate them by indices “a” and “b”. Because buildings PP-7 and RT-8 have the same structural building plan, figures superimpose results for PP-7a and RT-8a, and PP-7b and RT-8b.

Shown in Figure 3-1 and Figure 3-2 are the widths of the building plan in the X- and Y- directions b_x and b_y versus the normalized height of the structure. This property was obtained from structural plans by considering the maximum dimension of the slab in each story.

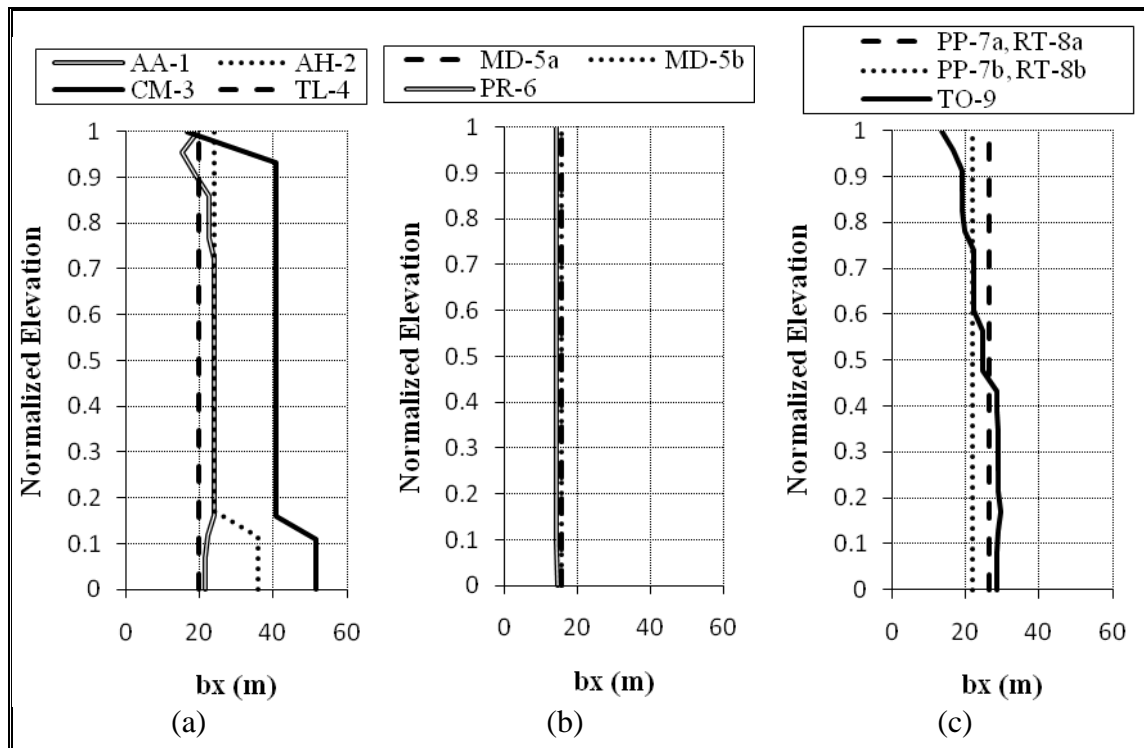


Figure 3-1: Width in the X-direction versus normalized height, b_x

For buildings TL-4, MD-5a, MD-5b, PR-6, PP-7a, PP-7b, RT-8a and RT-8b, b_x is approximately constant in height. In AA-1 and CM-3, b_x varies in the lower and top stories; in AH-2 variation occurs in the lower stories, and in TO-9, b_x decreases in stories above story 9.

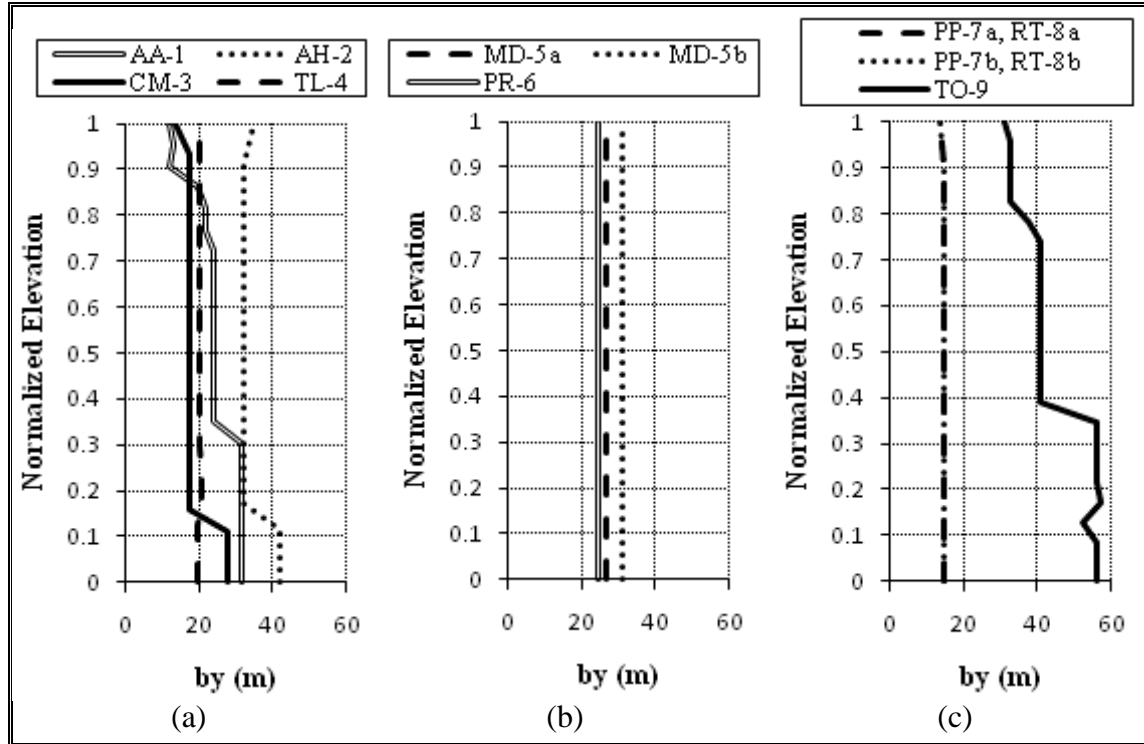


Figure 3-2: Width in the Y-direction versus normalized height, b_y

In TL-4, MD-5a, MD-5b, PR-6, PP-7a, PP-7b, RT-8a and RT-8b, b_y is approximately constant in height, while in AH-2 and CM-3 varies in the lower and upper stories. Plan widths decrease in AA-1 above story 6 and for TO-9 above story 7. For all these structures, widths ranges approximately from 15m to 40m and from 15m to 55m in the X- and Y-directions, respectively.

Shown in Figure 3-3 is the plan aspect ratio b_1/b_2 versus normalized height. This property was computed nominally from the structural drawings, where b_1 and b_2 are the maximum and minimum widths of the floor in each story. This plan aspect ratio remains approximately constant for buildings TL-4, MD-5a, MD-5b, PR-6, PP-7a, PP-7b, RT-8a

and RT-8b, while in AA-1, AH-2, and CM-3 it varies at the lower and upper stories. In TO-9 the aspect ratio varies in height, reaching its minimum value at the 7th and 8th stories; aspect ratios are in the range of 1 to 2.5.

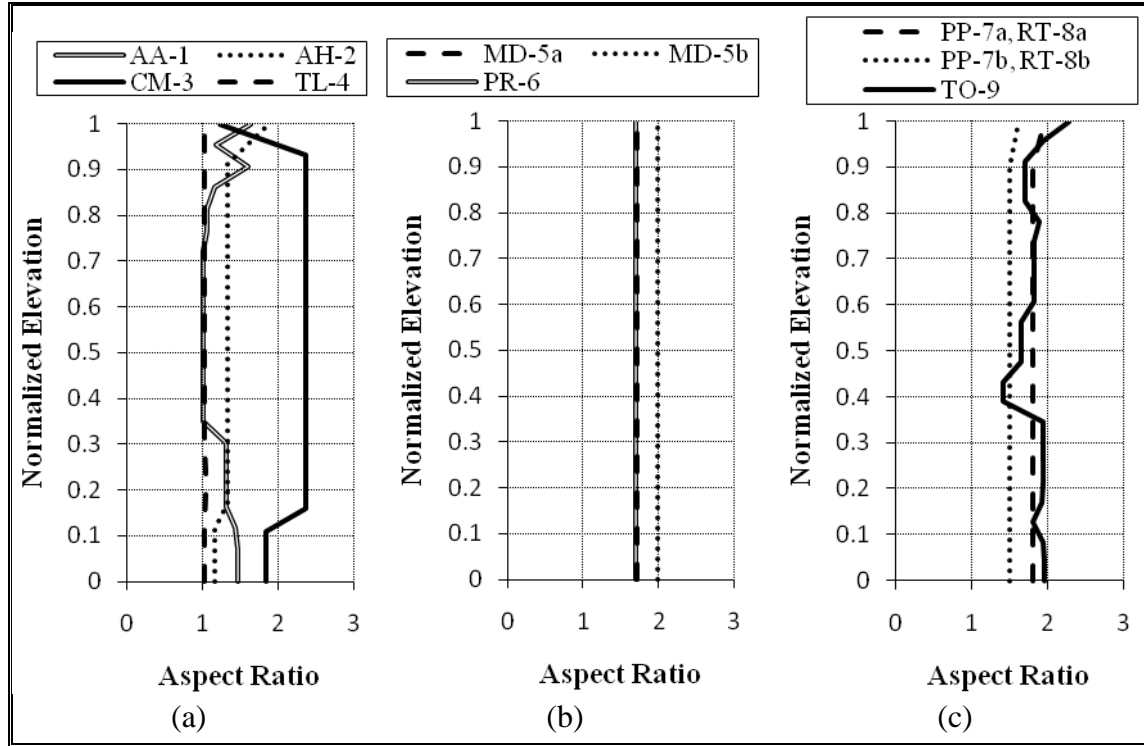


Figure 3-3: Aspect ratio versus normalized height, b_1/b_2

Figure 3-4 shows the slenderness ratio h/d versus normalized building height. This parameter was nominally obtained from structural drawings by taking the building height h over the minimum plan dimension, $d = \min(b_x, b_y)$. The slenderness ratio remains approximately constant for buildings TL-4, MD-5a, MD-5b, PR-6, PP-7a, PP-7b, RT-8a and RT-8b. For buildings AA-1 and CM-3, this ratio varies in the lower and upper stories, while for AH-2 it varies at the lower stories due to the additional parking space. In TO-9, the slenderness ratio is approximately constant up to the 8th story, and above that it increases considerably. These ratios are in the range from approximately 1.3 to 6.

The variation of the story surface A versus normalized height is shown in Figure 3-5. Surface areas remain approximately constant for buildings TL-4, MD-5a, MD-5b, PR-6, PP-7a, PP-7b, RT-8a and RT-8b. Building AA-1 shows a considerable reduction of surface in stories 6, 15 and 18. Building CM-3 shows surface variation in the lower and upper stories; AH-2 shows surfaces that are much larger in the lower stories with a minimum in the first story. In building TO-9, the surface area decreases monotonically in height from 1500m^2 to 350m^2 .

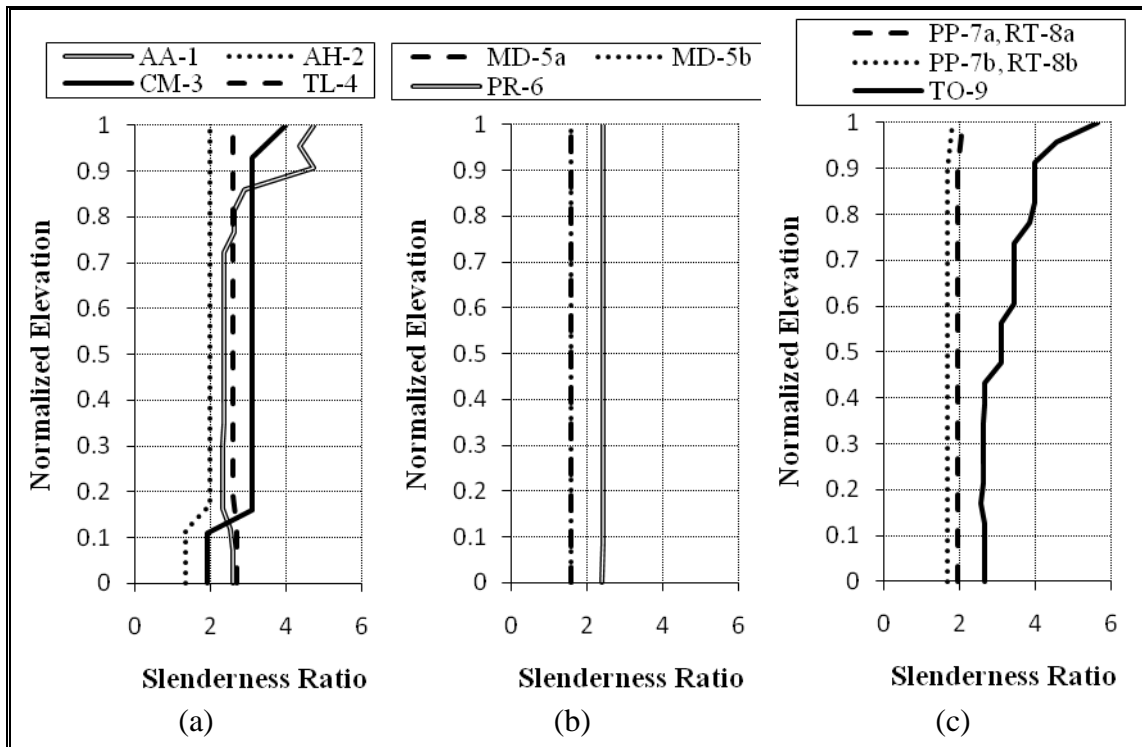


Figure 3-4: Slenderness ratio versus normalized height, h/d

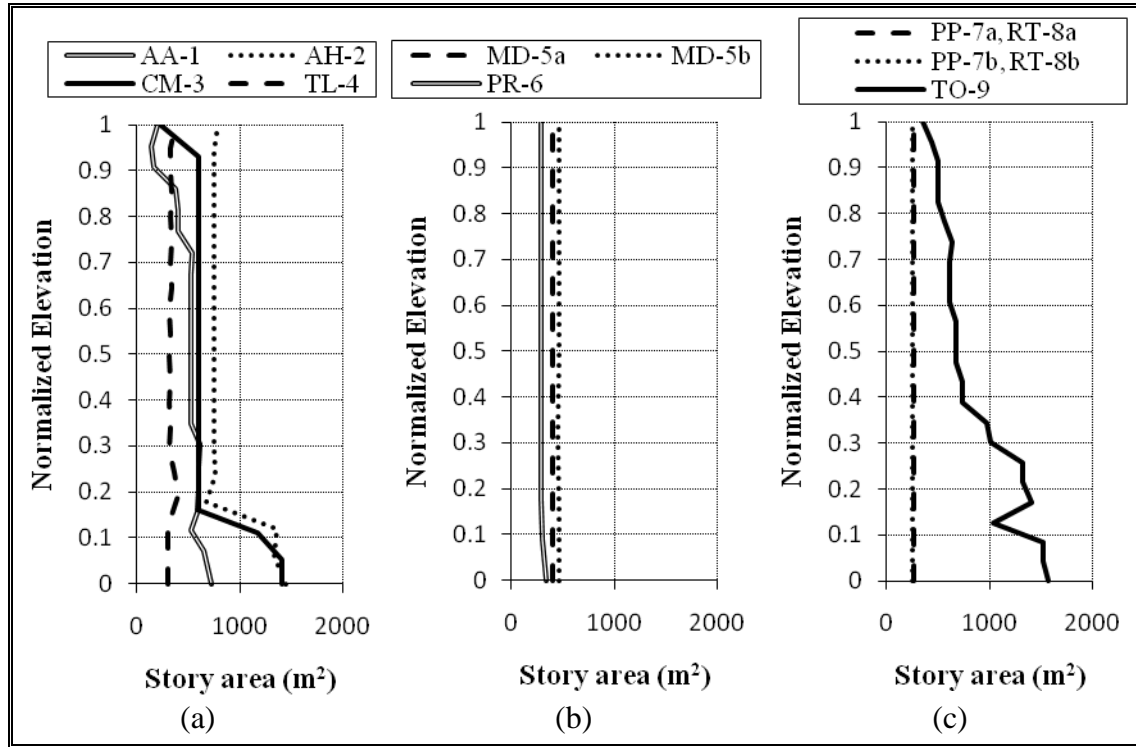


Figure 3-5: Story area versus normalized height, A

The variation of the nominal average thickness of walls in each story \bar{e} is presented as a function of normalized height in Figure 3-6. This parameter was computed by taking all shear wall elements present in the structural drawings, and constructing a weighted average thickness defined by:

$$\bar{e} = \frac{\sum_{i=1}^m e_i l_i}{\sum_{i=1}^m l_i} \quad (3.1)$$

Where e_i is the thickness of the i -th wall, l_i is the wall length, and m is the number of walls per story.

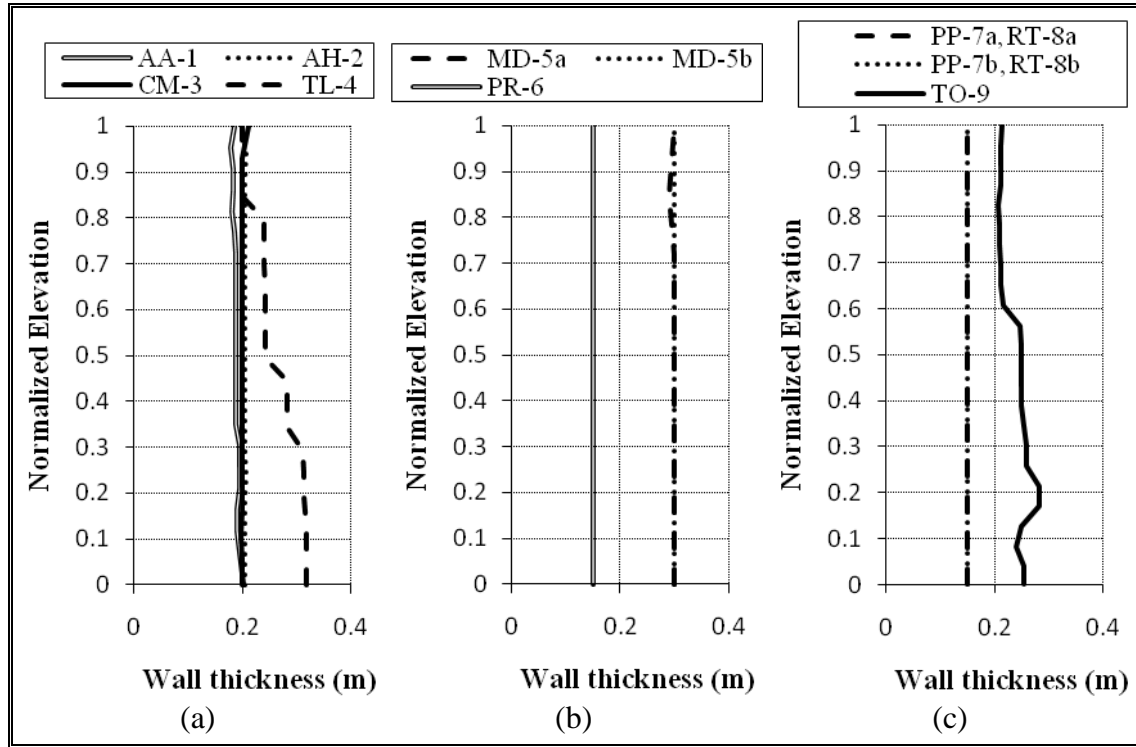


Figure 3-6: Average wall thickness versus normalized height, \bar{e}

It is apparent that the nominal average wall thickness remains approximately constant in buildings AA-1, AH-2, CM-3, MD-5a, MD-5b, PR-6, PP-7a, PP-7b, RT-8a and RT-8b. In building TL-4 there exist important reductions in wall thickness for the 4th, 7th, and 14th stories. For the TO-9 building, thickness reductions occur in stories -1, 4 and 12. As it is shown in Figure 3-6, average wall thicknesses are in the range of 0.15m to 0.30m. Shown in Figures 3-7 and 3-8 are the nominal X- and Y-direction densities of shear wall area ρ_x and ρ_y versus normalized height. This parameter was computed from the structural drawings and it is shown in the figures as a percentage of total story area. Also shown in Figure 3-9 is the total density of vertical elements ρ_z (shear walls and columns in both directions) versus normalized height.

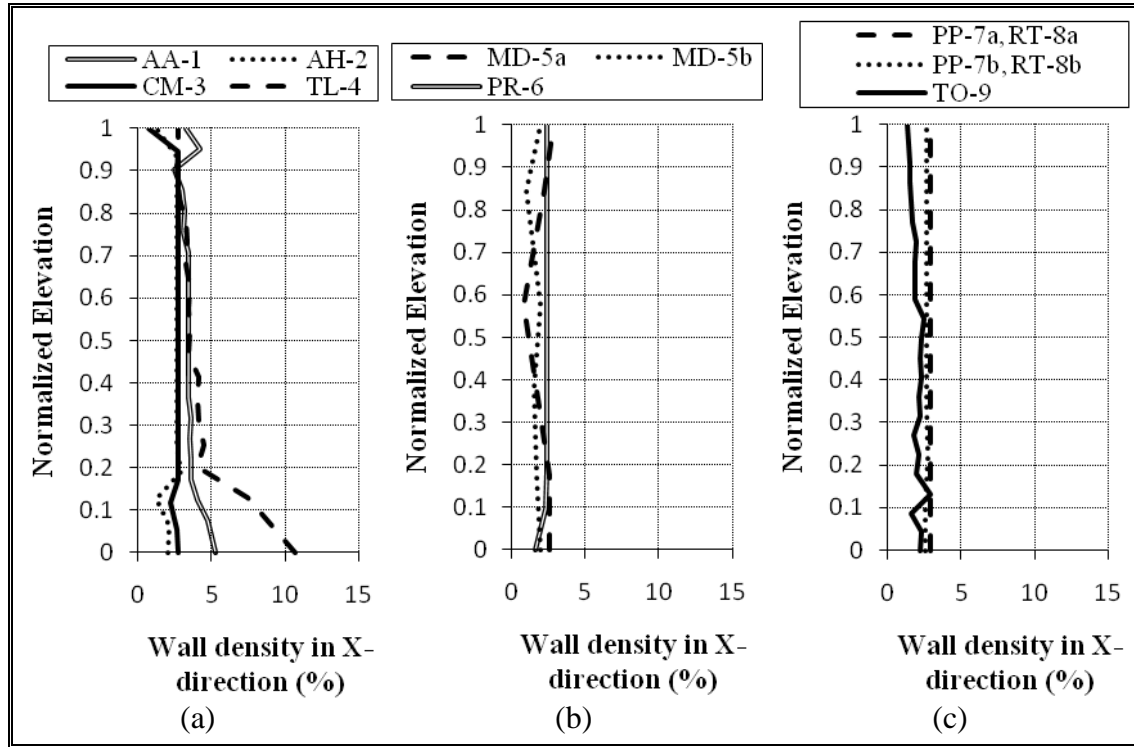


Figure 3-7: X-direction shear wall density versus normalized height, ρ_x

X-direction shear-wall densities remain approximately constant in buildings AH-2, PR-6, PP-7a, PP-7b, RT-8a and RT-8b. Also, an increase in wall density is shown in the 2nd story of building CM-3. The larger densities shown in the lower stories of TL-4 are due to the larger thickness of the walls. Building AA-1 shows higher density in upper stories with little variations in the 1st, 6th, and 15th stories. Building MD-5 shows larger variations in density due to fact that this building is a frame structure and has a double height story. Wall densities in the X-direction range from 1.5% to 3.5%, except for the high densities of TL-4 near the base.

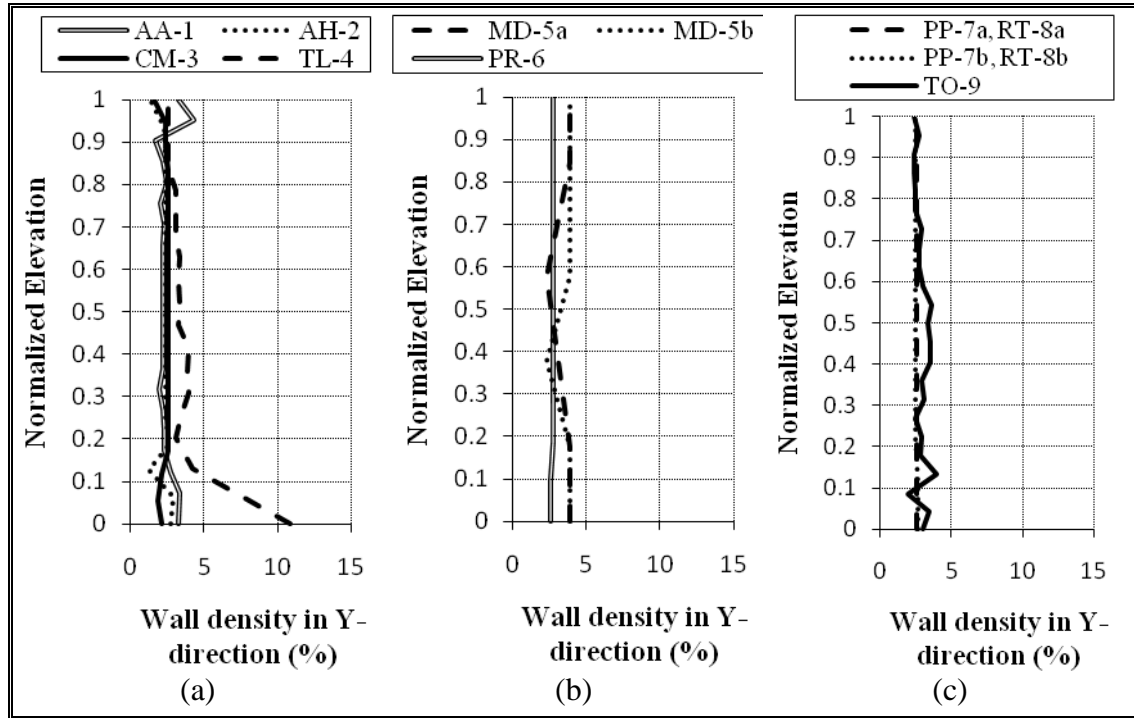


Figure 3-8: Y-direction shear wall density versus normalized height, ρ_y

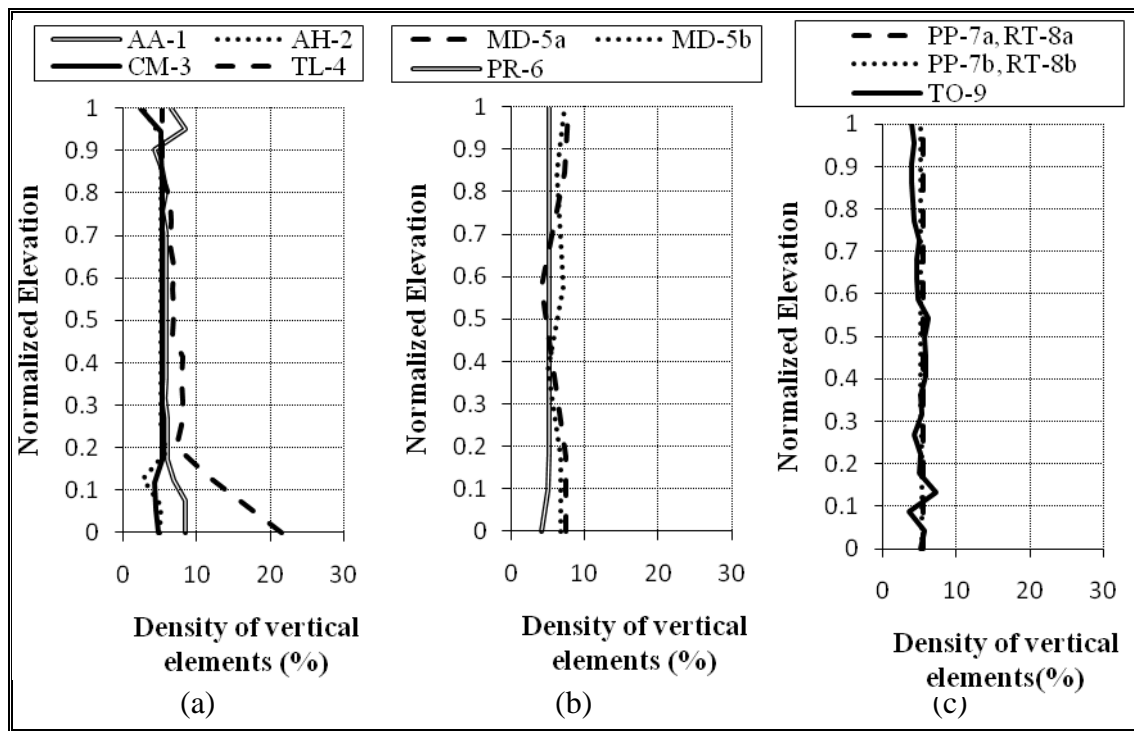


Figure 3-9: Density of vertical elements versus normalized height, ρ_z

Analogously, the Y-direction shear wall densities remain approximately constant for buildings AH-2, PR-6, PP-7a, PP-7b, RT-8a and RT-8b. Some of the observations are: building CM-3 shows an increase in density in story 2; TL-4 has higher densities in lower stories due to the larger thickness of the walls; AA-1 has higher densities in upper stories; and multiple variations are observed in building TO-9. Please notice that the Y-direction shear wall density in TO-9 is considerably larger than the one in the X-direction. Values of Y-direction shear wall densities range typically from 2% to 4%.

The total density of vertical elements remains approximately constant in height for buildings AH-2, PR-6, PP-7a, PP-7b, RT-8a and RT-8b. Variations are shown again in building MD-5 because of its moment resisting frame structural configuration and double height story. For building CM-3 an increase in density is apparent in the 1st story; TL-4 has higher densities in lower stories; AA-1 has higher densities in upper stories showing a slight variation in the 2nd, 10th, and 15th stories; and TO-9 shows continuous variations. Total vertical element densities vary in these buildings typically in the range of 4% to 7%. Values for all these building parameters are summarized in Table 3-1, where the bar represents mean values for each building.

Table 3-1: Summary of average building parameters

ID	\bar{b}_x (m)	\bar{b}_y (m)	\bar{b}_1 / \bar{b}_2	\bar{h} / \bar{d}	\bar{A} (m ²)	$\bar{\rho}_x$ (%)	$\bar{\rho}_y$ (%)	$\bar{\rho}_z$ (%)	\bar{e} (m)
AA-1	22.7	24.3	1.20	2.73	488	3.57	2.48	6.15	0.19
AH-2	26.1	33.9	1.34	1.87	848	2.44	2.34	4.88	0.20
CM-3	41.2	18.7	2.23	2.95	691	2.57	2.39	4.96	0.20
TL-4	19.9	19.9	1.03	2.61	332	4.09	3.68	7.77	0.27
MD-5a	15.53	26.54	1.71	1.59	408	2.21	3.61	6.82	0.30
MD-5b	15.53	30.89	1.99	1.59	465	1.69	3.66	6.52	0.30
PR-6	14.2	24.2	1.70	2.42	294	2.32	2.73	5.05	0.15
PP-7a	26.3	14.4	1.83	1.94	267	2.88	2.59	5.47	0.15
PP-7b	21.8	14.4	1.52	1.69	255	2.67	2.51	5.18	0.15
RT-8a	26.3	14.4	1.83	1.94	267	2.88	2.59	5.47	0.15
RT-8b	21.8	14.4	1.52	1.69	255	2.67	2.51	5.18	0.15
TO-9	24.5	44.5	1.83	3.25	855	1.95	2.91	4.90	0.24

Mean values of the aspect ratio b_1/b_2 are all less than 2 with the exception of CM-3, and the maximum mean slenderness ratio h/d is 3.25 and is obtained for TO-9. While the mean density of vertical elements $\overline{\rho_z}$ ranges from 4.88% to 7.77%, the shear wall density ranges from 1.69% to 4.09% in the X-direction, and from 2.34% to 3.68% in the Y-direction. The mean wall thickness \overline{e} ranges from 0.15m to 0.30m.

4 OTHER INDICES

Some indices (Building Seismic Safety Council, 2003; IS 1893 part 1, 2002; National Earthquake Hazards Reduction Program, 2009; Sarkar et al, 2010; Structural Engineers Association of California, 1999) for plan irregularities for the nine structures were computed and are presented in Table 4-1.

Table 4-1: Plan irregularities indices

ID	$\left \frac{A}{B} \right _{\max}$	$\left \frac{A_b}{A} \right _{\max}$	Maximum out of plane discontinuity in X-direction	Maximum out of plane discontinuity in Y-direction
AA-1	0.58	0.21	0	0.47
AH-2	0.28	0.08	0	0
CM-3	0.14	0.17	0	0
TL-4	0.16	0.18	0	0
MD-5a	0	0	0	0
MD-5b	0.25	0.04	0.81	0
PR-6	0.33	0.04	0.18	0
PP-7a	0.35	0.02	0	0
PP-7b	0.41	0.04	0	0
RT-8a	0.35	0.02	0	0
RT-8b	0.41	0.04	0	0
TO-9	0.72	0.14	0	0.50

The index $\left| A/B \right|_{\max}$ measures the re-entrant corners of the building and is calculated as the projection of the structure beyond a re-entrant corner divided by the plan dimension of the structure in the given direction. The maximum values of this index among all stories are presented in Table 4-1. It can be observed that all but two of the buildings has a maximum index greater than 15%, which classifies these buildings as irregular (Building Seismic Safety Council, 2003). Building TO-9 has the maximum value of 0.72

due to a re-entrant corner in the Y-direction of the 5th and 6th floors, and building AA-1 has a maximum index of 0.58 in the X-direction of the 2nd through 5th floors.

Additionally the index $|A_b / A|_{\max}$ measures the diaphragm discontinuity and is calculated as the cutout or open areas of the diaphragm divided by the gross enclosed diaphragm area. Table 4-1 presents the maximum value among all stories. None of the buildings present a maximum value above 50%, so none of them can be considered irregular by this index (Building Seismic Safety Council, 2003). Building AA-1 has the maximum value of 0.21 in the 1st floor, followed by TL-4 with a value of 0.18 in the subterranean level.

The last two indices shown in Table 4-1 refer to out of plane discontinuities in the X- and Y-directions of the vertical force-resisting elements. The basic index is defined as the dimension of the maximum out of plane discontinuity of the walls divided by the dimension of the wall immediately above the offset. This index was calculated for each floor plan of the buildings and its maximum value among all stories is presented in Table 4-1. Of the group of 9 buildings, only 4 present this type of offset in one direction. Notice that building MD-5b has a maximum out of plane discontinuity in the X-direction of 0.81 because of a wall offset present in the 3rd floor; building TO-9 has a maximum out of plane discontinuity in the Y-direction of 0.5 in the 4th floor.

Table 4-2 summarizes vertical irregularities for the eight buildings. The mass irregularity index $|M_i / M_{i+1}|_{\max}$ compares the mass of adjacent floors. This index was calculated for each floor of the buildings and the distribution in normalized elevation is shown in Figure 4-1, with the maximum value listed in Table 4-2. Buildings AA-1, CM-3, TL-4 and MD-5a have a maximum mass irregularity index above 1.5, being classified as irregular buildings (Building Seismic Safety Council, 2003). In particular, building TL-4 has a maximum index of 2.75 at the basement level mainly due to the larger wall density observed in this floor (Figure 3-9a). Building AA-1 has a maximum index of 2.29 in the 17th floor, meaning that the mass of the 17th floor is more than twice the mass of the 18th floor, which coincides with a decrease of the plan surface at the 18th floor (Figure 3-5a). Building CM-3 has a maximum index of 2.2 in the first floor mainly due

to the larger wall density in the 2nd story (Figures 3-9a). The rest of the indices shown in Table 4-2 refer to vertical geometric irregularities. It is important to note that these indices were calculated for all lateral force-resisting elevations of the buildings, and the maximum for each building summarized in Table 4-2.

The index $|A/L|_{\max}$ compares the maximum and minimum horizontal dimension of the lateral force-resisting system (IS 1893 part 1, 2002). Please note that 10 of the structures have a maximum value above 0.25, being classified as irregular buildings. Particularly buildings AA-1 and TO-9 have a maximum index value of 0.95, which occurs in highly irregular lateral force-resisting planes.

Table 4-2: Vertical irregularities indices

ID	$\left \frac{M_i}{M_{i+1}}\right _{\max}$	$\left \frac{A}{L}\right _{\max}$	$\left \frac{L_i}{L_{i+1}}\right _{\max}$	ϕ_s	Maximum in plane discontinuity in X direction	Maximum in plane discontinuity in Y direction
AA-1	2.29	0.95	17.0	2.5	9.70	7.00
AH-2	1.42	0.94	4.43	1.37	1.54	0.49
CM-3	2.20	0.90	8.52	1.47	2.60	1.00
TL-4	2.75	0.81	5.14	1.30	0	0
MD-5a	1.74	0.31	1.44	1.84	0	0
MD-5b	1.38	0.46	1.57	1.92	0	0
PR-6	1.10	0.90	7.28	1.59	0	0
PP-7a	1.25	0.55	2.20	1.24	0	0
PP-7b	1.21	0.01	1.01	1.11	0	0
RT-8a	1.25	0.55	2.20	1.24	0	0
RT-8b	1.21	0.01	1.01	1.11	0	0
TO-9	1.37	0.95	20.1	2.71	1.60	1.00

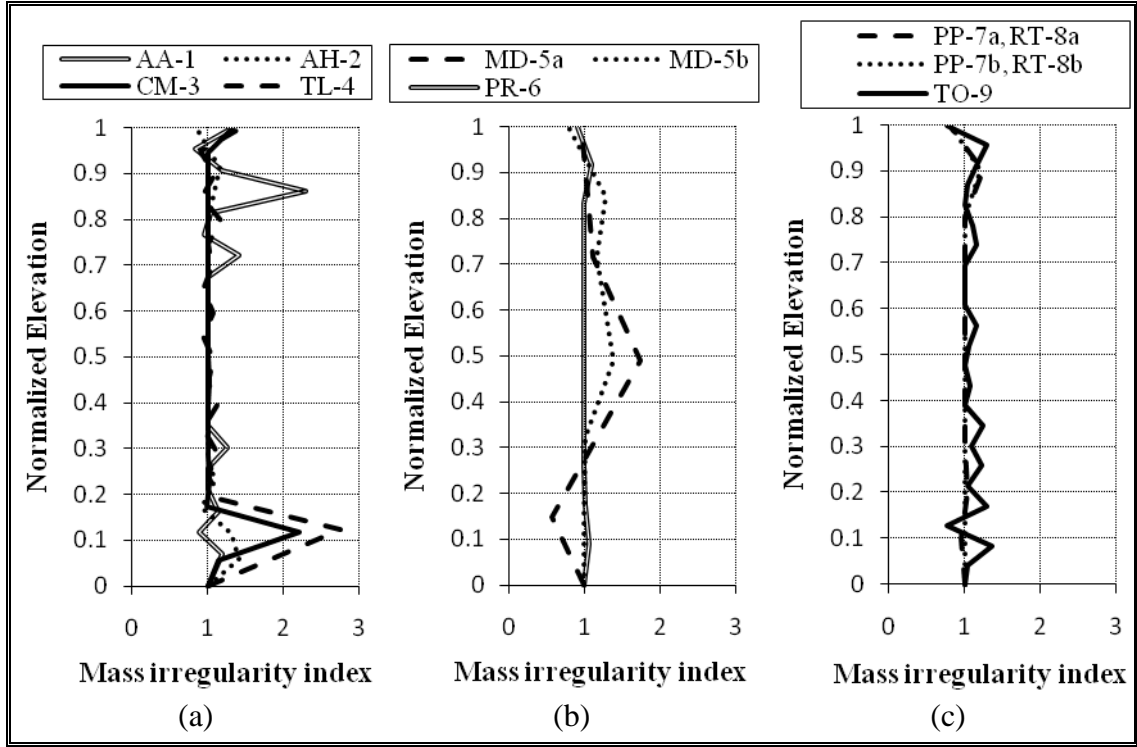


Figure 4-1: Mass irregularity index versus normalized height, $|M_i / M_{i+1}|$

The index $|L_i / L_{i+1}|_{\max}$ compares the horizontal dimension of the lateral force-resisting system of adjacent stories. All but two of the buildings have values exceeding 1.3, classifying them as vertically irregular buildings (National Earthquake Hazards Reduction Program, 2009), with highest values again for buildings AA-1 and TO-9.

As a measure of irregularity throughout the height of the building, the following index is presented:

$$\phi_s = \frac{1}{n_s - 1} \sum_{i=1}^{n_s-1} \frac{L_i}{L_{i+1}} \quad (4.1)$$

Where n_s is the number of stories (Sarkar et al., 2010). Buildings AA-1 and TO-9 have the highest indices, and represents how irregular are the force-resisting planes throughout the height of these structures.

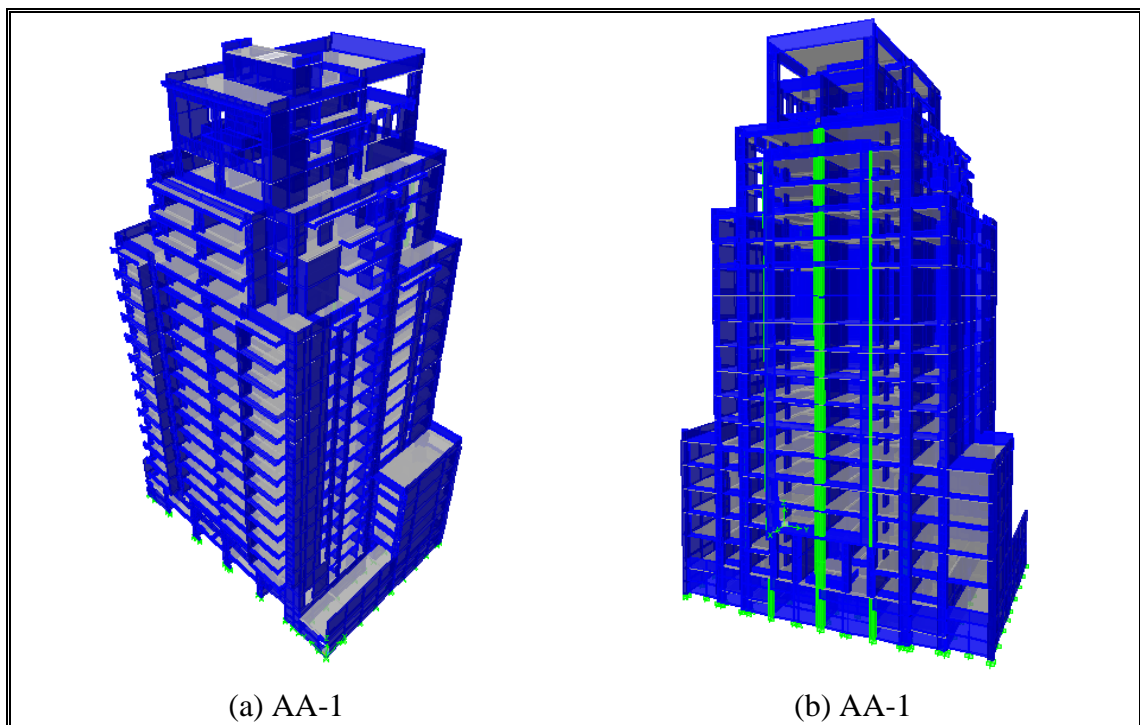
The last 2 indices shown in Table 4-2 refer to in-plane discontinuities in vertical lateral force-resisting planes. This index is defined as the ratio between the dimension of the in-

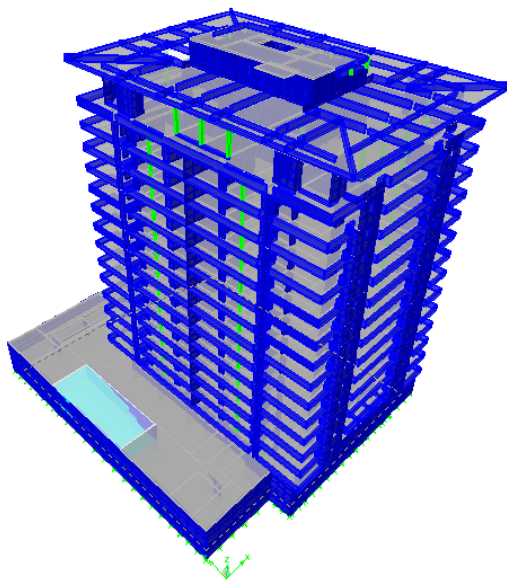
plane offset and the length of the element immediately below the offset (Building Seismic Safety Council, 2003). The building with maximum in-plane discontinuity is AA-1 with values of 9.7 and 7 in each direction. Again, buildings AA-1 and TO-9 are consistently irregular in height.

5 DYNAMIC BUILDING PROPERTIES

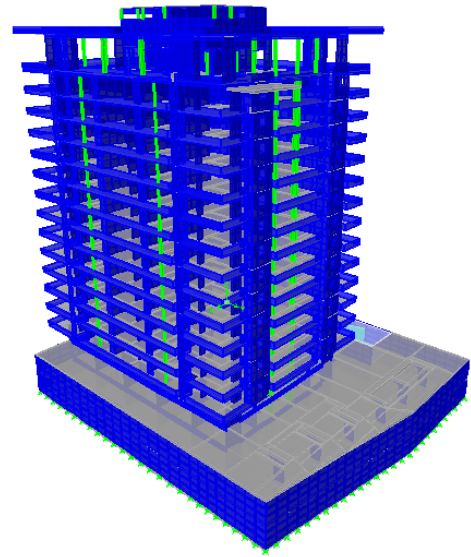
The building properties presented in the previous section try to characterize the geometry of the buildings considered. This section instead provides information on the dynamic properties of the nine buildings.

Three-dimensional linear models of each of the study buildings were developed using the software ETABS (2011). Figure 5-1 shows the linear models for each structure. Building mass and structural elements were based on building drawings believed to represent the as-built conditions. Material properties were tested in laboratory. Wall flexural and shearing stiffnesses were represented using gross sections. Diaphragms were modeled rigid in plane and completely flexible out of plane. Foundations were fixed except for buildings AH-2 and TO-9 where full soil-foundation-structure interaction was modeled. Seismic weight has been considered as indicated by the National Seismic Code (NCh 433 Of.96, 1996), i.e., a value of dead load plus 25% of the live load.

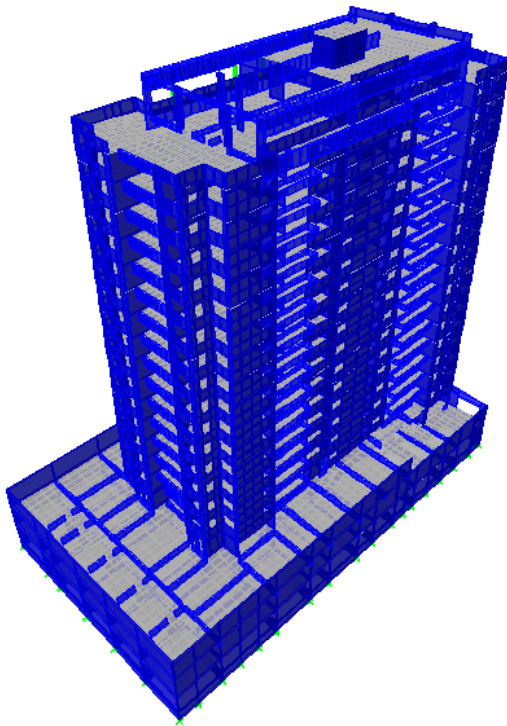




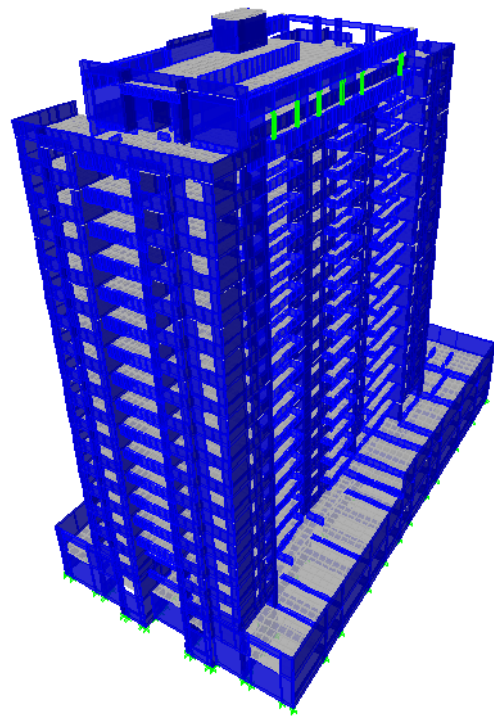
(c) AH-2



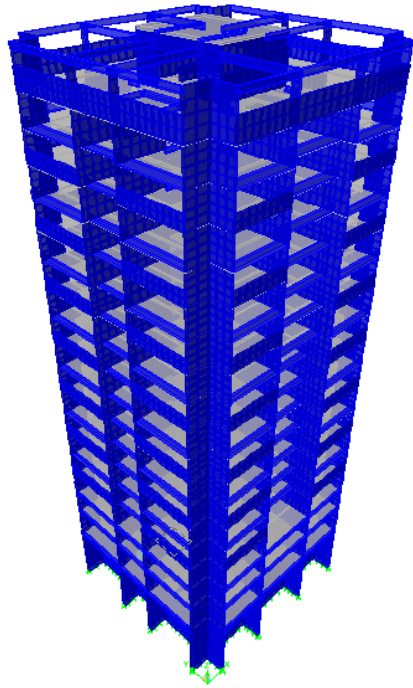
(d) AH-2



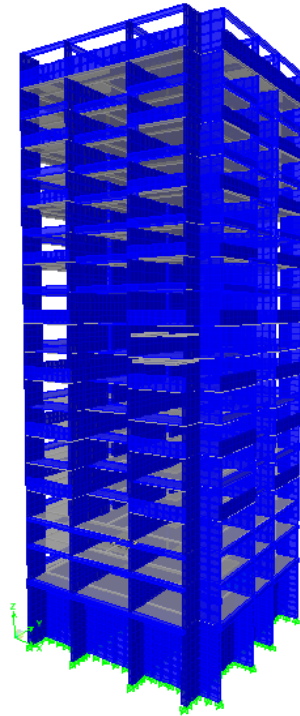
(e) CM-3



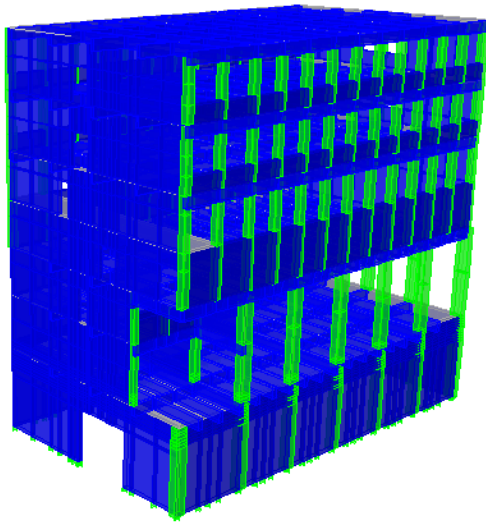
(f) CM-3



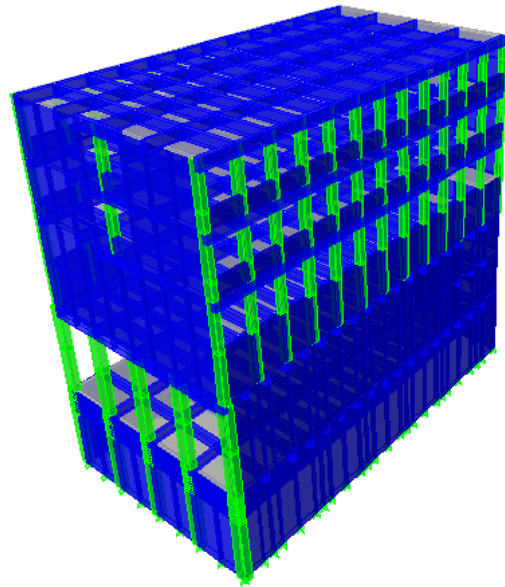
(g) TL-4



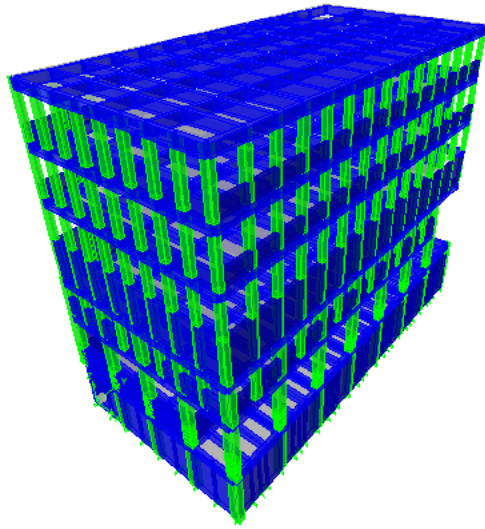
(h) TL-4



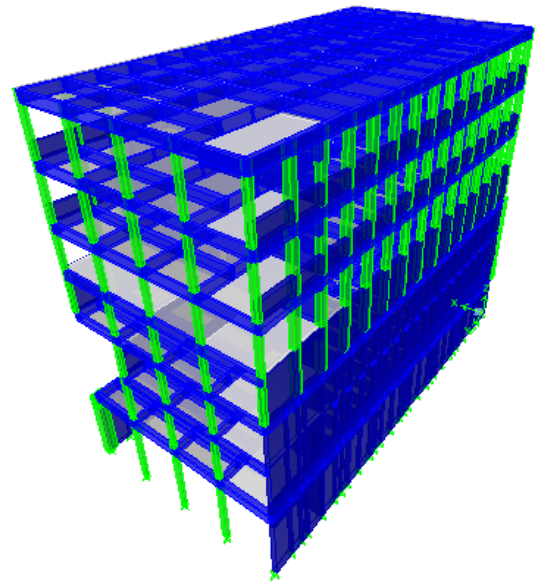
(i) MD-5a



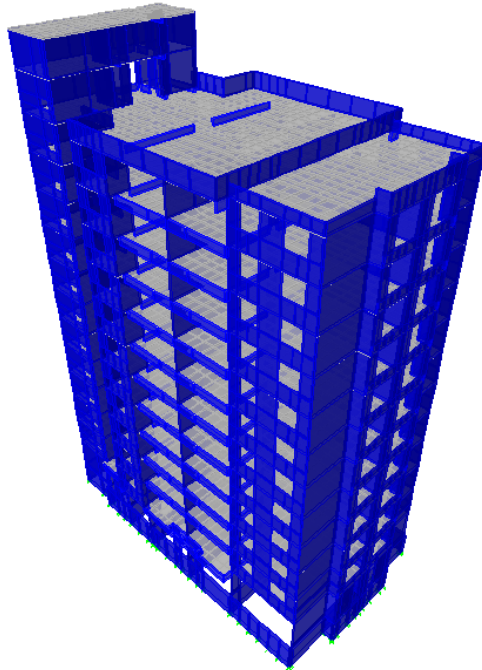
(j) MD-5a



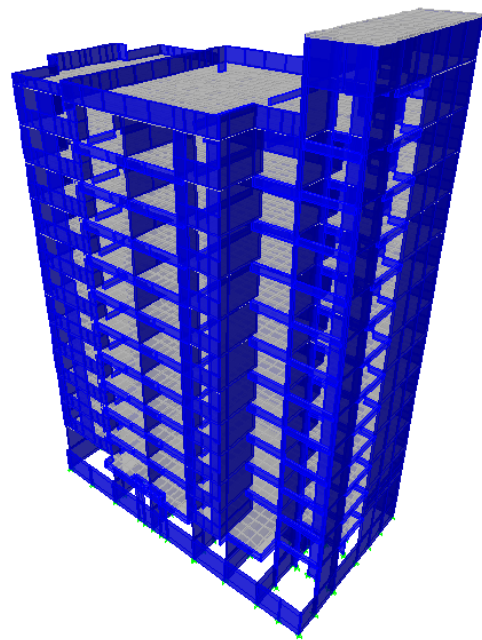
(k) MD-5b



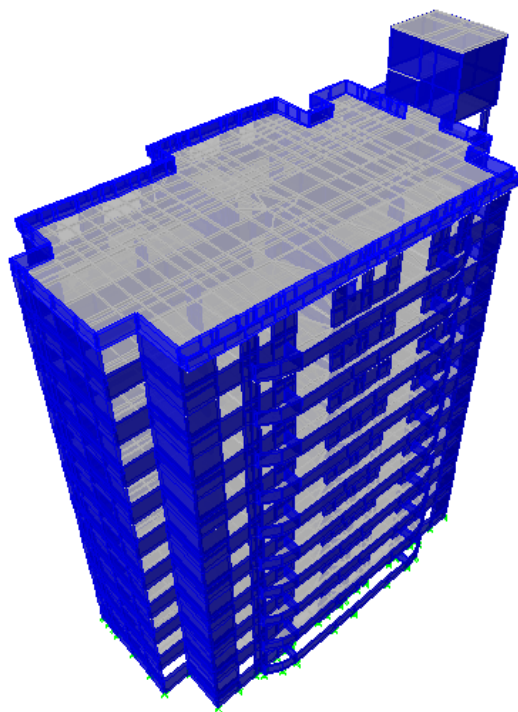
(l) MD-5b



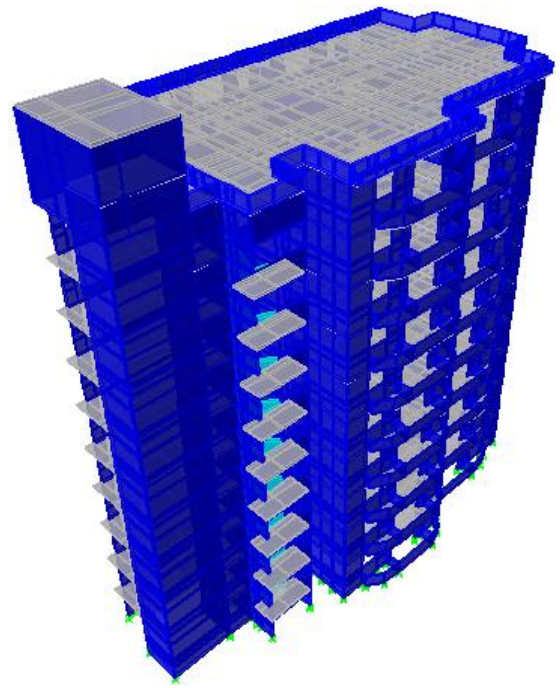
(m) PR-6



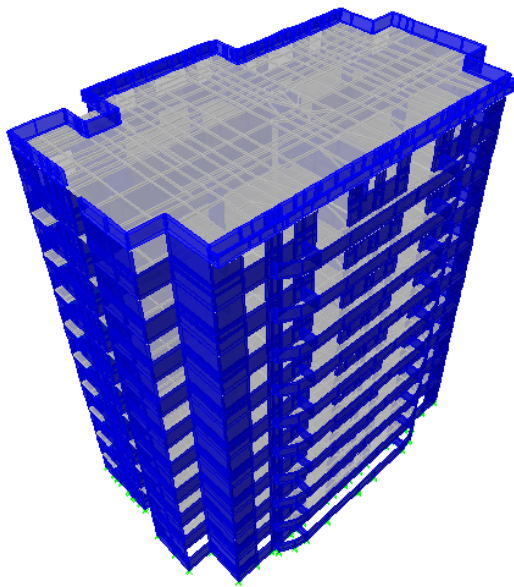
(n) PR-6



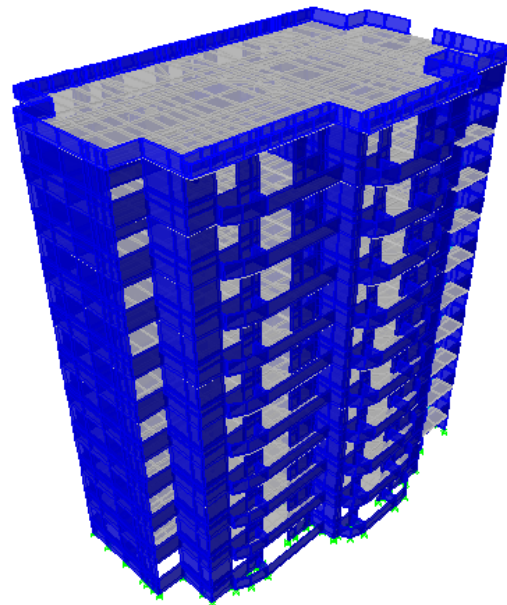
(o) PP-7a, RT-8a



(p) PP-7a, RT-8a



(q) PP-7b, RT-8b



(r) PP-7b, RT-8b

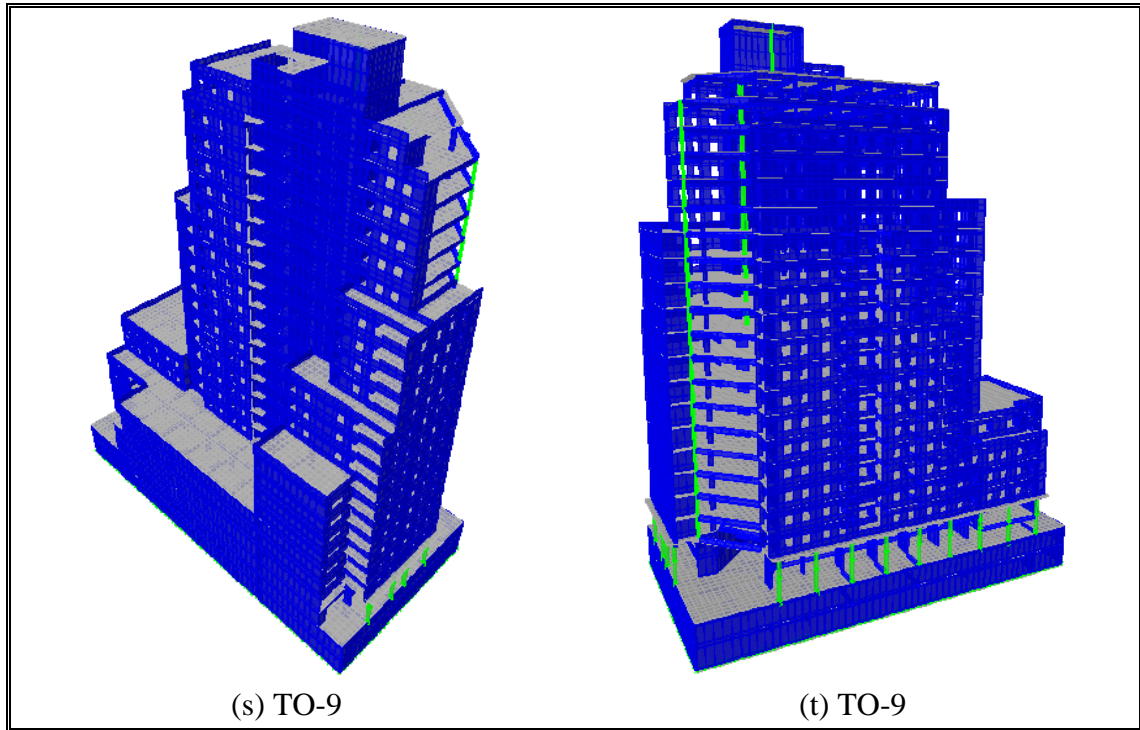


Figure 5-1: Linear 3-D models for analyzed buildings

Table 5-1 lists the first three calculated vibration periods in the X-, Y-, and Θ -directions, modal masses in these directions, and the total seismic weight. Note that modal masses are larger than 40% with the exception of building MD-5; however, torsional mass in TO-9 is substantially smaller than for other buildings. It is shown that fundamental vibration periods in X-direction range between 0.22s for PP-7a and RT-7a to 0.93s for TO-9; vibration periods in the Y-direction range from 0.31s in MD-5b and 0.80s in CM-3; and rotational periods range between 0.19s in MD-5b to 0.88s in TL-4. The seismic weight of the buildings varies approximately between 2000tonf to 18000tonf. The index period estimate $T = n_s/20$ gives period estimate longer than the fundamental period calculated by ETABS, except for building MD-5, which has a frame type configuration.

Table 5-1: Dynamic properties of analyzed buildings

ID	T_x (s)	T_y (s)	T_Θ (s)	X-direction modal mass (%)	Y-direction modal mass (%)	Θ -direction modal mass (%)	Seismic weight (ton)	$n_s/20$ (s)
AA-1	0.62	0.71	0.58	55.6	52.9	45.3	9850	1.0
AH-2	0.70	0.58	0.78	61.9	63.6	44.2	11900	0.75
CM-3	0.56	0.80	0.68	45.4	57.1	36.9	12300	0.90
TL-4	0.61	0.77	0.88	62.1	59.8	65.2	7510	0.85
MD-5a	0.34	0.50	0.22	27.1	35.5	30.5	3300	0.20
MD-5b	0.39	0.31	0.19	34.3	34.9	43.1	3650	0.25
PR-6	0.50	0.33	0.39	60.3	70.0	63.4	2940	0.60
PP-7a	0.22	0.36	0.27	70.5	65.9	68.6	4000	0.50
PP-7b	0.23	0.34	0.24	71.6	69.2	71.3	1970	0.50
RT-8a	0.22	0.36	0.27	70.5	65.9	68.6	4000	0.50
RT-8b	0.23	0.34	0.24	71.6	69.2	71.3	1970	0.50
TO-9	0.93	0.53	0.28	48.3	49.1	22.1	17900	1.1

Another dynamic index (Guendelman et al, 1997) for characterizing shear wall buildings is the ratio between the total height of the structure and the fundamental period, H/T . Table 5-2 lists the values for the study buildings. From the structural performance observed for shear wall buildings in past Chilean earthquakes (Moroni, 2011), $H/T > 70\text{m/s}$ corresponds to no structural damage, $50\text{-}70\text{m/s}$ to non-structural damage, $40\text{-}50\text{m/s}$ to light structural damage, and $30\text{-}40\text{m/s}$ to moderate structural damage. H/T ratios for the study buildings are 60m/s and higher, suggesting little damage would be expected. As discussed in the next sections, damage was much more severe.

Table 5-2: H/T ratios of analyzed buildings

ID	$\frac{H}{T_x}$ (m/s)	$\frac{H}{T_y}$ (m/s)	$\frac{H}{T_\theta}$ (m/s)
AA-1	0.62	0.71	0.58
AH-2	0.70	0.58	0.78
CM-3	0.56	0.80	0.68
TL-4	0.61	0.77	0.88
MD-5a	0.34	0.50	0.22
MD-5b	0.39	0.31	0.19
PR-6	0.50	0.33	0.39
PP-7a	0.22	0.36	0.27
PP-7b	0.23	0.34	0.24
RT-8a	0.22	0.36	0.27
RT-8b	0.23	0.34	0.24
TO-9	0.93	0.53	0.28

6 CHARACTERISTIC DAMAGE

Presented in this section is the characteristic damage observed of the study buildings. Several of the buildings have large footprints, with damage extending along many framing lines and over several stories. Only partial damage summaries are presented here. For more detailed information, see following sections.

6.1 Building AA-1

Building AA-1 had significant vertical irregularity at several levels (Figure 2-4b), but wall damage concentrated in the lower two stories. Wall setbacks at the lower level may have contributed to flexure-axial crushing failures beneath the setback, but the building also sustained shear failure (passing through vertical wall piers separated by openings) and crushing failure at multiple locations, in both EW and NS oriented walls in the North half of the building (Figure 2-4a). Building subsidence led to severe damage to upper level framing system as well. Figures 6-1 shows examples of wall damage.



Figure 6-1: Examples of wall damage in building AA-1

6.2 Building AH-2

This building sustained wall crushing and global wall buckling in the first story and in subterranean levels of EW walls toward the North end of the building (Figure 2-4c). Figure 6-2a and 6-2b show characteristic wall damage. The damage resulted in building subsidence especially toward the North-west corner of the building, resulting in sloping floors in several units.



Figure 6-2: Examples of wall damage in building AH-2

6.3 Building CM-3

CM-3 sustained failures in multiple EW-oriented walls in the first two elevated stories and the subterranean levels. Apparent failures involved shear failure through multiple piers separated by openings (a), compression or flexural compression failures (b), and shearing failures of horizontal wall segments at the bottom of a series of vertically aligned door openings (c). These cases are shown in Figure 6-3.

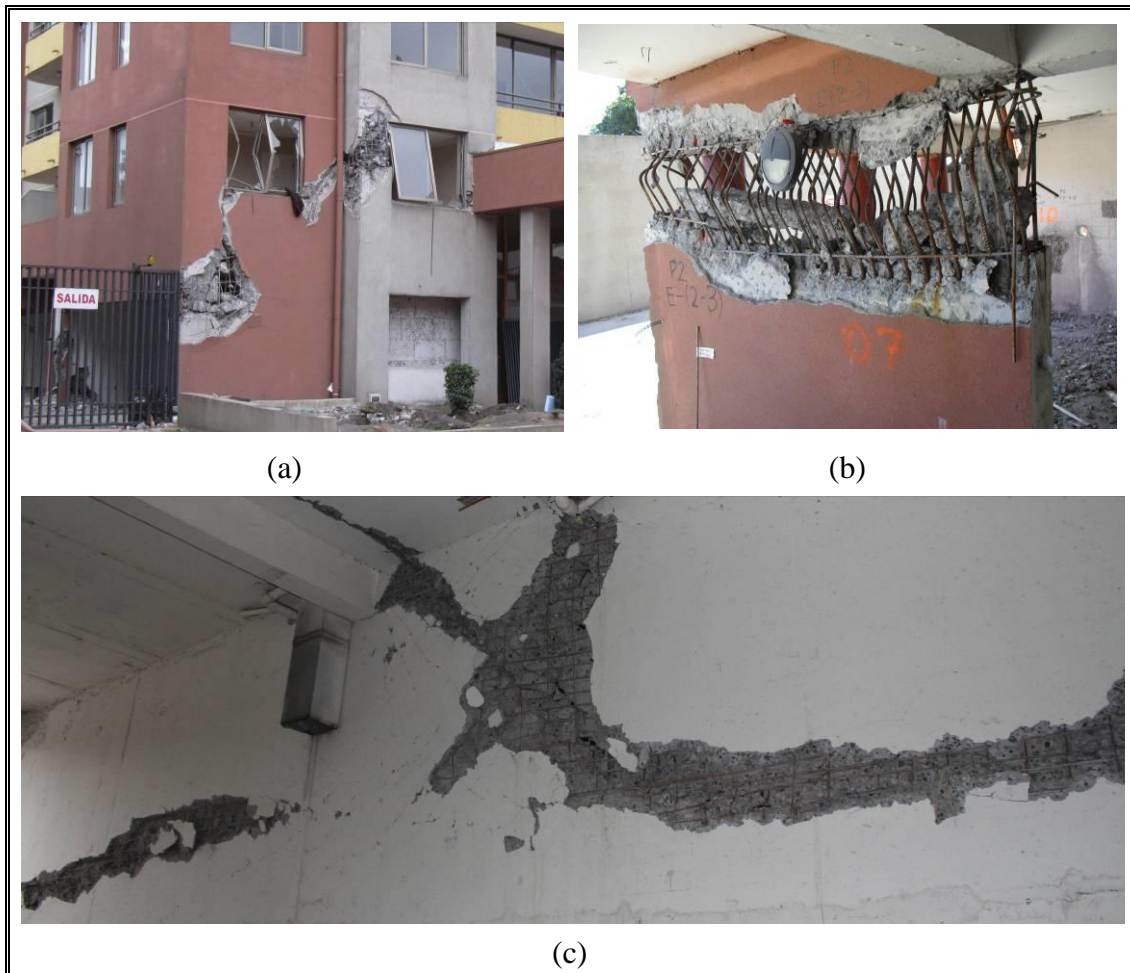


Figure 6-3: Examples of wall damage in building CM-3

6.4 Building TL-4

Shear walls sustained combined shear and flexure/axial failures in the lower story walls oriented in the EW direction (framing lines 2-5, Figure 2-4g). Failures also occurred over the building height due to flexural coupling of spandrels framing out-of-plane into the edges of L-walls at building corners. Figure 6-4 shows typical wall damage in lower stories, illustrating diagonally oriented web reinforcement.



Figure 6-4: Examples of wall damage in building TL-4

6.5 Building MD-5

Building MD-5 had significant damage in the columns of the 3rd story (double height level). While building MD-5a showed total hinge formation, building MD-5b showed partial hinge formation (in framing lines A and I, Figure 2-4i). Top stories in MD-5a moved to the West regarding its original configuration. Figure 6-5 shows typical column damage, illustrating smooth bars and corrosion.



Figure 6-5: Examples of column damage in building MD-5

6.6 Building PR-6

This building comprised two similarly configured wings separated by a construction joint (Figure 2-4k). The wing along framing lines A-M, with longitudinal axis oriented approximately EW, was relatively undamaged. The wing along lines N-W sustained severe wall flexural and shear damage in the EW (transverse) walls, with heaved soils around the foundation suggesting rocking response. Stories one and two were the most damaged ones. Figure 6-6a shows characteristics damage to transverse walls along lines O and Q while Figure 6-6b shows characteristic damage along lines V and W.



Figure 6-6: Examples of wall damage in building PR-6

6.7 Buildings PP-7 and RT-8

These similar, adjacent buildings sustained similar damage, concentrated in first-story EW-oriented walls (Figure 2-4m). Figure 6-7 shows damage characteristic of the most severe damage for these buildings. Building RT-8 was clearly more damaged than PP-7.



Figure 6-7: Examples of wall damage in buildings (a), (b) PP-7; (c), (d) RT-8

6.8 Building TO-9

This building was somewhat unique among the buildings for its multiple vertical and plan irregularities. Floor masses were eccentric to the core walls over many stories, with framing setbacks especially along the eastern portion of the building, possibly leading to accentuated torsional response. Damage was relatively light in the lower twelve stories. Partial story collapses occurred at each of levels 12, 16, and 20, each story corresponding to a significant vertical or plan irregularity (Figure 2-4q). Additionally, wall piers sustained shear failures over a significant

height of the building (Figure 6-8a). The main collapse area can be seen in Figure 6-8b.



Figure 6-8: Building TO-9; (a) Shear damage in axis 1A; (b) main collapse in story 12

7 STATISTICS OF BUILDING DAMAGE

Several teams visited this group of structures and contributed to a very thorough damage survey. This section is not exhaustive in describing that damage, but presents the most relevant observations from these visits and detailed inspection carried out during 2010 in the nine structures. Damage was surveyed by considering every structural element in the building, including walls, columns, beams, and slabs. Damage was defined as being light, moderate, or severe using a qualitative assessment of the likely loss of resistance due to the damage (e.g., Figure 7-1).

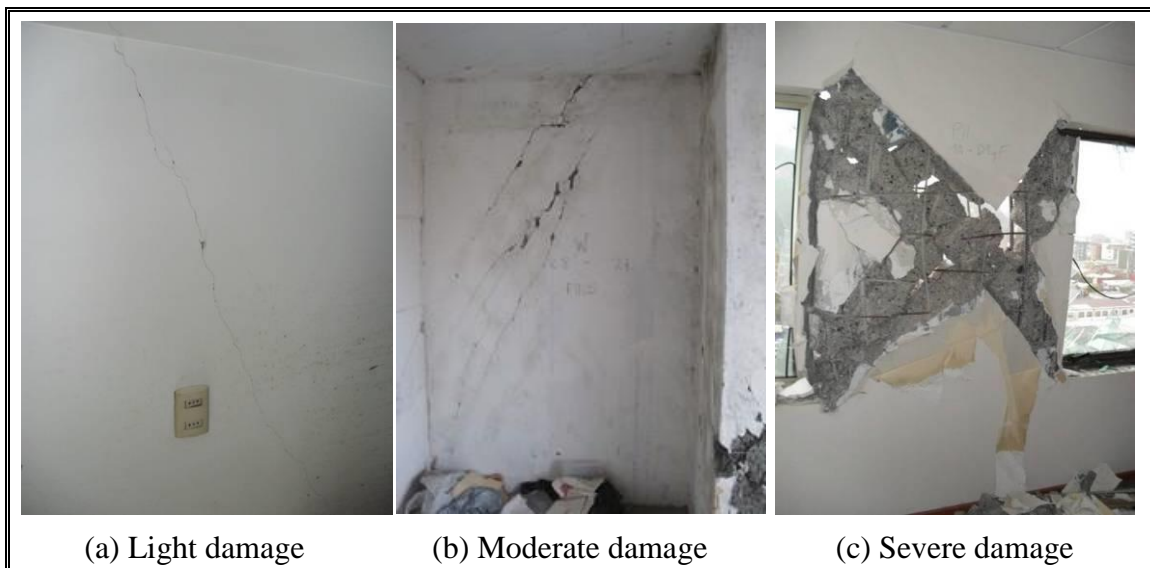


Figure 7-1: Examples of light, moderate and severe damage

The classification “Light Damage” was assigned to elements with minor cracking that lost approximately 20% or less of the original strength capacities. “Moderate Damage” referred to elements with more severe damage, likely corresponding to a modest reduction in force-resistance capacity, on the order of 50% of the original capacity. “Severe Damage” was assigned to elements that appeared to have lost a significant portion of their original force-resistance capacity, on the order of 80% of the original

capacity. Considerable information regarding damage was collected for each structure and is available for future analysis (DICTUC, 2010); detailed videos of every story and element in each structure were also recorded and are available. Note that data collection was done by two independent teams, so there is also capability for cross-checking the information gathered.

7.1 Wall Damage

Figures 7-2, 7-3 and 7-4 plots damage percentages for shear walls classified with light, moderate, and severe damage versus the normalized height of the structure. The damage is measured by the volume of damaged elements relative to the shear wall volume in each story. Buildings show the most damage in lower stories, with the exception of TO-9, which had a story failure in story 12, with additional damage in upper stories.

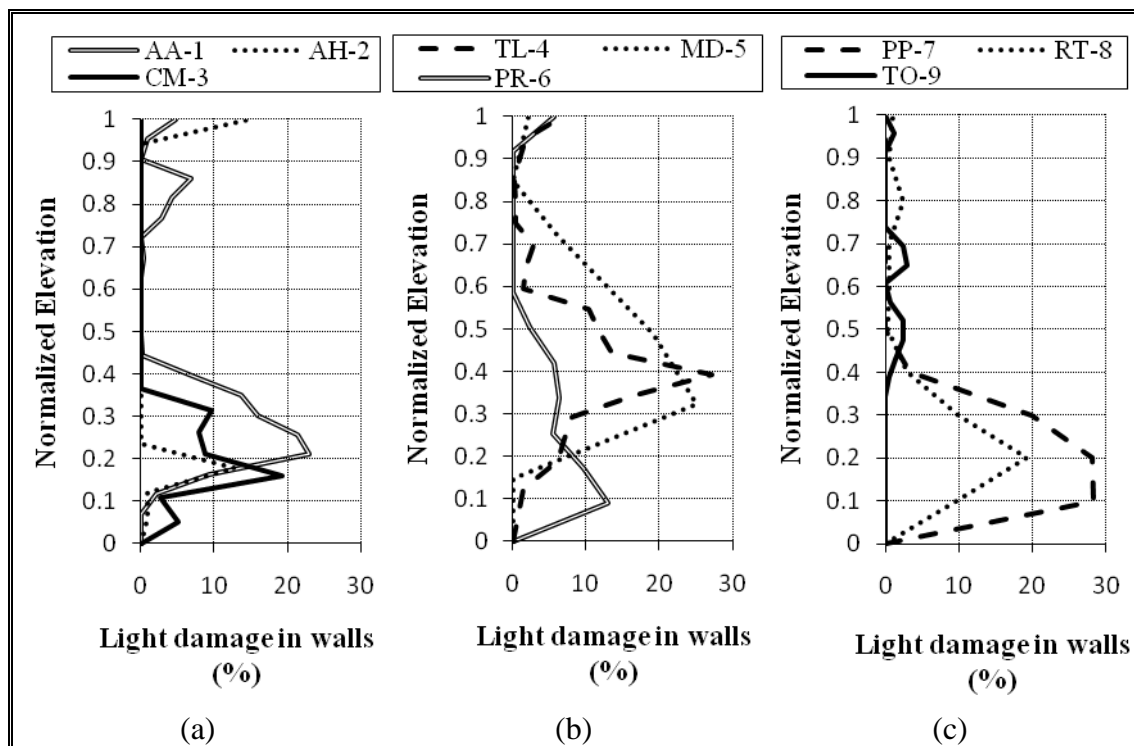


Figure 7-2: Light damage in walls

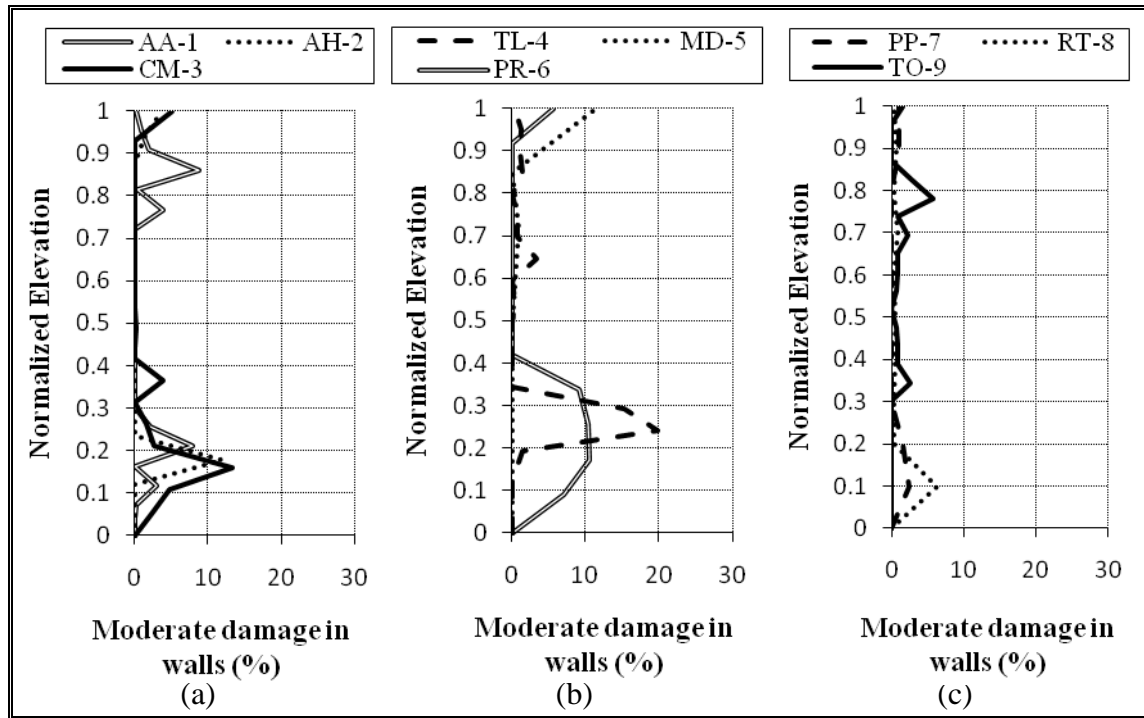


Figure 7-3: Moderate damage in walls

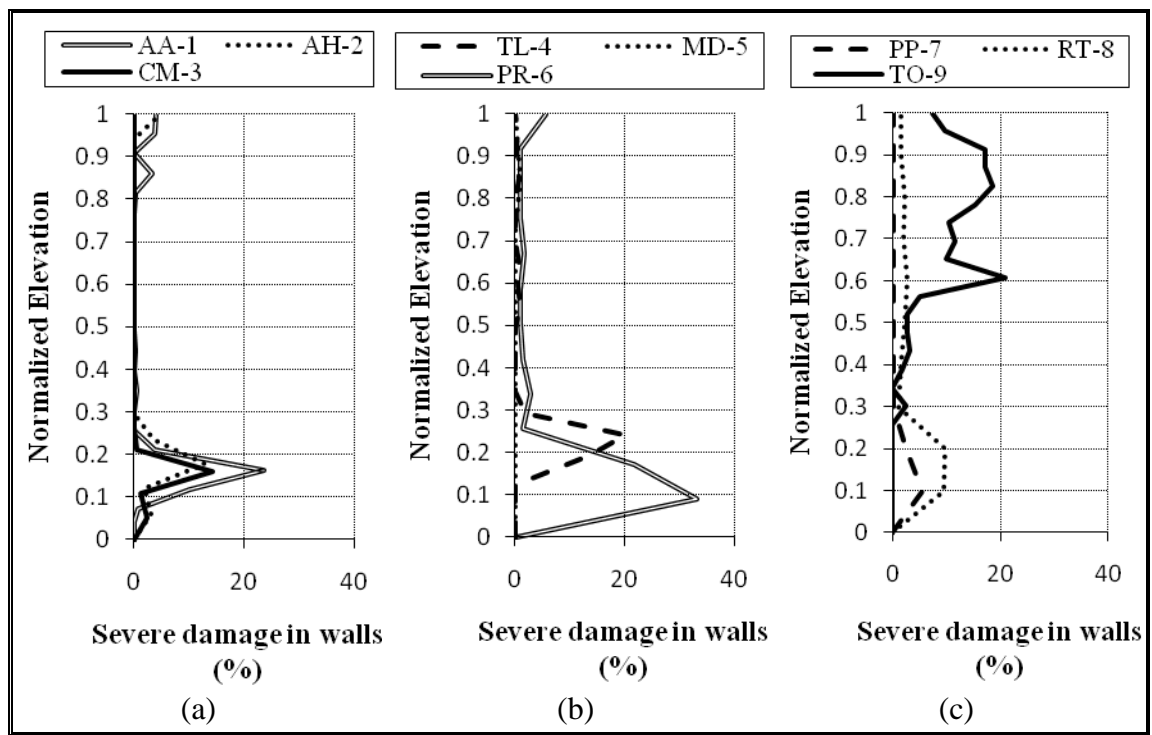


Figure 7-4: Severe damage in walls

Shown in Figure 7-5 is the damaged volume of walls (the sum of light, moderate and severe damage) as a percentage of total volume of walls in each story versus the normalized height of the structure.

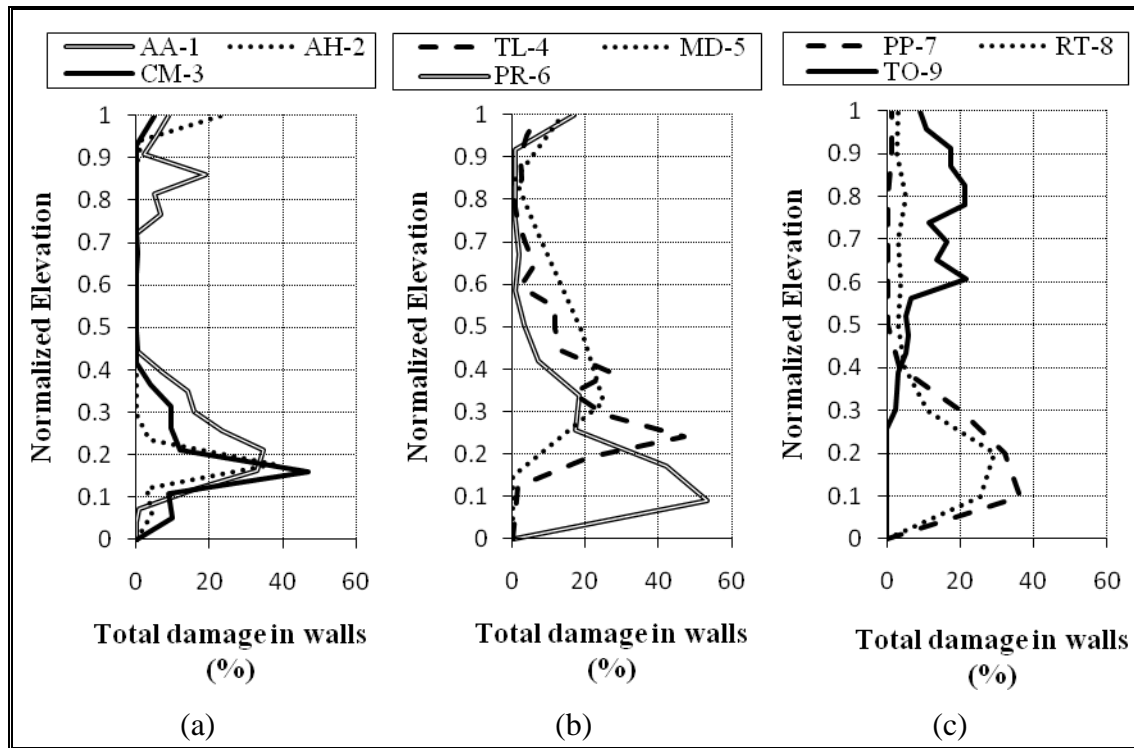


Figure 7-5: Total damage in walls

It is apparent that for building AA-1, damage in walls is concentrated in lower stories, reaching a maximum in the 2nd story. An increase in damaged walls is observed at the location of setbacks in higher stories. Building AH-2 has wall damage concentrated in lower and upper stories; severe damage occurs in lower stories, specifically from the 2nd basement to the 1st story; total damage peaks in the 1st story. Building CM-3 has intensive wall damage in stories -1, 1 and 2; maximum damage is reached in story 2. For TL-4, severely damaged walls are concentrated in the 1st and 2nd stories. In PR-6, damage is concentrated in the 1st and 2nd stories, having its maximum at the 2nd story. Severe damage at the 1st story is considerably larger than for other stories or even other buildings since approximately 33% of walls are severely damaged in this story. For Building PP-7,

light damage predominates over moderate or severe damage, the latter being localized in the structure in the 1st and 2nd stories. Analogously, damage in RT-8 concentrates in the same 1st and 2nd stories. Although PP-7 and RT-8 are nominally identical buildings, please note the different damage intensity in walls. PP-7 has light damage in walls, while RT-8 has an important percentage of severe damage in walls. For building TO-9, the amount of severely damaged walls predominates over lightly or moderately damaged ones. Damage in TO-9 starts in the 5th story and increases dramatically from the 12th story and up. The 12th story has the maximum value in damaged walls; part of this story collapses into the 11th story bringing the upper stories down. The axis of walls that collapses is J (Figure 2-4p, TO-9). Apart from having the building major setbacks in this story, walls reduce their thickness in this axis from 0.25m to 0.20m.

Table 7-1 shows the total percentage of damaged walls in each building relative to the total volume of shear walls in the structure, classified by damage category. The story with the most intensive wall damage is identified, and the amount it contributed to the percentage of total damage is indicated in the last column.

Table 7-1: Damage in walls

ID	% Light Damage	% Moderate Damage	% Severe Damage	% Total damage	Story with more damaged walls	
					Story	% From total damage
AA-1	5.31	1.26	2.60	9.17	2	1.84
AH-2	1.37	0.77	1.63	3.77	1	1.65
CM-3	3.01	1.86	1.10	5.98	2	2.24
TL-4	5.63	2.28	2.12	10.03	2	2.31
MD-5	7.16	1.21	0.09	8.46	2	3.09
PR-6	3.90	3.42	6.09	13.40	1	4.67
PP-7	7.87	0.59	0.95	9.40	1	3.58
RT-8	4.61	1.00	3.38	9.00	2	2.91
TO-9	0.49	0.62	4.22	5.34	12	0.66

Excluding building AH-2, which has localized damage in the walls of lower stories, damage in the rest of the buildings involves more than 5% of the shear walls. Buildings with considerable severe wall damage are PR-6, TO-9, RT-8 and AA-1; maximum wall damage occurs in PR-6. Damaged walls tend to occur in lower stories, 1st or 2nd with the exception of TO-9 where damage concentrates in the 12th story. Examples of the severe wall damage observed are shown in Figure 7-6.



(a) AA-1



(b) AA-1



(c) AH-2



(d) CM-3



Figure 7-6: Examples of severe wall damage

7.2 Beam Damage

It is possible now to extend this analysis to beam damage as shown in Figures 7-7, 7-8 and 7-9. Damage is measured by the volume of damaged elements relative to the beam volume in each story.

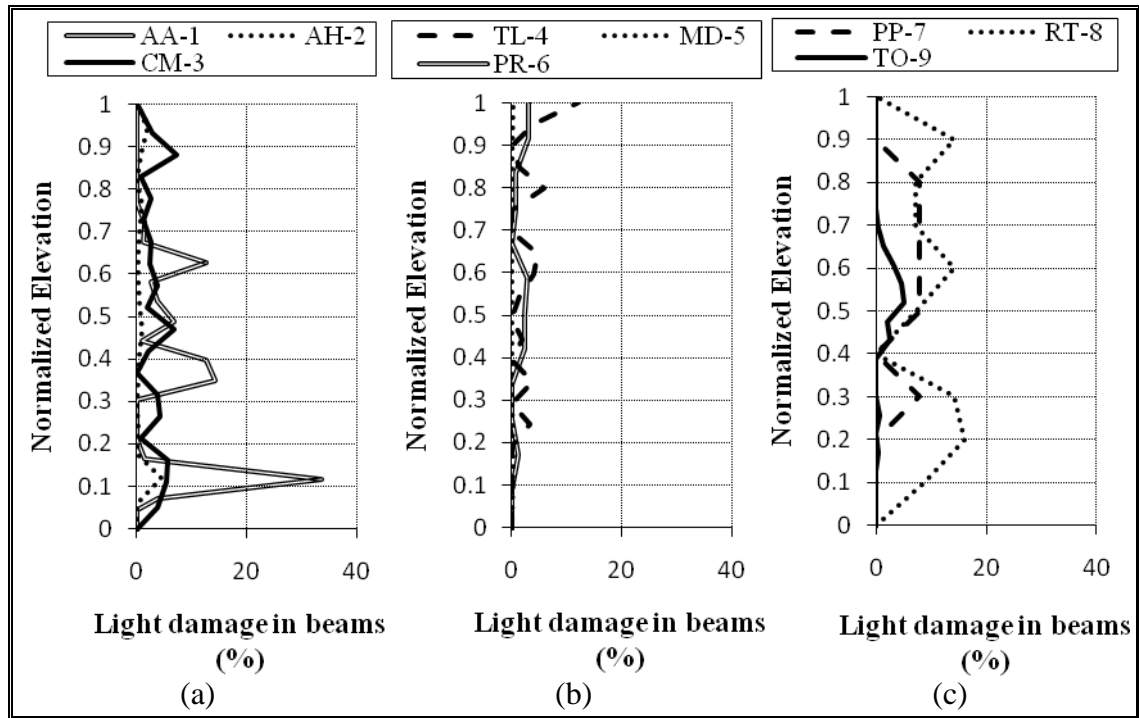


Figure 7-7: Light damage in beams

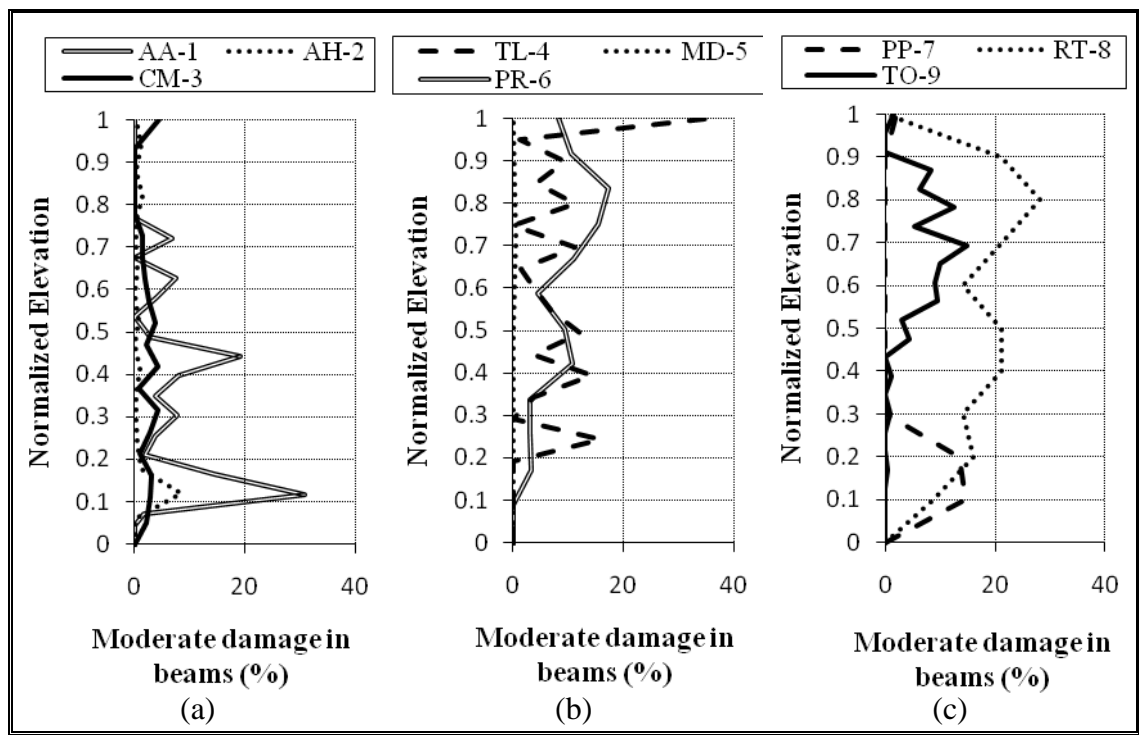


Figure 7-8: Moderate damage in beams

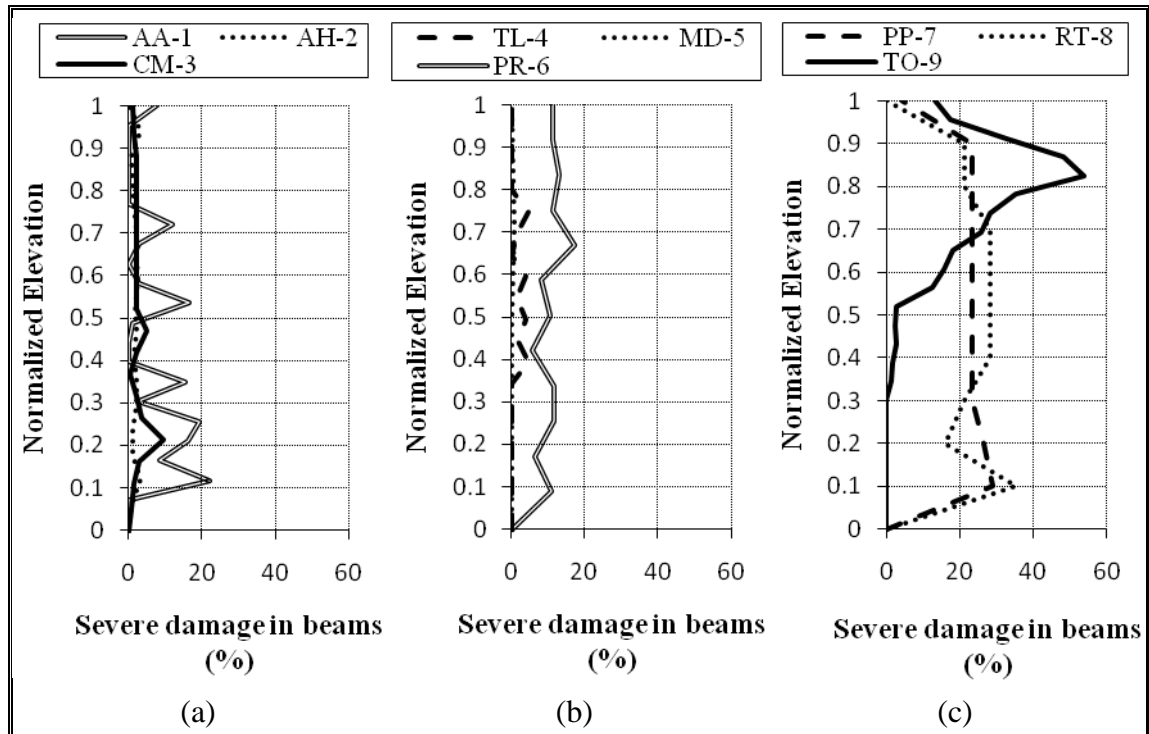


Figure 7-9: Severe damage in beams

Shown in Figure 7-10 is the damaged volume of beams (the sum of light, moderate and severe damage) as a percentage of total volume of beams in each story versus the normalized height of the structure.

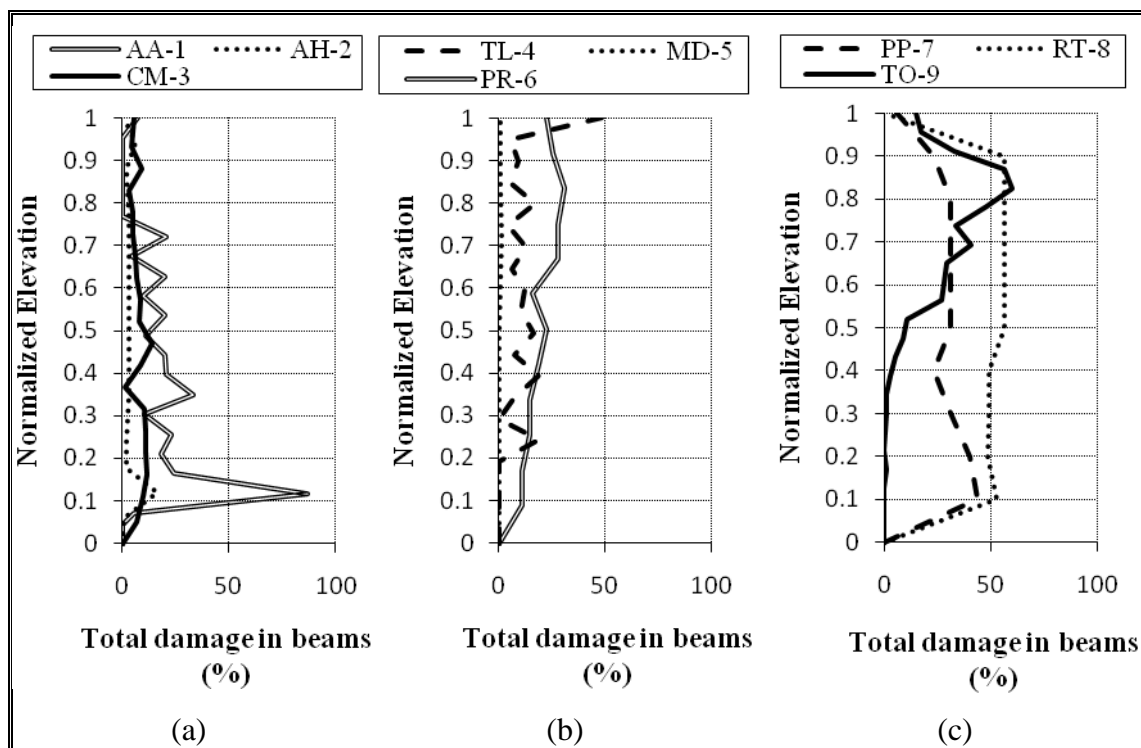


Figure 7-10: Total damage in beams

For building AA-1, beam damage is larger in stories 1 and 14, where setbacks in the structure exist. Damage in floor 14 is considerably higher than in other stories (as more beams exist in this level). Beam damage in AH-2 is rather uniform, having again an increase in lower and upper stories, consistent again with changes in the structural configuration. Building CM-3 has light damaged beams concentrated in bottom and top stories, moderate damaged beams scattered through the building while severely damaged beams are focused in lower stories, coincident with heavy wall damage. Notice that total beam damage matches the distribution of the total wall damage (Figure 7-5). Beams in TL-4 reach its maximum damage on the 2nd story. It is important to note that this structure has considerably more lightly and moderately damaged beams than severely damaged ones. MD-5 has a huge amount of beams (grillage of beams between columns) which damaged ones are not an important percentage of the total number of beams. This building shows moderate and severe beam damage in top stories,

where the slab failed and dragged the corresponding beams. Although PR-6 has a distribution of severely damaged beams approximately uniform in height, total damage concentrates in upper stories. This building experienced considerable rocking, which may have aggravated this behavior. Buildings PP-7 and RT-8 are the ones with the most damaged beams, approximately 20% and 30% of total beams. This type of damage occurred in the perimeter beams (axis B and near axis J, Figure 2-4m), where they break off, causing punching to perpendicular shear walls and the generation of hinges at their ends (axes 10-12, and 14-16, Figure 2-4m). Building TO-9 shows severe beam damage that is highly correlated with wall damage. Most of the severe beam damage observed in this building happened because of the very large deformations caused by the collapse of the 12th story into the 11th story.

Table 7-2 shows the total percentage of damaged beams in each building relative to the total volume of beams in the structure, classified by damage category. The story with the most intensive beam damage is also identified, and the amount it contributed to the percentage of total damage is indicated in the last column.

Table 7-2: Damage in beams

ID	% Light Damage	% Moderate Damage	% Severe Damage	% Total damage	Story with more damaged beams	
					Story	% From total damage
AA-1	3.35	4.82	5.69	13.87	1	1.91
AH-2	0.63	0.80	1.60	3.02	14	0.49
CM-3	2.44	1.62	1.96	6.02	1	0.72
TL-4	4.08	5.89	1.02	10.99	2	1.08
MD-5	0.14	0.17	0.26	0.57	3	0.23
PR-6	1.08	6.20	8.44	15.71	10	1.99
PP-7	2.69	2.17	15.61	20.47	1	2.43
RT-8	5.87	11.25	15.17	32.29	9	3.91
TO-9	0.84	2.95	9.30	13.09	17	1.50

Excluding AH-2, CM-3 and MD-5, all buildings have damage ratios larger than 10% in damaged beams, being larger for buildings PP-7 and RT-8. Total damage is significant for AA-1, PR-6, PP-7, RT-8 and TO-9. In TO-9 the percentage of severely damaged beams than other type of damage is considerably higher (9.30% against 0.84% for light damage and 2.95% for moderate damage). In all buildings, the stories with larger beam damage correspond to lower or upper stories, except for MD-5. This building had specific damage at story 3 which made beams at ends suffer local damage. Examples of the severe beam damage observed are shown in Figure 7-11.



(a) AA-1



(b) AH-2



(c) CM-3



(d) CM-3



Figure 7-11: Examples of severe beam damage

7.3 Column Damage

Figures 7-12, 7-13 and 7-14 plots damage percentages for columns versus the normalized height of the structure. The damage is measured by the volume of damaged elements relative to the column volume in each story. It is apparent that damage concentrates primarily in the lower and upper stories.

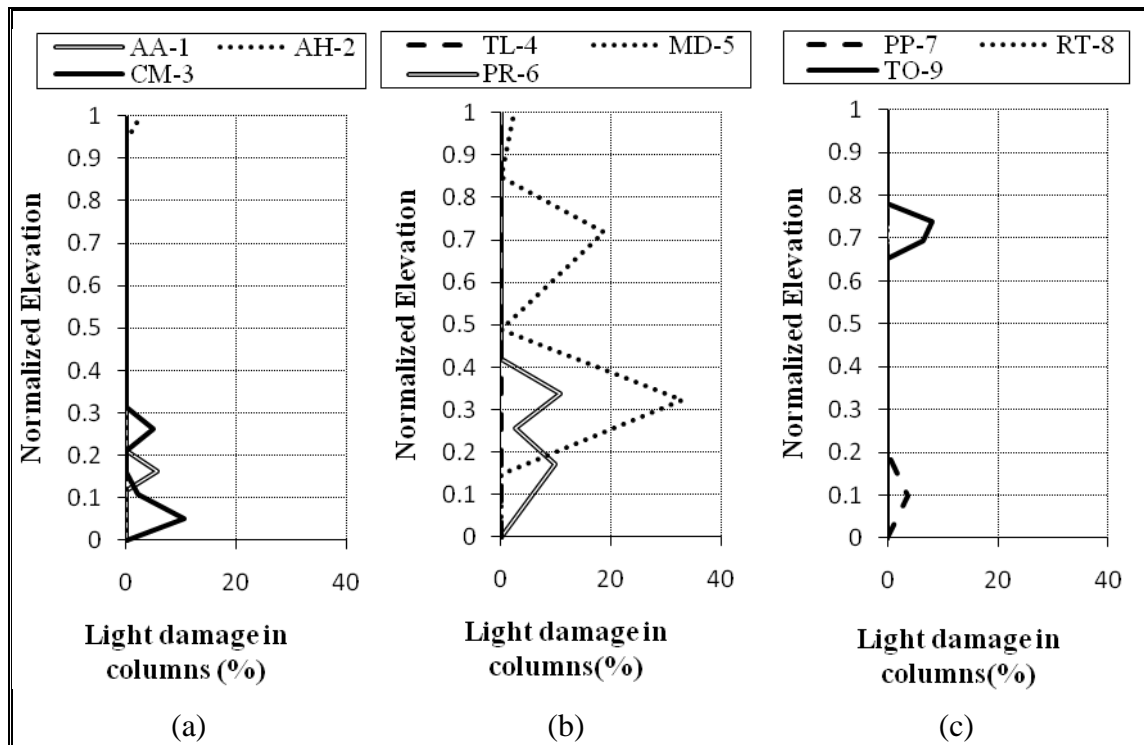


Figure 7-12: Light damage in columns

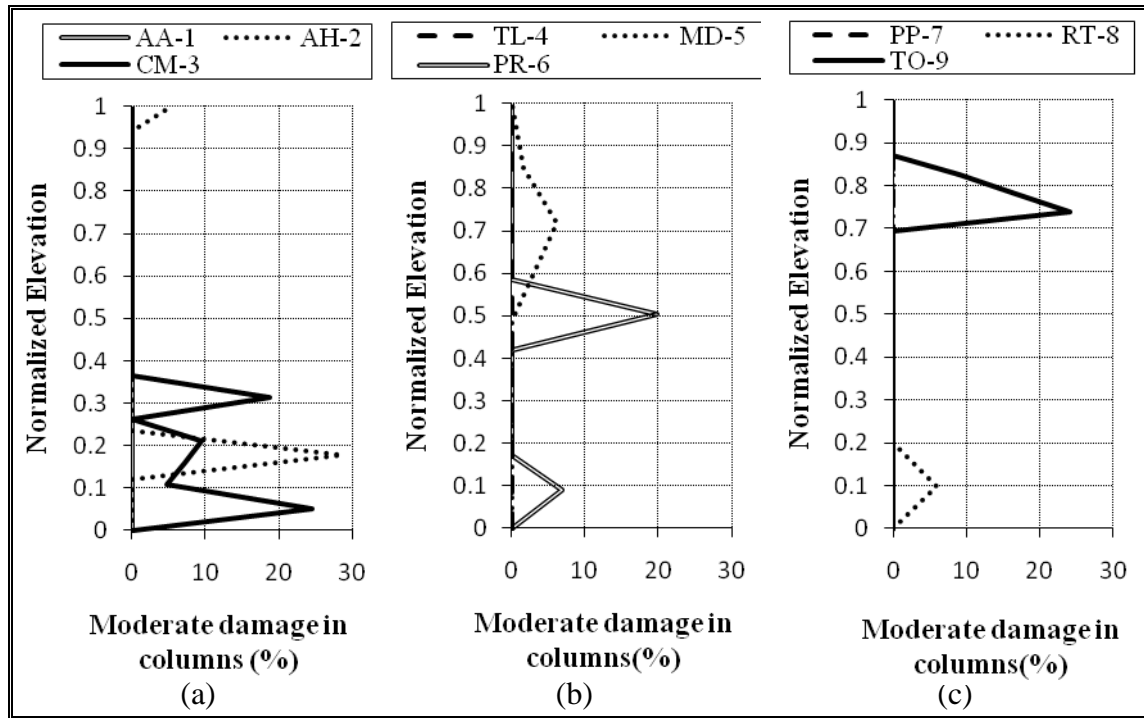


Figure 7-13: Moderate damage in columns

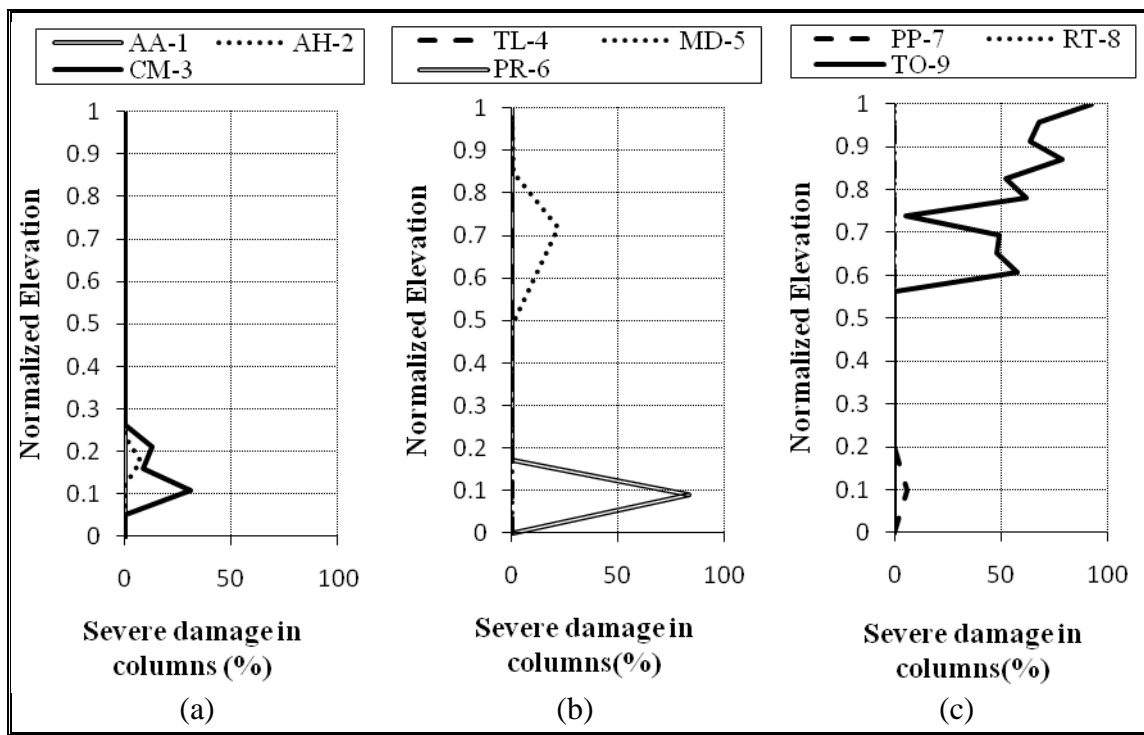


Figure 7-14: Severe damage in columns

Shown in Figure 7-15 is the damaged volume of columns (the sum of light, moderate and severe damage) as a percentage of total volume of columns in each story versus the normalized height of the structure.

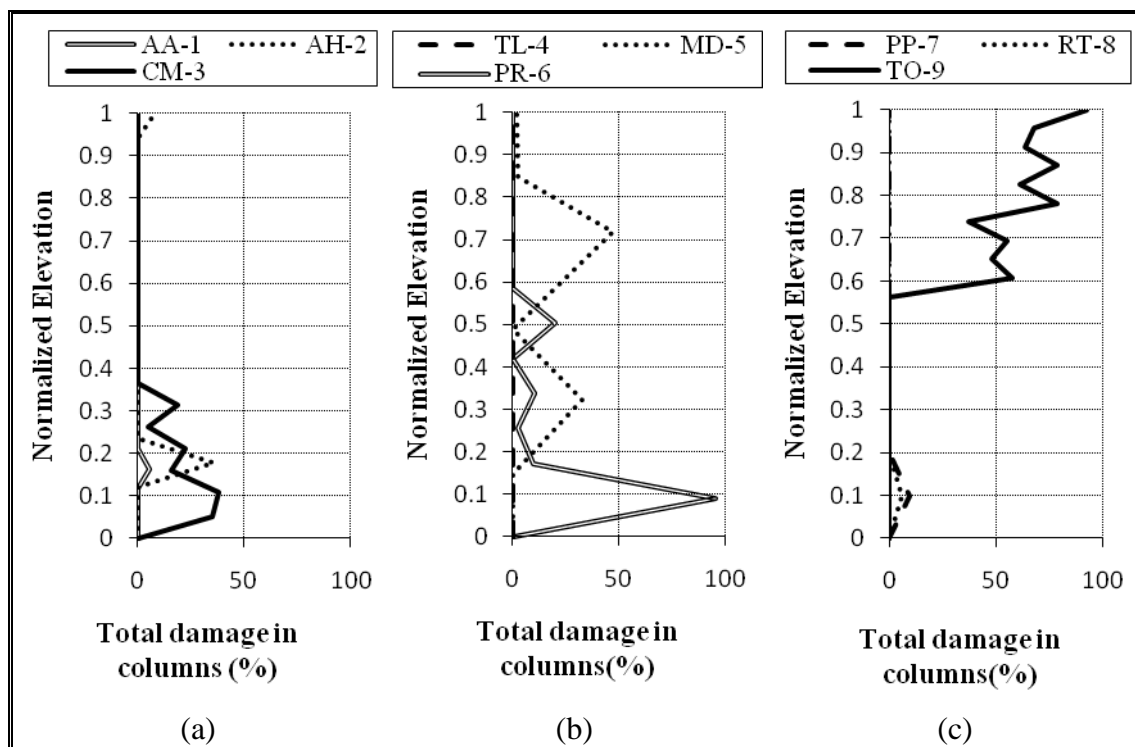


Figure 7-15: Total damage in columns

Please note that in general, with the exception of MD-5 and TO-9, the total plan area of columns is considerably smaller than that of shear walls. Damage in columns may be summarized as follows: building AA-1 shows light damage in story 2; column damage in AH-2 was observed in stories 1 and 15, with moderate damage in story 1; CM-3 shows damage between stories -1 and 5, with maximum severe damage in columns of story 1; severe damage in PR-6 concentrates in the first story and decreases in upper stories; buildings PP-7 and RT-8 show column damage only in the first story. In TO-9 severe damage in columns starts at the 12th story and upward, and compromises seriously the stability of the structure—column joints lack concrete and bars are buckled while punching of the slabs is

frequent. The only true frame structure is MD-5, and shows a great percentage of columns with damage localized on the 3rd story, which is double height ($h=6.30\text{m}$). Table 7-3 shows the total percentage of damaged columns in each building relative to the total volume of columns in the structure, classified by damage category. The story with the most intensive column damage is identified, and the amount it contributed to the percentage of total damage is indicated in the last column.

Table 7-3: Damage in columns

ID	% Light Damage	% Moderate Damage	% Severe Damage	% Total damage	Story with more damaged columns	
					Story	% From total damage
AA-1	0.43	0.00	0.00	0.43	2	0.43
AH-2	0.26	3.44	1.19	4.90	1	3.31
CM-3	0.61	2.86	3.10	6.57	1	2.05
TL-4	0.00	0.00	0.00	0.00	-	0.00
MD-5	8.89	1.87	5.99	16.75	3	12.36
PR-6	2.43	2.27	7.03	11.73	1	8.07
PP-7	0.37	0.00	0.58	0.95	1	0.95
RT-8	0.00	0.58	0.00	0.58	1	0.58
TO-9	0.56	1.88	20.00	22.45	16	2.95

Critical conditions in columns are found in buildings TO-9, PR-6 and MD-5. These structures present about 20%, 7% and 6% of their columns severely damaged, respectively. Column damage in TO-9 is uniformly distributed between stories 12 and higher. For building PR-6, almost 70% of column damage is concentrated in story 1, while in MD-5 approximately 75% of total column damage concentrates in story 3. Examples of the severe column damage observed are shown in Figure 7-16.



(a) AH-2



(b) CM-3



(c) MD-5



(d) MD-5



(e) PR-6



(f) PR-6



(g) TO-9



(h) TO-9



(i) TO-9



Figure 7-16: Examples of severe column damage

7.4 Slab Damage

Figures 7-17, 7-18 and 7-19 plots damage percentages for slabs versus the normalized height of the structure. The damage is measured by the volume of damaged elements relative to the slab volume in each story. Shown in Figure 7-20 is the damaged volume of slabs (the sum of light, moderate and severe damage) as a percentage of total volume of slabs in each story versus the normalized height of the structure.

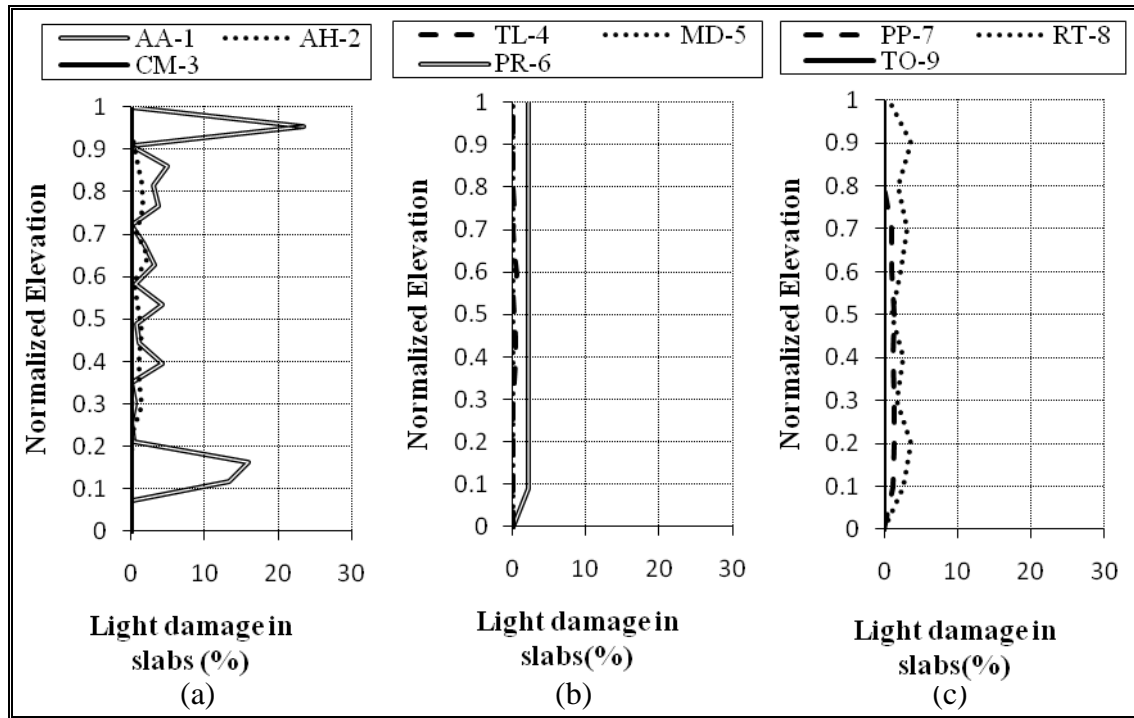


Figure 7-17: Light damage in slabs

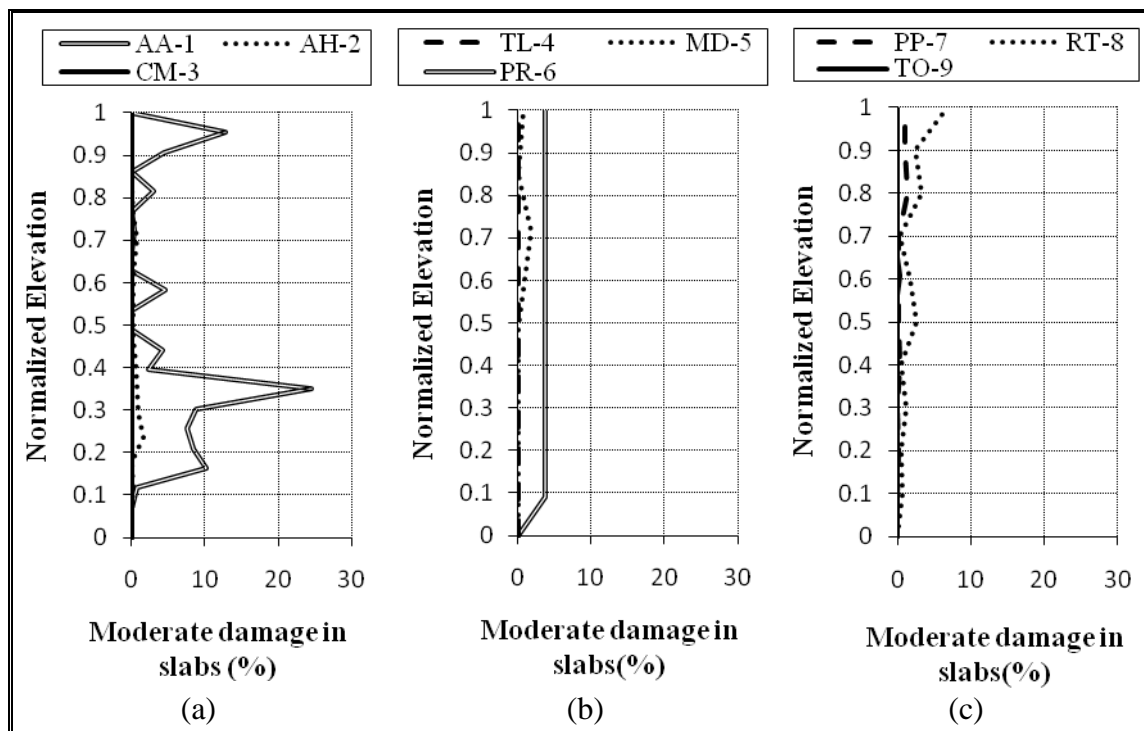


Figure 7-18: Moderate damage in slabs

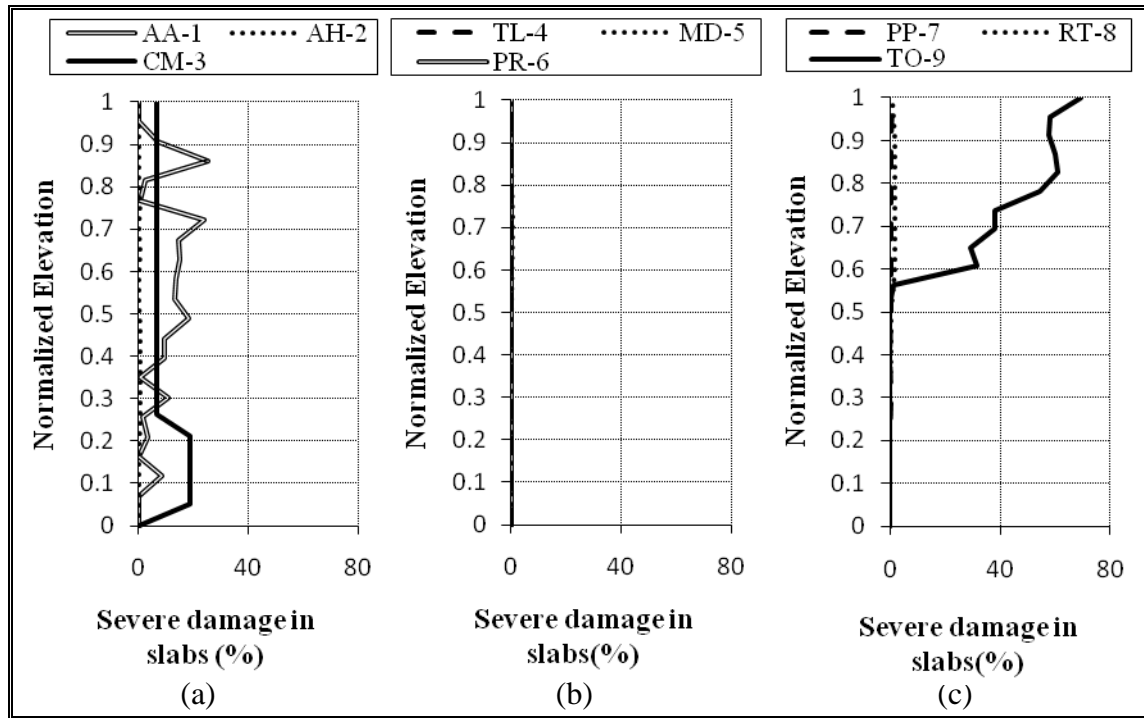


Figure 7-19: Severe damage in slabs

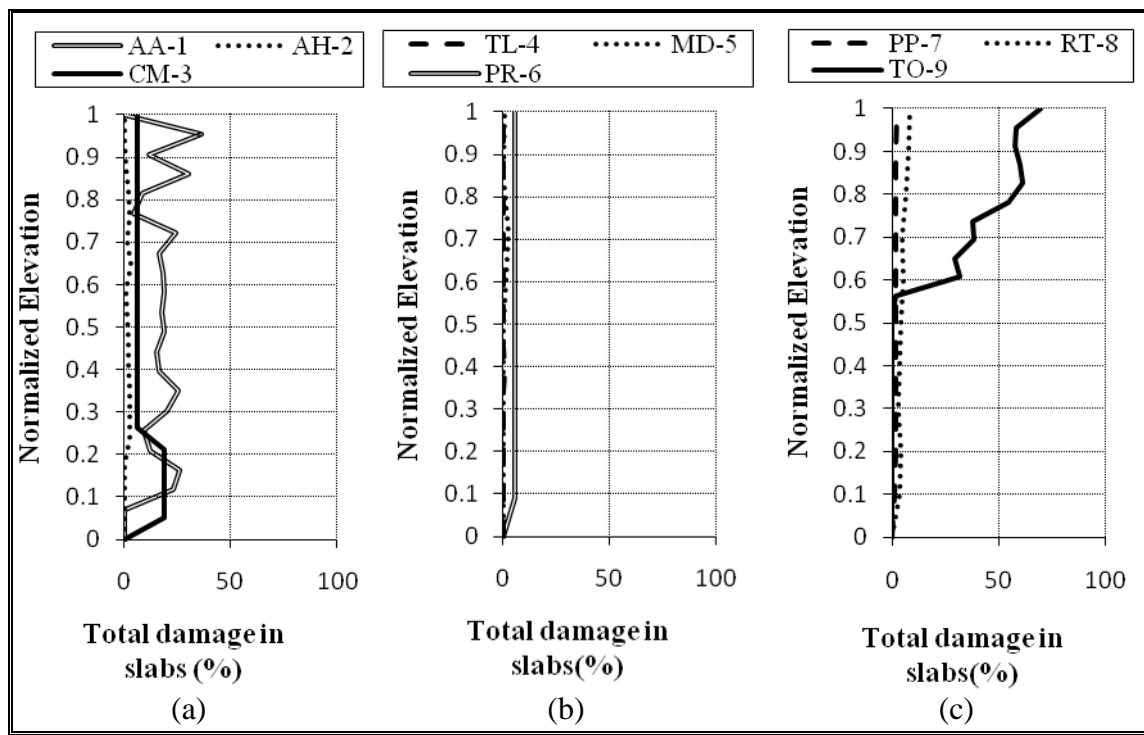


Figure 7-20: Total damage in slabs

This damage may be summarized as follows: building AA-1 shows a scattered pattern of damage of slabs with severe damage occurring at upper stories where the structure shows important setbacks; AH-2 shows punching of walls at the four building corners of the structure and at the intermediate levels—the slabs at each corner present a big cantilever portion making them particularly sensitive to vertical vibration; in building CM-3 severe slab damage occurred in lower stories; TL-4 has no or little damage in slabs; damage in building MD-5 concentrates in the 3rd story where slabs at the end of the longitudinal axes of MD-5a failed locally—there is an increase in damage at story 5 due to pounding of structures MD-5a and MD-5b; damage in slabs of building PR-6 is approximately constant in height and of moderate intensity; PP-7 and RT-8 showed light damaged in slabs and the fact that damage increases in elevation is likely due to pounding; building TO-9 has severe slab damage from the 12th story upward—some of the damage is a consequence of the partial collapse observed in this structure.

Table 7-4 shows the total percentage of damaged slabs in each building relative to the total volume of slabs in the structure, classified by damage category. The story with the most intensive slab damage is identified, and the amount it contributed to the percentage of total damage is indicated in the last column.

Table 7-4: Damage in slabs

ID	% Light Damage	% Moderate Damage	% Severe Damage	% Total damage	Story with more damaged slabs	
					Story	% From total damage
AA-1	3.19	4.25	8.41	15.85	2	1.52
AH-2	0.68	0.31	0.26	1.25	9	0.16
CM-3	0.00	0.00	6.85	6.85	-1	1.42
TL-4	0.17	0.02	0.00	0.19	5	0.03
MD-5	0.01	0.50	0.17	0.68	3	0.54
PR-6	1.92	3.24	0.00	5.16	12	0.43
PP-7	0.82	0.40	0.22	1.44	10	0.19
RT-8	2.30	1.94	0.75	4.98	10	0.81
TO-9	0.00	0.01	13.44	13.45	17	1.61

Buildings AA-1 and TO-9 are the ones with the largest slab damage ratios, 15.9% and 13.5%, respectively. In AA-1 slab damage peaks in 2nd story (matching damage in other elements). Practically all slab damage in TO-9 is severe and well distributed through stories above floor 12. For MD-5, approximately 80% of damage in slabs is present at story 3. Examples of the severe slab damage observed are shown in Figure 7-21.



(a) AA-1



(b) AH-2



(c) CM-3



(d) MD-5



(e) PP-7



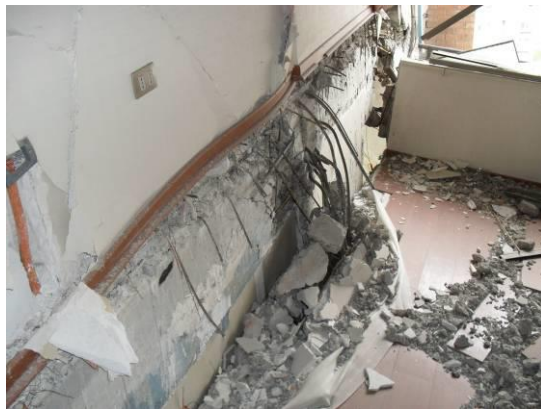
(f) RT-8



(g) TO-9



(h) TO-9



(i) TO-9



(j) TO-9

Figure 7-21: Examples of severe slab damage

7.5 Total Damage

Figures 7-22, 7-23 and 7-24 plots damage percentages for all elements classified with light, moderate, and severe damage versus the normalized height of the structure. The damage is measured by the volume of damaged elements relative to the total volume in each story.

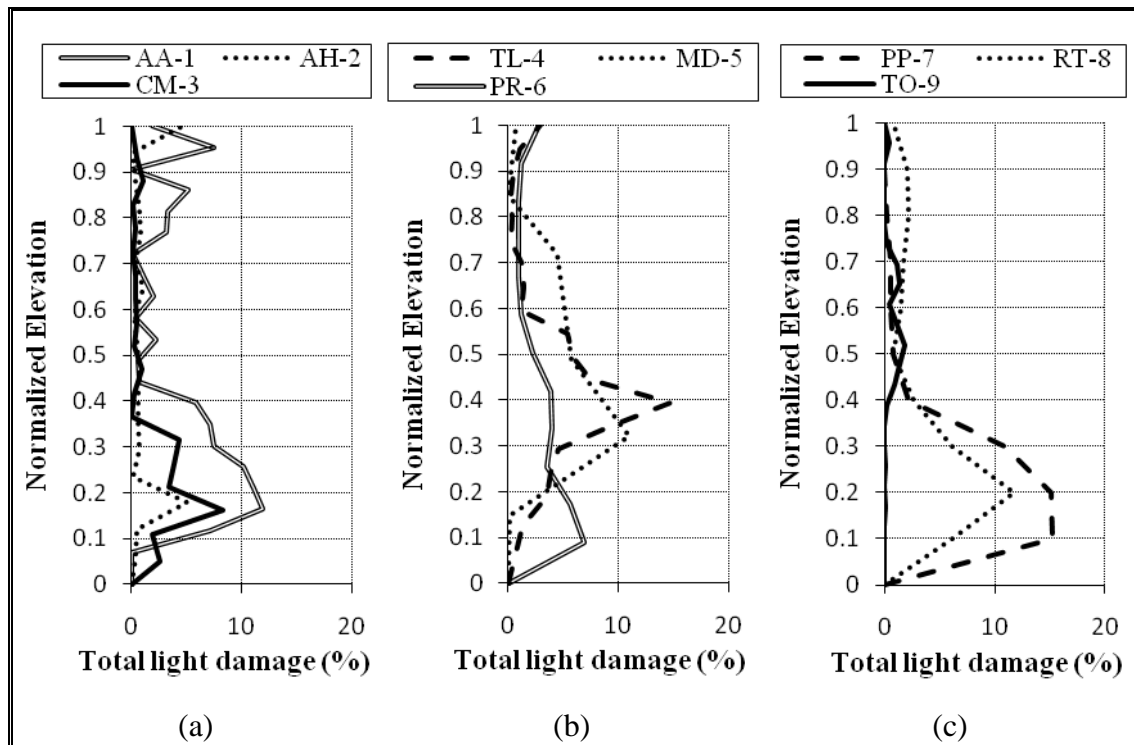


Figure 7-22: Total light damage

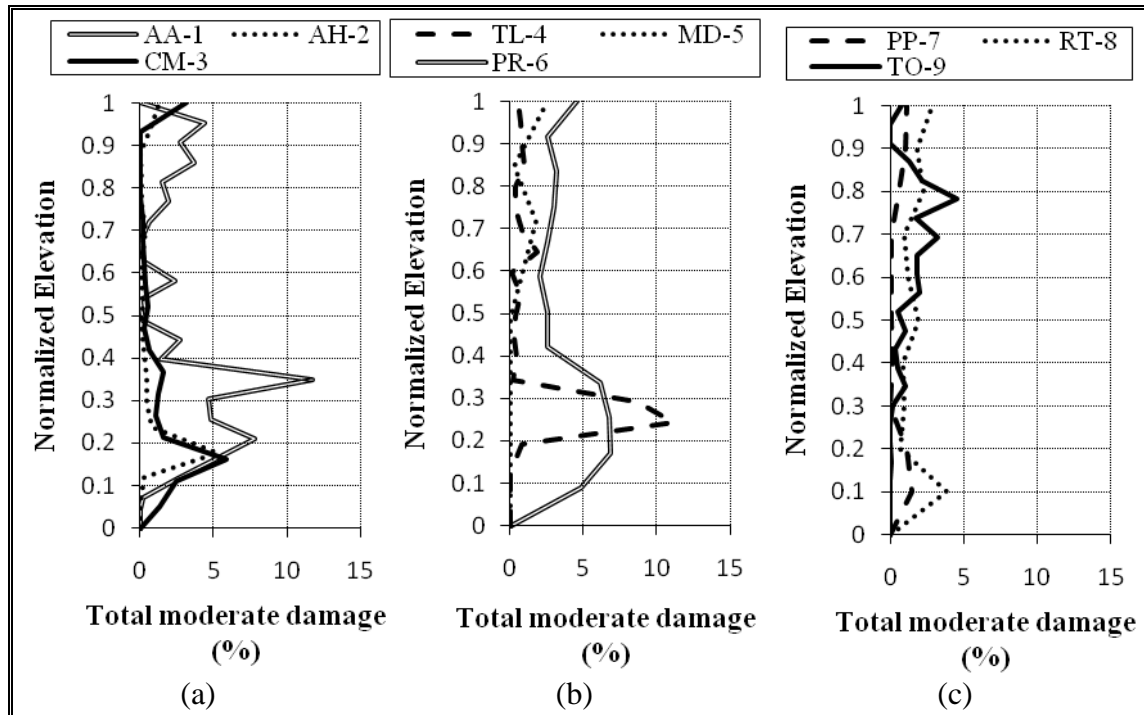


Figure 7-23: Total moderate damage

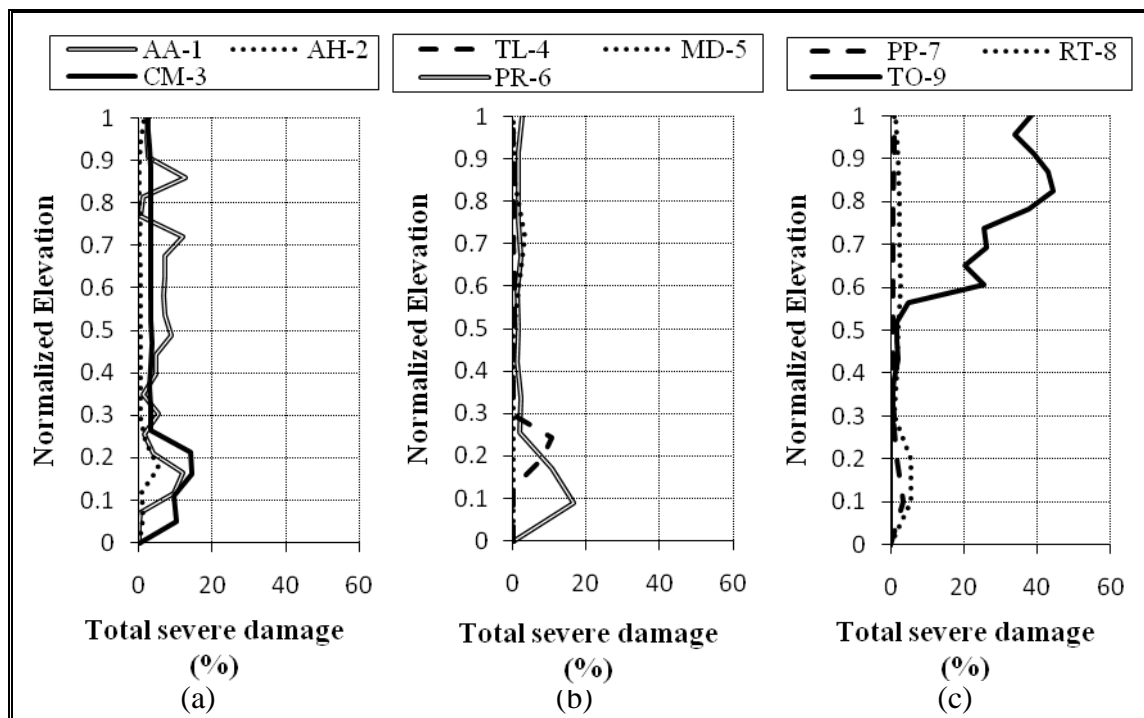


Figure 7-24: Total severe damage

Shown in Figure 7-25 is the damaged volume of elements (the sum of light, moderate and severe damage) as a percentage of total volume in each story versus the normalized height of the structure.

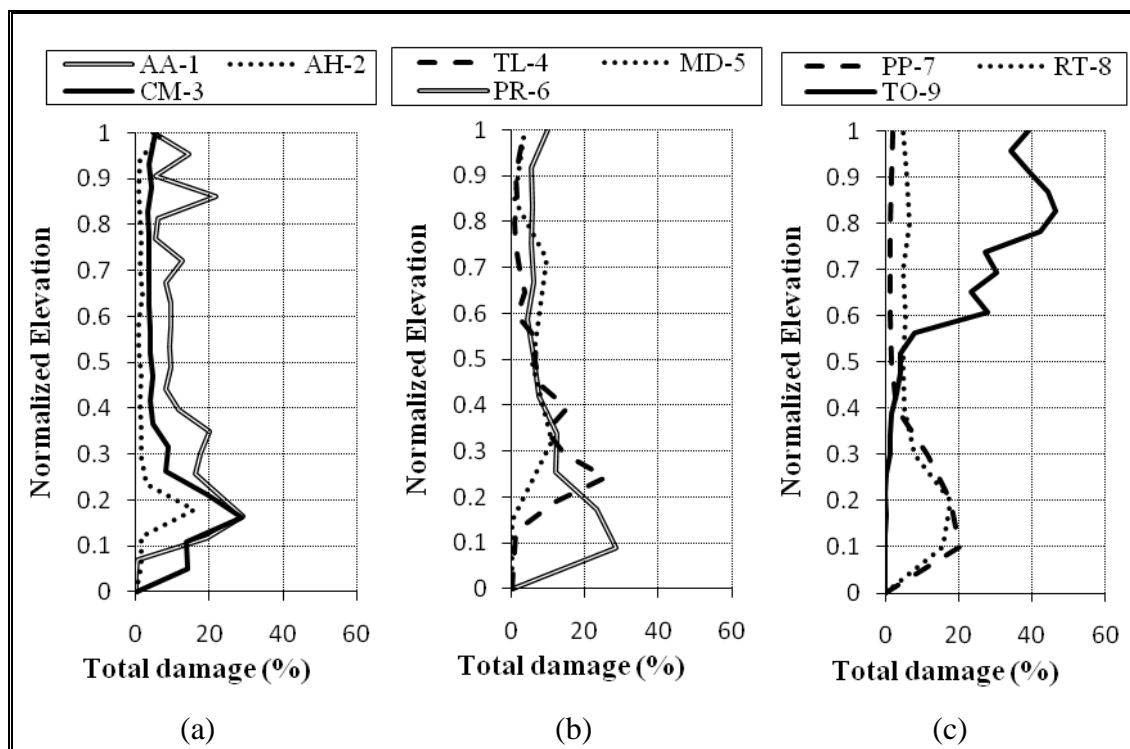


Figure 7-25: Total damage

As expected, damage tends to concentrate in the lower stories, but the damage pattern varies among structures. Building AA-1 shows more elements with severe damage than with other intensities. This damage is higher in its lower stories. Note that moderate, severe and total damage peaks locally at stories 14 and 17 where significant irregularities are found. In AH-2 all kind of damage follows the same distribution, reaching its maximum at lower stories with a local rise at upper levels. The same behavior (but more severe) in lower levels occurs in building CM-3. For this structure maximum is reached in story -1 (with similar values at story 1 and 2). Severe damaged elements in building TL-4 are mainly present in stories 1 and 2. Maximum total damaged elements are observed in 2nd story. MD-5 shows mainly severe damage in its MD-5a structure. At story 3; moderate, severe

and total damage is focused mainly because of the failure of columns at this double height story. Severely damaged elements in PR-6 are the most common ones. This damage is concentrated at story 1. PP-7 and RT-8 shows same distribution of damaged elements with intensity variation (RT-8 has more severely damaged elements than PP-7). Damage in both of this structures peaks at lower stories. Almost all of the damage observed in TO-9 is severe. It peaks at story 17 but similar values are found in stories 12 and 16 (where partial collapses exist). For stories between 5 and 11 few elements were observed mainly with light or moderate damage, while for stories lower than 5 approximately no damage was observed.

Table 7-5 shows the total percentage of damaged elements in each building relative to the total volume in the structure, classified by damage category. The story with the most intensive damage is identified, and the amount it contributed to the percentage of total damage is indicated in the last column.

Table 7-5: Total damage

ID	% Light Damage	% Moderate Damage	% Severe Damage	% Total damage	Story with more damaged elements	
					Story	% From total damage
AA-1	4.24	2.75	5.33	12.31	2	1.66
AH-2	0.95	0.56	0.93	2.44	1	0.71
CM-3	1.31	0.89	4.40	6.60	-1	1.14
TL-4	3.51	1.60	1.27	6.38	2	1.38
MD-5	3.20	0.76	0.72	4.68	3	1.90
PR-6	2.65	3.64	3.50	9.79	1	2.28
PP-7	4.46	0.54	1.08	6.07	1	1.98
RT-8	3.52	1.70	2.51	7.73	2	1.75
TO-9	0.34	0.74	9.16	10.23	16	1.15

Consolidated damage is largest in Building AA-1 and TO-9 and reaches values of the order of 12%. Note that in TO-9 approximately 90% of damage observed is

severe. In PP-7 almost the 75% of damage in elements is light damage. Except for MD-5 (with particular column damage) and TO-9 (with partial collapse of story 12) all other buildings had their most damaged elements in lower stories. For most damaged high rise buildings (AA-1, CM-3, PR-6 and TO-9) code-analysis information will be presented further. It is apparent that only a small proportion of the structure in volume was compromised for the critical condition of the structure, which certainly shows the lack of efficiency of the building in terms of developing redundancy and energy dissipation. A second aspect that supports this observation is the lack of graduation of damage observed in these structures. For instance building TO-9 shows that most damage is severe, showing the incapacity of the structure to distribute its damage. It is also interesting to observe that damage is highly correlated with places where structural irregularities exist.

8 TYPES OF DAMAGE

The damage data also can be organized according to type, location, and the geometry of the damaged elements.

8.1 Wall Damage



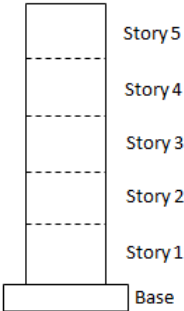
Table 8-1 summarizes damage in walls classified by: (i) the type of damage, shear or flexure, (ii) continuity of the wall from roof-to-base of the building, (iii) geometric discontinuity of the walls produced by sudden changes of the wall cross section in intermediate stories, (iv) “soft” story due to change in wall thickness, and (v) “flag-shaped” walls, that is, walls having significant reduction of the wall length in one story compared with the story immediately above.

A wall was designated as having shear damage if visible damage mainly involved diagonally oriented cracks or other distress. A wall was designated as having flexural damage if the damage mainly involved horizontal cracks or crushing; in many cases this included buckled longitudinal reinforcement especially near the wall boundary. Where a wall had mainly horizontal damage at the boundary but this propagated diagonally within the wall web, it was designated as having both flexure and shear damage. This categorization is subjective, as damage to all walls generally involved some combination of shear, axial load, and flexure. Information is presented as percentage of total damage observed.

Global building results show that more walls have shear than flexural damage, except for buildings CM-3 and TL-4, where percentages are similar. Except for building TO-9, where partial collapse imposed large rotations and stresses due to impact, flexural damage tends to occur in the lower stories. On the other hand, the location of shear damage varied. In buildings AA-1, TL-4 and MD-5, it is present

in most stories; in buildings AH-2, CM-3, PR-6, PP-7 and RT-8 it is present mainly in lower stories; and in building TO-9 it occurs only above the 6th story.

Table 8-1: Type of wall damage and stories where behavior is observed

Type of damage	AA-1	AH-2	CM-3	TL-4	MD-5	PR-6	PP-7	RT-8	TO-9
	-1, 1-9, 13, 15-20	-2, 1-2, 14-15	-1, 1-6, 18	-1, 2-5, 7-10, 14-17	1-5	1-5, 12	1-4	1-4, 8-10	6-21
Shear failure	69.1%	51.0%	50.7%	40.5%	74.0%	76.7%	91.2%	61.3%	66.4%
	-1,1-3	-2, -1,1	-1,1-3	1-3	-	1, 2	1, 2	1, 2	5, 11-19
Flexural failure	24.9%	32.0%	47.1%	37.6%	0%	17.9%	4.5%	17.4%	21.5%
	-1, 1-8, 17-18	-2, -1, 1-2, 15	-1, 1-6	1-17	2-3, 5	1-5, 12	1-10	1-10	4, 7-21
Damage in continuous walls	73.1%	79.4%	91.9%	100%	51.9%	98.3%	100%	100%	37.8%

<div><div></div><div></div><div></div><div></div><div></div></div> <div>Story5 Story4 Story3 Story2 Story1</div>	1-4, 8-9, 13, 15-20 15- - - 1-5 - - - 6-21									
Damage in discontinuous walls	15.9%	3.8%	0.0%	0.0%	36.5%	0.0%	0.0%	0.0%	51.0%	
<div><div></div><div></div></div> <div>Story2 Story1</div>	2-9, 13, 17-20 1, 151-2, 184-1722-3- - 12-20									
“Soft” story	35.3%	8.9%	6.0%	30.0%	34.0%	11.7%	0.0%	0.0%	17.1%	
<div><div></div><div></div><div></div><div></div><div></div><div></div></div> <div>Story5 Story4 Story3 Story2 Story1 Base</div>	1-4, 19-201-2, 14-152-3, 18- - 54- - 5-8, 11, 13-14, 16-17									
“Flag-shaped” walls	11.0%	16.9%	8.1%	0.0%	11.6%	1.7%	0.0%	0.0%	11.1%	

Building AA-1 shows 73.1% of its damage in continuous walls, and if compared with other buildings, damage due to discontinuous, soft-story, or “flag-shaped” walls is also very high. This is the result of its irregular configuration and multiple setbacks. Damage in discontinuous walls and “soft” stories is present throughout the structure, while damage in “flag-shaped” walls occurs primarily in the lower and upper levels. Please note that for this building, a concrete with specified compressive strength $f'_c=250 \text{ kg/cm}^2$ was used in the first five stories, with specified compressive strength reduced to $f'_c=200 \text{ kg/cm}^2$ in upper stories.




Building AH-2 has damage in continuous wall elements in lower and upper stories; it also shows some localized damage in discontinuous walls in the 15th story, and moderate damage adjacent to “soft” stories. However, this building leads the percentage of damaged “flag-shaped” walls with 16.9%. Building CM-3 shows 91.9% of its damage in continuous walls, and other type of damage occurs in lower stories and story 18. Essentially all wall damage in building PR-6 occurs in continuous elements. Just a few “flag-shaped” walls were damaged in the 4th story. Buildings TL-4, PP-7, and RT-8 showed damage only in continuous walls. Please note that 30% of damaged walls in TL-4 had a “soft” story characteristic above the 4th story. This is because wall thickness changes in several stories from 0.40m (lower levels) to 0.20m (upper levels, Figure 3-6a). Building TO-9 showed about 40% of wall damage in continuous elements and 50% in discontinuous walls. This significant percentage of damage in discontinuous walls insinuates some of the configuration problems present in this structure. “Soft” story conditions also are present in TO-9 at the 12th and 20th stories. Note that in the J-axis that collapsed, wall thickness changes in the 12th story from 0.25m to 0.20m (Figure 3-6c). In this case, damage in “flag-shape” configurations accounts for 10% of total wall damage observed.

8.2 Beam Damage

A similar analysis is presented in Table 8-2 for beams. Shear damage represents elements showing evidence of this kind of behavior; rotational or moment based damage accounts for elements that underwent flexural cracking; continuous rotation reflects damage in the connection and punching of the connecting elements; heavy rotation implies the formation of plastic hinges at one end; and connection failures problems in connectivity with other elements.

Beams damaged in shear in building AA-1 were observed up to the 14th story. Large rotations of perimeter beams were one of the most common types of behavior observed in this building; this rotation caused hinges at both beam ends. Buildings AH-2, CM-3, and PR-6 show internal beams with shear damage in all stories, in particular door lintels, accounting for approximately 80% of beam damage in these buildings. There is also moment based damage in beams of buildings AH-2 and CM-3 in lower and upper stories at places where the plan configuration changes, accounting for about 25% of the beam damage observed; connection damage also occurs in lower and upper stories. Building PR-6 shows rotations of perimeter beams in some stories. Damage due to flexural and rotation of perimeter beams was also observed in TL-4; shear failures occurred at the 4th story where the thickness of walls decreases. Beams of building MD-5 showed severe flexural and shear cracking. The most compromised beams occurred at stories 3-5 and are contiguous to the collapsed slab area at both building ends. Rotation induced damage was present in all perimeter beams of structures PP-7 and RT-8. These beams punched the perpendicular walls and damaged the corresponding connections. A wide variety of beam damage is present in Building TO-9 including shear damage at levels above 12, large rotations due to partial collapse of the floor, leading in some cases to hinge formation, and flexural damage. Approximately 80% of beams show evidence of damage as a result of the induced moments.

Table 8-2: Type of beam damage and stories where behavior is observed

Type of damage	AA-1	AH-2	CM-3	TL-4	MD-5	PR-6	PP-7	RT-8	TO-9
	-1, 1-14	-2, -1, 1-15	-1, 1-18	4-7, 9-17	3-5	1-12	-	-	4-21
Shear damage	37.7%	79.4%	87.4%	11.3%	49.2%	75.9%	0%	0%	35.3%
	1-14, 20	-1, 2, 14-15	-1, 1-3, 18	2-17	-1, 3-5	1, 5-6	1-10	1-9	2, 5, 8-21
Rotational or moment based damage	66.2%	28.6%	22.8%	91.9%	62.2%	24.1%	100%	100%	83.1%
	1-4, 6-14, 20	2, 14-15	-1, 1-3, 18	2-17	-1, 5	1, 5-6	1-10	1-9	2, 8-21
Damage at connection	71.1%	18.0%	20.1%	90.9%	29.6%	19.0%	100%	100%	80.2%



8.3 Slab Damage

Shown in Table 8-3 is structural damage of slabs, namely, pounding in seismic joints and coupling shear-bending behavior.

As it would be expected, with the exception of PR-6 where damage is uniform in height, slab damage due to pounding was heavier in higher stories. In PR-6 the predominant movement of this building was parallel to the neighbor structure. Moreover, and as a result of torsion, the area of the building close to the seismic joint has much less damage than the opposite end. Building MD-5 shows partial collapse at both longitudinal ends in stories 3-5, being this the most important slab

damage in the structure. For PP-7 and RT-8, a large percentage of damage in slabs was due to the badly executed construction joints between slabs and walls showing cracking in all stories.

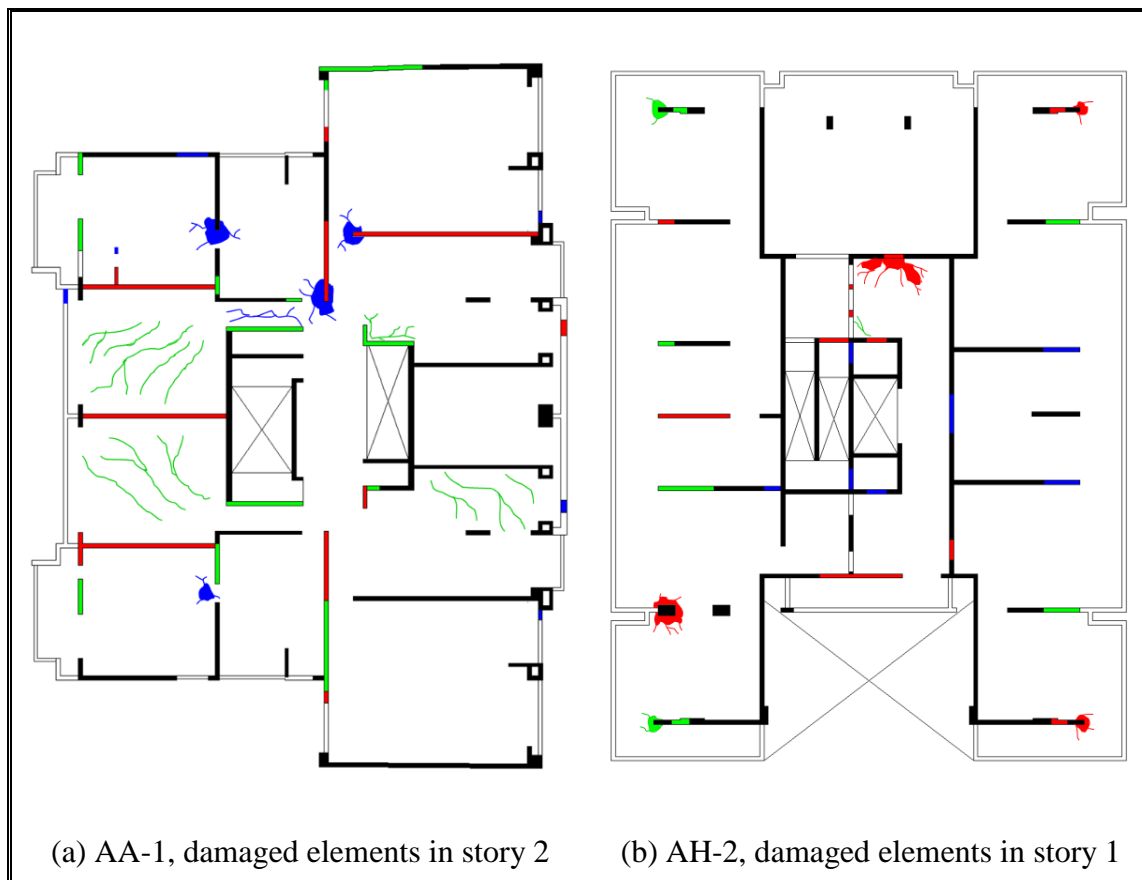
Table 8-3: Type of slab damage and stories where behavior is observed

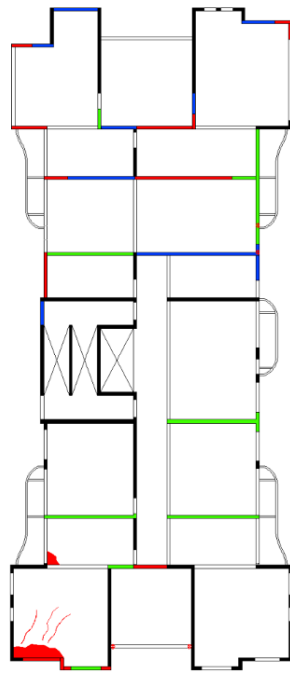
Type of damage	AA-1	AH-2	CM-3	TL-4	MD-5	PR-6	PP-7	RT-8	TO-9
	-	-	-	-	2-5	1-12	1-10	1-10	-
Slab pounding	0%	0%	0%	0%	19.1%	23.4%	6.2%	14.9%	0%
	1-19	-2, -1, 1-13	-1, 1-18	4-10, 12, 14-15, 17	-1, 2-5	1-12	1-10	1-10	11-21
Shear-bending action and other	100%	100%	100%	100%	80.9%	76.6%	93.8%	85.2%	100%

9 REPRESENTATION OF DAMAGE

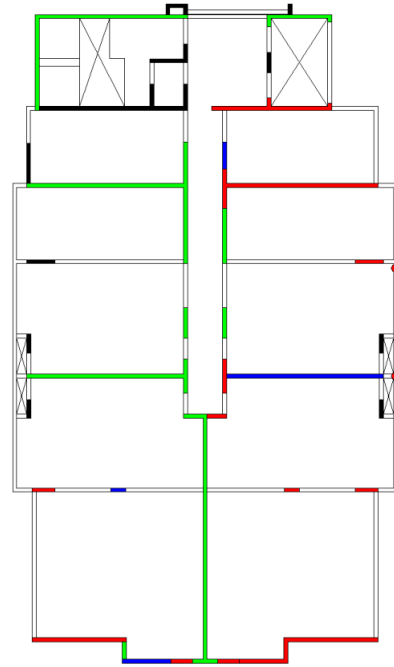
In order to help understanding the seismic behavior of these structures, the observed damage in these buildings was transferred into elevations of all resisting planes. These damage drawings include every single element damaged in the structure, the type of damage observed, and a classification of intensity based on the predefined scale. All these drawings are available and could be used in detailed future building studies.

The convention in these drawings is: lightly damaged elements (green), moderately damaged elements (blue), and severely damaged elements (red). A schematic representation of the information available is presented in Figure 9-1. See Appendix A to view the most damaged story in each structure.

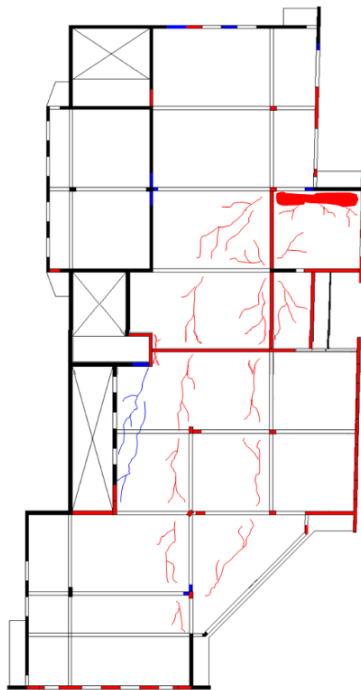




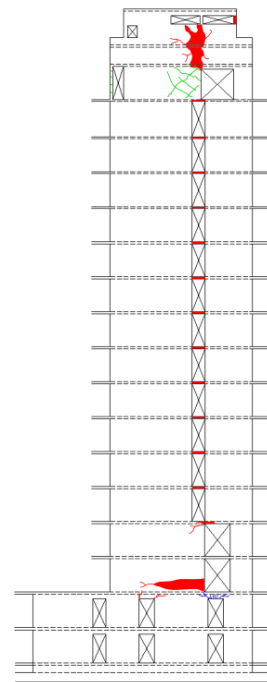
(c) CM-3, damaged elements in story 2



(d) PR-6, damaged elements in story 1



(e) TO-9, damaged elements in story 12



(f) AH-2, damaged elements in axis U

Figure 9-1: Example of damage observed in structural drawings

A comparison between damage recorded in structural drawings with real damage is observed in Figure 9-2 for axis 1A of building TO-9.

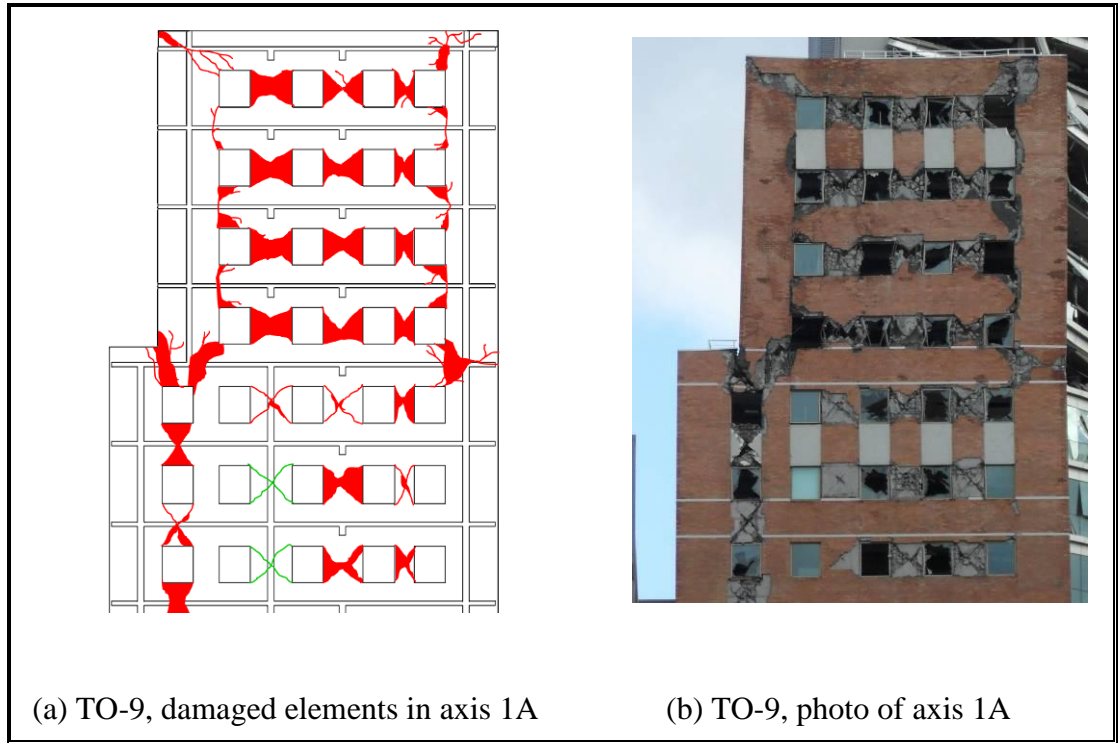


Figure 9-2: Comparison between recorded and actual damage for axis 1A of TO-9

10 TRENDS IN SEISMIC BUILDING BEHAVIOR

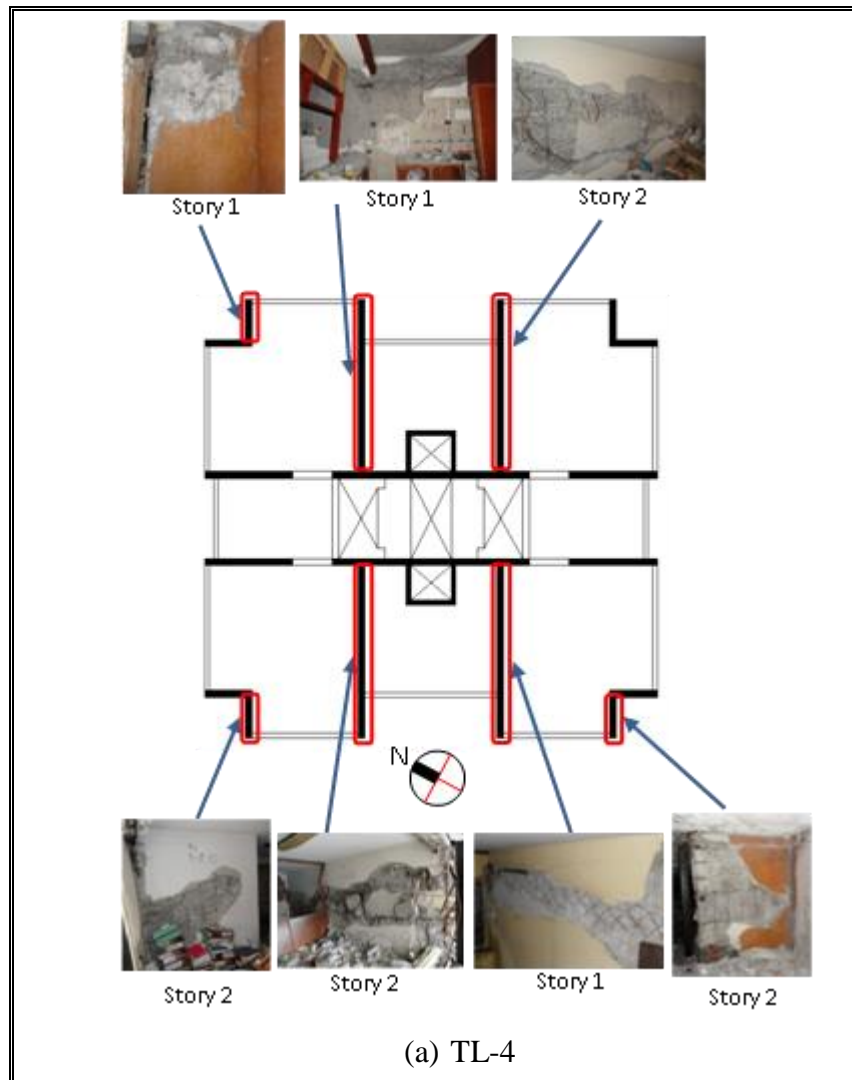
In this section an identification of some relevant and repetitive aspects observed in the damage of these structures will be presented. The intention is to provide with some interpretation of design and performance aspects that may be of use to current practice, some of them, never considered in the conventional design process. The description has been organized in 5 main areas: (i) orientation of the building relative to the ground motion axes; (ii) existence of vertical and plan irregularities; (iii) detailing of walls and construction aspects; (iv) damage propagation within the structure; and (v) energy dissipation capacity of the structure.

Note that the most typical plan architecture of RC apartment buildings in Chile usually has a longitudinal central shear wall corridor with transverse walls used to separate building apartments and interior spaces. A number of transverse shear walls run from the corridor outward creating a topology, commonly denoted locally as “fish-bone”. Results presented next are for the Concepcion buildings but the damage patterns observed also occurred in other buildings at distant places with different base motions and soil conditions. This is indeed a proof that the observed repetitive wall damage is somewhat invariant to local anomalies present in the base motions and that there is space for the hypothesis of a more general trend in this damage that has to do with design issue.

10.1 Orientation of the Building

It is apparent that the orientation of the structure relative to the ground motion had an influence in the performance of the buildings. Damage in essentially all the structures considered tend to concentrate along their shorter axes, and predominantly in the E-W direction, with the exception of MD-5 that will be

discussed later. Just as an example of this effect, shown in Figure 10-1 is a summary of the severely damaged walls affecting the stability of two of the structures, AH-2 and TL-4.



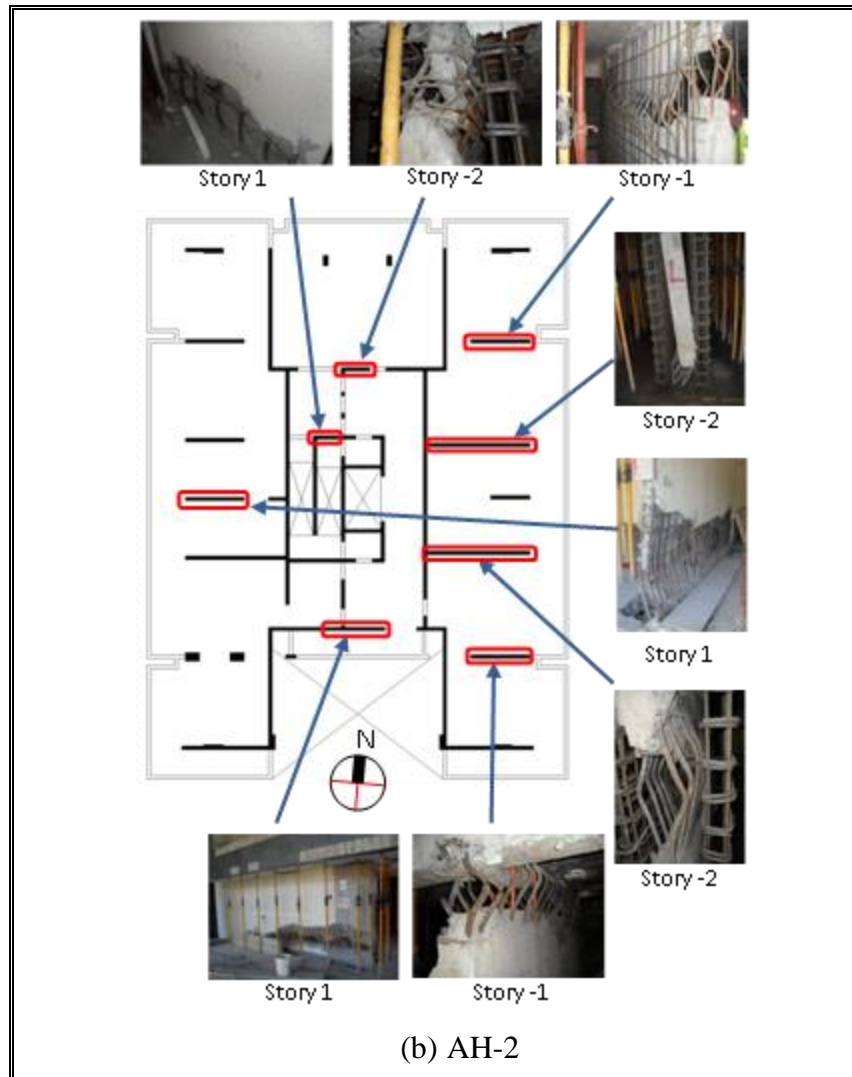


Figure 10-1: Severely damaged walls at buildings (a) TL-4, (b) AH-2

Damage is presented only for the critical story and occurs predominantly along the E-W walls. Structural damage in the perpendicular walls was minor. As a first general comment, it is quite remarkable that buildings with such severe damage in critical walls were able to survive without collapsing. One hypothesis is that the less damaged longitudinal walls may have played a role in stabilizing the structure; such is the case also for damage observed in buildings in other cities such as Santiago and Viña del Mar. There is empirical proof that some of these buildings

ended up balancing about the longitudinal corridor with indication of tension of the walls at one side of the corridor and compression driven failures at the other. The clearest example on how directionality may affect the behavior of the buildings is PR-6. This building is actually two structures perpendicularly oriented in plan, forming an “L-shaped” footprint (Figure 10-2).

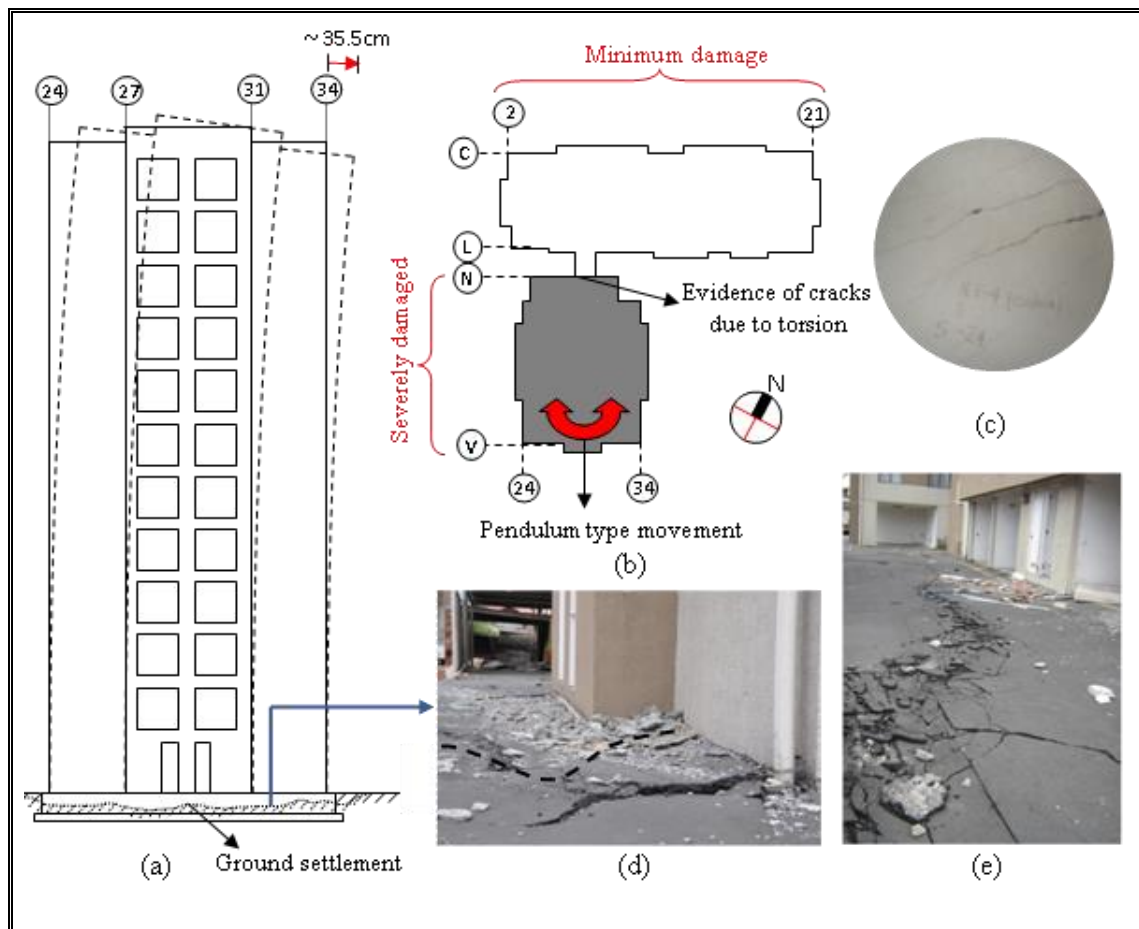


Figure 10-2: Building PR-6; (a) Schematic elevation V-W, (b) Story plan and damaged area, (c) Torsion in axis N, (d) Ground settlement near axis V, (e) Settlement in PR-6

Despite the similarity of these structures, only the building with its short axis oriented in the E-W direction suffered severe damage. Most of transverse shear walls have clear signs of tension, flexural, and shear damage, indicative of the lateral cycles underwent by the structure. Evidence of torsional cracking in the

axis N and the most severe damage near axis V is indicative of rotation of the building plan relative to the much stiffer shear wall core near axis N. As shown earlier, most of the severe damage occurs in stories 1 and 2, tilting the structure towards the East. The building is tilted almost as a rigid body with a roof displacement of about 35.5cm. This rigid body displaced shape implies perhaps foundation rotation, which is consistent with the ground settlement around the building caused by an eventual incursion into the inelastic range of the soil.

One exception to this rule of damage along the short axis is MD-5. This is an old RC building consisting of two different structures, MD-5a and MD-5b, joined by a construction joint. The main difference between buildings MD-5a and MD-5b is that structure MD-5a has two stories with double height, stories 1 and 3, while MD-5b has only one (Figure 10-3). Building MD-5a suffered larger damage than MD-5b and most of the columns collapsed along axes A and I at the 3rd story. Note that the buildings had signs of reinforcement corrosion and that they used plain undeformed bars. However, MD-5b also shows evidence of the onset of hinge formation also at columns in the 3rd story.

Moment diagrams for collapsed columns in each direction are shown in Figures 10-3d and 10-3e. Along the E-W direction, walls constrain columns at mid height. It is simple to prove that because of the constraint, simultaneous motion in both directions would result in higher bending moments at the top of the columns, exactly where hinges were formed. Although a combination of seismic excitation in both directions explains the observed damage in MD-5, the larger E-W damage intensity is still present and collapsed stories are clearly displaced in this direction (Figure 10-3b). Despite its age, this is a case where the designer must be aware of the 3D behavior of a structure, regardless of the code analysis which neglects the simultaneous action of two horizontal components for a regular structure.

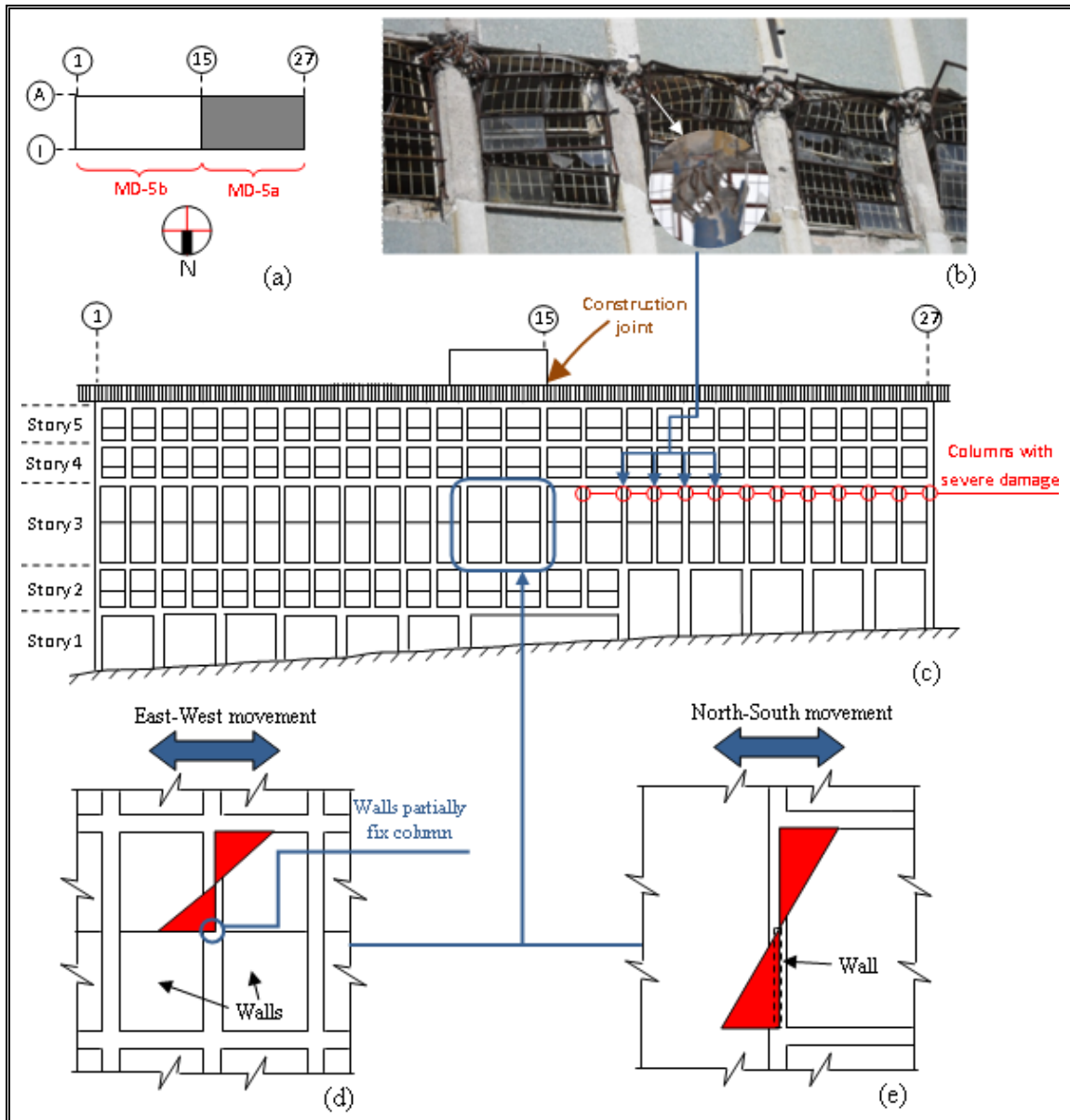
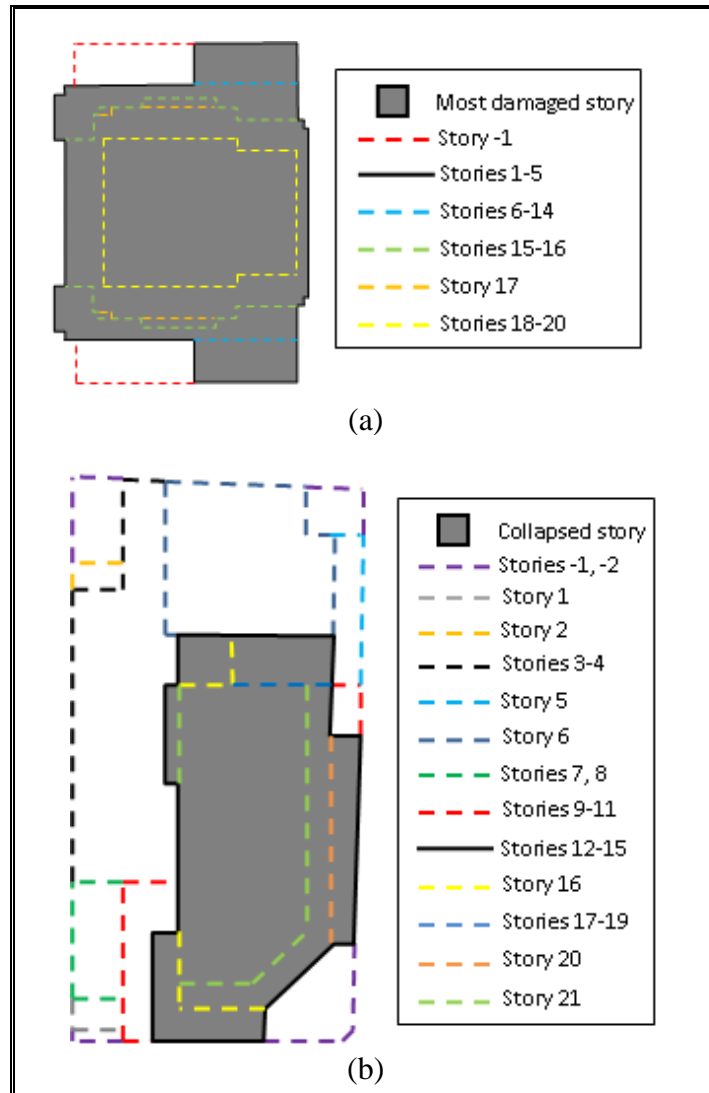


Figure 10-3: Building MD-5: (a) schematic plan; (b) collapsed columns; (c) elevation I; bending moment diagram in collapsed columns for (d) E-W, and (e) N-S

10.2 Vertical and Plan Irregularities

Another relevant aspect to look at is the existence of horizontal and vertical irregularities in most damaged buildings. Irregularities seem to be a common

denominator present in most of the observed damage patterns (Arnold, 1990). Some dramatic configuration issues are found in buildings such as AA-1 and TO-9. To get an idea of these irregularities, shown in Figures 10-4a and 10-4b are schematic plan views of these buildings, respectively, indicating by different segmented traces how the plan changes in height. As an example, shown in Figure 10-4c is a beam at the 11th story of TO-9 which dropped about 1.2m, as a result of having an inverted wall in higher stories and leading to the observed damage.



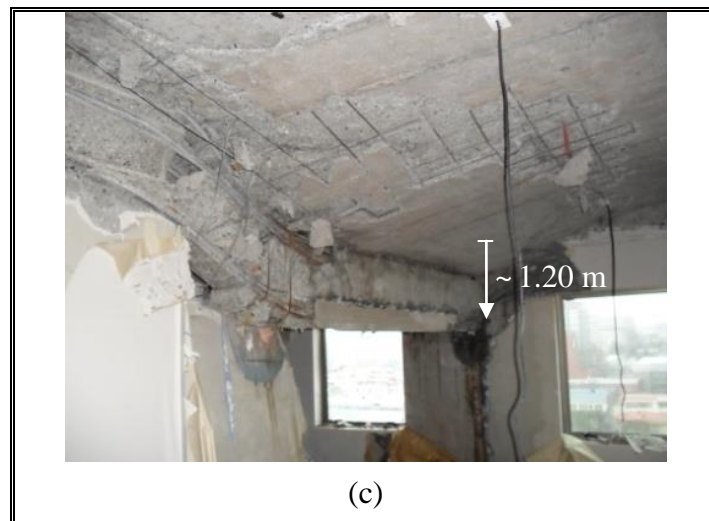


Figure 10-4: Severe irregularities in buildings (a) AA-1, (b) TO-9, (c) inverted wall and damage at the 11th story of TO-9, axis 10

A very common irregularity observed in most damaged buildings is the so called flag-shaped pattern. In that case, shear walls reduce in length due to architectural and functional constraints in the first stories (open spaces at the lobby) and parking levels (ramp and circulation requirements). A schematic view of observed damage is shown in Figure 10-5b, where large stress concentrations occur at the contraction region of the wall. It became evident that the usual design assumption that the floor slab would be capable of distributing locally such concentration does not work. Typical examples of wall damage are shown in Figures 10-5c and 10-5d. It can be shown that refining the meshes of the usual finite element models of the buildings clearly shows this concentration effect, but more important than that is to be sure in design not only how the usual transfer of shear forces occurs through the slab, but how a smoother transition of the combined axial and bending capacity is achieved since moments are similar above and below the slab, but the axial stresses below are considerably larger.

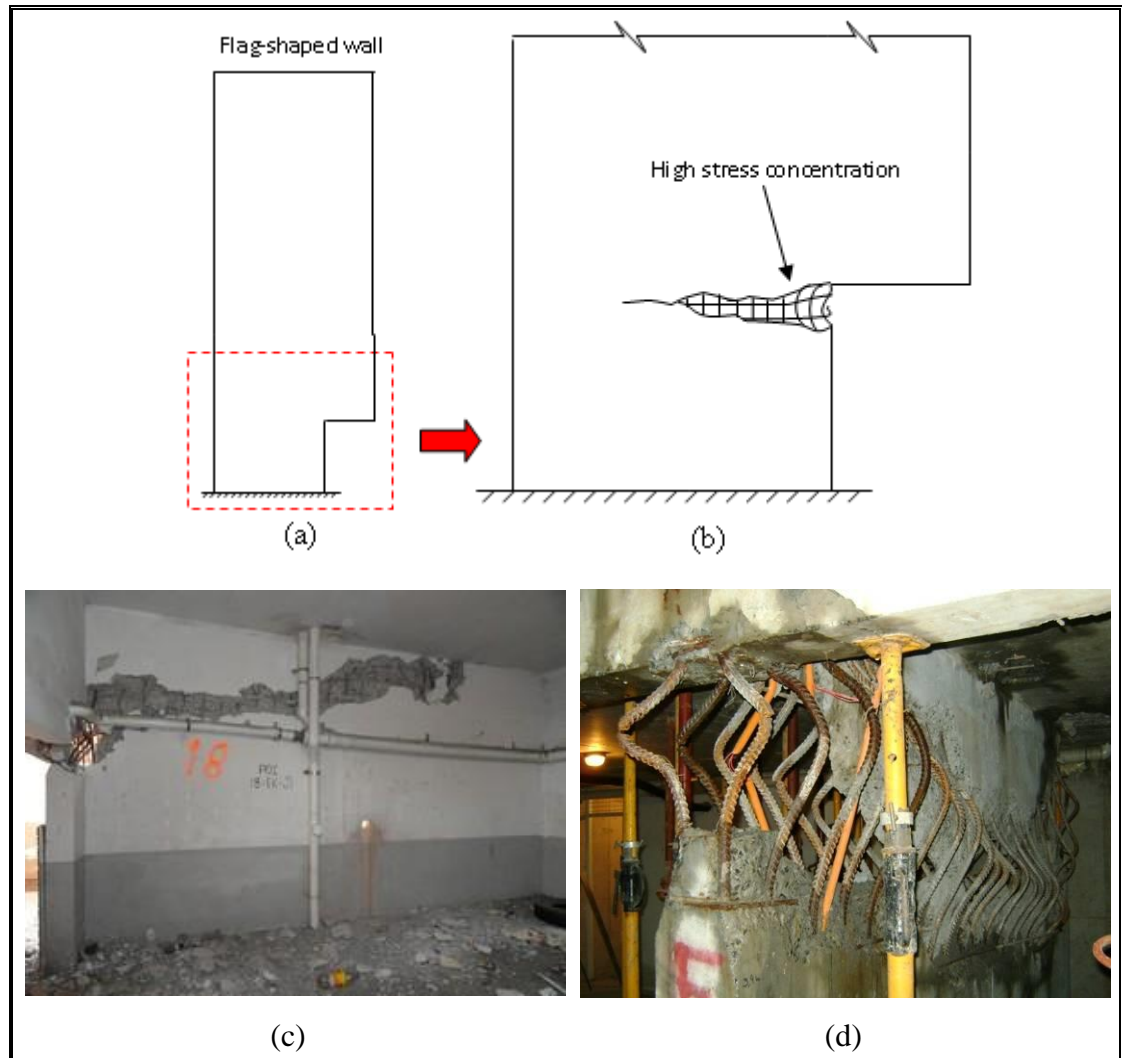


Figure 10-5: (a) Typical flag-shaped wall; (b) damage observed in flag shaped walls;
Examples at buildings (c) AA-1 and (d) AH-2

Another aspect of vertical irregularity that caused repetitive damage occurred where two different walls become coupled in upper and/or lower stories. This situation is common in the case of closing openings of coupled walls. A scheme and examples of this damage are shown in Figure 10-6. As both walls try to move independently, the coupling shear stresses between elements are very high, and tend to fracture the lintel and try to form the opening. In some cases such damage

may affect the vertical load carrying capacity of perpendicular gravitational elements causing serious problems.

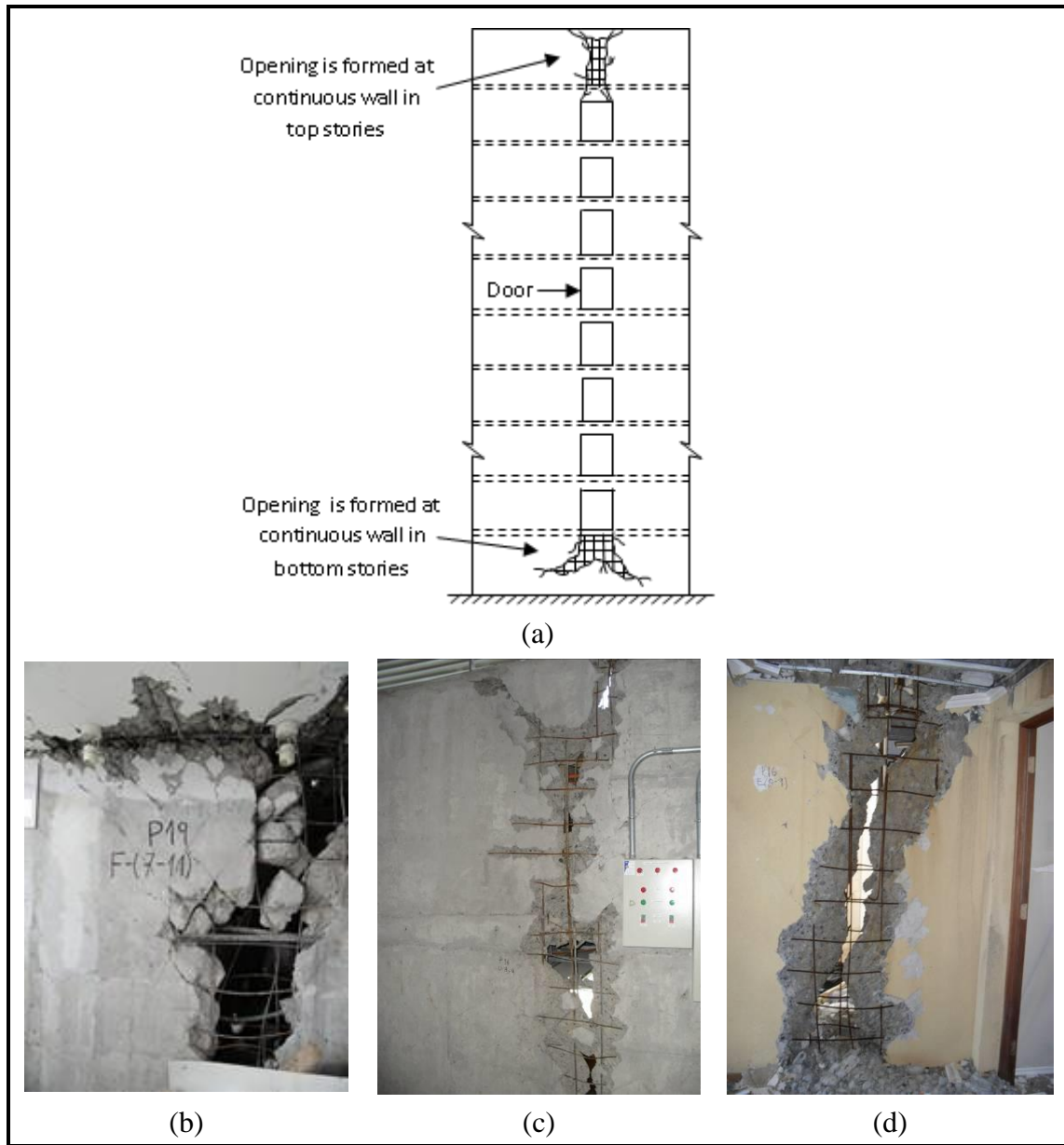




Figure 10-6: (a) Opening formation at vertical irregularities; damage in upper stories of (b) AA-1, (c) AH-2, (d) CM-3; damage in lower stories of (e) CM-3, (f) building in Chillan

Configuration issues in building AH-2 also caused unseen damage patterns. Firstly, shear failure in walls with variable thickness was observed. Shown in Figures 10-7a and 10-7b are structural drawings of stories 1 and 2, and highlighted in blue is a wall of thickness 30cm that in lower stories has at its edges walls of thickness 20cm. As shown in Figure 10-7c there is almost a perfect shear failure between the two walls of different thickness, mainly due to their relative displacement. Secondly, inspection of higher stories showed that there was slab damage at the four edges of the building, with wall punching and notorious permanent slab deformations. Apart from having the corners of the building a considerable slab area in cantilever, walls marked in red go from stories 2 through 15 and do not reach story 1 (Figure 10-7b). Slabs flapped up and down freely with the help of these discontinuous elements, punching walls nearby and leaving permanent deformation at all stories above 2. Although this damage due to the configuration is localized and completely avoidable, reparation costs are high and the building will probably be demolished, at least in part, because of the settlement of floors.

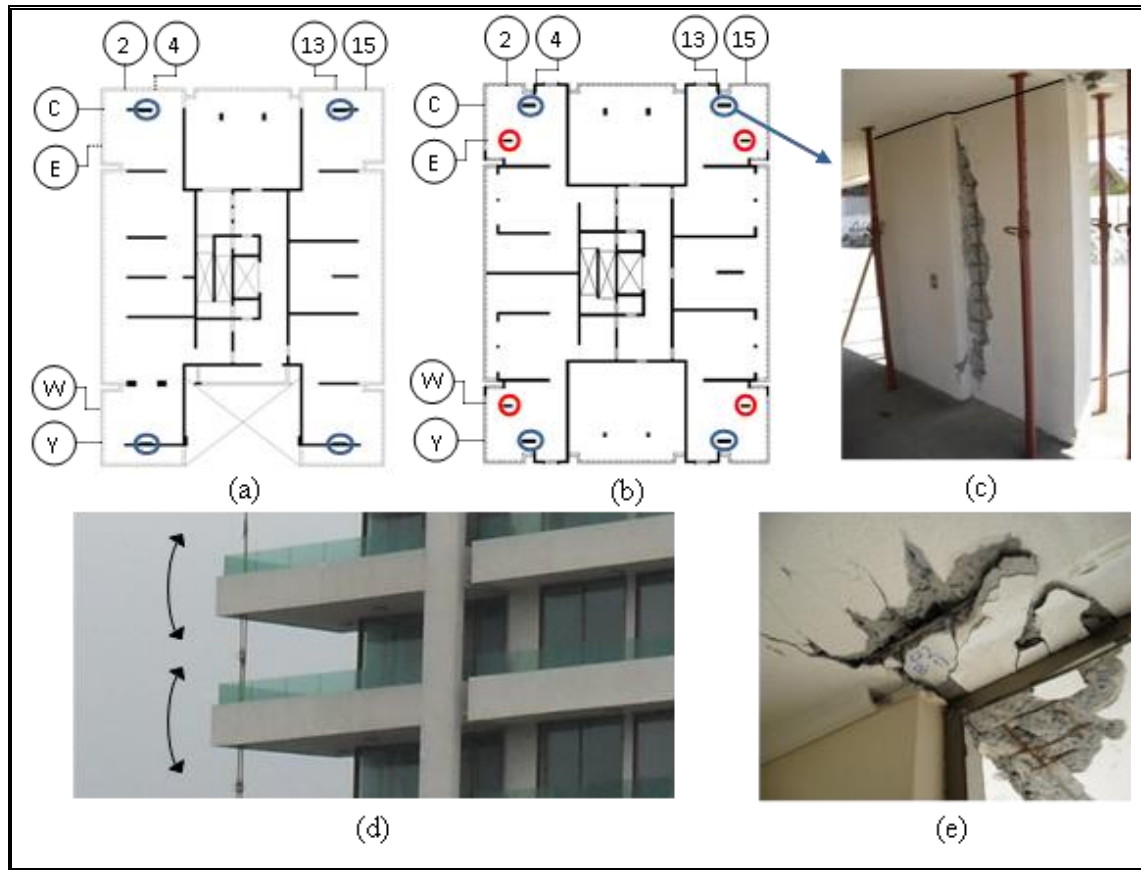


Figure 10-7: Building AH-2. (a) Story 1 of AH-2, (b) story 2 of AH-2, (c) shear damage in first story wall, (d) slab movement and (e) punching of walls through slabs

In several buildings, damage due to the configuration issues and support of beams was also observed. Because beams carry sometimes considerable gravitational load, this effect may compromise the stability of the structure. One remarkable example is beams supported by orthogonal walls. Cyclic motion in these buildings made beams to pull out and punch the walls as shown in Figure 10-8. Another case is perimeter spandrel beams coupled with transverse shear walls. Damage in this case occurred due to the direction of motion, mainly at buildings PP-7 and RT-8 (Figure 10-8f). It is clear that modeling of these deep beams as frame elements in a structural model would not capture the real state of stress in the connection.

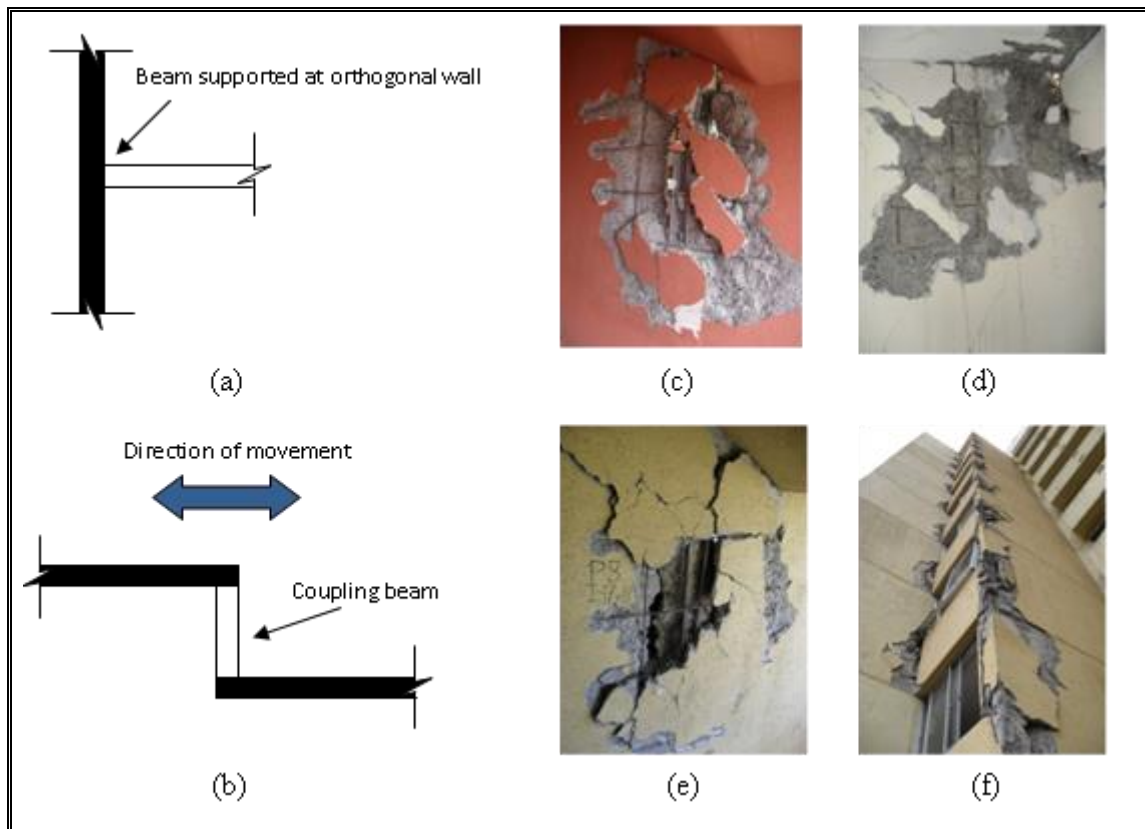


Figure 10-8: (a) Beams supported at orthogonal walls and (b) beams coupled with transverse shear walls. Beam punching at (c) RT-8, (d) TO-9, (e) PP-7. (f) Damage in coupling beams of PP-7

10.3 Structural Detailing of Walls and Construction

Typical Chilean construction changed after the 3-M, 1985 earthquake. Buildings became taller and in some cases walls became thinner as a result of having no limit in the wall axial forces. Previous to 1985 wall thicknesses of 30cm and above were common for mid-rise RC buildings (Wood, 1991), while in the current buildings the average thickness was only 20cm (Westenenk et al, 2011), and in several cases structural walls were as thin as 15cm. This proved to be a general problem for this

earthquake, as thin walls with high flexural and axial stresses were severely damaged in a brittle manner in this earthquake.

As bending occurs, the boundaries of the wall are subjected to very high axial stresses due to the combination of axial and flexural demand. Small areas of the walls were partially confined—and most of times not confined because the Chilean seismic code (NCh 433Of.96, 1996) excluded the ACI confinement requirements. Thus, at boundaries cover concrete spalls-off and longitudinal boundary reinforcement buckles due to the large stirrup spacing and poor detailing. Consequently, the wall loses considerable flexural capacity while keeping the axial load. As the wall cycles, it is the web reinforcement the one that pretends to carry the bending moment, but the demand exceeds the bending capacity of the wall, the wall lateral cover spalls-of, the web reinforcement yields and fractures, and the wall cuts in the tension part of becomes unstable in compression. There is evidence also that this occurs in a brittle manner, which is consistent with the high axial loads, and that the “unzipping” crack quickly propagates throughout the length of the wall. Due to the localized nature of the failure, the building is not capable to develop large ductility or energy dissipation making the assumption of the R-factor used in design unwarranted. Naturally, if the wall has a large flange in compression as a result of a perpendicular longitudinal wall, no damage occurs at that side, which also demonstrates that compression stresses played an important role in the failure pattern. Shown in Figures 10-9a through 10-9d are examples of “unzipping” wall damage for the buildings considered.

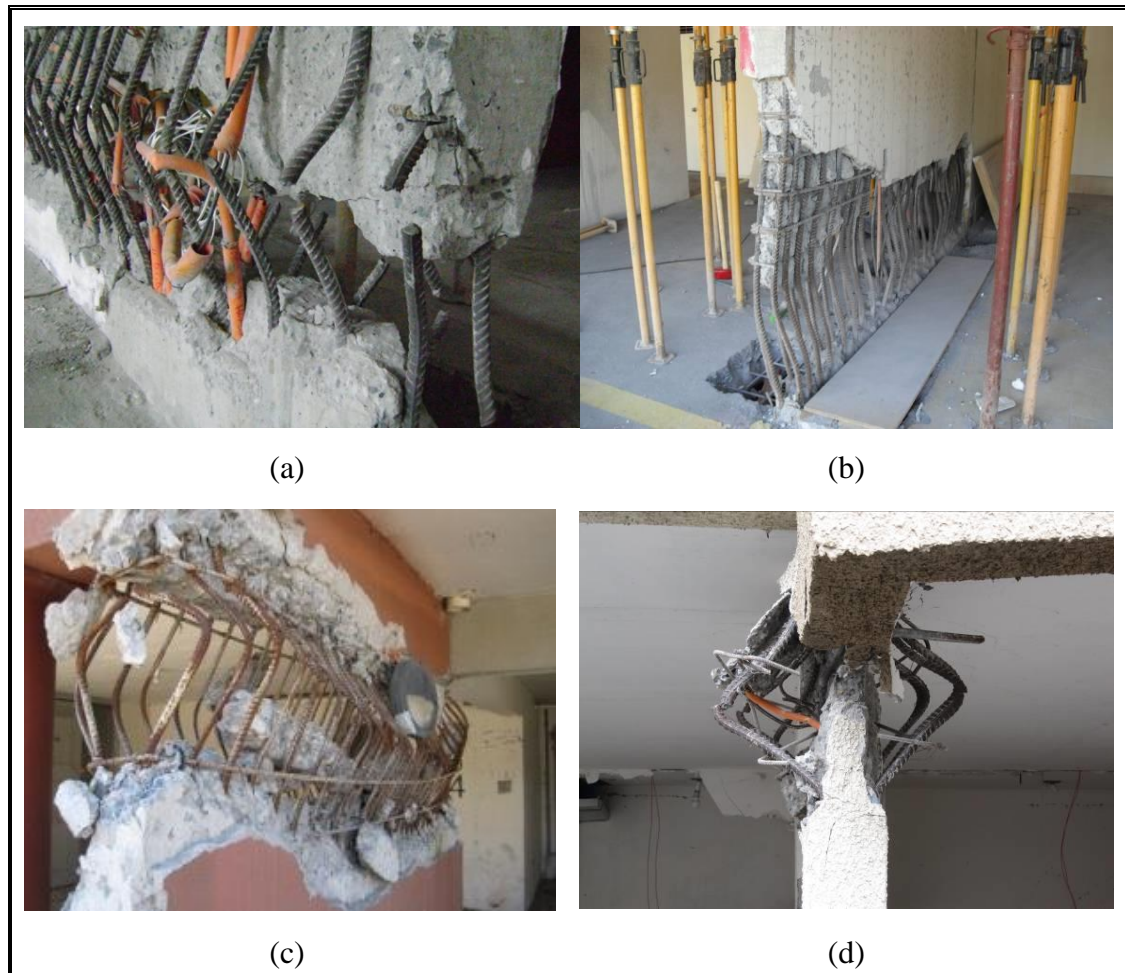


Figure 10-9: Typical thin wall failure. Buildings (a), (b): AH-2, (c) CM-3 and (d) PR-6.

Serious problems regarding reinforcement detailing and construction were observed in the analyzed buildings, especially TO-9. Poor anchorages between beams and walls were repetitively observed. Longitudinal reinforcement of beams was anchored outside of the confined area of the wall, in the concrete cover. This happens because beams have the same thickness of the wall and there is no space to anchor the reinforcement inside the web of the wall. Moreover, building TO-9 showed severe construction problems finding beams without stirrups or that have been cut. As mentioned earlier also, confinement of the boundary elements in shear walls was poor or inexistent (Wallace, Moehle, 1995; Wallace, Moehle, 1992) due to the elimination of the requirement in 1996 (NCh 433Of.96, 1996).

The typical detailing in boundaries of walls considers the mesh with legs bent in 90° but without hooks around the longitudinal bars. This confinement proved to be highly insufficient; other examples of poor detailing and construction are shown in Figure 10-10.

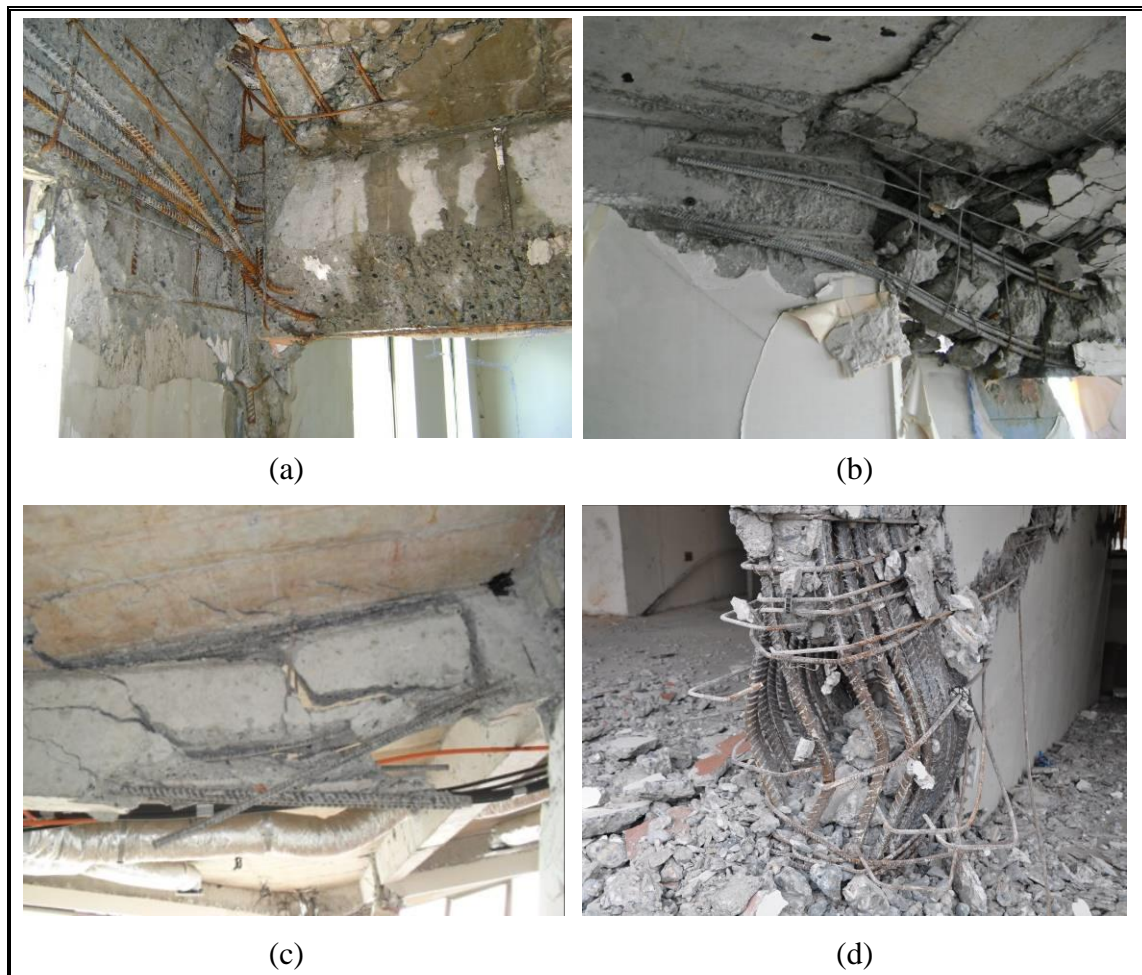


Figure 10-10: (a) Inadequate anchorage of beam-wall connection, (b) reinforcement outside of the confined area, (c) unconfined longitudinal reinforcement and lack of stirrups, (d) typical observed hooks.

10.4 Inter-Story Damage Patterns

In some cases, building damage involved more than one story. This is somewhat difficult to capture in design because structural models treat building elements as units in each story. However, it is evident that fracture will occur in the simplest and least demanding way to the structure. We have denoted this phenomenon as multistory damage. Shown in Figure 10-11 is the case of CM-3 where three of the four corners of the building experienced this behavior. Buildings should be analyzed and designed as 3D systems, considering all possible failure mechanisms crossing stories and connecting weak elements in neighbor stories.

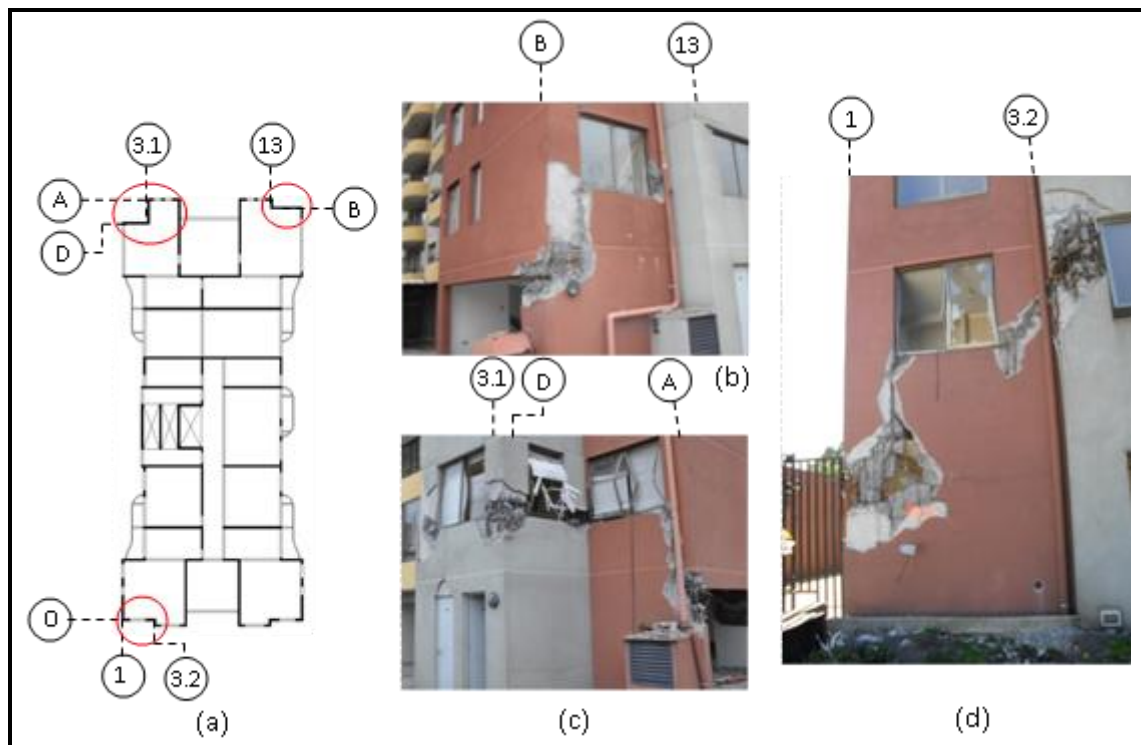


Figure 10-11: Multistory damage at CM-3. (a) Structural plan of story 2, (b) N-E corner, (c) N-W corner and (d) S-W corner.

Moreover, damage propagated not only between stories, but also along elements of the same story. An example is shown in Figure 10-12, where flexural damage at the external walls caused shear damage in the central portion of the wall of building CM-3. Figure 10-12d shows the flexural damage at one of these edges.

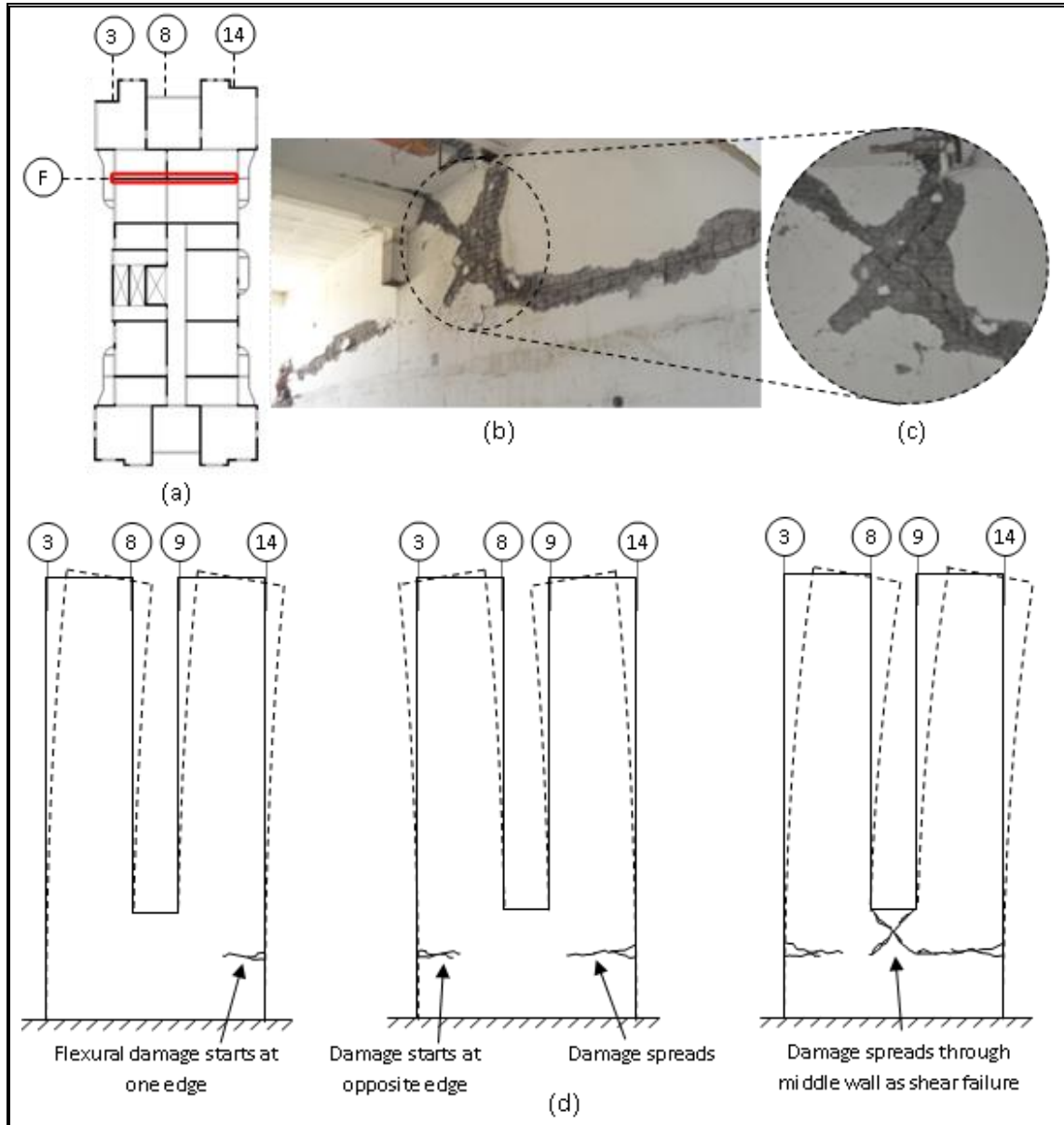


Figure 10-12: (a) Location of walls in plan CM-3, (b) observed damage, (c) shear failure at central wall and (d) induced damage in elevation F.

It is apparent that is not enough to analyze in design each element separately, since damage in one element could lead to a different behavior and severe damage in others. This observation and behavior repeats among buildings. Multistory damage propagation is also apparent in building PR-6 (see Figure 10-13d). Propagation of damage into orthogonal elements and slabs was also observed. Shown in Figure 10-13 is the case of building PR-6. Specifically, Figure 10-13b shows how shear damage started on a wall along axis V, propagated through the slab (zoom at Figure 10-13c) and reached a wall along axis W. The effect of shear at the central part of the wall together with flexural and axial stress at the boundaries of the wall lead to the peculiar trace of the crack shown in Figure 10-13c.

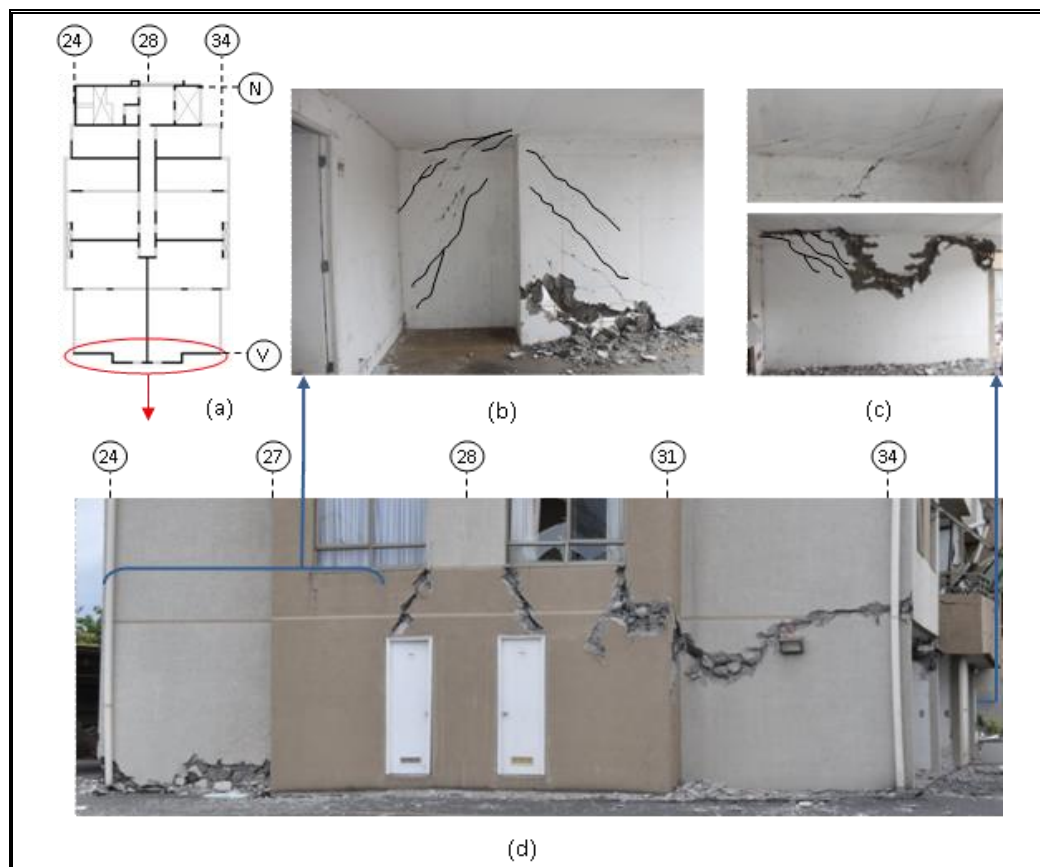


Figure 10-13: Building PR-6. (a) Structural plan of 1st story, (b) shear damage propagation through the slab, (c) zoom of damaged slab and superimposed flexural and shear stress cracking. (d) Multistory damage.

10.5 Energy Dissipation Sources

A final aspect worth mentioning is the true energy dissipation capacity of current shear wall structures. Apart from using higher axial loads, thinner walls, and lower densities of shear walls in plan, the architectural topology of the Chilean apartment building also changed by drastically reducing or even eliminating lintels. The justification to do so was that they are essentially impossible to design, or even if we could, they end up being so heavily reinforced that why to bother. Unfortunately, with this change a very good source for energy dissipation in the structure was eliminated. With that change in practice, the seismic reduction coefficient (R factor in the Chilean code) should have been reduced because it was calibrated for a different structural configuration that considered coupling beams. Since the structure requires dissipating energy to stop vibrating, in many cases slabs turned into flat coupling beams and underwent severe structural damage. Examples of such behavior are shown in Figure 10-14. With the effect also of increasing building flexibility, some non-structural elements suffered heavy damage.





Figure 10-14: Slabs working as coupling beams in buildings (a) AA-1, (b), (c) AH-2 and (d) PP-7.

The absence of coupling beams makes non-structural components in a building to increase their role as energy dissipators. Indeed, in buildings PP-7 and RT-8, non-structural elements may justify the different intensities in the observed damage of these two identical structures. As mentioned elsewhere, RT-8 showed larger damage than PP-7, although they have the same nominal plans, same orientation, and are next to each other. Building PP-7 had very stiff partition elements made of plaster; RT-8 had very flexible partitions. While non-structural elements in PP-7 were practically shattered, in RT-8 were practically undamaged. Although it may be somewhat speculative, it seems that the energy dissipation coming from non-structural elements in PP-7 contributed to reduce structural damage as opposed to RT-8. This behavior shows some relevance since building PP-7 will be saved and RT-8 will be demolished.

To reinforce this concept, it is worth mentioning that all buildings in Chile with seismic isolation or energy dissipation devices showed no damage in contents or structure. As an example, shown in Figure 10-15 is the Titanium tower, the highest building in Chile at the time of the earthquake, and its dissipation devices responsible in part of the outstanding behavior. The metallic dampers used considered 72 (in the longitudinal direction) and 84 (in the transverse direction) C-shaped plates each, and every single of the plates yielded substantially in each of the 45, 280-ton, metallic dampers. The total

energy dissipated by these dampers during the earthquake has been estimated in 2200 Joules for the longitudinal direction and 2800 Joules for the transverse direction.

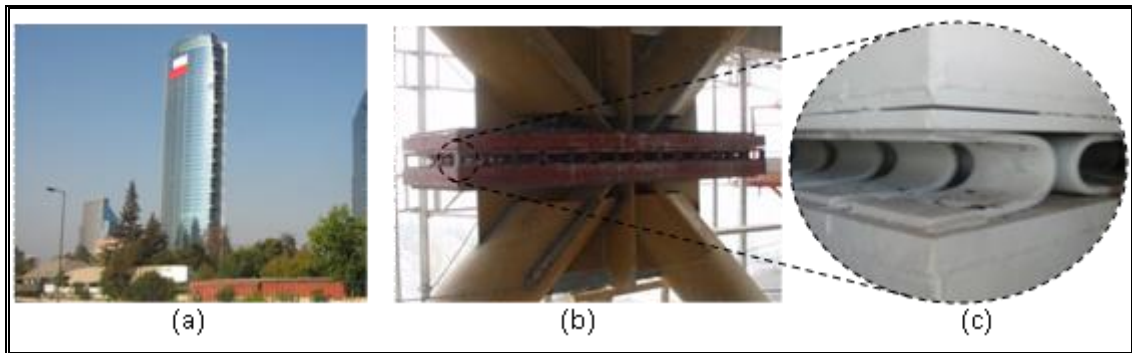


Figure 10-15: (a) Titanium building, (b) 280-ton energy dissipation device used and (c) C-shaped dissipators.

11 INTERPRETATION OF TO-9 BUILDING

This section describes the behavior of one particular case within the group of these 9 buildings, mainly because it has additional aspects of interest to researchers and practitioners. Although its stability condition is precarious, building TO-9 was inspected completely, element by element, from which videos are available.

Building TO-9 had a main collapse at story 12, where a section of the building fell and dragged with it the upper stories. Shown in Figure 11-1 is an external view of this building. North and West elevations (Figure 11-1a) show very little damage as compared with the East and South elevations (Figures 11-1b and 11-1c). In addition to this main collapse, there are two other partial areas of collapse of the building at stories 16 and 20, which can be seen from the East side of the building (Figure 11-1b). Note that in these stories there are important setbacks, so the location of irregularities matches with that of the collapsed areas. The main collapse in axis J is shown in Figure 11-1e; walls between axes 4 and 7 dropped one story while elements between axis 9 and 10 dropped half a story. As mentioned elsewhere, walls in axis J change their thickness from 25cm to 20cm at story 12. On the other hand, this axis is out of plumb by approximately 13cm in lower stories (Figure 11-1c). Another repetitive damage present in most of the structures is the short-column effect. The most severe case is shown axis 1A (Figure 11-1f), where short perimeter walls between spandrel beams were severely damaged in shear. Between stories 12 and 15, this axis presents a mechanism that tilted slightly toward the collapsed area. The slab in this structure is tying the whole damaged part of the structure to the core walls and prevents it from collapsing. Once the short walls failed, the spandrel beams worked as a long span moment frame, causing the hinges and damage at both ends (Figure 11-1f). It can be shown that stories 20 and 21 are in critical condition, as columns farther from the core are all severely damaged and slabs are highly deformed. Practically these stories are hanging in the remaining of the damaged beams and slabs. Figure 11-1g shows the condition of the 21st story from outside.



Figure 11-1: Building TO-9. (a) West view, (b) East view, (c) South view and deformed axis J, (d) top view, (e) main collapse at story 12, (f) short column damage along axis 1A and (g) condition of 21st story.

By analyzing the structural drawings of the building it can be seen that the 12th story shows a stiff section that remained with light or no damage (Figure 11-2a); axis C can be seen undamaged on the west face of the structure (Figure 11-1a). The collapsed zone happens to be in a much more flexible area, with a number of short walls and columns, which have larger cross sections in lower stories. During the inspection, the interior of the building shows signs of wall torsion in axis C (Figure 11-2a), which could be attributed to post-earthquake events. Shown in Figures 11-2b and 11-2c are the partial collapses at stories 16 and 20, respectively, mainly due to columns being completely displaced out of their axes, losing the support of the slab. The collapsed area in story 12 is enclosed by axes 4 and 7, and axes G and J, with the slabs being supported at the ceiling of the 11th story. Columns in this area were pulverized as observed in Figures 11-2e and 11-2f. All other elements were driven to this deformed shape, as it is shown in Figure 11-2d.

Damage in all internal building elements increases in height. A short summary is as follows: little to no damage was observed in stories -2 through 4; severe damage in a single wall is present in the 5th story; stories 6 through 11 show increasing damage in height; the main collapse at the 12th story augmented damage in every upper story, especially slabs and columns. As a reference, shown in Figure 11-3 is the inside condition of some stories.

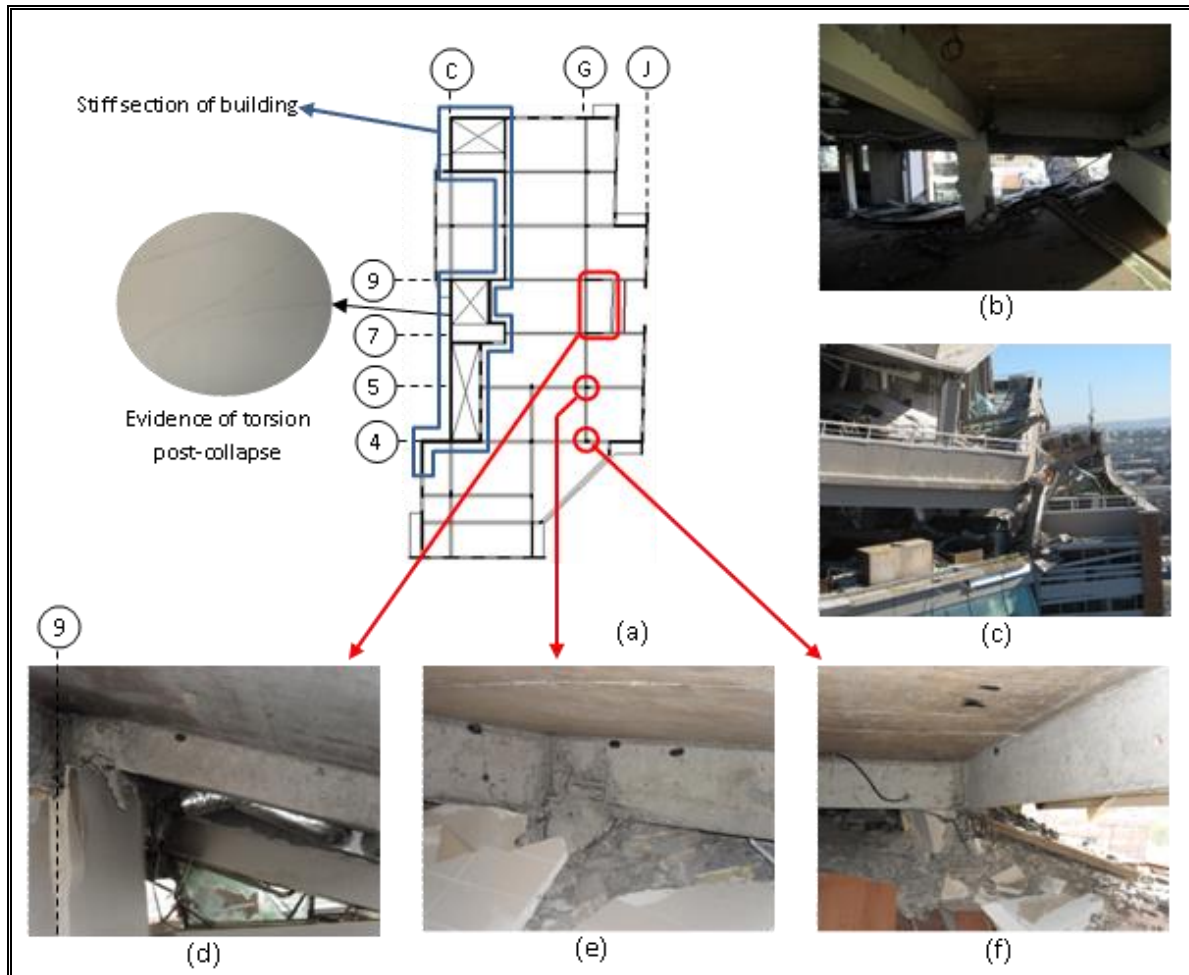


Figure 11-2: Building TO-9. (a) Structural plan of 12th story, (b) partial collapse of the 16th story, (c) partial collapse of the 20th story, (d) beams at 12th story, (e) column in axes G-5 of 12th story and (f) column in axes G-4.

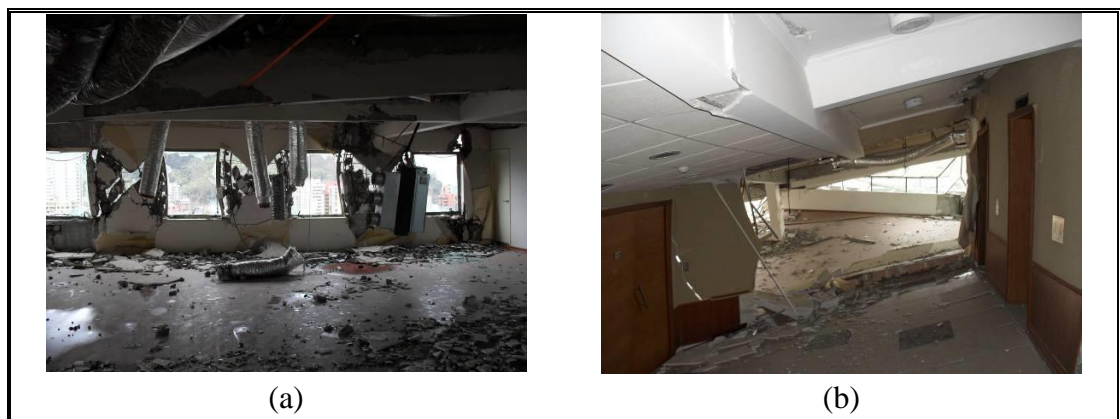




Figure 11-3: Building TO-9. (a) Axis 1A at story 14, (b) slab deformation at story 16, (c) damage at 18th story, (d) severely damaged column at 21st story.

Internal inspection was possible because the central core did not show important damage in height. The exception to this are stories 11 and 12, where severe damage of a wall on axis 4 was observed (Figure 11-4b). Interestingly, this wall shows shear cracking in opposite direction to the one that would have been predicted by the type of failure of the structure. To explain this damage, irregularities become important once again. This wall is a flag-shaped wall that underwent flexural-axial damage in a corner of story 11 (Figure 11-4a). As before, damage in story 11 reduced the axial capacity of the wall producing an unzipping failure. As a result, the axial stresses were too high and the wall in story 12 split from the lower part of the flag shape through a shear failure. Shear induced damage is shown and explained in further Figure 11-4. This damage makes the building more flexible at the 12th story creating a sudden change in lateral stiffness. There is intuitive consensus that these types of irregularities and setbacks in the building play a crucial role in its collapse.

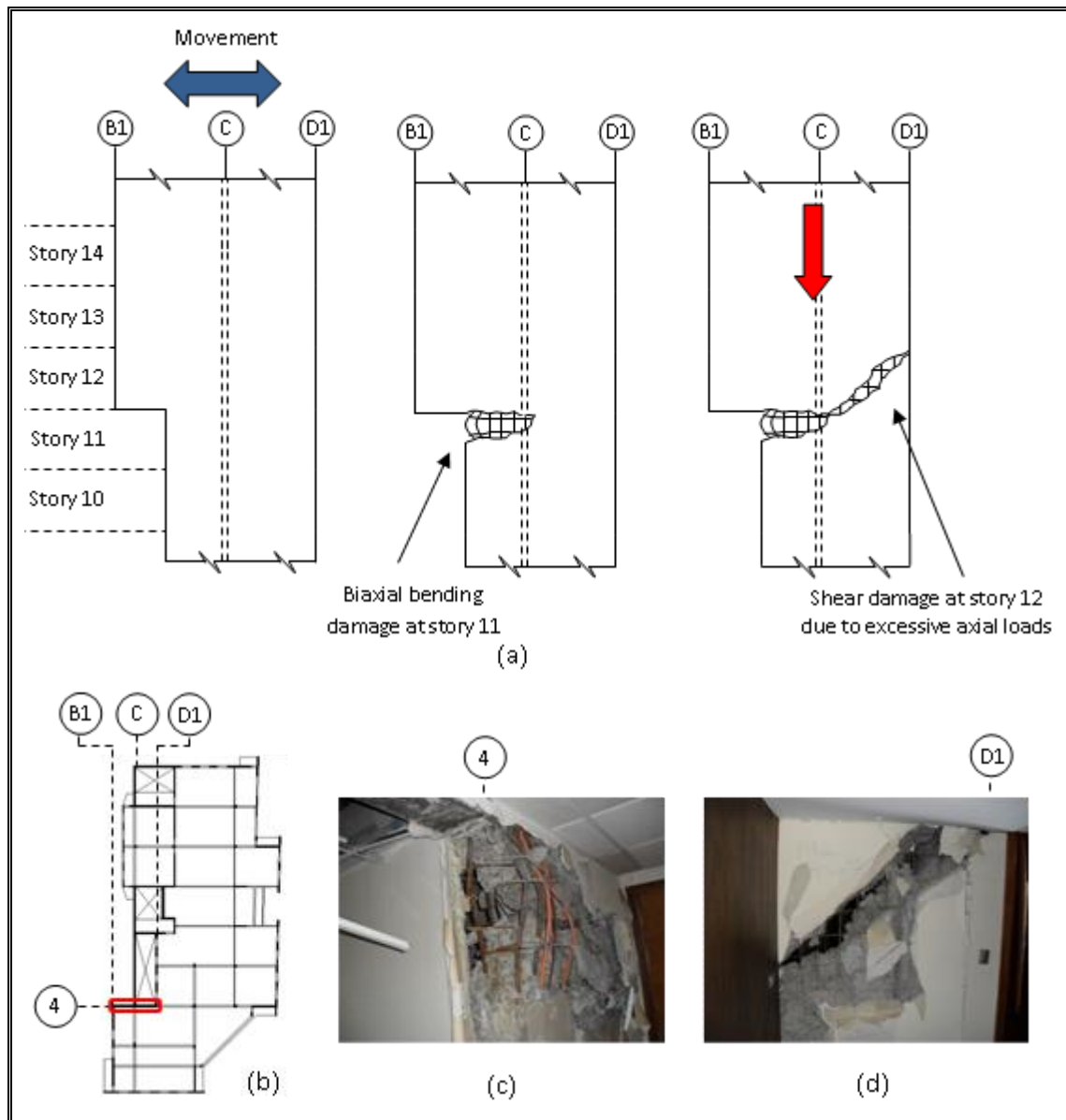


Figure 11-4: Important damage at core. (a) Explanation of observed behavior, (b) location of wall in story 12, (c) flexure-axial damage in story 11, (d) shear induced damage in story 12.

12 BUILDING CODE TYPE ANALYSIS

A thorough code review of the structural design was performed for buildings AA-1, CM-3, PR-6 and TO-9. Some of these results will be discussed next as they provide a first glimpse of the nominal structural condition of the structure. Please note that the code used in this review was NCh433-1996, used in its design. This code makes reference to ACI318-95 (American Concrete Institute Committee 318, 1995) for the design of RC elements.

For the sake of brevity just Demand/Capacity (D/C) ratios will be presented in shear and flexure of walls. For beam design, D/C ratios were calculated in shear, positive, and negative bending. For each different type of behavior, D/C ratios were classified as shown in Table 12-1.

Table 12-1: Grouping of D/C ratios

Properly designed elements	Slightly deficient elements	Moderately deficient elements	Significant strength deficit
D/C ratio < 1	$1 < \text{D/C ratio} \leq 1.25$	$1.25 < \text{D/C ratio} \leq 1.5$	D/C ratio > 1.5

12.1 Walls Analysis

For the performance evaluation of walls in shear, D/C ratios are defined as $V_u/\phi V_n$.

Results for the four groups defined in Table 12-1 are shown in Figure 12-1 as a percentage of analyzed elements in each story.

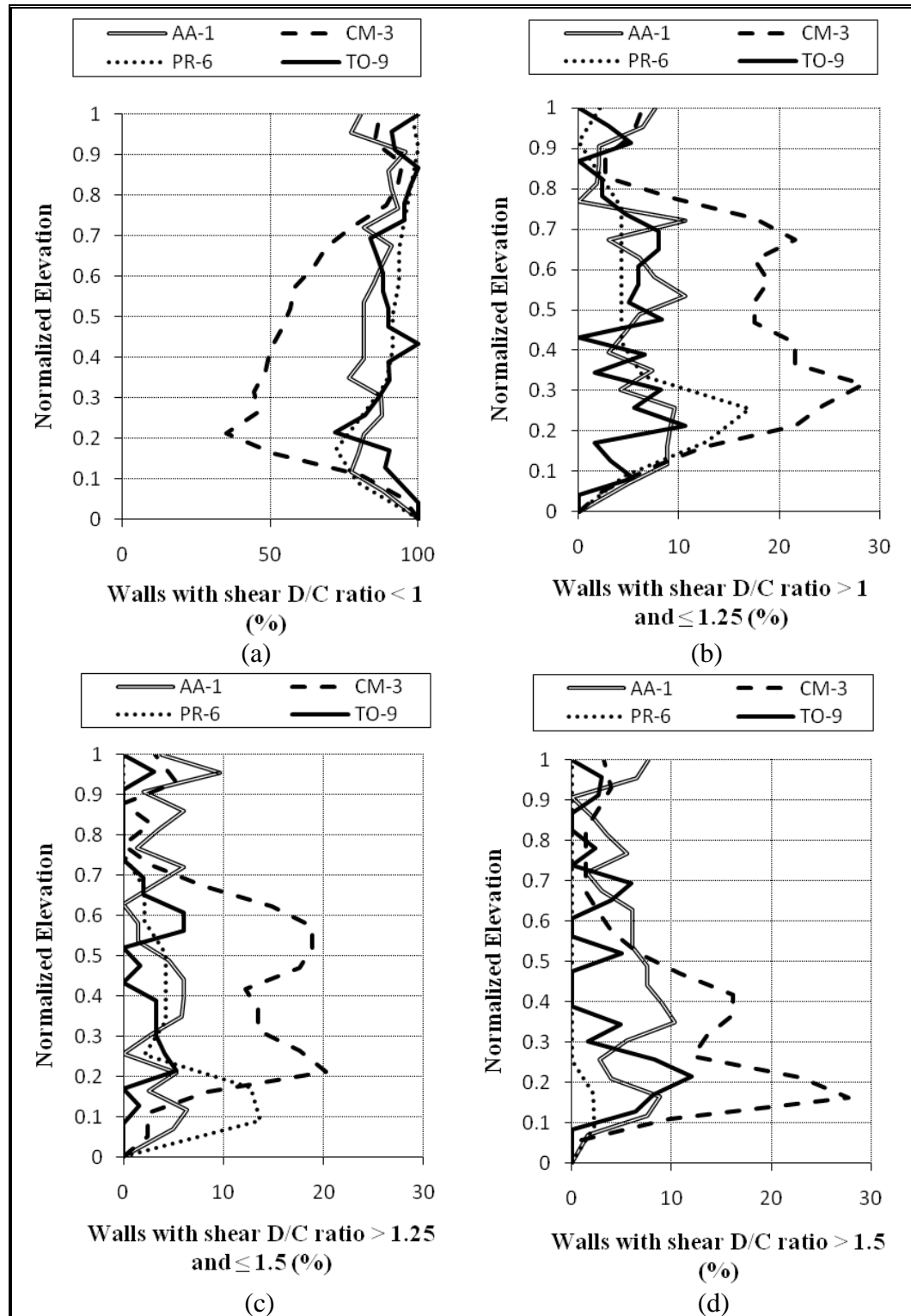


Figure 12-1: Percentage of analyzed walls with shear D/C ratios within each group

Buildings AA-1 and TO-9 show shear D/C ratios of every category well distributed among different stories. PR-6 shows higher D/C ratios in lower stories while CM-3 presents higher values at lower and intermediate levels. In building AA-1 walls with significant strength deficit were found on almost all stories (except on story 18), with higher percentages concentrated in stories 1, 2, 6, 7, 8 and 9. For CM-3 elements with significant strength deficit are focused on stories 2 and 3, reaching approximately 25% of analyzed walls on these stories. PR-6 shows maximum percentages for the most severe category in stories 1 and 2, which matches the observed damage, while TO-9 shows maximum code deficiencies on the 3rd story.

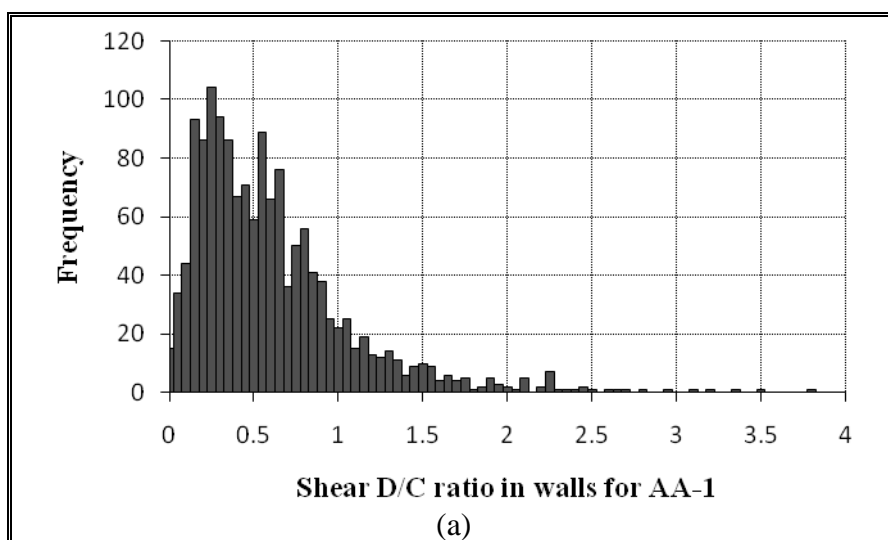
Summarized in Table 12-2 is the distribution of D/C ratios, its mean, and standard deviation for the 4 buildings analyzed. The first observation is that buildings show elements with D/C ratios greater than one, which implies a deficit in the code design. However, the number of elements with D/C greater than one is not large in general, which implies that the design of these structures is not balanced in terms of D/C requirements and just a few elements cause essentially the high level of damage observed. The building with the largest proportion of D/C ratios greater than 1 is CM-3, and it is also the one with the greatest proportion of elements with $D/C > 1.5$.

Table 12-2: Total results for shear in walls

ID	N° of walls analyzed	$D/C < 1$ (%)	$1 < D/C \leq 1.25$ (%)	$1.25 < D/C \leq 1.5$ (%)	$D/C > 1.5$ (%)	$\mu_{D/C}$	$\sigma_{D/C}$
AA-1	1458	85.87	5.76	3.43	4.94	0.58	0.48
CM-3	1383	67.25	14.68	9.69	8.39	0.82	0.47
PR-6	593	90.89	5.23	3.54	0.34	0.50	0.33
TO-9	1152	89.67	4.86	2.08	3.39	0.52	0.38

Building CM-3 shows a significant lower percentage of walls properly designed than other buildings (67.25 % of analyzed elements against approximately 90% of analyzed elements in other buildings). Mean values $\mu_{D/C}$ show the same tendency,

reaching the highest value of 0.82 for building CM-3. Note that PR-6 has a significant lower percentage of walls with severe strength deficit in shear behavior (lower than 1 % of analyzed walls), while CM-3 has approximately double the percentage of buildings AA-1 and TO-9. For building AA-1, walls with severe strength deficit are located on axes 7, 8, I and H, between stories 5 and 13. For building CM-3, several walls with significant strength deficit correspond to short perimeter walls coupled with spandrel beams, thus leading to high shear stresses. In PR-6, moderate deficiencies occur in axis W. For TO-9, axis J is the one that concentrates the highest D/C ratios, which coincides with the axis that collapsed at story 12. For buildings AA-1, CM-3 and TO-9, the highest D/C ratios are found in zones with vertical irregularities. D/C ratios were organized in intervals of 0.05 and frequencies regarding each D/C ratio are shown in Figure 12-2 as histograms for every building.



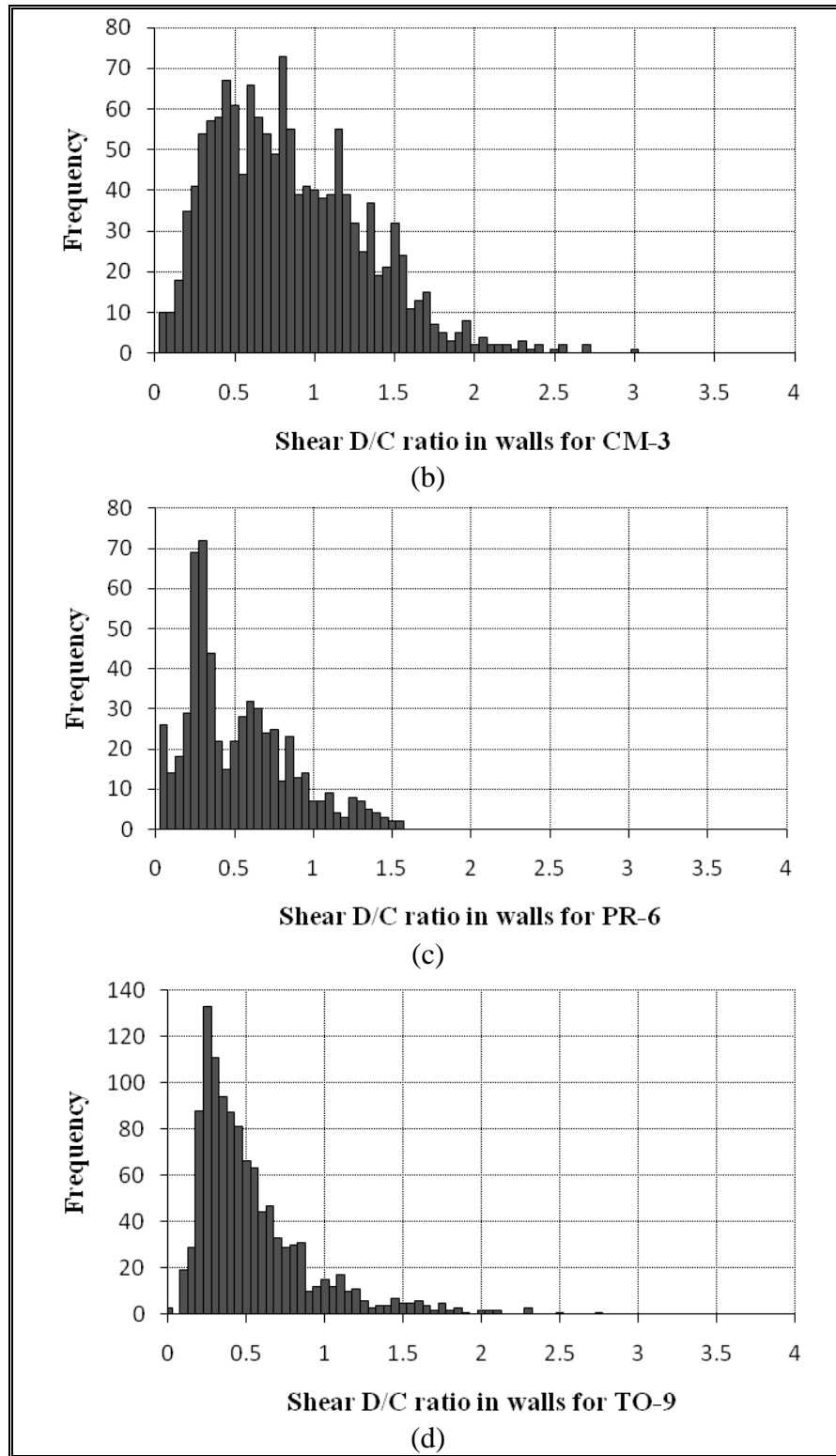


Figure 12-2: Shear D/C ratios in walls as histograms

All buildings show distributions with a clearly marked positive skew. Data in CM-3 is more scattered than in other buildings, having the worst designed walls in shear behavior (elements were designed to the limit of their capacities). Shown in Figure 12-3 is the shear D/C ratios in walls presented as a cumulative probability for every building analyzed.

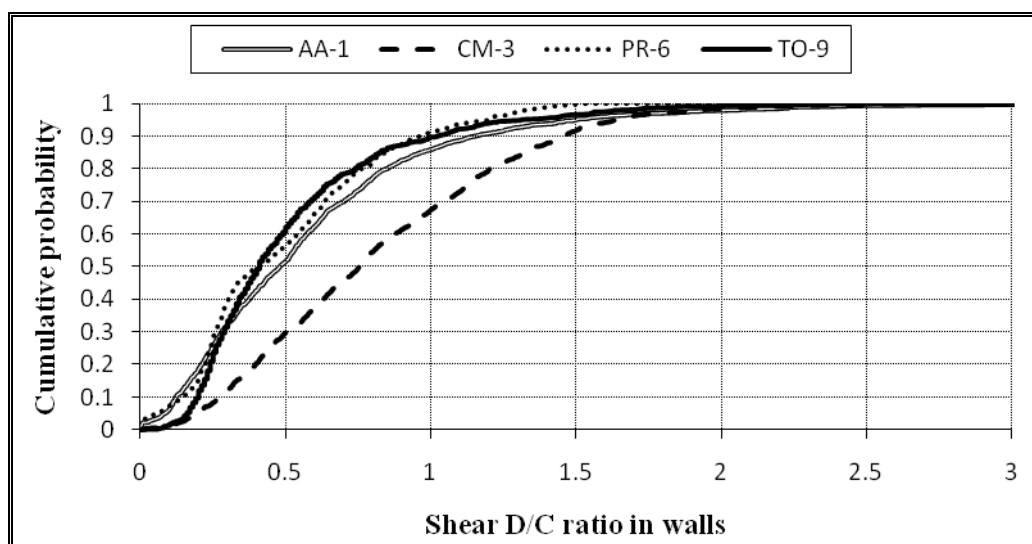


Figure 12-3: Shear D/C ratios in walls as cumulative probability

Although buildings AA-1, PR-6 and TO-9 show similar D/C distributions, the CM-3 curve is far below the others. Assuming that walls with higher D/C ratios were the ones that failed, limit values for these ratios will be proposed. 6.34 % of all walls in building AA-1 showed damage due to shear stress, which would account for walls with a D/C ratio limit of 1.39. On the other hand, 3.03 % of all walls in building CM-3 showed damage due to shear stress, which would match walls with a D/C ratio limit of 1.79. For PR-6, 10.28 % of all walls showed damage due to shear stress, which would mean walls having a D/C ratio limit of 0.95. Finally for TO-9, 3.55 % of all walls showed damage due to shear stress, which would account for a D/C ratio limit of 1.48. Note that in PR-6 the D/C limit is lower than one, which means that more walls were observed having shear

damage than the ones the code could prevent. Further analysis and future corrections of the code can be approached by checking behavior in PR-6.

In the case of flexure in walls, interaction curves ($\phi M_n, \phi P_n$) were computed for a large number of walls in every building. In general, the complete wall macro-element was considered (C-shaped, T-shaped, L-shaped, and other more complex shapes), not just the rectangular parts that compose the section. D/C ratios are defined in this case as a ratio of radial distances between the origin of the interaction curve and the farthest point of demand, and the origin and point of intersection on the interaction curve along the same ray. For buildings CM-3 and PR-6 the analysis was focused in macro-elements in lower stories, while in AA-1 it was concentrated in lower and higher stories. For building TO-9 the analysis was made in all stories and statistical data is presented for this building. Global results for flexure in walls are shown in Table 12-3.

Table 12-3: Total results for flexure in walls

ID	N° of walls analyzed	D/C < 1 (%)	1 < D/C ≤ 1.25 (%)	1.25 < D/C ≤ 1.5 (%)	D/C > 1.5 (%)
AA-1	281	91.46	4.63	1.42	2.49
CM-3	69	68.12	8.70	10.14	13.04
PR-6	50	80.00	4.00	6.00	10.00
TO-9	205	93.17	2.44	2.93	1.46

Again, building CM-3 shows the largest percentage of walls not properly designed—68% of analyzed elements versus 90% in the AA-1 and TO-9 cases. For building AA-1, walls with severe strength deficit are focused at story 14, matching again the structure setbacks. Note that CM-3 and PR-6 have a significantly higher percentage of walls with severe strength deficit in flexural behavior; building PR-6 has higher D/C ratios on the first story. Please notice, however, that for CM-3 and PR-6, D/C analysis was concentrated on the lower stories, which could explain in part the difference in percentages with other buildings.

For building TO-9, D/C ratios were organized in intervals of 0.05 and frequencies regarding each D/C ratios are shown in Figure 12-4 as a histogram.

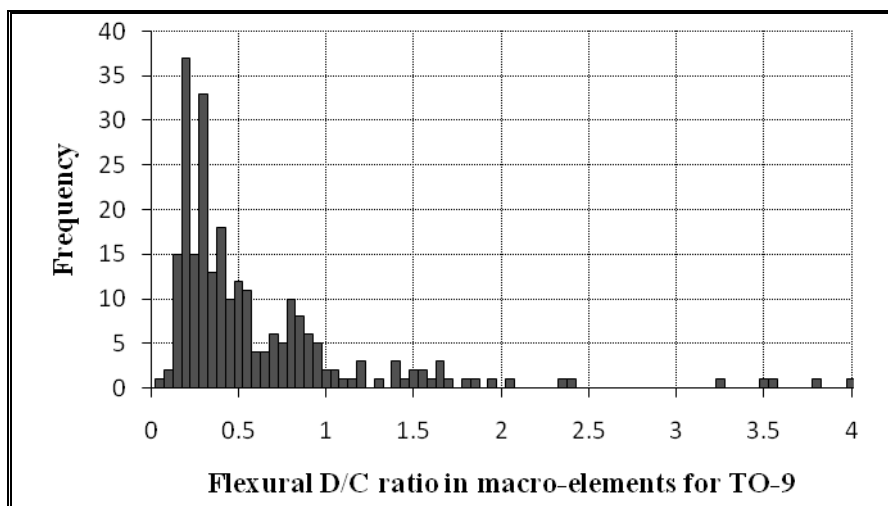


Figure 12-4: Flexural D/C ratios in walls as histogram for building TO-9

Note that in flexure, TO-9 also shows a distribution with a clearly marked positive skew. The mean value of D/C ratios for TO-9 is 0.44 with a standard deviation of 0.33, showing better designed walls for biaxial behavior than in shear. Shown in Figure 12-5 are the flexural D/C ratios in walls of building TO-9 presented as a cumulative probability.

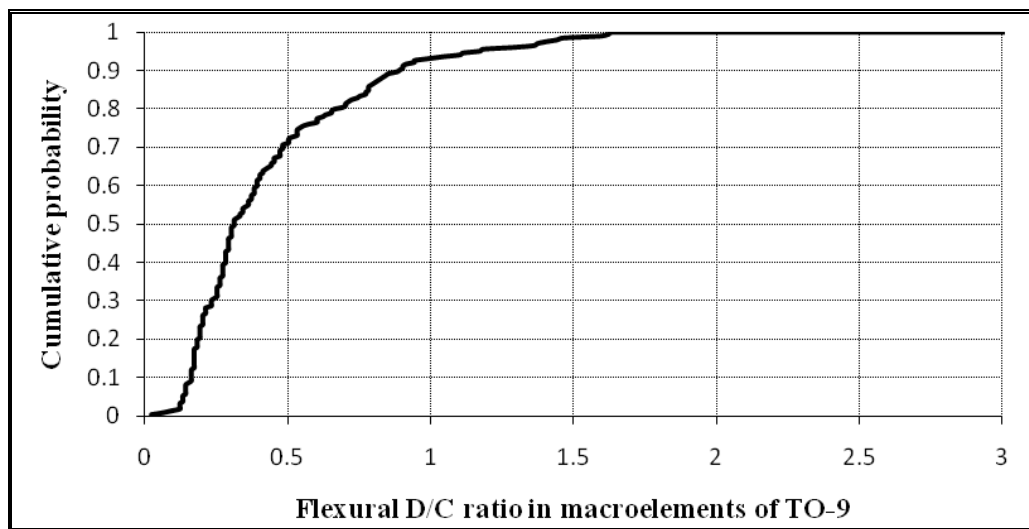
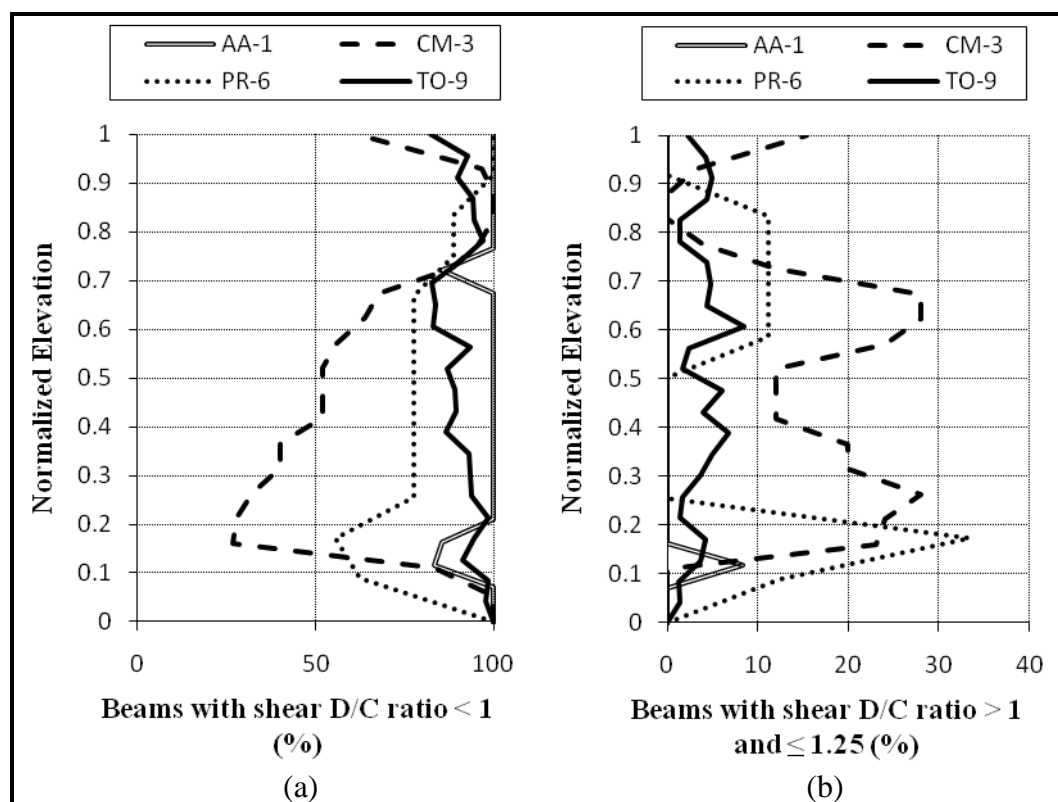


Figure 12-5: Flexural D/C ratios in walls of TO-9 as cumulative probability

Assuming that walls with higher D/C ratios were the ones that failed, limit values for these ratios will be proposed for TO-9. 1.15 % of all walls in building TO-9 showed damage due to flexure, which would account for walls with a D/C ratio limit of 1.53. In this case, the code was available to predict damage in walls, regarding that the D/C limit is greater than one.

12.2 Beam Analysis

As for walls, D/C ratios in beams are defined as $V_u/\phi V_n$. Results for the four groups defined in Table 12-1 are shown in Figure 12-6 as a percentage of analyzed elements in each story.



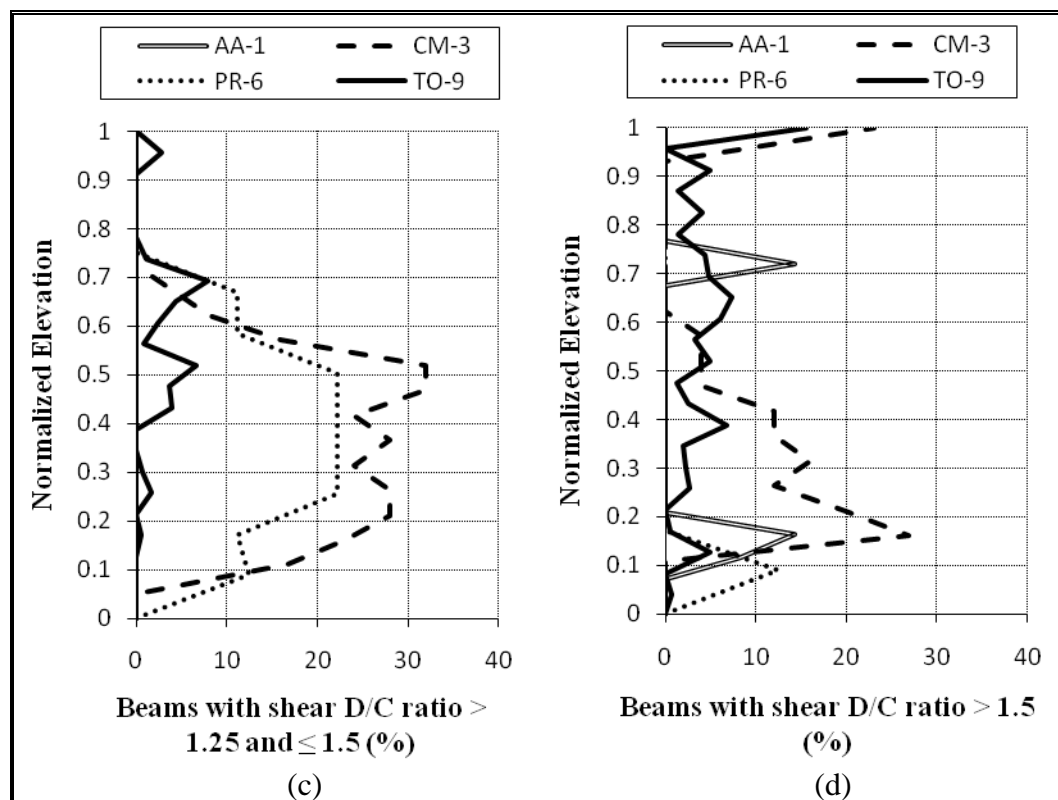


Figure 12-6: Percentage of analyzed beams with shear D/C ratios within each group

In building AA-1 beams with significant strength deficit were found in stories 1, 2, and 14. CM-3 and PR-6 show higher D/C ratios for intermediate and lower stories. For CM-3, elements with significant strength deficit are localized in stories 2, and 18, reaching approximately 25% of the analyzed beams in these stories. PR-6 shows beams with severe strength deficiencies on the 1st story. Building TO-9 shows shear D/C ratios in D/C category well distributed in height.

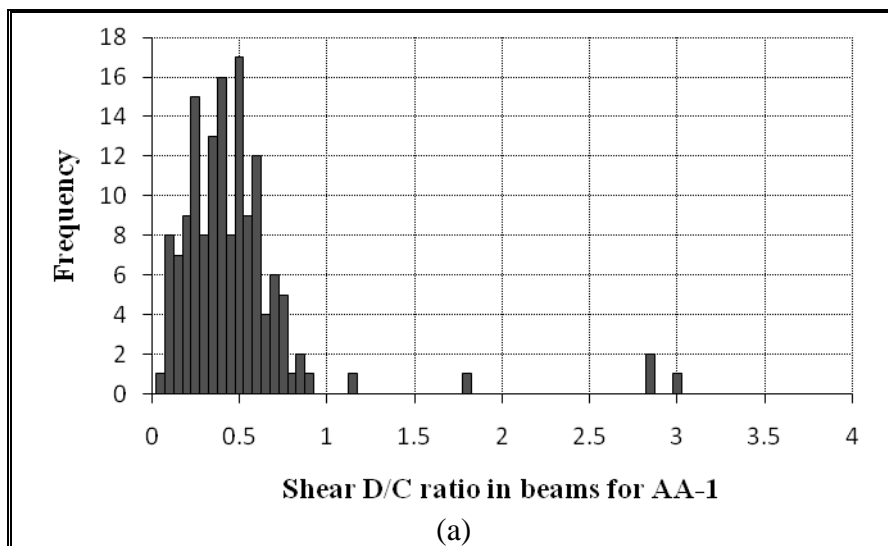
Summarized in Table 12-4 is the distribution of D/C ratios, its mean, and standard deviation for the 4 buildings analyzed. Building CM-3 is the one that shows the highest percentage (63%) of beams with D/C shear ratios greater than 1. Mean values show the same, reaching for the CM-3 building a D/C shear ratio equal to 0.87. For building CM-3, beams with severe D/C ratios occur in axes A and O. In TO-9, axes 1A, 4 and 6 are the ones with the highest D/C ratios. Note that precisely in axis 1A, a large number of beams presented shear failures as viewed

from the outside of the building (Figure 11-1c). PR-6 has less than 1 % of the analyzed beams with D/C ratios > 1.5 .

Table 12-4: Total results for shear in beams

ID	N° of beams analyzed	D/C < 1 (%)	$1 < \text{D/C} \leq 1.25$ (%)	$1.25 < \text{D/C} \leq 1.5$ (%)	D/C > 1.5 (%)	$\mu_{\text{D/C}}$	$\sigma_{\text{D/C}}$
AA-1	147	96.60	0.68	0.00	2.72	0.45	0.42
CM-3	433	63.05	15.01	14.78	7.16	0.87	0.50
PR-6	120	82.05	6.67	10.00	0.83	0.64	0.35
TO-9	2076	92.53	3.56	1.40	3.08	0.56	0.40

D/C ratios were organized in intervals of 0.05 and frequencies regarding each D/C ratio are shown in Figure 12-7 as histograms for every building.



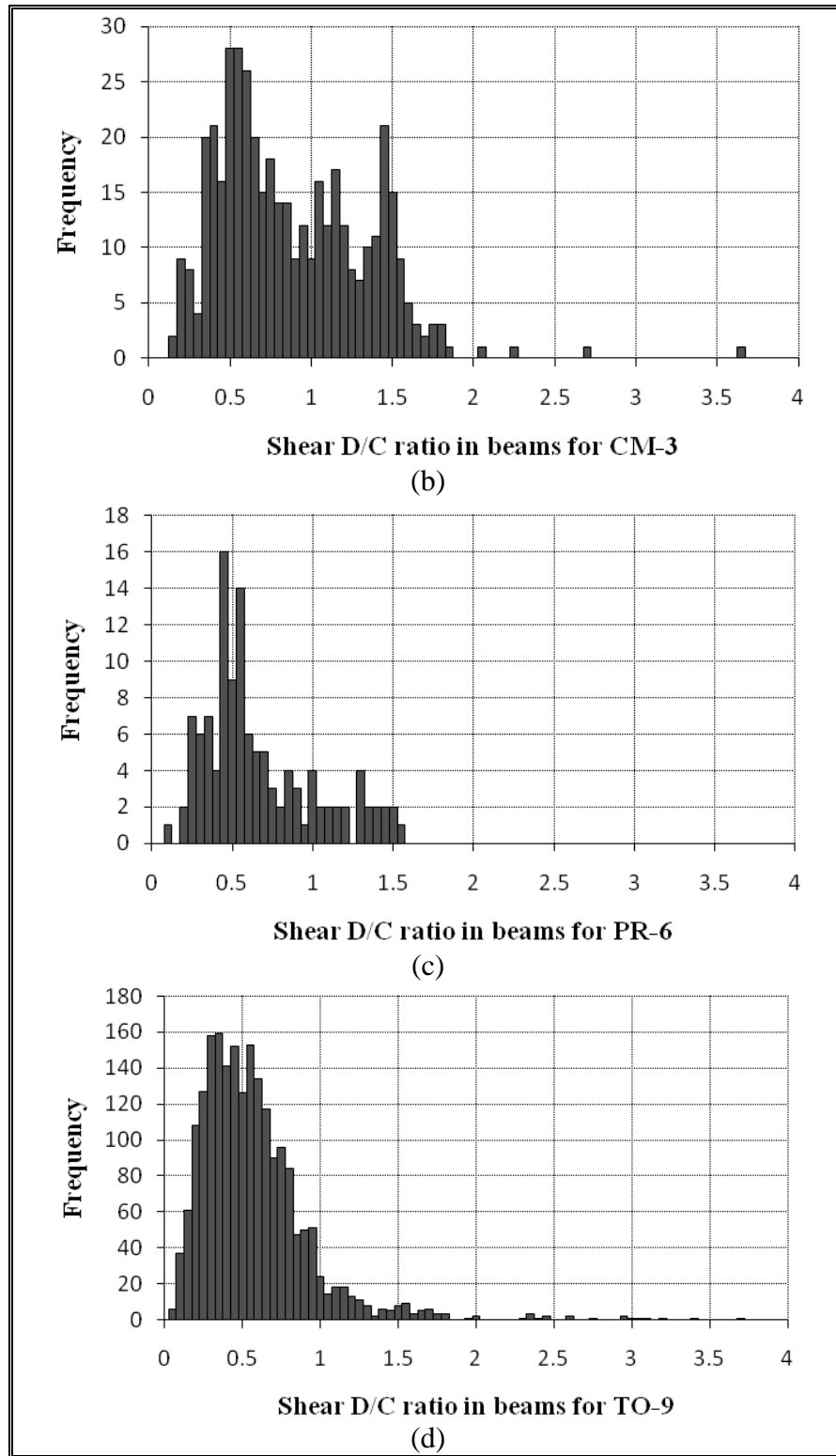


Figure 12-7: Shear D/C ratios in beams as histograms

All buildings show distributions with a clearly marked positive skew. Again, data in CM-3 is more scattered than in other buildings, having the worst designed beams in shear behavior (elements were designed to the limit of their capacities). Shown in Figure 12-8 are the shear D/C ratios in beams presented as a cumulative probability function for every building analyzed.

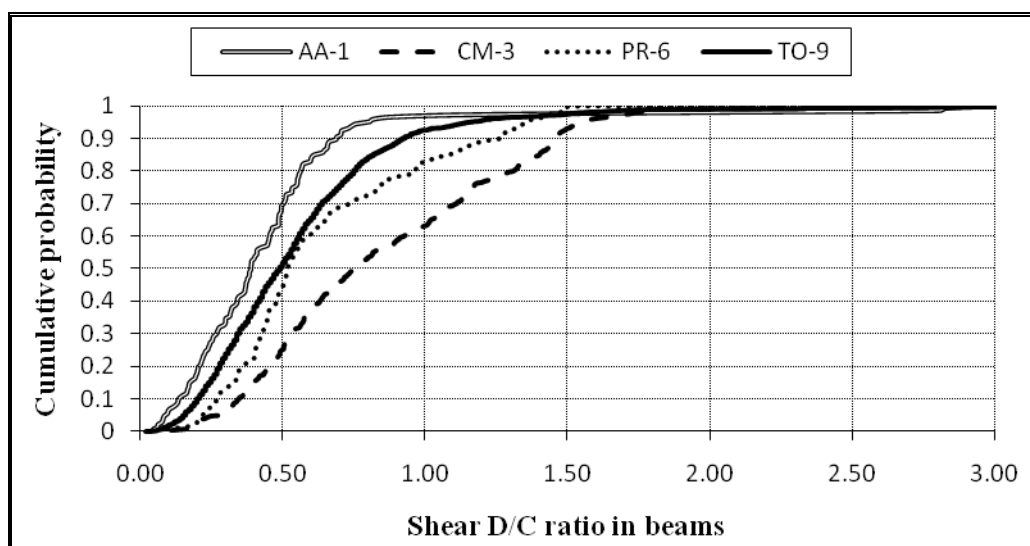
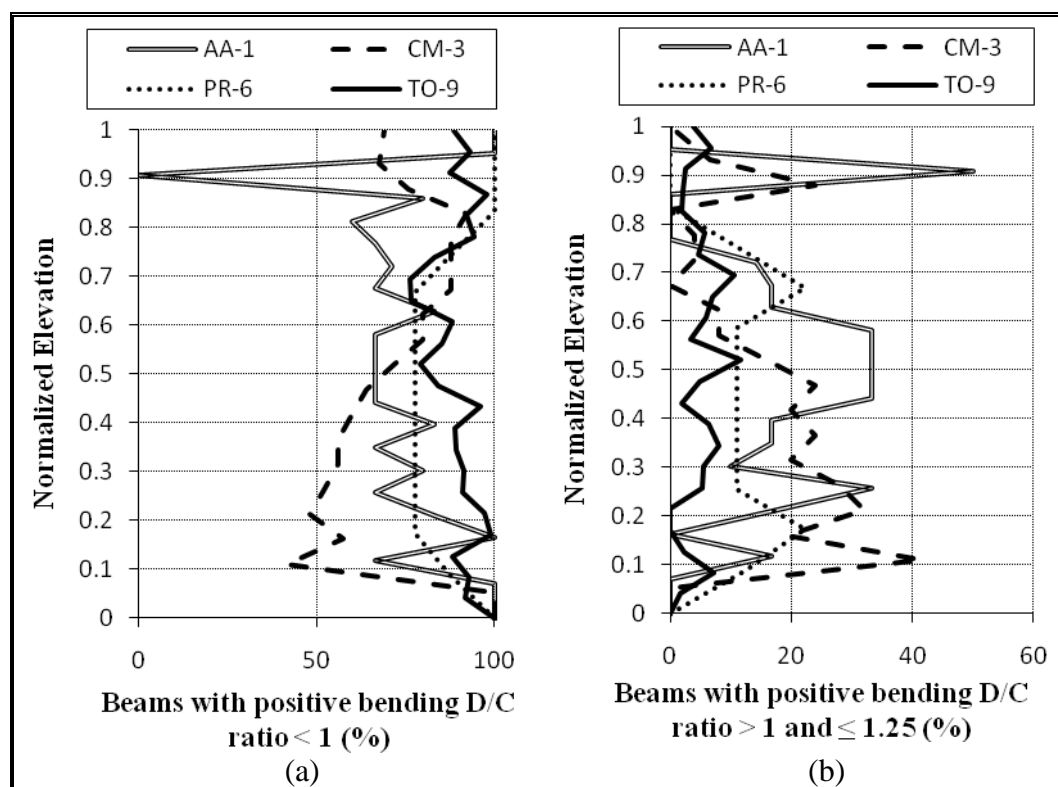


Figure 12-8: Shear D/C ratios in beams as cumulative probability

In shear behavior of beams, building AA-1 shows best designed elements while CM-3 again shows big deficiencies on D/C ratios. Assuming that beams with higher D/C ratios were the ones that failed, limit values for these ratios will be proposed for every building. 5.22 % of all beams in building AA-1 showed damage due to shear stress, which would account for beams with a D/C ratio limit of 0.79. On the other hand, 5.26 % of all beams in building CM-3 showed damage due to shear stress, which would match beams with a D/C ratio limit of 1.54. For PR-6, 11.93 % of all beams showed damage due to shear stress, which would mean beams having a D/C ratio limit of 1.17. Finally for TO-9, 4.62 % of all beams showed damage due to shear stress, which would account for a D/C ratio limit of 1.20. Note that in AA-1 the D/C limit is lower than one, which means that more beams were observed having shear damage than the ones the code could

prevent. Further analysis and future corrections of the code can be approached by checking behavior in AA-1.

For positive bending, D/C ratio is defined as $M_u^+ / \phi M_n^+$. Results for the four groups defined in Table 12-1 are shown in Figure 12-9 as percentage of analyzed elements in each story. Building TO-9 shows positive bending D/C ratios of every category well distributed among different stories. AA-1 shows greater deficits in beams at high stories where setbacks exist. PR-6 shows bigger D/C ratios for intermediate stories while for CM-3 positive bending D/C ratios are bigger in lower and higher levels. PR-6 shows no beam with severe strength deficiencies. In building AA-1 beams with significant strength deficit were found in stories 1, 14, 15, 16 and 17, with higher percentages concentrated in upper stories. For CM-3 elements with significant strength deficit are focused on stories 2, 3, 17 and 18, reaching approximately 20 % of analyzed beams on these stories.



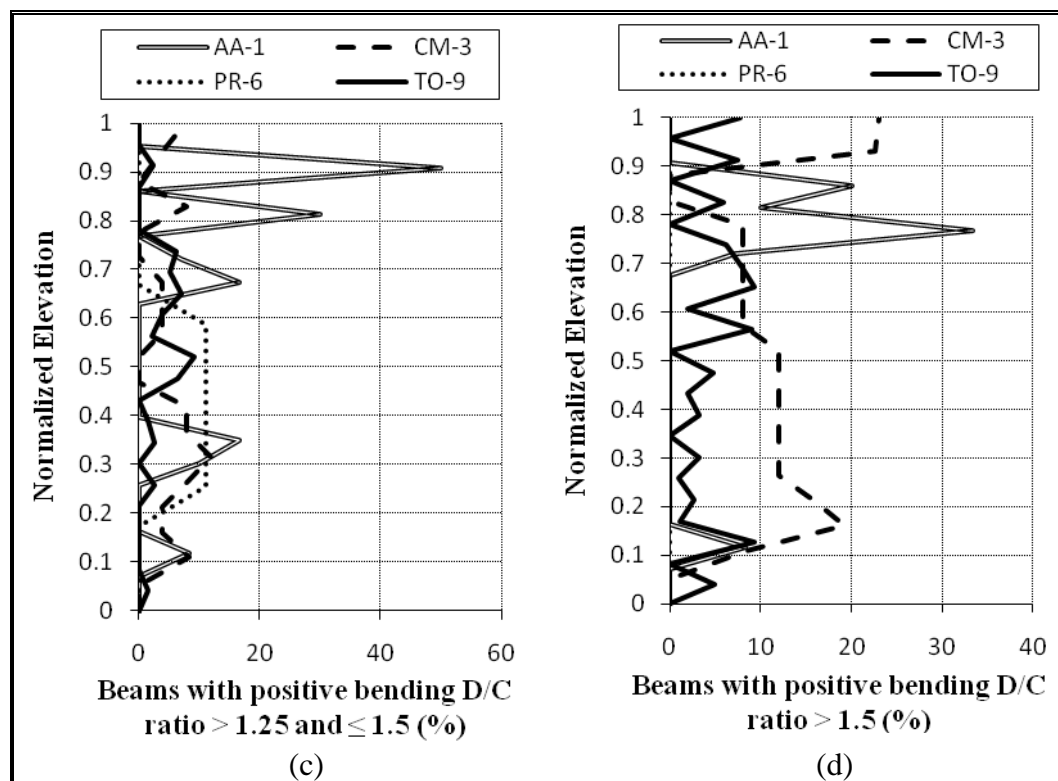


Figure 12-9: Percentage of analyzed beams with positive bending D/C ratios within each group

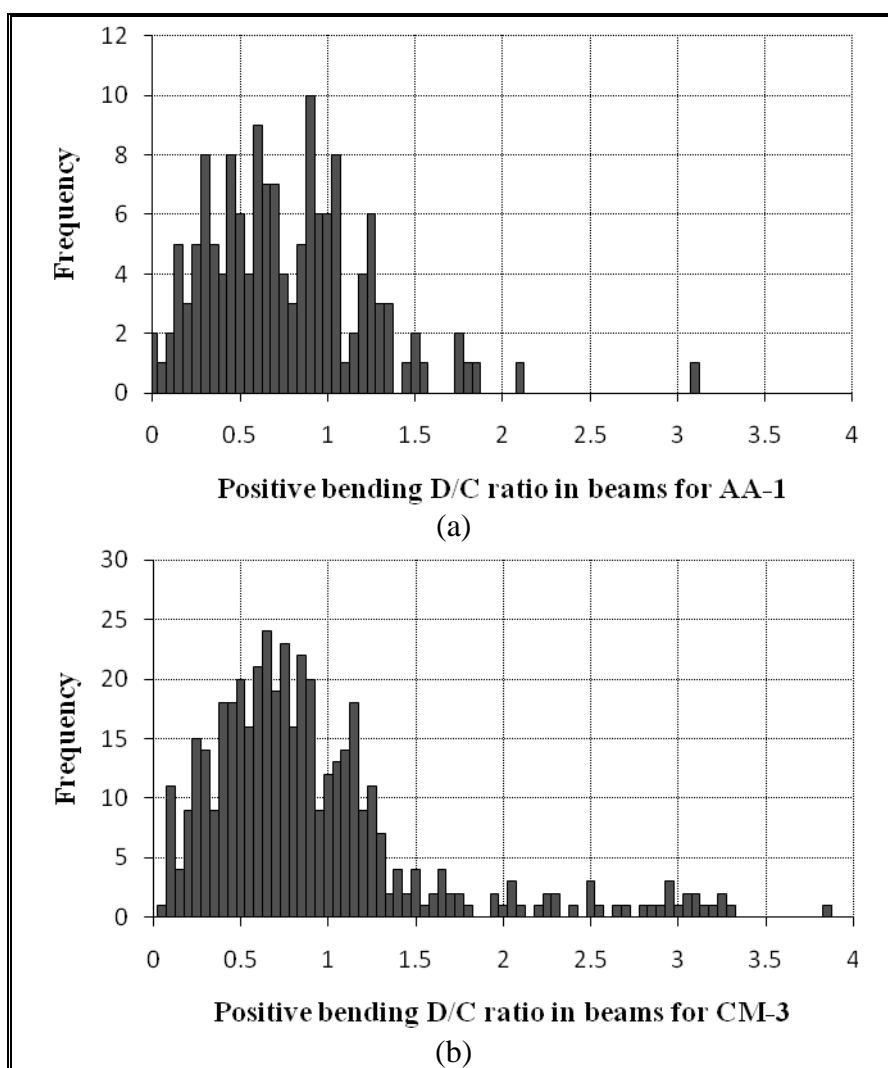
Summarized in Table 12-5 is the distribution of D/C ratios, its mean, and standard deviation for the 4 buildings analyzed.

Table 12-5: Total results for positive bending in beams

ID	N° of beams analyzed	D/C < 1 (%)	1 < D/C ≤ 1.25 (%)	1.25 < D/C ≤ 1.5 (%)	D/C > 1.5 (%)	$\mu_{D/C}$	$\sigma_{D/C}$
AA-1	147	74.83	14.29	6.12	4.76	0.74	0.46
CM-3	433	69.52	15.01	4.39	11.09	0.89	0.65
PR-6	120	86.67	9.17	4.17	0.00	0.52	0.35
TO-9	1315	89.66	4.56	2.21	3.57	0.49	0.50

Buildings AA-1 and CM-3 show the lowest percentages of beams properly designed (approximately 70% of analyzed elements against 90% of analyzed elements in other buildings). Mean values shows the same, reaching in AA-1 a

D/C ratio of 0.74 and in CM-3 a value of 0.89. Note that PR-6 has no beams with severe strength deficit in positive bending behavior while CM-3 has 11.09 % of the analyzed elements. For building CM-3, beams with severe strength deficit are focused in axes A and O. In TO-9, axis 1A is the one where most of the highest D/C ratios are found. Note that in axis 1A there is a big number of damaged beams. D/C ratios were organized in intervals of 0.05 and frequencies regarding each D/C ratio are shown in Figure 12-10 as histograms for every building.



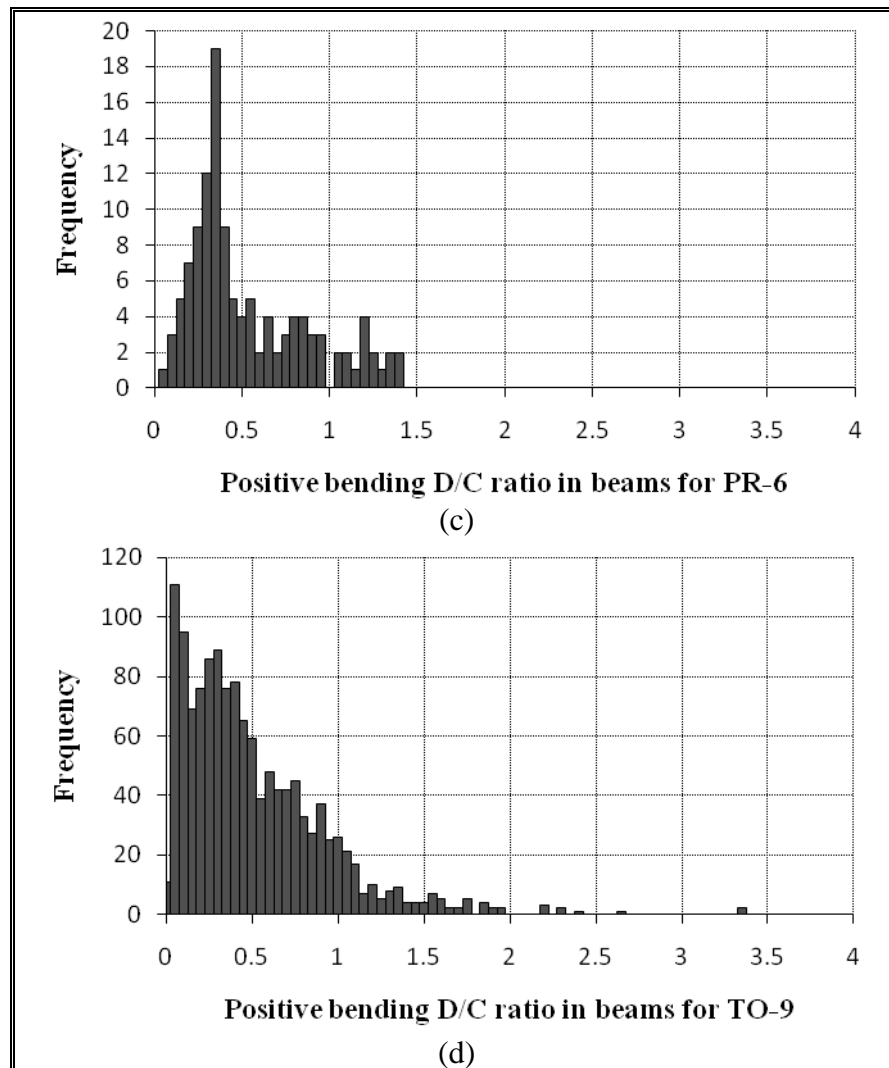


Figure 12-10: Positive bending D/C ratios in beams as histograms

As with shear, all buildings show distributions with a clearly marked positive skew, being stronger in TO-9. Data in AA-1 and CM-3 is more scattered than in other buildings, having the worst designed beams in positive bending behavior (elements were designed to the limit of their capacities). Shown in Figure 12-11 are the positive bending D/C ratios in beams presented as a cumulative probability function for every building analyzed.

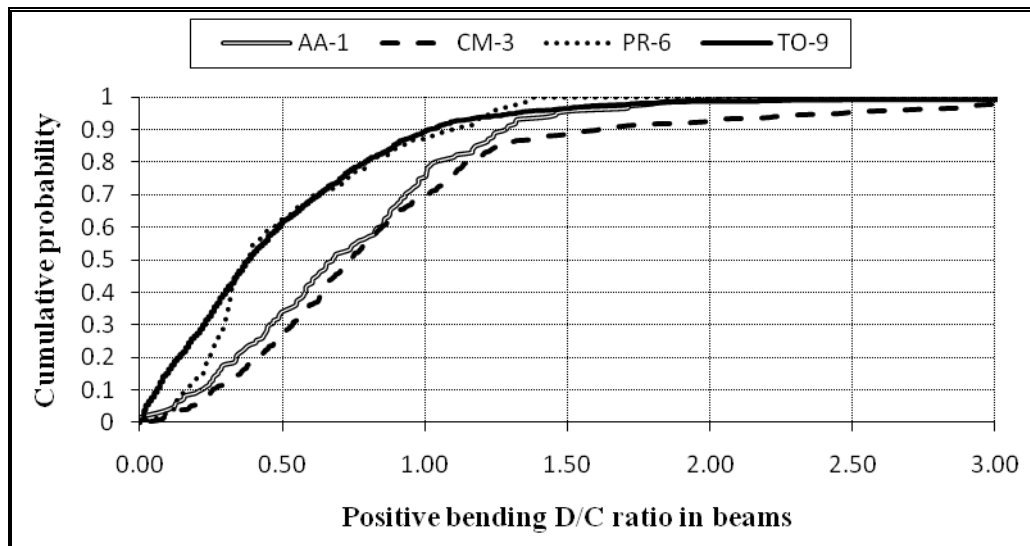
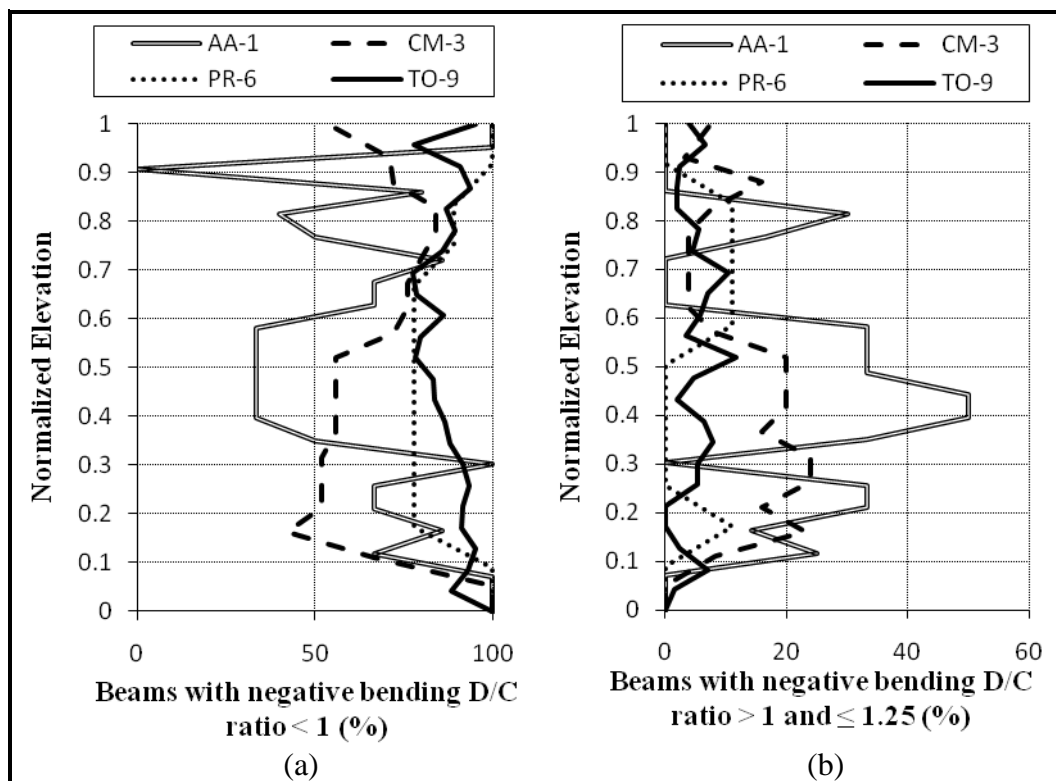


Figure 12-11: Positive bending D/C ratios in beams as cumulative probability

In positive bending of beams, building PR-6 and TO-9 shows the best behavior, while buildings AA-1 and CM-3 have poorly designed elements. Assuming that beams with higher D/C ratios were the ones that failed, limit values for these ratios will be proposed for every building. 9.19 % of all beams in building AA-1 showed evidence of damage due to flexural stress, which would account for beams with a D/C ratio limit of 1.29. On the other hand, 1.37 % of all beams in building CM-3 showed evidence of damage due to flexural stress, which would match beams with a D/C ratio limit of 3.08. For PR-6, 3.78 % of all beams showed evidence of damage due to flexural stress, which would mean beams having a D/C ratio limit of 1.18. Finally for TO-9, 10.87 % of all beams showed evidence of damage due to flexural stress, which would account for a D/C ratio limit of 0.85. Note that in TO-9 the D/C limit is lower than one, which means that more beams were observed having shear damage than the ones the code could prevent. Regarding that most of the beams in TO-9 that showed flexural evidence failed due to interaction with other elements (partial collapse takes big importance), no further code-analysis for positive bending in beams will be performed.

For negative bending, D/C ratio is defined as $M_u^-/\phi M_n^-$. Results for the four groups defined in Table 12-1 are shown in Figure 12-12 as percentage of analyzed elements in each story. Building TO-9 shows negative bending D/C ratios of every category well distributed among different stories. AA-1 shows greater deficits in beams at intermediate and higher stories where setbacks exist. PR-6 shows bigger D/C ratios for intermediate stories while for CM-3 negative bending D/C ratios are bigger in lower and intermediate levels. In building AA-1 beams with significant strength deficit were found in story 1 and stories 13 to 19, with higher percentages concentrated in upper stories. For CM-3 elements with significant strength deficit are focused on story 2, reaching approximately 35 % of analyzed beams on that story. PR-6 shows beams with severe strength deficiencies at stories 4 and 5.



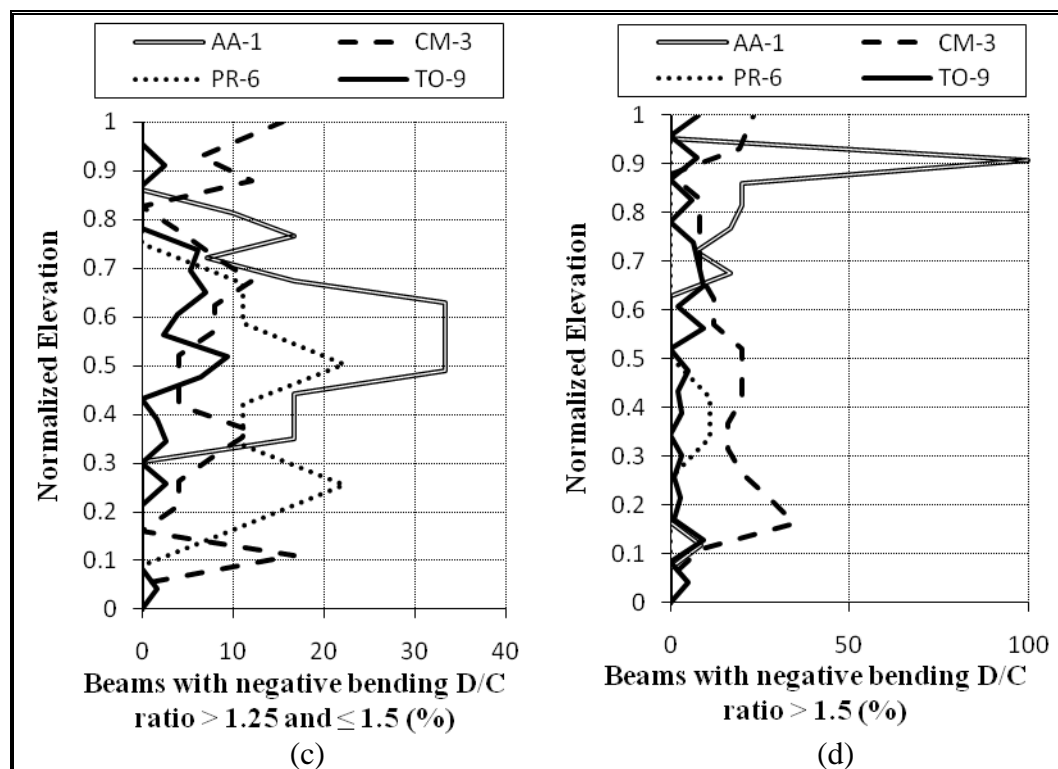


Figure 12-12: Percentage of analyzed beams with negative bending D/C ratios within each group

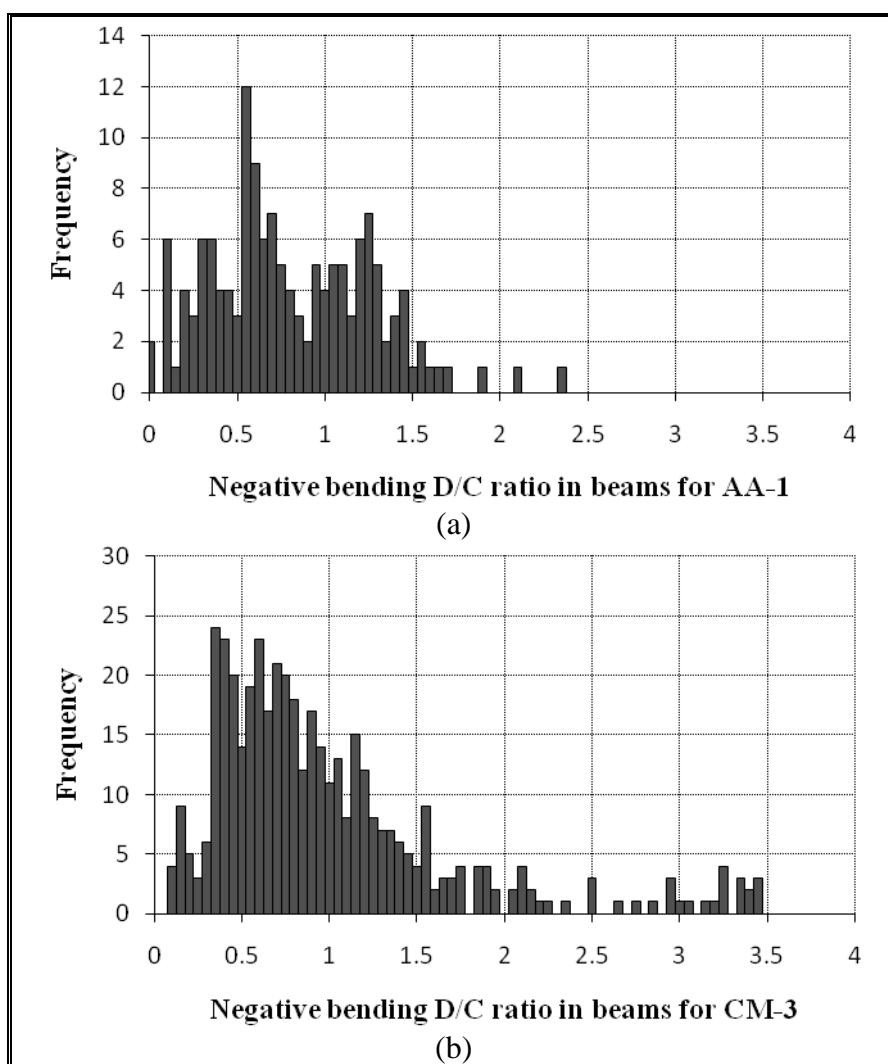
Summarized in Table 12-6 is the distribution of D/C ratios, its mean, and standard deviation for the 4 buildings analyzed.

Table 12-6: Total results for negative bending in beams

ID	N° of beams analyzed	D/C < 1 (%)	1 < D/C ≤ 1.25 (%)	1.25 < D/C ≤ 1.5 (%)	D/C > 1.5 (%)	$\mu_{D/C}$	$\sigma_{D/C}$
AA-1	147	65.31	17.69	10.20	6.80	0.83	0.60
CM-3	433	64.67	12.93	6.70	15.70	0.97	0.72
PR-6	120	86.67	4.17	7.50	1.67	0.52	0.36
TO-9	1988	87.68	4.38	2.82	5.13	0.60	0.62

Buildings AA-1 and CM-3 shows a significant lower percentage of beams properly designed than other buildings (approximately 65 % of analyzed elements against 90 % of analyzed elements in other buildings). Mean values shows the same, reaching in AA-1 a D/C ratio of 0.60 and in CM-3 a value of 0.72. Note that

PR-6 has a significant lower percentage of beams with severe strength deficit in negative bending behavior (lower than 2 % of analyzed beams), while building CM-3 shows the biggest percentage (15.70 % of analyzed elements). For building CM-3, beams with severe strength deficit are focused in axes A and O. In TO-9, axes G, I and 7 are the ones where most of the highest D/C ratios are found. These ratios were organized in intervals of 0.05 and frequencies regarding each D/C ratio are shown in Figure 12-13 as histograms for every building.



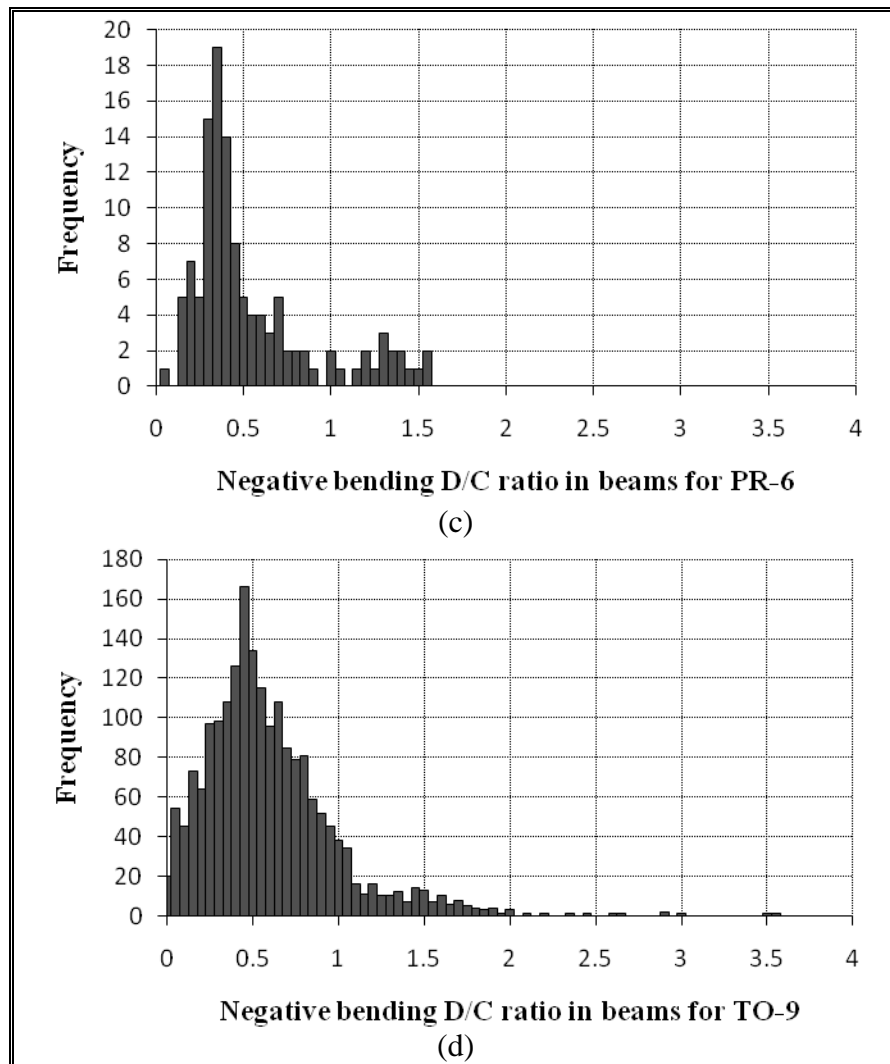


Figure 12-13: Negative bending D/C ratios in beams as histograms

As with positive bending, all buildings show distributions with a clearly marked positive skew. Again, data in AA-1 and CM-3 is more scattered than in other buildings, having the worst designed beams in negative bending behavior (elements were designed to the limit of their capacities). Shown in Figure 12-14 are the negative bending D/C ratios in beams presented as a cumulative probability function for every building analyzed.

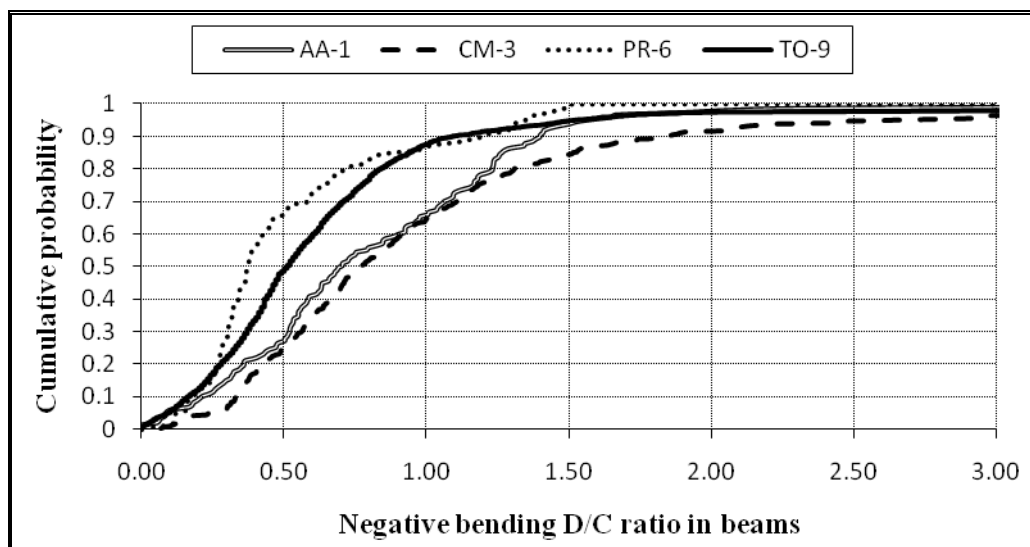


Figure 12-14: Negative bending D/C ratios in beams as cumulative probability

In negative bending of beams, building PR-6 and TO-9 shows best behavior, while buildings AA-1 and CM-3 shows poorly designed elements. Assuming that beams with higher D/C ratios were the ones that failed, limit values for these ratios will be proposed for every building. Percentages of damaged beams showing flexural evidence in every building were presented previously in the positive bending section. Limits for D/C ratios are 1.40 for AA-1, 3.34 for CM-3, 1.37 for PR-6 and 1.02 for TO-9. In this case, the code was available to predict damage in beams, regarding that all D/C limits are bigger than one.

12.3 General Comments

In general, CM-3 shows a deficient design with a considerable amount of elements with D/C ratios higher than one. For other buildings (excluding flexural behavior in beams of AA-1), approximately 90% of the analyzed elements have D/C ratios lower than one, implying that though these structures have design deficiencies, they are localized. Please note that all code analysis results used the more detailed soil mechanics performed after the earthquake by part of this team. Original soil

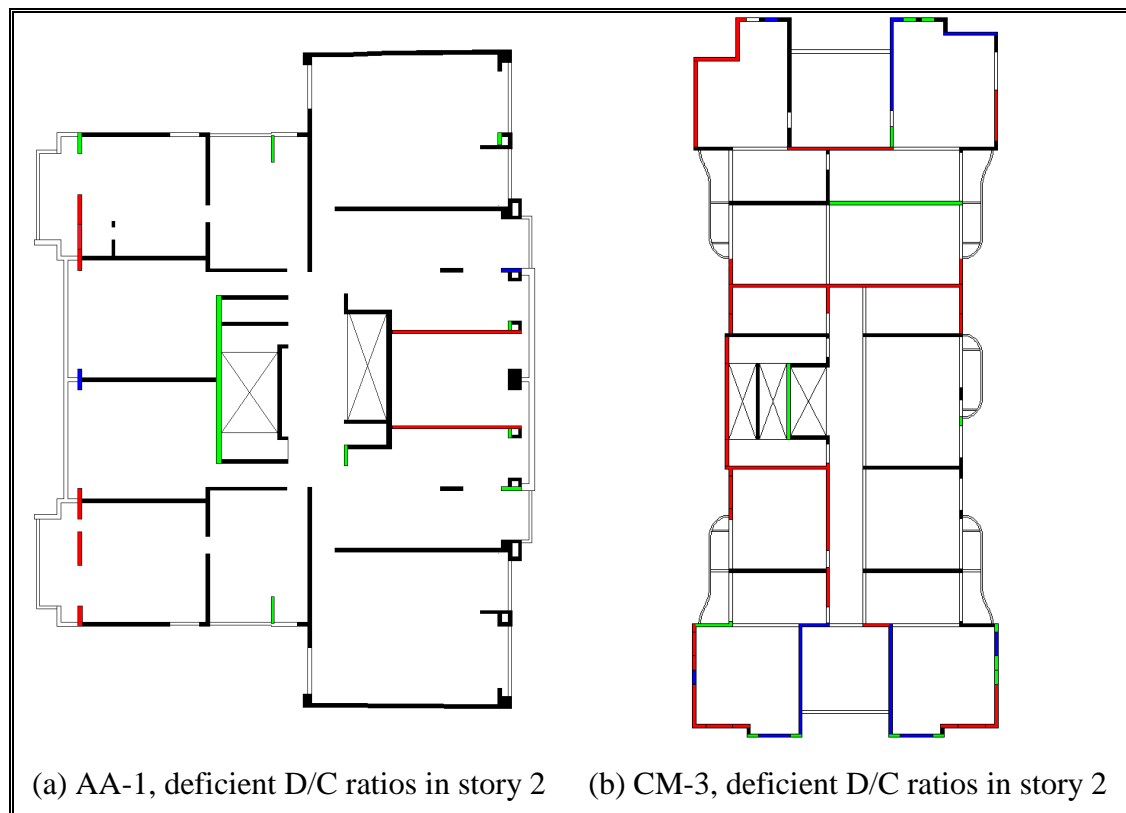
mechanics differs from the one used in design in buildings CM-3 and TO-9. The original soil mechanics for building TO-9 indicated soil type II, and according to this study, it should be type III (softer). This change implies a considerable larger seismic demand on the structure. On the other hand, the original soil mechanics for CM-3 states soil type III and our study indicate soil type II. If this soil condition were accepted, D/C ratios would increase considerably from the ones shown earlier. The soil classification seems to be critical in these projects.

Regarding details of reinforcement, buildings AA-1 and PR-6 shows adequate steel ratios, proper anchorage and development lengths. Although most details of reinforcement are met for CM-3, several beams with longitudinal reinforcement of diameter 22 mm end with a 90° hook of inadequate length, according to ACI318-95 section 12.5.3. TO-9 has very poor reinforcement details, for instance, with non- anchored top reinforcement bars at the ends of tall beams. Structural specifications do not detail the specific length of standard hooks of 90°, but state a general 90° hook with 30 cm. According to ACI318-95, sections 7.1.2. and 7.2.1, this detail would be adequate for bars with a diameter less than 18 mm, but inadequate for larger diameters, which are present in the structure. In some cases, development lengths in beams and connections with walls are insufficient. In walls, boundary reinforcement specifies a lap splice of 100 cm, which in some cases shows to be inadequate for bars with diameters 22 mm and larger.

12.4 Comparison with Observed Damage

In this section a comparison between the observed damage with some of the code analysis results will be performed. With that idea in mind, structural drawings showing D/C ratios were created for all four buildings. For D/C drawings, elements with D/C ratios between 1 and 1.25 are associated with green, between

1.25 and 1.5 with blue, and larger than 1.5 with red. These drawings can be compared with the ones mentioned in chapter 9 of this thesis which shows the observed damage in every analyzed building (Figure 9-1). A schematic representation of the information available is presented in Figure 12-15. See Appendix B to view the most damaged story in each structure with code analysis revision.



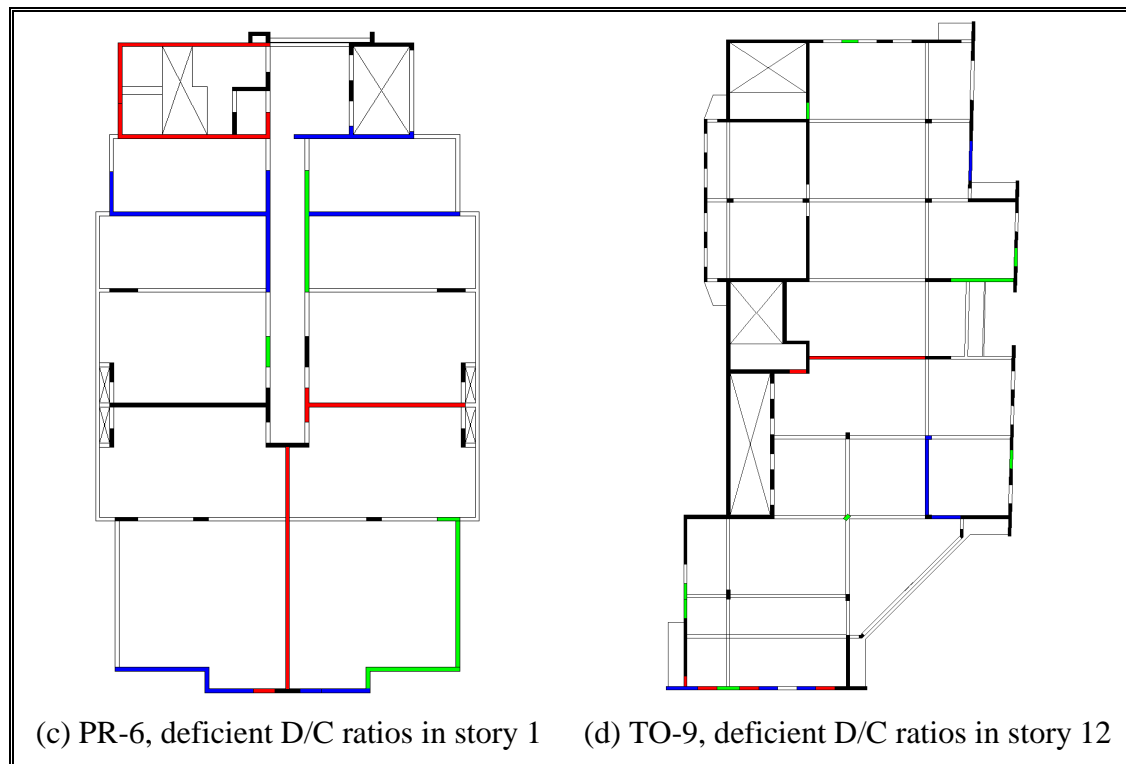


Figure 12-15: Example of deficient D/C ratios in structural drawings

It is apparent that there are cases where D/C ratios and design deficit match the damaged elements; there are also cases where damage cannot be explained by high D/C ratios. Such is the case mainly because of load transfer between elements when the first element collapse occurs, and load gets distributed within the structure. There is evidence of significant redistributions of loads in these buildings; otherwise, it is difficult to explain why they did not collapse.

For better understanding and comparison, fragility curves showing the probability of exceeding a prescribed level of damage given its D/C ratio can be performed in future research. This will ultimately prove if the code is conservative or if it underestimates the demand in shear wall buildings.

12.5 Drifts and Displacements

Nominal interstory drifts and displacements were checked in all structures. Note that code NCh433-96 states that the drift in the center of mass (CM) must be smaller than 2 ‰, and that maximum drift in any point must not exceed in more than 1 ‰ the drift at the CM. Detailed results are shown only for the four most severely damaged structures.

Figure 12-16 shows drifts of center of mass, maximum story drifts, and center of mass displacements for each direction in normalized elevation for building AA-1. Note that seismic deformations are quite similar in both directions, implying similar stiffness in the center of mass for both directions. Maximum drifts in Y-direction are considerably higher than drifts in the center of mass, probably because there is torsion involved due to plan asymmetry. Discontinuities can be observed where setbacks exist. All limits given by the code are met; expected behavior for very rigid structures.

Figure 12-17 shows drifts of center of mass, maximum story drifts, and center of mass displacements for each direction in normalized elevation for building CM-3. Note that seismic deformations are very different in both directions (regarding magnitude rather than shape), expected behavior due to the narrow plan. Maximum drifts in Y-direction are quite similar than drifts in the center of mass, implying no significant torsion occurred. Again, all limits given by the code are met.

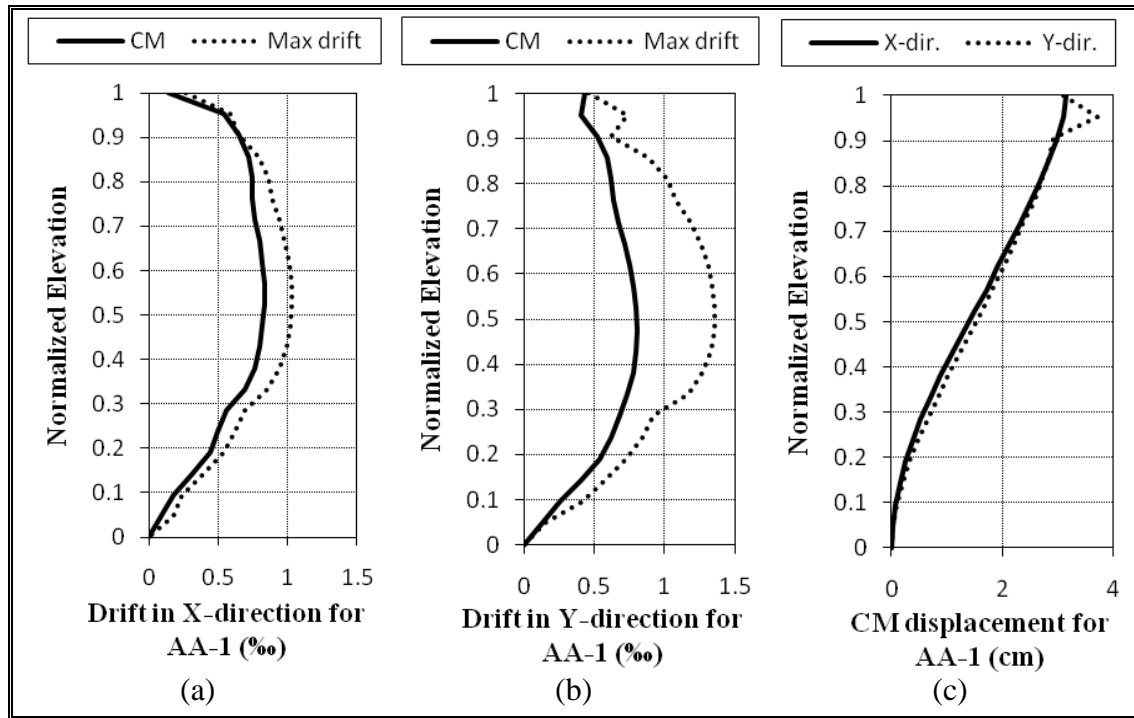


Figure 12-16: Drifts and displacements for building AA-1

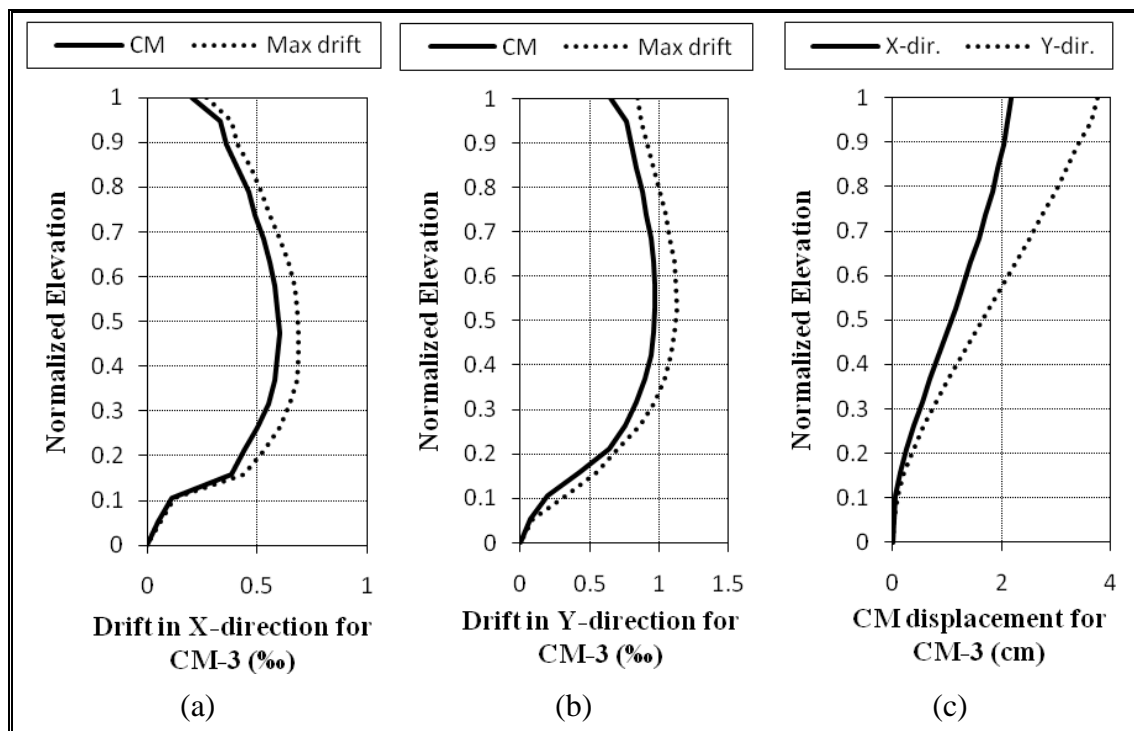


Figure 12-17: Drifts and displacements for building CM-3

Figure 12-18 shows drifts of center of mass, maximum story drifts, and center of mass displacements for each direction for building PR-6.

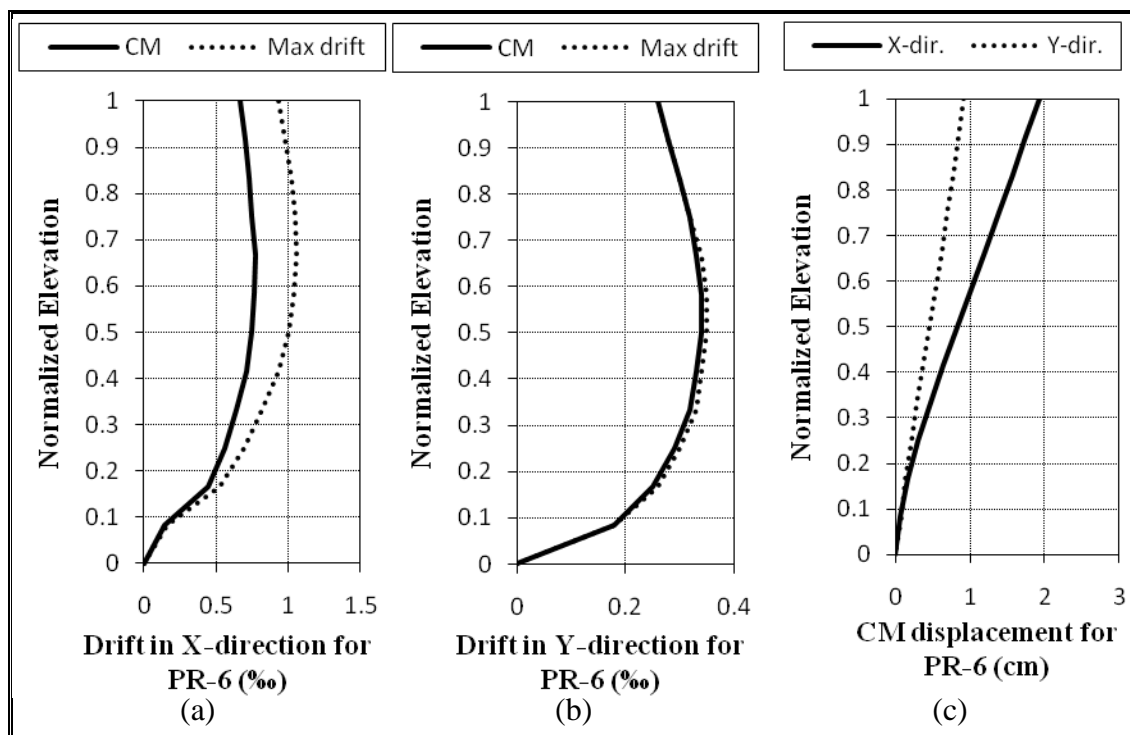


Figure 12-18: Drifts and displacements for building PR-6

Again, seismic deformations are very different in both directions (regarding magnitude rather than shape), expected behavior due to the narrow plan. Maximum drifts in X-direction are very different than drifts in the center of mass, implying significant torsion occurred in X-direction. Axes V and W are the ones with maximum drifts, which differs approximately in a 30% with drifts in the center of mass. Again, all limits given by the code are met.

Figure 12-19 shows drifts of center of mass, maximum story drifts, and center of mass displacements for each direction for building TO-9.

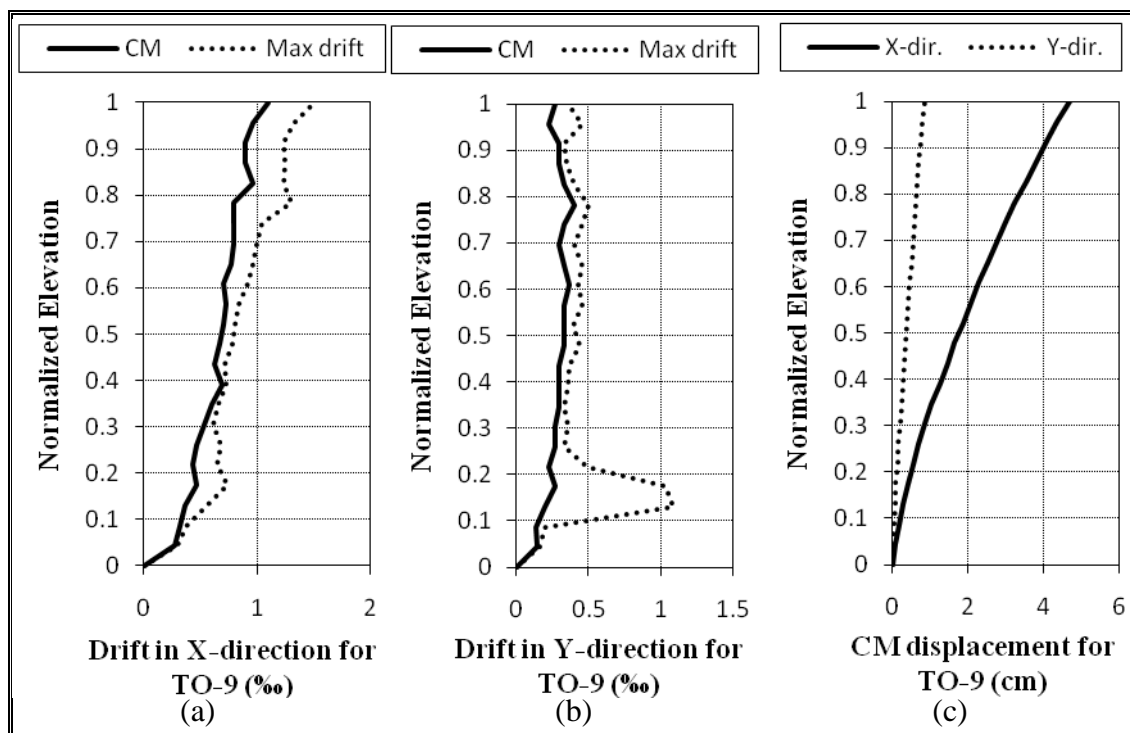


Figure 12-19: Drifts and displacements for building TO-9

TO-9 shows an important difference in seismic deformations for both directions. Center of mass displacements at story 21 reaches 4.69 cm in X-direction and 0.84 cm for Y-direction. Note the discontinuities on drift behavior, given by a capricious configuration. Maximum drifts in Y-direction shows a great difference with center of mass drifts in lower stories, mainly due to the double height columns present at these stories. At higher stories, X-direction shows a greater difference between maximum and center of mass drifts, implying more torsion at this direction in higher levels. Again, all limits given by the code are met.

Table 12-7 summarizes the information regarding drifts and displacements for all buildings.

Table 12-7: Drifts and displacements for all considered buildings

ID	Max. CM drift in X-direction (%)	Max. drift in X-direction (%)	Max. CM drift in Y-direction (%)	Max. drift in Y-direction (%)	Max. CM displ. in X-direction (cm)	Max. CM displ. in Y-direction (cm)
AA-1	0.83	1.03	0.81	1.36	3.15	3.72
AH-2	0.90	1.14	0.73	0.83	3.26	2.59
CM-3	0.60	0.69	0.97	1.13	2.18	3.76
TL-4	0.88	0.94	1.17	1.25	3.01	3.80
MD-5a	0.57	2.23	0.50	1.54	0.95	0.96
MD-5b	0.41	1.52	0.55	0.99	0.85	0.79
PR-6	0.77	1.06	0.34	0.35	1.94	0.91
PP-7a	0.21	0.25	0.66	0.89	0.44	1.34
PP-7b	0.21	0.23	0.51	0.58	0.43	1.02
RT-8a	0.21	0.25	0.66	0.89	0.44	1.34
RT-8b	0.21	0.23	0.51	0.58	0.43	1.02
TO-9	1.10	1.51	0.40	1.09	4.69	0.84

Buildings PP-7a, PP-7b, RT-8a and RT-8b showed very different seismic deformations in both directions. The difference between maximum drifts and drifts at the CM for buildings PP-7a and RT-8a, implies also nominal torsional coupling. When building MD-5 was built, the code limits regarding drifts and displacements did not apply, being the only building that did not meet the requirements. Differences between MD-5a and MD-5b can be due to the fact that MD-5a is a much more flexible structure (story 1 and story 2 in MD-5a are double height stories, while in MD-5b only story 3 is a double height level). Finally, it is clear that almost every building with a predominant shear wall configuration meets the displacement and drift requirements of the code, which says, in light of the earthquake results, little about the quality of its configuration in plan and height.

13 CONCLUSIONS

This thesis summarizes the observations obtained in 9 reinforced concrete buildings that were severely damaged during the 2010, Chile earthquake. The buildings were a small subset of the total shear wall building population in Chile, but account for approximately half of the severely damaged, moderately tall shear wall buildings from the Biobío region. The study buildings range in height from 5 to 21 stories, with all but two constructed after 2000. Some observations and conclusions derived from the data are intuitive at this point. In general, it is fair to conclude that buildings in Chile had a reasonable behavior during the past earthquake, with only some exceptions, less than 1%, which underwent damage of the type and intensity presented herein.

The study buildings have relatively high ratios of structural wall area to floor area, as is typical of Chilean wall buildings. Typical wall areas in a single direction ranged from around 1.5% to 4% of floor plan area. The buildings have relatively short calculated fundamental vibration periods, ranging from 0.22s to 0.62s, consistent with the high wall-to-floor-area ratios. Several of the study buildings have irregularities in plan or elevation; this aspect may have contributed to building damage, but damage occurred in regularly configured buildings also.

Most of the study buildings have their principal axes oriented predominantly N-S and E-W. Field observations suggest that the most serious damage occurred in the E-W oriented resisting planes. Apparent damage was subjectively associated with shear (inclined “cracks”), flexure and axial load (horizontal cracks and crushed regions, buckled longitudinal reinforcement, and globally buckled wall sections). Survey results show that more walls had shear damage than had flexural damage, though both shear and flexural damage affected several of the buildings. In most of the buildings, severe damage associated with axial load and flexure, shear, or both, concentrated in the lower

stories without significant spread of inelastic response. In one of the buildings, however, structural irregularities apparently contributed to severe shear-related damage and collapse in the upper stories.

As opposed to buildings in the cities of Viña del Mar and Santiago, the Concepción buildings did show in more cases shear failures of the walls. Damage of poorly confined vertical elements such as columns is extensive in some of the structures, such as TO-9. Beams also underwent substantial damage in part as a result of wall connection details that are poorly implemented and developed in several cases. It is seen that floor slabs acted in many cases as coupling lintels between walls, while presenting a very limited energy dissipation capacity.

Some of the shear damage observed was expected, but the other combined flexural and compression damage was not. Although Chilean reinforced concrete design code is mainly ACI 318 code (American Concrete Institute Committee 318, 1995), the current seismic code NCh 433Of.96, excluded the chapters regarding walls boundary confinement, mainly because of the successful structural behavior during the 1985 Chilean earthquake. Even if high levels of wall density in Chilean buildings would make boundary confinement less necessary, it was empirically demonstrated during this earthquake that the 2008 change in the RC Chilean codes that included ACI boundary confinement requirements was probably necessary. Unfortunately, nothing has been said about limiting the axial load in shear walls, which seems to be a highly controlling factor.

Global and local observations of wall damage indicate that the seismic behavior in these buildings was probably non ductile, or at least, with a ductility less than the one implicit in the strength R-factor used in design. The concentration of damage observed within the element and throughout the structure, and the fact that similar structures did not experience damage at all, are indicative of a rather brittle behavior. However, we are still tremendously ignorant about this earthquake and the observed structural behavior, so further studies are required to investigate the impact in building performance of each of these factors. From the analysis of linear D/C ratios and their mediocre correlation with

damage, it becomes apparent that inelastic analyses are mandatory in order to clarify what really happened within these structures and how did it happen. Predicting the observed behavior of these structures has value per se, since it could provide the base of information to support corrections of some usual design practices of shear wall buildings that did not work.

Soil related problems and irregularities present in buildings were also two very important factors in explaining their damage. Although most damage occurs in lower stories for most buildings, in buildings such as TO-9 damage occurred at level 12 and above, where building vertical irregularities were most notorious. In at least one of the buildings, PR-6, soil problems were apparent.

Based on the results presented herein, unfortunately it is impossible to rule out problems in the design and construction of the buildings considered. The observation shows that there are apparent errors in design and construction of these structures, but to be fair those errors are likely to be present to some extent in other similar structures with no damage. Under this assumption, it becomes interesting to explore more deeply on the reasons for such critical behavior. Severe damage is the result of multiple physical factors, and there is some clear indication that correlates positively in this case with ground motion directionality, soil quality, building irregularities in plan and height, slenderness and plan aspect ratio, high levels of compression loads, lack of confinement, and minimum values of wall thickness.

There are short term and long term implications that can be derived from all this information. Chilean and probably international codes should be revised in relation to shear wall design. Revisions could include many aspects, from the ground motion characterization in longer periods to stricter confinement requirements, but two related aspects that seem simple and crucial to implement shortly in wall design are: (i) to limit axial loads, and (ii) to limit minimum wall thicknesses for constructability and damage integrity purposes. Please note that confinement is not included because it requires further analysis. If the ACI provisions are applied at face value, Chilean engineers will find incentive to abandon the typical apartment building with high density of shear

walls, and move toward a system with much less but well confined walls. It could be the solution, but it needs to be studied further. In the long run, other aspects such as simultaneity of horizontal and vertical components in wall design, plan and vertical irregularities, participation of non-structural elements, reincorporation of energy dissipation lintels, and new drift limits may find room for improvement in the codes. Besides, seismic codes should try to promote the concept of conceptual 3D building design, suggesting procedures to include not only element or story based designs, but 3D designs including formation of mechanisms with critical sections that travel through stories.

Buildings studied are common Chilean housing and office buildings, i.e., include high densities of shear walls and building plans that are simple (with exceptions like TO-9); and because of that, their study is quite useful to improve the design of shear wall buildings reflected in new codes and practices.

There is no doubt that the only way to address this complex problem more effectively is worldwide collaborative research. The importance of earthquake behavior and well-designed facilities goes beyond the structural engineering realm. The society trust structural engineers to build safely, but more and more, it has become clearer that safety is not enough. Society is not willing to accept damage that impairs the use of structures after an earthquake, and hence, performance based engineering and clear communication of that expected performance to people is a crucial aspect of the profession. Apart from the incommensurable effect on people lives, it is a fact that the performance of structures during earthquakes hits the core of the society and must be taken with maximum rigor.

REFERENCES

Alimoradi, A., & Naeim, F. (2010). Did the large coseismic displacement cause the global overturning collapse of the Alto Río building during the 27 February 2010 offshore Maule, Chile earthquake? *The Structural Design of Tall and Special Buildings*, 19(8), 876-884.

American Concrete Institute Committee 318 (1995). *Building Code Requirements for Reinforced Concrete*. (ACI 318-95). Detroit, USA: Author.

Arnold, C. (1990). *The 1985 Chile Earthquake: Architectural and Structural Configurations as Determinants of Seismic Performance – Reinforced Concrete Buildings in Viña del Mar* (Report to the National Science Foundation). Building Systems Development, Inc., San Mateo, California.

Building Seismic Safety Council (2003). *NEHRP recommended provisions for seismic regulations for new buildings and other structures*. (FEMA 450). Washington D. C., USA: Author.

Bureau of Indian Standards (2002). *Indian standard criteria for earthquake resistant design of structures*. (IS 1893 part 1). New Delhi, India: Author.

Computers & Structures, Inc (2011). ETABS (9.6). Berkeley, California, USA.

DICTUC S. A. (2010). *Structural evaluation and diagnosis studies of severely damaged buildings from the February 27th earthquake*. Santiago, Chile: Author.

Guendelman, T., Lindenberg, J., & Guendelman, M. (1997). Bio-Seismic profile of buildings. *Proceedings of the VII Chilean Conference on Seismology and Earthquake Engineering*. La Serena, Chile.

Hayes, G., & U. S. Geological Survey (2010). Finite Fault Model. In USGS. Recovered January 12 of 2011, from http://earthquake.usgs.gov/earthquakes/eqinthenews/2010/us2010utc5/finite_fault2.php

Instituto de la Construcción (2010). *30 proposals regarding the February 27th earthquake of 2010*. Santiago, Chile: Author.

Instituto Nacional de Estadísticas de Chile (2010). *Information based on approved building permits*. Santiago, Chile: Author.

Instituto Nacional de Normalización (1996). *Seismic design of buildings*. (NCh433Of.96). Santiago, Chile: Author.

Moehle, J. P. (2010). Briefing on Chile earthquake of February 27, 2010. *Briefing on Chile earthquake of February 27, 2010*. Earthquake Engineering Research Institute. San Francisco, USA.

Moroni, O. (2011). Concrete shear wall construction. In *World Housing Encyclopedia*. Recovered February 4th of 2011, from <http://www.world-housing.net/>.

National Earthquake Hazards Reduction Program (2009). *2009 NEHRP recommended seismic provisions for new buildings and other structures*. (FEMA P749). Washington D.C., USA: Author.

Riddell, R. (1992). Performance of RC buildings in the 1985 Chile earthquake. *Earthquake engineering, Tenth world conference*. Rotterdam, Netherlands: Author.

Riddell, R., Wood, S. L., and de la Llera, J. C. (1987). *The 1985 Chile Earthquake: Structural Characteristics and Damage Statistics for the Building Inventory in Viña del Mar* (Structural Research No. 534). Civil Engineering Studies, University of Illinois, Urbana.

Sarkar, P., Prasad, A. M., & Menon, D. (2010). Vertical geometric irregularity in stepped building frames. *Engineering Structures*, 32(8), 2175-2182.

Structural Engineers Association of California (1999). *Recommended Lateral Force Requirements and Commentary*. (SEAOC Blue Book). Sacramento, USA: Author.

Wallace, J. W., & Moehle, J. P. *The 1985 Chile Earthquake: An evaluation of Structural Requirements for Bearing Wall Buildings* (Report No. UCB/EERC-89-05). Earthquake Engineering Research Center, University of California at Berkeley.

Wallace, J. W., & Moehle, J. P. (1992). Ductility and Detailing Requirements of Bearing Wall Buildings. *Journal of Structural Engineering*, 118(6), 1625-1644.

Wood, S. L. (1991). Performance of reinforced concrete buildings during the 1985 Chile earthquake: Implications for the design of structural walls. *Earthquake Spectra*, 7(4), 607-638.

Wood S. L., Wight, J. K., & Moehle, J. P. (1987). *The 1985 Chile Earthquake: Observations on Earthquake-Resistant Construction in Viña del Mar* (Structural Research Series No. 532). Civil Engineering Studies, University of Illinois, Urbana.

Westenenk, B., de la Llera, J. C., Besa, J. J., Jünemann, R., Moehle, J. P., Lüders, C.,...,Hwang, S. (2011). Response of Reinforced Concrete Buildings in Concepción during the Maule Earthquake. *Earthquake Spectra* (To be published).

Westenenk, B., de la Llera, J. C., Besa, J. J., Jünemann, R., Lüders, C., Inaudi, J. A.,...,Jordán, R. (2011). Seismic response in RC buildings in Concepción during the February 27, Maule Earthquake. Qualitative analysis and Interpretation. *Earthquake Spectra* (To be published).

APPENDICES

APPENDIX A: DAMAGE DRAWINGS

As mentioned earlier, this Appendix shows structural drawings with damage. Only the most damaged story is presented for every building. Convention is: light damage: green, moderate damage: blue, severe damage: red.

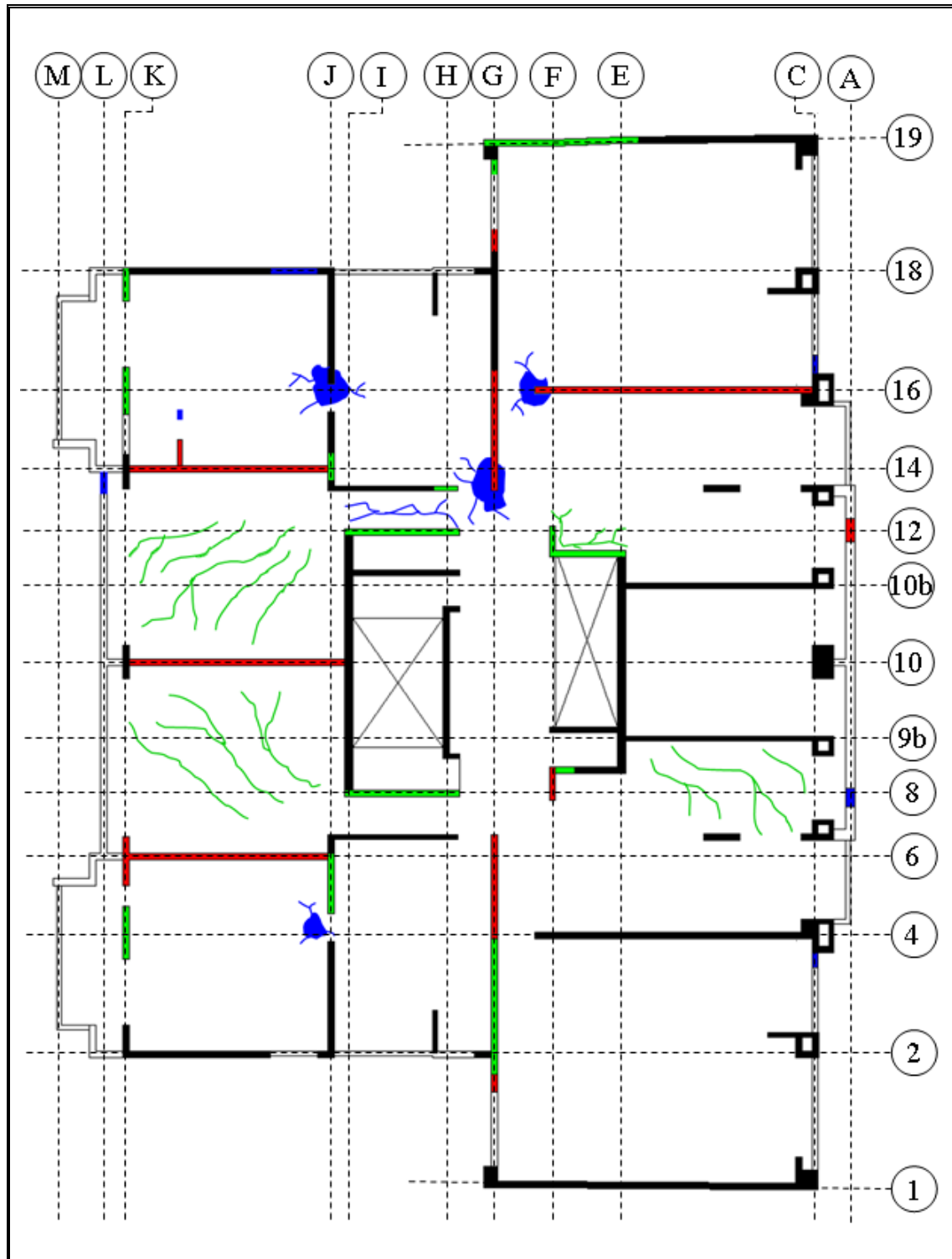


Figure A-1: Damaged elements in story 2 of building AA-1

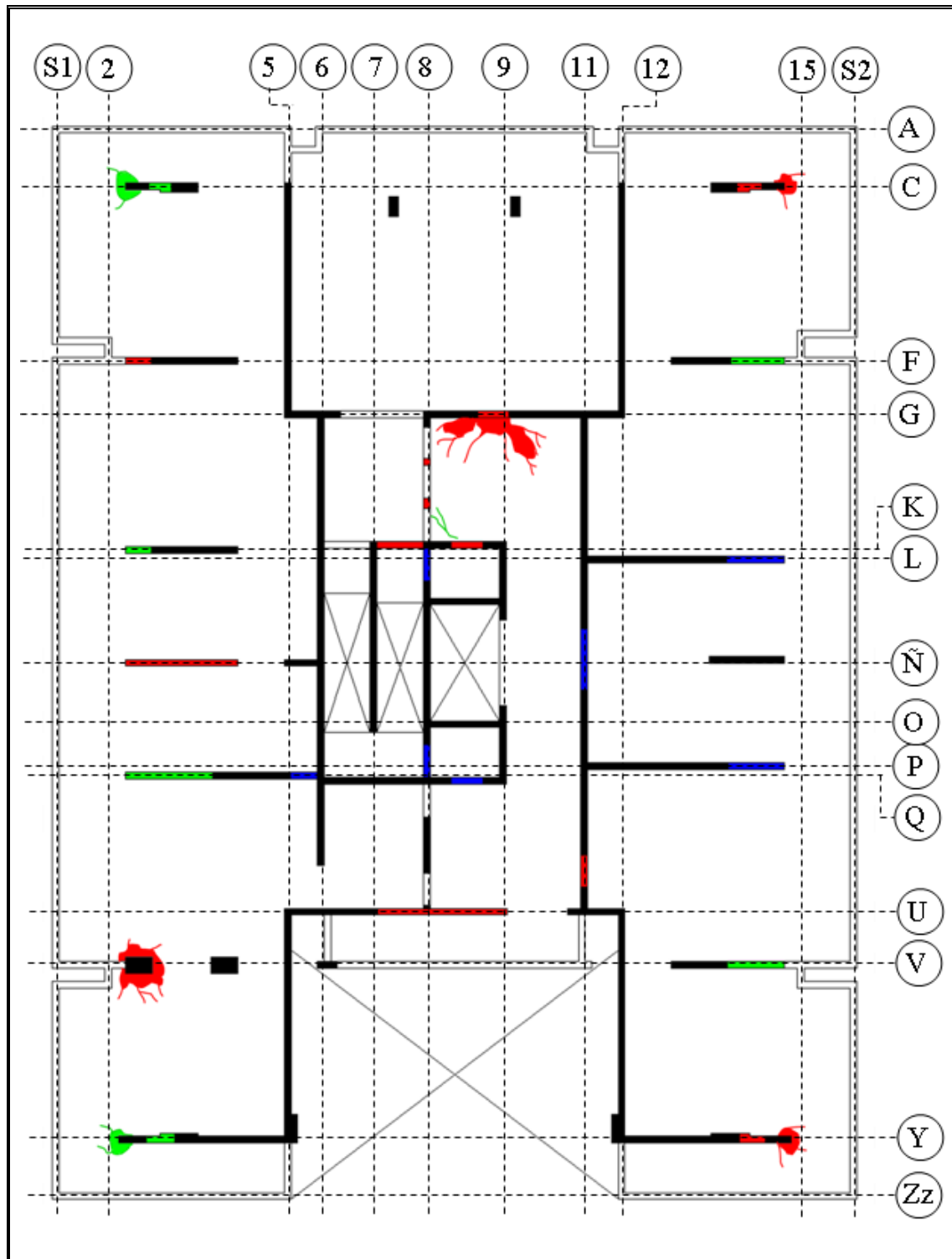


Figure A-2: Damaged elements in story 1 of building AH-2

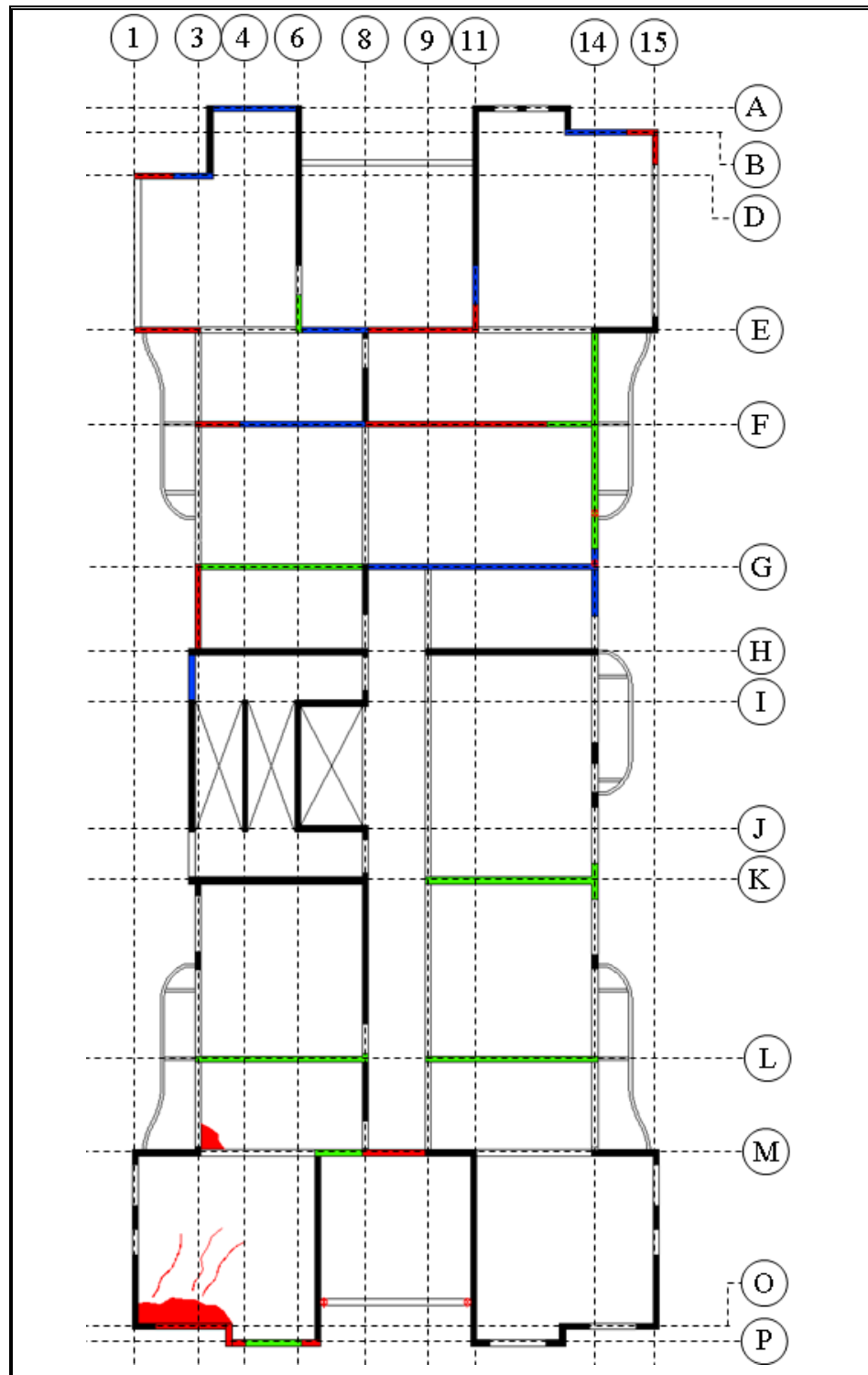


Figure A-3: Damaged elements in story 2 of building CM-3

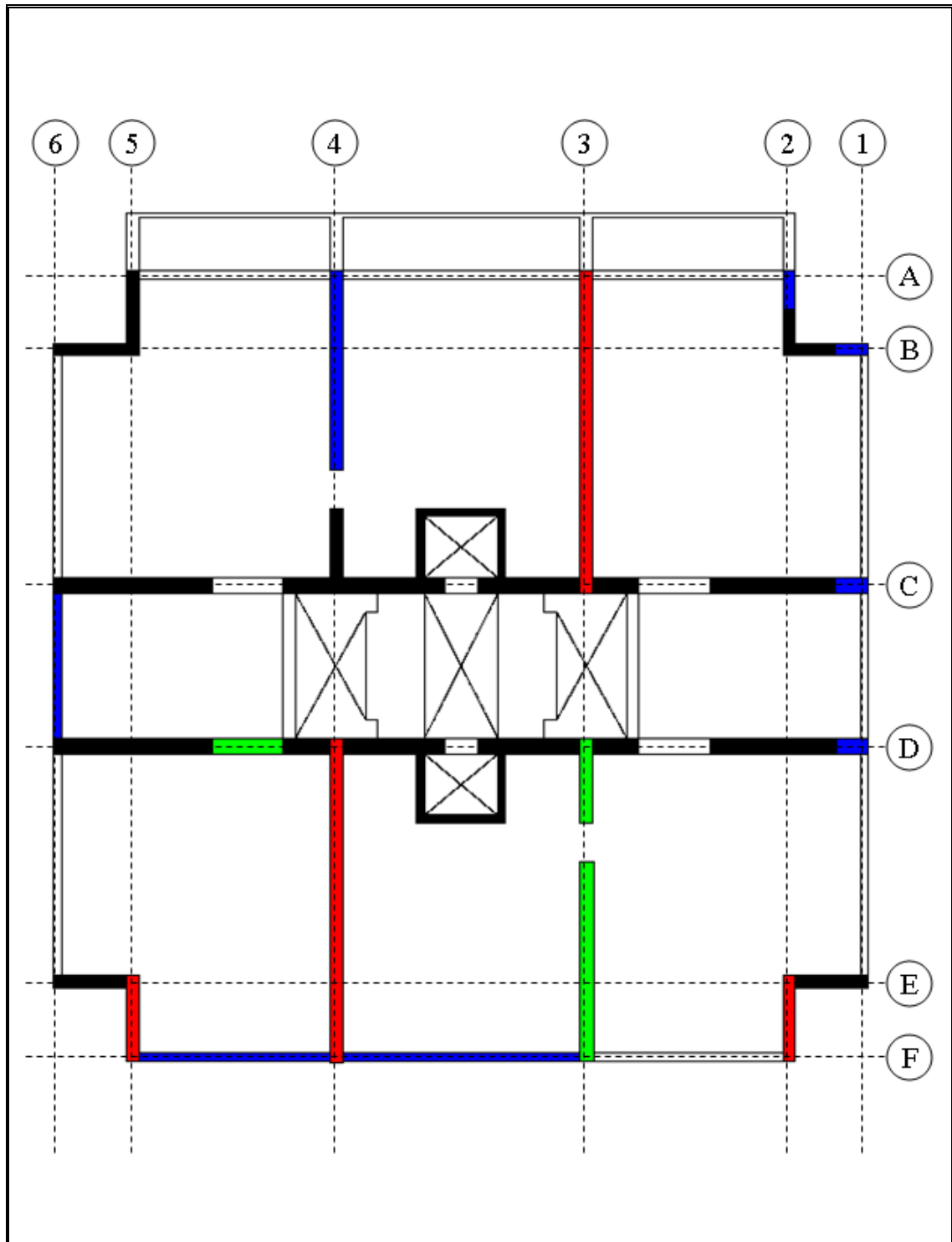


Figure A-4: Damaged elements in story 2 of building TL-4

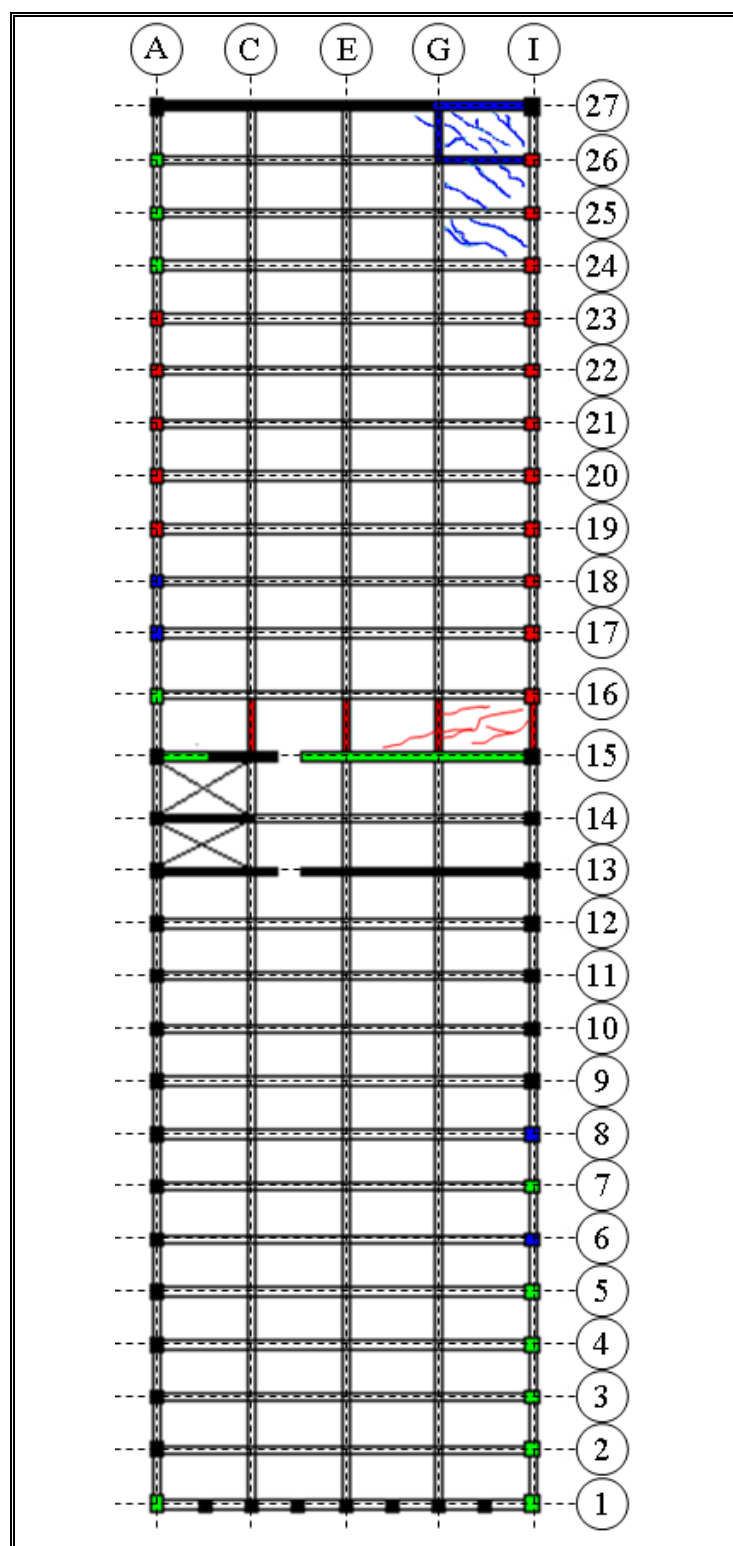


Figure A-5: Damaged elements in story 3 of building MD-5

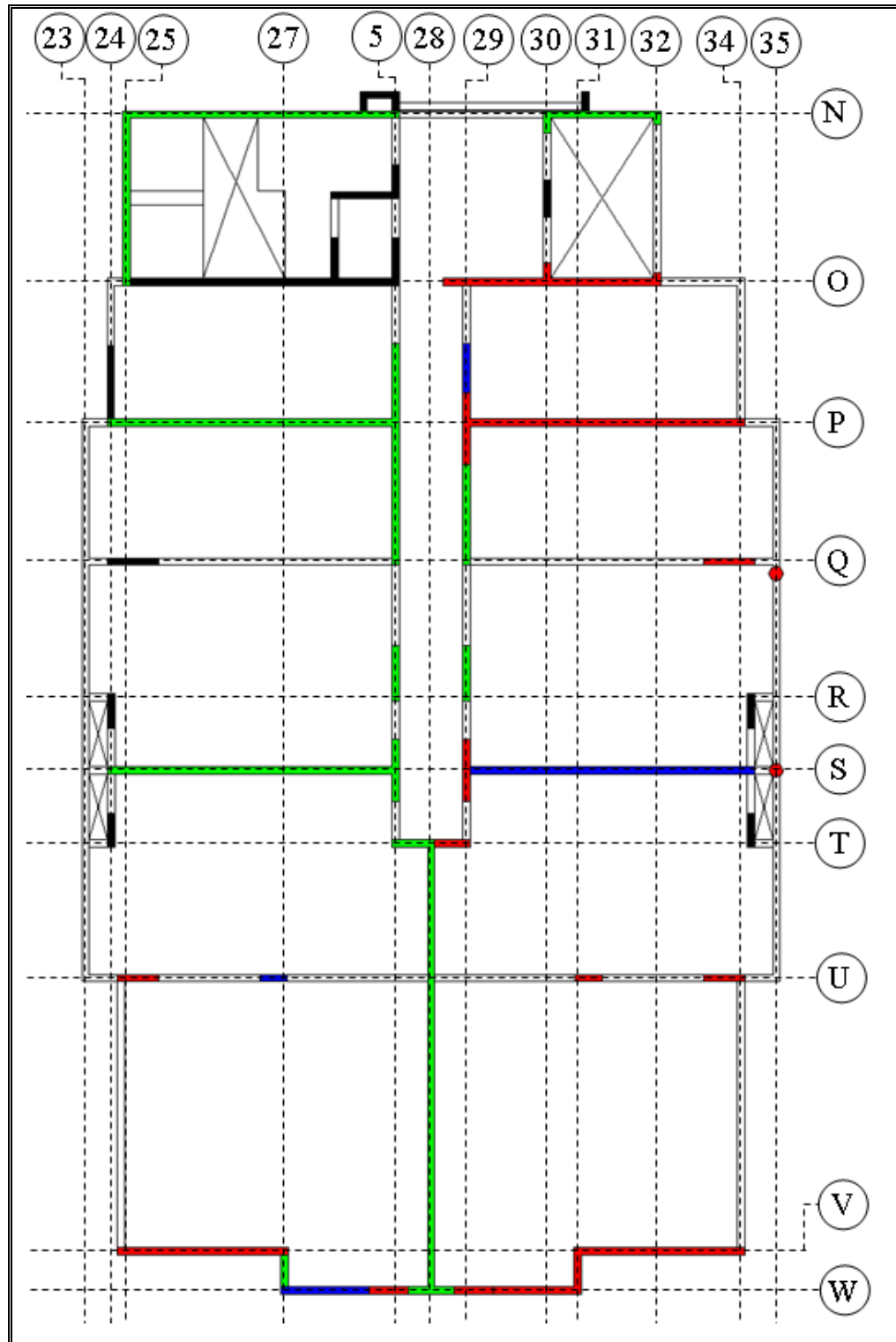


Figure A-6: Damaged elements in story 1 of building PR-6

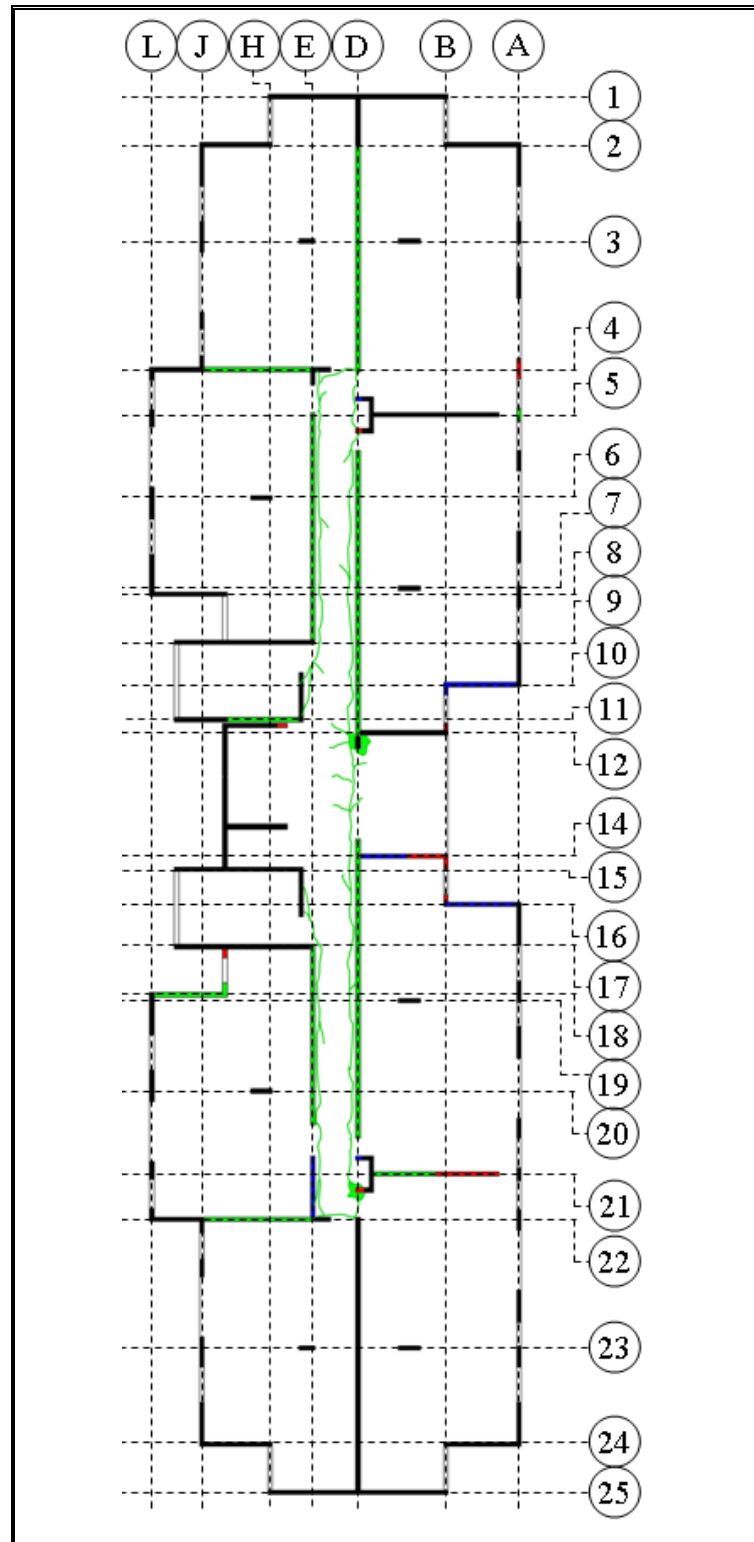


Figure A-7: Damaged elements in story 1 of building PP-7

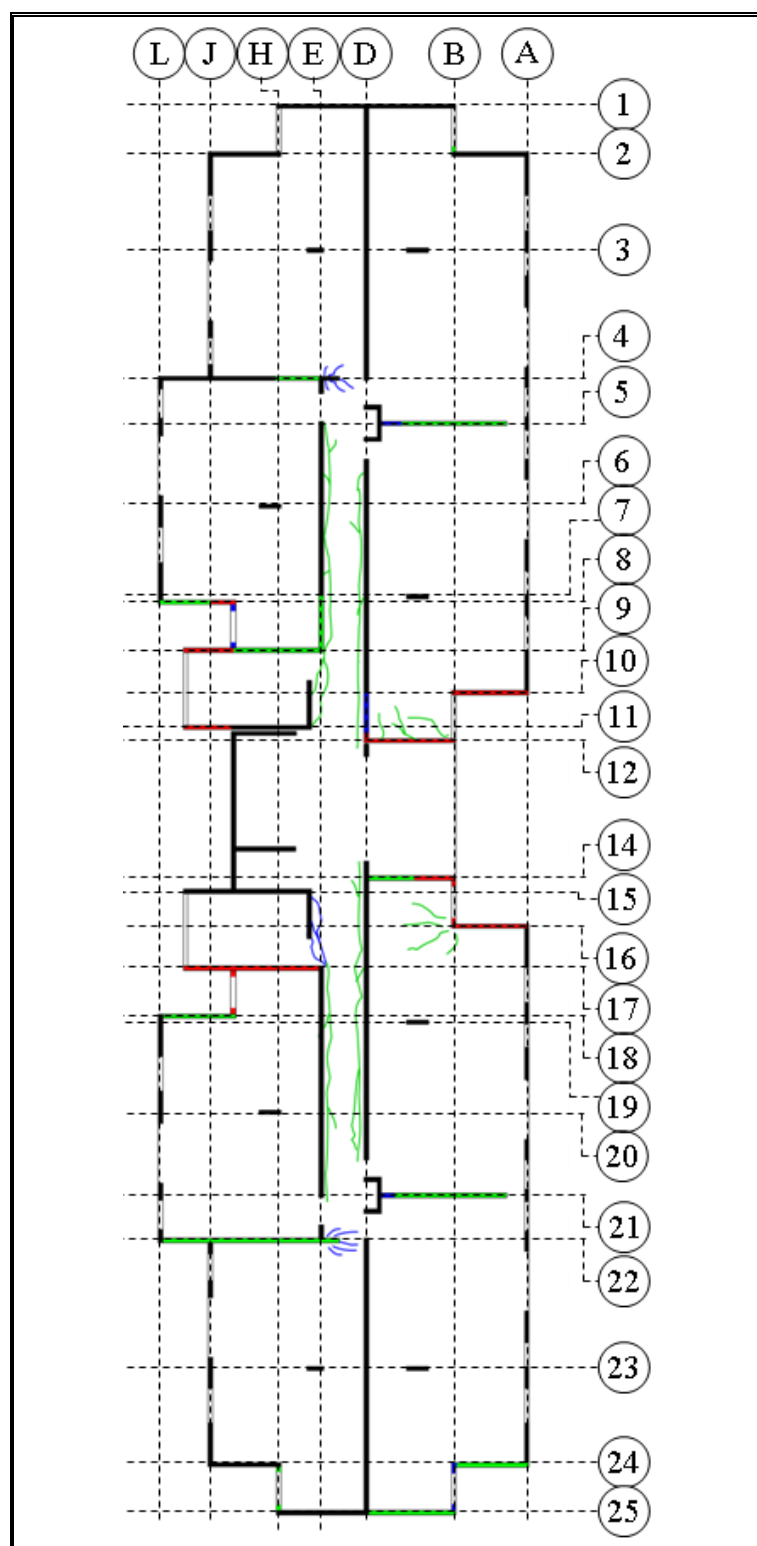


Figure A-8: Damaged elements in story 2 of building RT-8

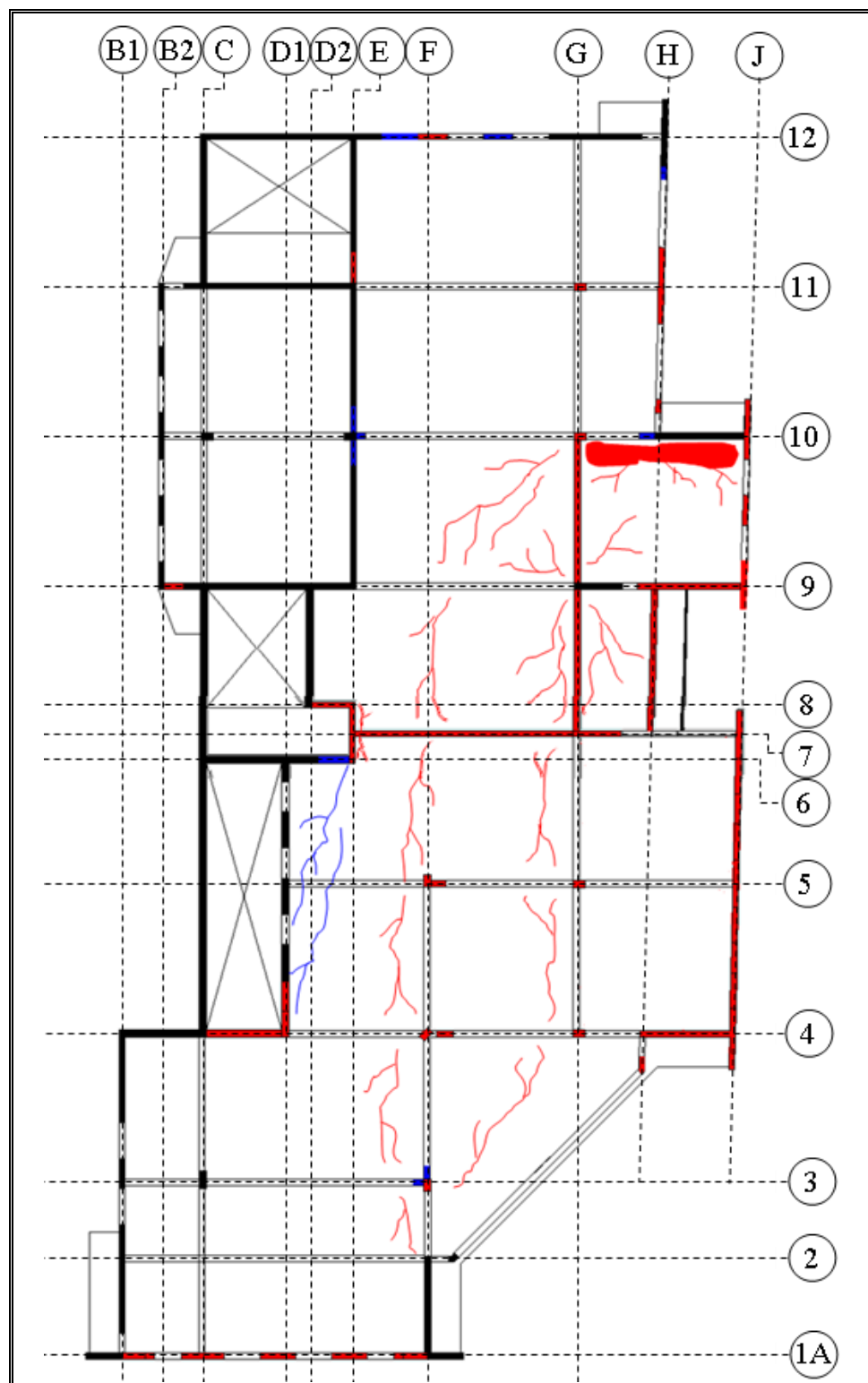


Figure A-9: Damaged elements in story 12 of building TO-9

APPENDIX B: D/C DRAWINGS

As mentioned earlier, this Appendix shows structural drawings with deficient D/C ratios. Only the most damaged story is presented for every building. Convention is: D/C ratio between 1 and 1.25: green, D/C ratio between 1.25 and 1.5: blue, D/C higher than 1.5: red. Note that if the same element has deficient D/C ratios in more than one behavior, the highest prevails.

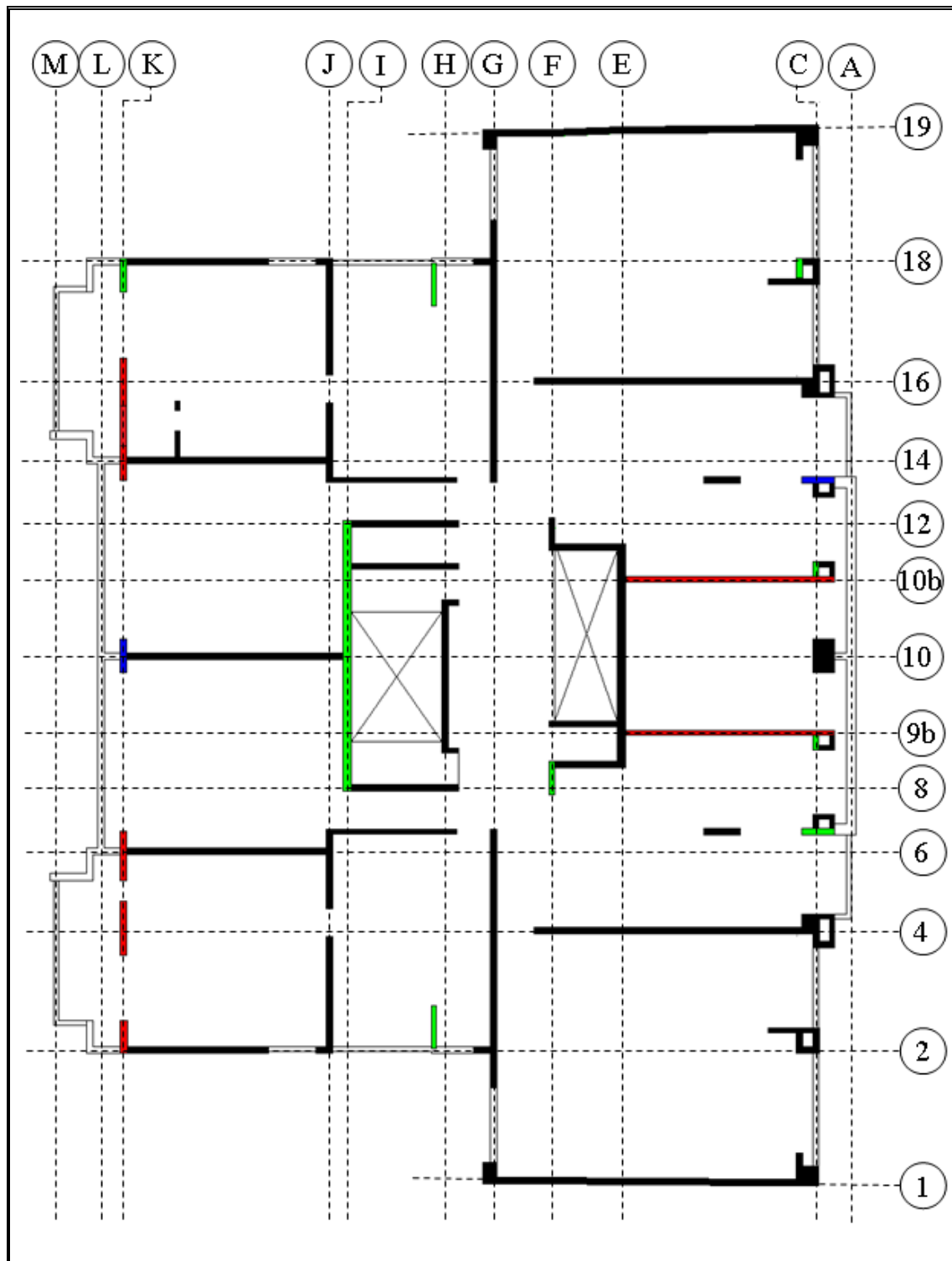


Figure B-1: D/C ratios in story 2 of building AA-1

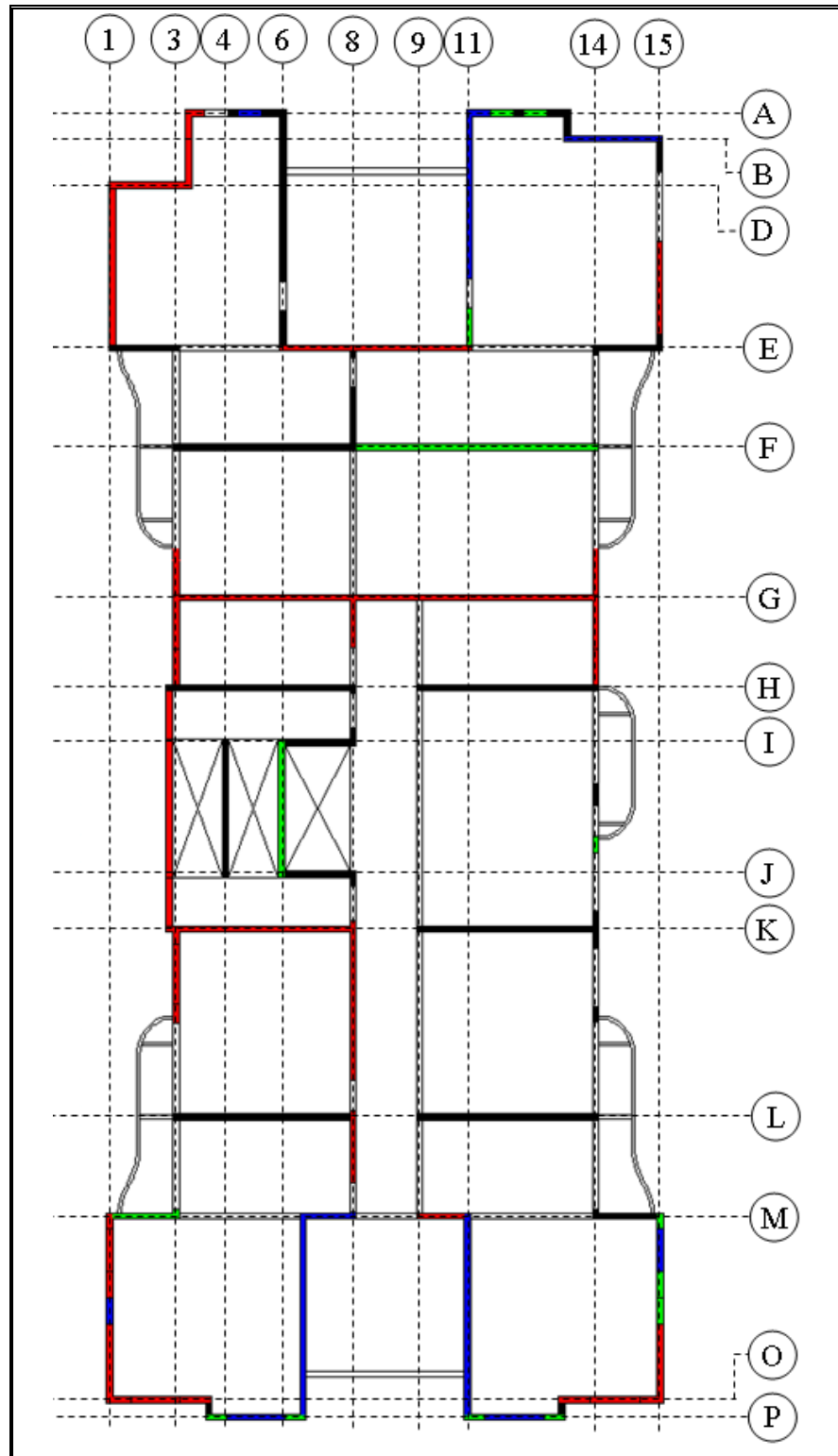


Figure B-2: D/C ratios in story 2 of building CM-3

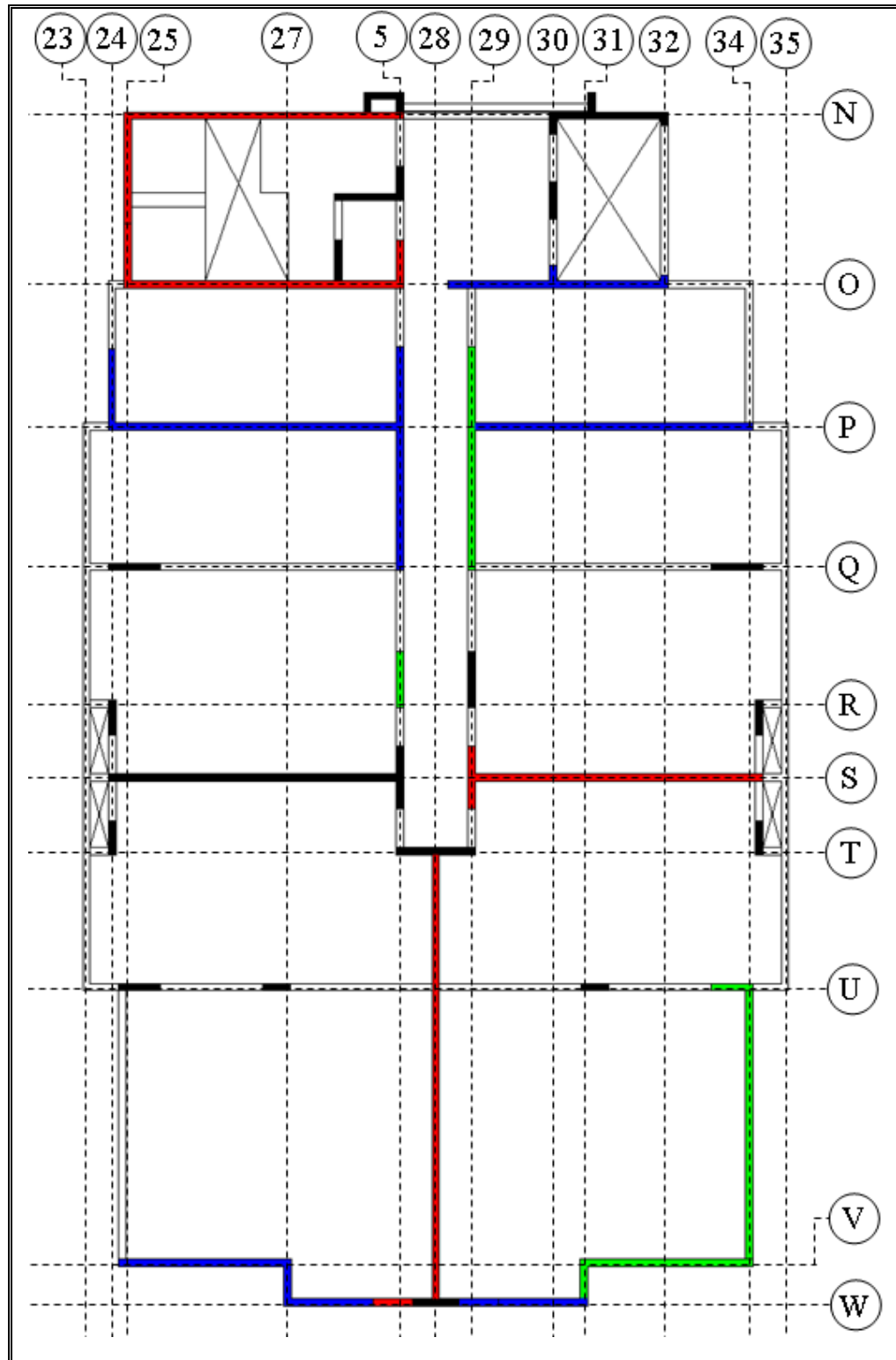


Figure B-3: D/C ratios in story 1 of building PR-6

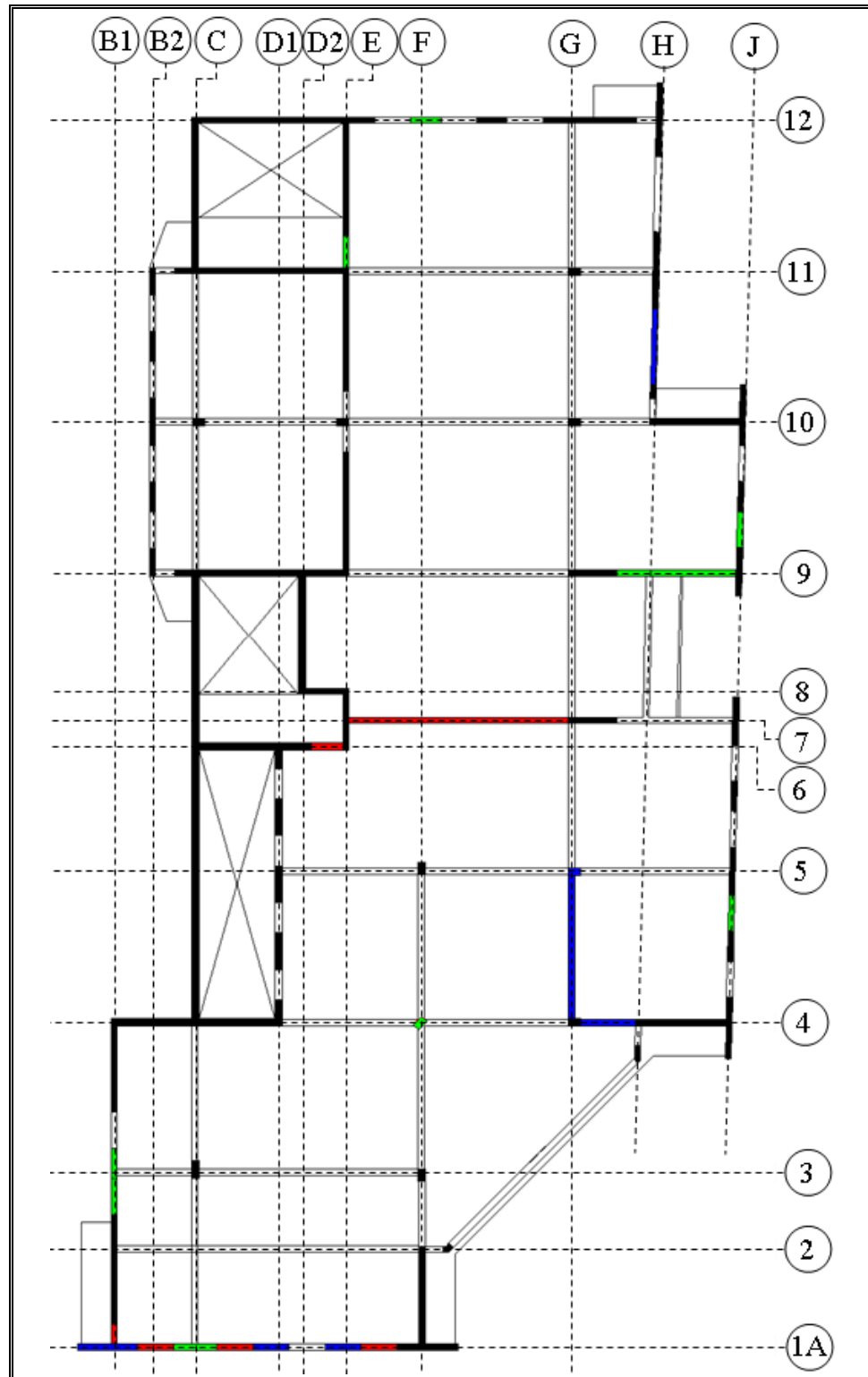


Figure B-4: D/C ratios in story 12 of building TO-9